250p.

MTP-P&VE-F-63-3) OTS: $
July 16, 1963

60

N63 22173

CODE-1

GEORGE C. MARSHALL SPACE FLIGHT CENTER

HUNTSVILLE, ALABAMA

(NASA TMX 50816)

Lunar Escape

By

Rowland E. Burns

and

Larry G. Singleton

OTS PRICE

XEROX $ 16.00 ph

MICROFILM $ 7.70 mf

NASA

[redacted]

NATIONAL AERONAUTICS AND SPACE ADMINISTRATION

MSFC - Form 523 (Rev. November 1960)

GEORGE C. MARSHALL SPACE FLIGHT CENTER

MTP-P&VE-F-63-3

LUNAR ESCAPE

By

Rowland E. Burns

and

Larry G. Singleton

ABSTRACT

22173

The problem of escape from the Moon is treated in this report using the techniques of the calculus of variations. The Moon is assumed to be spherical and rotating. Only single stage vehicles of constant thrust are considered. The three-dimensional equations used in a previous study (Ref. 1) are modified to allow a smooth transition to planar segments of the trajectory.

Numerical data considers three escape modes: *direct* escape, escape *through* orbit, and escape *from* orbit. For the first two modes, a further subdivision is made according to whether the altitude or angle of attack is specified at cutoff. For certain trajectories which escape through orbit, a discontinuity is inserted at circular orbit in order to specify the angle of attack at cutoff.

For the last two modes, post-orbital trajectory segments are planar. In all cases, parabolic energy (with respect to the Moon) is taken as the thrust termination criterion.

Data are presented in both tabular and graphical form. The initial lunar thrust-to-weight ratio varies from 1 to 7 for the first two modes and from 0.2 to 7 for the last mode. Specific impulses are taken to be 300, 350, 400, and 450 sec. Initial orbital altitudes are 50, 100, 150, 200, 250, and 300 kilometers for those trajectories which escape from orbit. Numerical examples illustrate applications of the data to preliminary design studies.

GEORGE C. MARSHALL SPACE FLIGHT CENTER

MTP-P&VE-F-63-3

LUNAR ESCAPE

By

Rowland E. Burns

and

Larry G. Singleton

PROPULSION AND VEHICLE ENGINEERING DIVISION

ADVANCED FLIGHT SYSTEMS BRANCH

TABLE OF CONTENTS

Summary 1

Introduction 1

Summary of Previous Theory 2

Derivation of Planar Equations 5

End Conditions 8

Numerical Integration Procedure 11

Numerical Results 13

Graphical Presentation of Results 112

Numerical Examples 208

Conclusions 222

Computer Diagrams (Appendix) 223

References 230

LIST OF ILLUSTRATIONS

Figure	Title	Page
1	Coordinate System	3
2	Gimbal Angle Coordinates	3
3	Mass Fraction at Escape vs Initial Lunar Thrust-to-Weight Ratio for Direct Escape at 15 km.	113
4	λ_1 vs Initial Lunar Thrust-to-Weight Ratio for Direct Escape at 15 km	114
5	λ_1 vs Initial Lunar Thrust-to-Weight Ratio for Direct Escape at 15 km	115
6	λ_4 vs Initial Lunar Thrust-to-Weight Ratio for Direct Escape at 15 km	116
7	λ_4 vs Initial Lunar Thrust-to-Weight Ratio for Direct Escape at 15 km	117
8	λ_5 vs Initial Lunar Thrust-to-Weight Ratio for Direct Escape at 15 km	118
9	Gamma at Escape vs Initial Lunar Thrust-to-Weight Ratio for Direct Escape at 15 km	119
10	Burning Time to Escape vs Initial Lunar Thrust-to-Weight Ratio for Direct Escape at 15 km	120
11	Mass Fraction at Escape vs Initial Lunar Thrust-to-Weight Ratio for Direct Escape. Altitudes Matched with Corresponding Specific Impulses and Thrust-to-Weight Ratios of Tables 33 Through 42	121
12	λ_1 vs Initial Lunar Thrust-to-Weight Ratio for Direct Escape. Altitudes Matched with Corresponding Specific Impulses and Thrust-to-Weight Ratios of Tables 33 Through 42	122
13	λ_4 vs Initial Lunar Thrust-to-Weight Ratio for Direct Escape. Altitudes Matched with Corresponding Specific Impulses and Thrust-to-Weight Ratios of Tables 33 Through 42	123
14	λ_5 vs Initial Lunar Thrust-to-Weight Ratio for Direct Escape. Altitudes Matched with Corresponding Specific Impulses and Thrust-to-Weight Ratios of Tables 33 Through 42	124
15	Gamma at Escape vs Initial Lunar Thrust-to-Weight Ratio for Direct Escape. Altitudes Matched with Corresponding Specific Impulses and Thrust-to-Weight Ratios of Tables 33 Through 42	125
16	Burning Time to Escape vs Initial Lunar Thrust-to-Weight Ratio for Direct Escape. Altitudes Matched with Corresponding Specific Impulses and Thrust-to-Weight Ratios of Tables 33 Through 42	126
17	Altitude, Initial Lunar Thrust-to-Weight Ratio, and Mass Fraction vs Specific Impulse for Escape Through a 15 km. Circular Orbit. m_{esc}/m_0 Maximized with Respect to T/W_0 .Thrust and Velocity Vectors not Aligned at Escape	127
18	Initial Values of λ_1, λ_4, and λ_5 vs Specific Impulse for Escape Through a 15 km. Circular Orbit. m_{esc}/m_0 Maximized with Respect to T/W_0 . Thrust and Velocity Vectors not Aligned at Escape	128

List of Illustrations (Continued)

Figure	Title	Page
34	Gamma at Escape vs Initial Lunar Thrust-to-Weight Ratio for Escape Through a 15 km. Circular Orbit. Thrust and Velocity Vectors Aligned at Escape via λ_4 Discontinuity at Circular Orbit	144
35	Burning Time to Escape vs Initial Lunar Thrust-to-Weight Ratio for Escape Through a 15 km. Circular Orbit. Thrust and Velocity Vectors Aligned at Escape via λ_4 Discontinuity at Circular Orbit	145
36	Adjusted Value of λ_4 at Circular Orbit vs Initial Lunar Thrust-to-Weight Ratio	146
37	Mass Fraction, Initial Lunar Thrust-to-Weight Ratio, and Altitude vs Specific Impulse. $r_{esc} - r_0$ Maximized with Respect to T/W_0. Thrust and Velocity Vectors Aligned at Orbit; Alignment at Escape via λ_4 Discontinuity at Orbit	147
38	Initial Values of λ_1, λ_4, and λ_5 vs Specific Impulse. $r_{esc} - r_0$ Maximized with Respect to T/W_0. Thrust and Velocity Vectors Aligned at Orbit; Alignment at Escape via λ_4 Discontinuity at Orbit	148
39	Mass Fraction vs Initial Lunar Thrust-to-Weight Ratio. Thrust and Velocity Vectors Aligned at Orbit: Alignment at Escape via λ_4 Discontinuity at Orbit	149
40	Altitude vs Initial Lunar Thrust-to-Weight Ratio. Thrust and Velocity Vectors Aligned at Orbit: Alignment at Escape via λ_4 Discontinuity at Orbit	150
41	Altitude vs Initial Lunar Thrust-to-Weight Ratio. Thrust and Velocity Vectors Aligned at Orbit: Alignment at Escape via λ_4 Discontinuity at Orbit	151
42	Gamma at Escape vs Initial Lunar Thrust-to-Weight Ratio. Thrust and Velocity Vectors Aligned at Orbit: Alignment at Escape via λ_4 Discontinuity at Orbit	152
43	Burning Time to Escape vs Initial Lunar Thrust-to-Weight Ratio. Thrust and Velocity Vectors Aligned at Orbit: Alignment at Escape via λ_4 Discontinuity at Orbit	153
44	Adjusted Value of λ_4 at Circular Orbit vs Initial Lunar Thrust-to-Weight Ratio	154
45	Altitude, Initial Lunar Thrust-to-Weight Ratio, and Mass Fraction vs Specific Impulse for Escape Through a 15 km. Circular Orbit. m_{esc}/m_0 Maximized with Respect to T/W_0. Thrust and Velocity Vectors Aligned at Escape via λ_3 Discontinuity at Circular Orbit	155
46	Initial Values of λ_1, λ_4, and λ_5 vs Specific Impulse for Escape Through a 15 km. Circular Orbit. m_{esc}/m_0 Maximized with Respect to T/W_0. Thrust and Velocity Vectors Aligned at Escape via λ_3 Discontinuity at Circular Orbit	156
47	Mass Fraction vs Initial Lunar Thrust-to-Weight Ratio for Escape Through a 15 km. Circular Orbit. Thrust and Velocity Vectors Aligned at Escape via λ_3 Discontinuity at Circular Orbit	157
48	Altitude vs Initial Lunar Thrust-to-Weight Ratio for Escape Through a 15 km. Circular Orbit. Thrust and Velocity Vectors Aligned at Escape via λ_3 Discontinuity at Circular Orbit	158

List of Illustrations (Continued)

Figure	Title	Page
19	Mass Fraction vs Initial Lunar Thrust-to-Weight Ratio for Escape Through a 15 km. Circular Orbit. Thrust and Velocity Vectors not Aligned at Escape	129
20	Altitude at Escape vs Initial Lunar Thrust-to-Weight Ratio for Escape Through a 15 km. Circular Orbit. Thrust and Velocity Vectors not Aligned at Escape	130
21	Gamma at Escape vs Initial Lunar Thrust-to-Weight Ratio for Escape Through a 15 km. Circular Orbit. Thrust and Velocity Vectors not Aligned at Escape	131
22	Burning Time to Escape vs Initial Lunar Thrust-to-Weight Ratio for Escape Through a 15 km. Circular Orbit. Thrust and Velocity Vectors not Aligned at Escape	132
23	Altitude, Initial Lunar Thrust-to-Weight Ratio, and Mass Fraction vs Specific Impulse. $r_{esc} - r_0$ Maximized with Respect to T/W_0. Thrust and Velocity Vectors Aligned at Circular Orbit but not Aligned at Escape	133
24	Initial Values of λ_1, λ_4 and λ_5 vs Specific Impulse, $r_{esc} - r_0$ Maximized with Respect to T/W_0. Thrust and Velocity Vectors Aligned at Circular Orbit but not Aligned at Escape	134
25	Mass Fraction vs Initial Lunar Thrust-to-Weight Ratio. Thrust and Velocity Vectors Aligned at Circular Orbit but not Aligned at Escape	135
26	Altitude vs Initial Lunar Thrust-to-Weight Ratio. Thrust and Velocity Vectors Aligned at Circular Orbit but not Aligned at Escape	136
27	Altitude vs Initial Lunar Thrust-to-Weight Ratio. Thrust and Velocity Vectors Aligned at Circular Orbit but not Aligned at Escape	137
28	Gamma at Escape vs Initial Lunar Thrust-to-Weight Ratio. Thrust and Velocity Vectors Aligned at Circular Orbit but not Aligned at Escape	138
29	Burning Time to Escape vs Initial Lunar Thrust-to-Weight Ratio. Thrust and Velocity Vectors Aligned at Circular Orbit but not Aligned at Escape	139
30	Altitude, Initial Lunar Thrust-to-Weight Ratio, and Mass Fraction vs Specific Impulse for Escape Through a 15 km. Circular Orbit. m_{esc}/m_0 Maximized with Respect to T/W_0. Thrust and Velocity Vectors Aligned at Escape via λ_4 Discontinuity at Circular Orbit	140
31	Initial Values of λ_1, λ_4, and λ_5 vs Specific Impulse for Escape Through a 15 km. Circular Orbit. m_{esc}/m_0 Maximized with Respect to T/W_0. Thrust and Velocity Vectors Aligned at Escape via λ_4 Discontinuity at Circular Orbit	141
32	Mass Fraction vs Initial Lunar Thrust-to-Weight Ratio for Escape Through a 15 km. Circular Orbit. Thrust and Velocity Vectors Aligned at Escape via λ_4 Discontinuity at Circular Orbit	142
33	Altitude vs Initial Lunar Thrust-to-Weight Ratio for Escape Through a 15 km. Circular Orbit. Thrust and Velocity Vectors Aligned at Escape via λ_4 Discontinuity at Circular Orbit	143

List of Illustrations (Continued)

Figure	Title	Page
49	Gamma at Escape vs Initial Lunar Thrust-to-Weight Ratio for Escape Through a 15 km. Circular Orbit. Thrust and Velocity Vectors Aligned at Escape via λ_3 Discontinuity at Circular Orbit	159
50	Burning Time to Escape vs Initial Lunar Thrust-to-Weight Ratio for Escape Through a 15 km. Circular Orbit. Thrust and Velocity Vectors Aligned at Escape via λ_3 Discontinuity at Circular Orbit	160
51	Adjusted Value of λ_3 at Circular Orbit vs Initial Lunar Thrust-to-Weight Ratio	161
52	Adjusted Value of λ_3 at Circular Orbit vs Initial Lunar Thrust-to-Weight Ratio	162
53	Mass Fraction, Initial Lunar Thrust-to-Weight Ratio, and Altitude vs Specific Impulse. $r_{esc} - r_0$ Maximized with Respect to T/W_0. Thrust and Velocity Vectors Aligned at Orbit: Alignment at Escape via λ_3 Discontinuity at Orbit	163
54	Initial Values of λ_1, λ_4, and λ_5 vs Specific Impulse. $r_{esc} - r_0$ Maximized with Respect to T/W_0. Thrust and Velocity Vectors Aligned at Orbit: Alignment at Escape via λ_3 Discontinuity at Orbit	164
55	Mass Fraction vs Initial Lunar Thrust-to-Weight Ratio. Thrust and Velocity Vectors Aligned at Orbit: Alignment at Escape via λ_3 Discontinuity at Orbit	165
56	Altitude vs Initial Lunar Thrust-to-Weight Ratio. Thrust and Velocity Vectors Aligned at Orbit: Alignment at Escape via λ_3 Discontinuity at Orbit	166
57	Altitude vs Initial Lunar Thrust-to-Weight Ratio. Thrust and Velocity Vectors Aligned at Orbit: Alignment at Escape via λ_3 Discontinuity at Orbit	167
58	Gamma at Escape vs Initial Lunar Thrust-to-Weight Ratio. Thrust and Velocity Vectors Aligned at Orbit: Alignment at Escape via λ_3 Discontinuity at Orbit	168
59	Burning Time to Escape vs Initial Lunar Thrust-to-Weight Ratio. Thrust and Velocity Vectors Aligned at Orbit: Alignment at Escape via λ_3 Discontinuity at Orbit	169
60	Adjusted Value of λ_3 at Circular Orbit vs Initial Lunar Thrust-to-Weight Ratio	170
61	Adjusted Value of λ_3 at Circular Orbit vs Initial Lunar Thrust-to-Weight Ratio	171
62	Escape Altitude vs Initial Orbital Altitude for Specific Impulse of 300 sec	172
63	Escape Altitude vs Initial Orbital Altitude for Specific Impulse of 350 sec	173
64	Escape Altitude vs Initial Orbital Altitude for Specific Impulse of 400 sec	174
65	Escape Altitude vs Initial Orbital Altitude for Specific Impulse of 450 sec	175
66	Mass Fraction vs Initial Orbital Altitude for Initial Lunar Thrust-to-Weight Ratio = 0.2	176
67	Mass Fraction vs Initial Orbital Altitude for Initial Lunar Thrust-to-Weight Ratio = 0.4	177
68	Mass Fraction vs Initial Orbital Altitude for Initial Lunar Thrust-to-Weight Ratio = 0.6	178
69	Mass Fraction vs Initial Orbital Altitude for Initial Lunar Thrust-to-Weight Ratio = 0.8	179
70	Mass Fraction vs Initial Orbital Altitude for Initial Lunar Thrust-to-Weight Ratio = 1.0	180

Figure	Title	Page
71	Mass Fraction vs Initial Orbital Altitude for Initial Lunar Thrust-to-Weight Ratio = 2.0	181
72	Mass Fraction vs Initial Orbital Altitude for Initial Lunar Thrust-to-Weight Ratio = 3.0	182
73	Mass Fraction vs Initial Orbital Altitude for Initial Lunar Thrust-to-Weight Ratio = 4.0	183
74	Mass Fraction vs Initial Orbital Altitude for Initial Lunar Thrust-to-Weight Ratio = 5.0	184
75	Mass Fraction vs Initial Orbital Altitude for Initial Lunar Thrust-to-Weight Ratio = 6.0	185
76	Mass Fraction vs Initial Orbital Altitude for Initial Lunar Thrust-to-Weight Ratio = 7.0	186
77	Value of λ_4 at Circular Orbit vs Initial Orbital Altitude for Specific Impulse of 300 sec	187
78	Value of λ_4 at Circular Orbit vs Initial Orbital Altitude for Specific Impulse of 350 sec	188
79	Value of λ_4 at Circular Orbit vs Initial Orbital Altitude for Specific Impulse of 400 sec	189
80	Value of λ_4 at Circular Orbit vs Initial Orbital Altitude for Specific Impulse of 450 sec	190
81	Burning Time to Escape vs Initial Orbital Altitude for Initial Lunar Thrust-to-Weight Ratio = 0.2	191
82	Burning Time to Escape vs Initial Orbital Altitude for Initial Lunar Thrust-to-Weight Ratio = 0.4	192
83	Burning Time to Escape vs Initial Orbital Altitude for Initial Lunar Thrust-to-Weight Ratio = 0.6	193
84	Burning Time to Escape vs Initial Orbital Altitude for Initial Lunar Thrust-to-Weight Ratio = 0.8	194
85	Burning Time to Escape vs Initial Orbital Altitude for Initial Lunar Thrust-to-Weight Ratio = 1.0	195
86	Burning Time to Escape vs Initial Orbital Altitude for Initial Lunar Thrust-to-Weight Ratio = 2.0	196
87	Burning Time to Escape vs Initial Orbital Altitude for Initial Lunar Thrust-to-Weight Ratio = 3.0	197
88	Burning Time to Escape vs Initial Orbital Altitude for Initial Lunar Thrust-to-Weight Ratio = 4.0	198
89	Burning Time to Escape vs Initial Orbital Altitude for Initial Lunar Thrust-to-Weight Ratio = 5.0	199
90	Burning Time to Escape vs Initial Orbital Altitude for Initial Lunar Thrust-to-Weight Ratio = 6.0	200
91	Burning Time to Escape vs Initial Orbital Altitude for Initial Lunar Thrust-to-Weight Ratio = 7.0	201
92	Mass Fraction vs Initial Lunar Thrust-to-Weight Ratio for Initial Circular Orbital Altitude = 50 km	202
93	Mass Fraction vs Initial Lunar Thrust-to-Weight Ratio for Initial Circular Orbital Altitude = 100 km	203

List of Illustrations (Concluded)

Figure	Title	Page
94	Mass Fraction vs Initial Lunar Thrust-to-Weight Ratio for Initial Circular Orbital Altitude = 150 km	204
95	Mass Fraction vs Initial Lunar Thrust-to-Weight Ratio for Initial Circular Orbital Altitude = 200 km	205
96	Mass Fraction vs Initial Lunar Thrust-to-Weight Ratio for Initial Circular Orbital Altitude = 250 km	206
97	Mass Fraction vs Initial Lunar Thrust-to-Weight Ratio for Initial Circular Orbital Altitude = 300 km	207
98	Gamma, Mass Fraction at Escape, and Time to Escape vs Specific Impulse for $T/W_0 = 2.7$	209
99	Initial Values of λ_1, λ_4, and λ_5 vs Specific Impulse for $T/W_0 = 2.7$	210
100	Burning Time to Escape, Mass Fraction at Escape, and Initial Lunar Thrust-to-Weight Ratio vs Specific Impulse for $r_{esc} - r_0 = 20$ km	213
101	Mass Fraction at Escape vs Specific Impulse for $T/W_0 = 1$	216
102	Altitude at Escape vs Initial Lunar Thrust-to-Weight Ratio for Initial Circular Orbital Altitude of 185 km	219
103	Altitude at Escape vs Specific Impulse for Initial Circular Orbital Altitude of 185 km. and Initial Lunar Thrust-to-Weight Ratio of 0.75	221
104	Mass Fraction at Escape vs Initial Lunar Thrust-to-Weight Ratio for Initial Circular Orbital Altitude of 185 km	223
105	Mass Fraction at Escape vs Specific Impulse for Initial Circular Orbital Altitude of 185 km. and Initial Lunar Thrust-to-Weight Ratio of 0.75	224

LIST OF TABLES

Table	Title	Page
1	Direct Escape at 15 Kilometers; Initial Lunar Thrust-to-Weight Ratio = 1.	15
2	Direct Escape at 15 Kilometers; Initial Lunar Thrust-to-Weight Ratio = 1.1	16
3	Direct Escape at 15 Kilometers; Initial Lunar Thrust-to-Weight Ratio = 1.3	17
4	Direct Escape at 15 Kilometers; Initial Lunar Thrust-to-Weight Ratio = 1.5	18
5	Direct Escape at 15 Kilometers; Initial Lunar Thrust-to-Weight Ratio = 2.	19
6	Direct Escape at 15 Kilometers; Initial Lunar Thrust-to-Weight Ratio = 3	20
7	Direct Escape at 15 Kilometers; Initial Lunar Thrust-to-Weight Ratio = 4	21
8	Direct Escape at 15 Kilometers; Initial Lunar Thrust-to-Weight Ratio = 5	22
9	Direct Escape at 15 Kilometers; Initial Lunar Thrust-to-Weight Ratio = 6	23
10	Direct Escape at 15 Kilometers; Initial Lunar Thrust-to-Weight Ratio = 7	24
11	Direct Escape: Altitudes Matched with Corresponding Cases of Table 33; Initial Lunar Thrust-to-Weight Ratio = 1.	25
12	Direct Escape: Altitudes Matched with Corresponding Cases of Table 34; Initial Lunar Thrust-to-Weight Ratio = 1.1	26
13	Direct Escape: Altitudes Matched with Corresponding Cases of Table 35; Initial Lunar Thrust-to-Weight Ratio = 1.3	27
14	Direct Escape: Altitudes Matched with Corresponding Cases of Table 36; Initial Lunar Thrust-to-Weight Ratio = 1.5	28
15	Direct Escape: Altitudes Matched with Corresponding Cases of Table 37; Initial Lunar Thrust-to-Weight Ratio = 2	29
16	Direct Escape: Altitudes Matched with Corresponding Cases of Table 38; Initial Lunar Thrust-to-Weight Ratio = 3	30
17	Direct Escape: Altitudes Matched with Corresponding Cases of Table 39; Initial Lunar Thrust-to-Weight Ratio = 4	31
18	Direct Escape: Altitudes Matched with Corresponding Cases of Table 40; Initial Lunar Thrust-to-Weight Ratio = 5	32
19	Direct Escape: Altitudes Matched with Corresponding Cases of Table 41; Initial Lunar Thrust-to-Weight Ratio = 6	33
20	Direct Escape: Altitudes Matched with Corresponding Cases of Table 42; Initial Lunar Thrust-to-Weight Ratio = 7	34
21	Escape Through a 15 Kilometer Circular Orbit; m_{esc}/m_0 Maximized Via Choice of T/W_0	35
22	Escape Through a 15 Kilometer Circular Orbit. Thrust and Velocity Vectors Not Aligned at Escape; Initial Lunar Thrust-to-Weight Ratio = 1	36
23	Escape Through a 15 Kilometer Circular Orbit. Thrust and Velocity Vectors Not Aligned at Escape; Initial Lunar Thrust-to-Weight Ratio = 1.1	37
24	Escape Through a 15 Kilometer Circular Orbit. Thrust and Velocity Vectors Not Aligned at Escape; Initial Lunar Thrust-to-Weight Ratio = 1.3	38
25	Escape Through a 15 Kilometer Circular Orbit. Thrust and Velocity Vectors Not Aligned at Escape; Initial Lunar Thrust-to-Weight Ratio = 1.5	39

List of Tables (Continued)

Table		Page
26	Escape Through a 15 Kilometer Circular Orbit. Thrust and Velocity Vectors Not Aligned at Escape; Initial Lunar Thrust-to-Weight Ratio = 2.0	40
27	Escape Through a 15 Kilometer Circular Orbit. Thrust and Velocity Vectors Not Aligned at Escape; Initial Lunar Thrust-to-Weight Ratio = 3.0	41
28	Escape Through a 15 Kilometer Circular Orbit. Thrust and Velocity Vectors Not Aligned at Escape; Initial Lunar Thrust-to-Weight Ratio = 4.0	42
29	Escape Through a 15 Kilometer Circular Orbit. Thrust and Velocity Vectors Not Aligned at Escape; Initial Lunar Thrust-to-Weight Ratio = 5.0	43
30	Escape Through a 15 Kilometer Circular Orbit. Thrust and Velocity Vectors Not Aligned at Escape; Initial Lunar Thrust-to-Weight Ratio = 6.0	44
31	Escape Through a 15 Kilometer Circular Orbit. Thrust and Velocity Vectors Not Aligned at Escape; Initial Lunar Thrust-to-Weight Ratio = 7.0	45
32	Escape Through Orbit. Thrust and Velocity Vectors Aligned at Orbit: No Alignment at Escape; $r_{esc} - r_0$ Maximized Via Choice of T/W_0	46
33	Escape Through Orbit. Thrust and Velocity Vectors Aligned at Orbit: No Alignment at Escape; Initial Lunar Thrust-to-Weight Ratio = 1	47
34	Escape Through Orbit. Thrust and Velocity Vectors Aligned at Orbit: No Alignment at Escape; Initial Lunar Thrust-to-Weight Ratio = 1.1	48
35	Escape Through Orbit. Thrust and Velocity Vectors Aligned at Orbit: No Alignment at Escape; Initial Lunar Thrust-to-Weight Ratio = 1.3	49
36	Escape Through Orbit. Thrust and Velocity Vectors Aligned at Orbit: No Alignment at Escape; Initial Lunar Thrust-to-Weight Ratio = 1.5	50
37	Escape Through Orbit. Thrust and Velocity Vectors Aligned at Orbit: No Alignment at Escape; Initial Lunar Thrust-to-Weight Ratio = 2	51
38	Escape Through Orbit. Thrust and Velocity Vectors Aligned at Orbit: No Alignment at Escape; Initial Lunar Thrust-to-Weight Ratio = 3	52
39	Escape Through Orbit. Thrust and Velocity Vectors Aligned at Orbit; No Alignment at Escape; Initial Lunar Thrust-to-Weight Ratio = 4	53
40	Escape Through Orbit. Thrust and Velocity Vectors Aligned at Orbit: No Alignment at Escape; Initial Lunar Thrust-to-Weight Ratio = 5	54
41	Escape Through Orbit. Thrust and Velocity Vectors Aligned at Orbit: No Alignment at Escape; Initial Lunar Thrust-to-Weight Ratio = 6	55
42	Escape Through Orbit. Thrust and Velocity Vectors Aligned at Orbit: No Alignment at Escape; Initial Lunar Thrust-to-Weight Ratio = 7	56
43	Escape Through a 15 Kilometer Circular Orbit. Thrust and Velocity Vectors Aligned at Escape Via λ_4 Discontinuity; m_{esc}/m_0 Maximized Via Choice of T/W_0	57
44	Escape Through a 15 Kilometer Circular Orbit. Thrust and Velocity Vectors Aligned at Escape Via λ_4 Discontinuity; Initial Lunar Thrust-to-Weight Ratio = 1	58

List of Tables (Continued)

Table	Title	Page
45	Escape Through a 15 Kilometer Circular Orbit. Thrust and Velocity Vectors Aligned at Escape Via λ_4 Discontinuity; Initial Lunar Thrust-to-Weight Ratio = 1.1	59
46	Escape Through a 15 Kilometer Circular Orbit. Thrust and Velocity Vectors Aligned at Escape Via λ_4 Discontinuity; Initial Lunar Thrust-to-Weight Ratio = 1.3	60
47	Escape Through a 15 Kilometer Circular Orbit. Thrust and Velocity Vectors Aligned at Escape Via λ_4 Discontinuity; Initial Lunar Thrust-to-Weight Ratio = 1.5	61
48	Escape Through a 15 Kilometer Circular Orbit. Thrust and Velocity Vectors Aligned at Escape Via λ_4 Discontinuity; Initial Lunar Thrust-to-Weight Ratio = 2	62
49	Escape Through a 15 Kilometer Circular Orbit. Thrust and Velocity Vectors Aligned at Escape Via λ_4 Discontinuity; Initial Lunar Thrust-to-Weight Ratio = 3	63
50	Escape Through a 15 Kilometer Circular Orbit. Thrust and Velocity Vectors Aligned at Escape Via λ_4 Discontinuity; Initial Lunar Thrust-to-Weight Ratio = 4	64
51	Escape Through a 15 Kilometer Circular Orbit. Thrust and Velocity Vectors Aligned at Escape Via λ_4 Discontinuity; Initial Lunar Thrust-to-Weight Ratio = 5	65
52	Escape Through a 15 Kilometer Circular Orbit. Thrust and Velocity Vectors Aligned at Escape Via λ_4 Discontinuity; Initial Lunar Thrust-to-Weight Ratio = 6	66
53	Escape Through a 15 Kilometer Circular Orbit. Thrust and Velocity Vectors Aligned at Escape Via λ_4 Discontinuity; Initial Lunar Thrust-to-Weight Ratio = 7	67
54	Escape Through Orbit. Thrust and Velocity Aligned at Orbit: Alignment at Escape Via λ_4 Discontinuity; $r_{esc} - r_0$ Maximized Via Choice of T/W_0	68
55	Escape Through Orbit. Thrust and Velocity Aligned at Orbit: Alignment at Escape Via λ_4 Discontinuity; Initial Lunar Thrust-to-Weight Ratio = 1	69
56	Escape Through Orbit. Thrust and Velocity Aligned at Orbit: Alignment at Escape Via λ_4 Discontinuity; Initial Lunar Thrust-to-Weight Ratio = 1.1	70
57	Escape Through Orbit. Thrust and Velocity Aligned at Orbit: Alignment at Escape Via λ_4 Discontinuity; Initial Lunar Thrust-to-Weight Ratio = 1.3	71
58	Escape Through Orbit. Thrust and Velocity Aligned at Orbit: Alignment at Escape Via λ_4 Discontinuity; Initial Lunar Thrust-to-Weight Ratio = 1.5	72
59	Escape Through Orbit. Thrust and Velocity Aligned at Orbit: Alignment at Escape Via λ_4 Discontinuity; Initial Lunar Thrust-to-Weight Ratio = 2	73
60	Escape Through Orbit. Thrust and Velocity Aligned at Orbit: Alignment at Escape Via λ_4 Discontinuity; Initial Lunar Thrust-to-Weight Ratio = 3	74
61	Escape Through Orbit. Thrust and Velocity Aligned at Orbit: Alignment at Escape Via λ_4 Discontinuity; Initial Lunar Thrust-to-Weight Ratio = 4	75
62	Escape Through Orbit. Thrust and Velocity Aligned at Orbit: Alignment at Escape Via λ_4 Discontinuity; Initial Lunar Thrust-to-Weight Ratio = 5	76
63	Escape Through Orbit. Thrust and Velocity Aligned at Orbit: Alignment at Escape Via λ_4 Discontinuity; Initial Lunar Thrust-to-Weight Ratio = 6	77
64	Escape Through Orbit. Thrust and Velocity Aligned at Orbit: Alignment at Escape Via λ_4 Discontinuity; Initial Lunar Thrust-to-Weight Ratio = 7	78

List of Tables (Continued)

Table	Title	Page
65	Escape Through a 15 Kilometer Circular Orbit. Thrust and Velocity Vectors Aligned at Escape Via λ_3 Discontinuity; m_{esc}/m_0 Maximized Via Choice of T/W_0 . . .	79
66	Escape Through a 15 Kilometer Circular Orbit. Thrust and Velocity Vectors Aligned at Escape Via λ_3 Discontinuity; Initial Lunar Thrust-to-Weight Ratio = 1 . . .	80
67	Escape Through a 15 Kilometer Circular Orbit. Thrust and Velocity Vectors Aligned at Escape Via λ_3 Discontinuity; Initial Lunar Thrust-to-Weight Ratio = 1.1 . .	81
68	Escape Through a 15 Kilometer Circular Orbit. Thrust and Velocity Vectors Aligned at Escape Via λ_3 Discontinuity; Initial Lunar Thrust-to-Weight Ratio = 1.3 . .	82
69	Escape Through a 15 Kilometer Circular Orbit. Thrust and Velocity Vectors Aligned at Escape Via λ_3 Discontinuity; Initial Lunar Thrust-to-Weight Ratio = 1.5 . . .	83
70	Escape Through a 15 Kilometer Circular Orbit. Thrust and Velocity Vectors Aligned at Escape Via λ_3 Discontinuity; Initial Lunar Thrust-to-Weight Ratio = 2	84
71	Escape Through a 15 Kilometer Circular Orbit. Thrust and Velocity Vectors Aligned at Escape Via λ_3 Discontinuity; Initial Lunar Thrust-to-Weight Ratio = 3. . . .	85
72	Escape Through a 15 Kilometer Circular Orbit. Thrust and Velocity Vectors Aligned at Escape Via λ_3 Discontinuity; Initial Lunar Thrust-to-Weight Ratio = 4	86
73	Escape Through a 15 Kilometer Circular Orbit. Thrust and Velocity Vectors Aligned at Escape Via λ_3 Discontinuity; Initial Lunar Thrust-to-Weight Ratio = 5	87
74	Escape Through a 15 Kilometer Circular Orbit. Thrust and Velocity Vectors Aligned at Escape Via λ_3 Discontinuity; Initial Lunar Thrust-to-Weight Ratio = 6	88
75	Escape Through a 15 Kilometer Circular Orbit. Thrust and Velocity Vectors Aligned at Escape Via λ_3 Discontinuity; Initial Lunar Thrust-to-Weight Ratio = 7	89
76	Escape Through Orbit. Thrust and Velocity Vectors Aligned at Orbit: Alignment at Escape Via λ_3 Discontinuity $r_{esc} - r_0$ Maximized Via Choice of T/W_0	90
77	Escape Through Orbit. Thrust and Velocity Vectors Aligned at Orbit: Alignment at Escape Via λ_3 Discontinuity; Initial Lunar Thrust-to-Weight Ratio = 1	91
78	Escape Through Orbit. Thrust and Velocity Vectors Aligned at Orbit: Alignment at Escape Via λ_3 Discontinuity; Initial Lunar Thrust-to-Weight Ratio = 1.1	92
79	Escape Through Orbit. Thrust and Velocity Vectors Aligned at Orbit: Alignment at Escape Via λ_3 Discontinuity; Initial Lunar Thrust-to-Weight Ratio = 1.3	93
80	Escape Through Orbit. Thrust and Velocity Vectors Aligned at Orbit: Alignment at Escape Via λ_3 Discontinuity; Initial Lunar Thrust-to-Weight Ratio = 1.5	94
81	Escape Through Orbit. Thrust and Velocity Vectors Aligned at Orbit: Alignment at Escape Via λ_3 Discontinuity; Initial Lunar Thrust-to-Weight Ratio = 2	95
82	Escape Through Orbit. Thrust and Velocity Vectors Aligned at Orbit: Alignment at Escape Via λ_3 Discontinuity; Initial Lunar Thrust-to-Weight Ratio = 3	96
83	Escape Through Orbit. Thrust and Velocity Vectors Aligned at Orbit: Alignment at Escape Via λ_3 Discontinuity; Initial Lunar Thrust-to-Weight Ratio = 4	97

Table	Title	Page
84	Escape Through Orbit. Thrust and Velocity Vectors Aligned at Orbit: Alignment at Escape Via λ_3 Discontinuity; Initial Lunar Thrust-to-Weight Ratio = 5	98
85	Escape Through Orbit. Thrust and Velocity Vectors Aligned at Orbit: Alignment at Escape Via λ_3 Discontinuity; Initial Lunar Thrust-to-Weight Ratio = 6	99
86	Escape Through Orbit. Thrust and Velocity Vectors Aligned at Orbit: Alignment at Escape Via λ_3 Discontinuity; Initial Lunar Thrust-to-Weight Ratio = 7	100
87	Escape From Orbit; Initial Lunar Thrust-to-Weight Ratio = .2	101
88	Escape From Orbit; Initial Lunar Thrust-to-Weight Ratio = .4	102
89	Escape From Orbit; Initial Lunar Thrust-to-Weight Ratio = .6	103
90	Escape From Orbit; Initial Lunar Thrust-to-Weight Ratio = .8	104
91	Escape From Orbit; Initial Lunar Thrust-to-Weight Ratio = 1	105
92	Escape From Orbit; Initial Lunar Thrust-to-Weight Ratio = 2	106
93	Escape From Orbit; Initial Lunar Thrust-to-Weight Ratio = 3	107
94	Escape From Orbit; Initial Lunar Thrust-to-Weight Ratio = 4	108
95	Escape From Orbit; Initial Lunar Thrust-to-Weight Ratio = 5	109
96	Escape From Orbit; Initial Lunar Thrust-to-Weight Ratio = 6	110
97	Escape From Orbit; Initial Lunar Thrust-to-Weight Ratio = 7	111
98	Initial Lunar Thrust-to-Weight Ratio = 2.7	208
99	Initial Lunar Thrust-to-Weight Ratio = 2.7 and Specific Impulse = 410 sec	208
100	Final Altitude = 20 km.	212
101	Initial Lunar Thrust-to-Weight Ratio = 3.44	212
102	Initial Lunar Thrust-to-Weight Ratio = 3.44 and Specific Impulse = 375 sec	212
103	Initial Lunar Thrust-to-Weight Ratio = 4.038 with no Alignment at Escape	214
104	Initial Lunar Thrust-to-Weight Ratio = 4.038 with λ_4 Alignment at Escape	214
105	Initial Lunar Thrust-to-Weight Ratio = 4.038 with λ_3 Alignment at Escape	214
106	Mass Fraction at Escape for I_{sp} = 300, 350, 400, and 450 sec	215
107	Initial Circular Orbital Altitude = 185 km.	218
108	Initial Circular Orbital Altitude = 185 km and Initial Lunar Thrust-to-Weight Ratio = 0.75	218
109	Initial Circular Orbital Altitude = 185 km.	220
110	Initial Circular Orbital Altitude = 185 km. and Initial Lunar Thrust-to-Weight Ratio = 0.75	222

LIST OF SYMBOLS

LATIN SYMBOLS

C_1	Constant of Integration, λ_6
E	Energy of Vehicle Per Unit Mass
f	Indicates Functional Relationship
G	Universal Gravitation Constant
g	Magnitude of Gravitational Acceleration
I	Orbital Inclination
I_{sp}	Specific Impulse
K	Intermediate Quantities of Numerical Integration Process
M	Mass of the Moon
m	Vehicle Mass
$\dot{m}$	Vehicle Mass Flow Rate
r	Scalar Radius
$\mathbf{T}$	Thrust Vector
T	Scalar Thrust
t	Time
u	Characteristic Velocity
$\hat{u}_r$, $\hat{u}_\theta$, $\hat{u}_\phi$	Vehicle Fixed Unit Vectors
$\hat{u}_{\mathbf{T}}$	Unit Vector Parallel to $\mathbf{T}$
$\hat{u}_{\mathbf{v}}$	Unit Vector Parallel to $\mathbf{v}$
$\mathbf{v}$	Vector Velocity
v	Scalar Velocity

GREEK SYMBOLS

α	Lunar Referenced Thrust-to-Weight Ratio
γ	Thrust Orientation Angle
Δ	Finite Increment in Numerical Integration
δ	Thrust Orientation Angle
ϵ	Convergence Tolerance
θ	Latitude Position Angle of the Vehicle
λ_i	Time Dependent Lagrange Multipliers ($i = 1,\ldots,7$)
ϕ	Longitudinal Position Angle of the Vehicle
Ω	Angular Velocity of the Moon

SUBSCRIPTS

c	Circular Condition
esc	Escape Condition
f	Final Condition
i	Dummy Subscript
m	Dummy Subscript
n	Dummy Subscript
p	Indicates Planar Variables
0	Initial Condition (Lunar Surface)
$\oplus$	Astronomical Subscript for the Earth
☾	Astronomical Subscript for the Moon

Arabic number subscripts indicate various integration constants or members of a set. Time derivatives are indicated by the dot notation.

GEORGE C. MARSHALL SPACE FLIGHT CENTER

MTP-P&VE-F-63-3

LUNAR ESCAPE

By
Rowland E. Burns

and

Larry G. Singleton

SUMMARY

The problem of escape from the Moon is treated in this report using the techniques of the calculus of variations. The Moon is assumed to be spherical and rotating. Only single stage vehicles of constant thrust are considered. The three-dimensional equations used in a previous study (Ref. 1) are modified to allow a smooth transition to planar segments of the trajectory.

Numerical data considers three escape modes: *direct* escape, escape *through* orbit, and escape *from* orbit. For the first two modes, a further subdivision is made according to whether the altitude or angle of attack is specified at cutoff. For certain trajectories which escape through orbit, a discontinuity is inserted at circular orbit in order to specify the angle of attack at cutoff.

For the last two modes, post-orbital trajectory segments are planar. In all cases, parabolic energy (with respect to the Moon) is taken as the thrust termination criterion.

SECTION I. INTRODUCTION

A previous report (Ref. 1) treated the problem of three-dimensional ascent from the surface of the Moon to low lunar orbit. Another problem of interest is lunar escape. Escape may occur either from the Moon's surface or from a lunar orbit, and both possibilities will be discussed here. Throughout this discussion, only single-stage vehicles of constant thrust will be considered.

Initially restricting the problem to escape from the lunar surface still leaves several options to be studied. The first of these would be to follow a flight program that ascends to a low circular lunar orbit and escape from this orbit as is usually done on earth-escape missions. A second possibility is direct escape, i.e., circular conditions are *not* attained between lift-off and escape. A third option is to first ascend to a low lunar orbit, perform a Hohmann maneuver to a higher circular orbit, and then escape from this orbit. This option is closely connected with lunar orbit rendezvous studies and will not be considered here.

Secondary options arise when consideration is given to various combinations of end point constraints that may be specified, such as alignment of the thrust and velocity vectors at escape,* or requirement of an altitude that is to be attained when escape occurs, etc.

---

* This condition minimizes deviations due to errors in the cutoff time.

Furthermore, the time (or position along the trajectory) at which the required value of the inclination is attained may be varied. The most probable application of a lunar escape trajectory is to return to the Earth or, possibly, a planetary mission. For a given earth-moon (or earth-moon-planet) configuration, the proper orbital inclination (with respect to the plane of interest) must be attained at or before escape conditions are reached. For example we might choose to ascend to a low lunar orbit having an inclination less than the value desired at escape and gain the remainder during the portion of the trajectory between orbit and escape. A more realistic assumption would be that the circular orbit has an inclination equal to the value which is finally sought, and escape from orbit along a planar trajectory.

Escape from lunar orbit also offers a number of choices, some of which are excluded if we reference our discussion to lunar orbit rendezvous considerations. Since the primary application of the work within this context will be escape of the Apollo spacecraft from orbit, there will be no need to consider plane changes since these can be achieved more economically by the lunar excursion module during the landing and ascent maneuvers. Even so, considerations of thrust alignment and altitude specification at escape are possible.

The theory of Reference 1 is sufficient to cover all of the above possibilities except the insertion of planar segments into a three-dimensional trajectory. We now proceed to investigate the results of such a modification.

SECTION II. SUMMARY OF PREVIOUS THEORY

We begin by summarizing the pertinent context of Reference 1.

The equations are referenced to a spherical coordinate system r, θ, ϕ, and the thrust vector orientation is given by the angles γ and δ (see FIG 1 and 2). The steering program, which maximizes gross weight at cutoff, is governed by a set of five time-dependent Lagrange multipliers ($\lambda_1, \ldots, \lambda_5$) and one constant Lagrange multiplier ($\lambda_6 \equiv C_1$).

The thrust-to-mass ratios (T/m) do not appear explicitly in the equations of motion; these have been replaced by an expression containing the gravitation acceleration at the surface of the Earth $[(g_0)_\oplus]$ and Moon $[(g_0)_☾]$, the specific impulse (I_{sp}), the *initial* lunar thrust-to-weight ratio (α), and the time (t). The quantity GM is the gravitational parameter of the Moon.

Vector equations are written in terms of the unit vectors $\hat{u}_r$, $\hat{u}_\theta$, and $\hat{u}_\phi$ (which are perpendicular to the surfaces described by constant values of r, θ, and ϕ, respectively).

The velocity vector is given by

$$\mathbf{v} = \dot{r}\,\hat{u}_r + r\dot{\theta}\,\hat{u}_\theta + r\dot{\phi}\cos\theta\,\hat{u}_\phi \tag{1}$$

The thrust vector is

$$\mathbf{T} = T\cos\delta\cos\gamma\,\hat{u}_r + T\sin\delta\,\hat{u}_\theta + T\cos\delta\sin\gamma\,\hat{u}_\phi \tag{2}$$

The energy of the vehicle during free flight (in particular, an arbitrarily short time after cutoff) is given by

$$E = \frac{1}{2}\left[\dot{r}^2 + r^2(\dot{\theta}^2 + \dot{\phi}^2\cos^2\theta)\right] - \frac{GM}{r} \tag{3}$$

A relationship between the latitude (θ), longitude (ϕ), and inclination (I) which is valid during free flight, is

$$\tan\theta = \tan I\,\sin(\phi + \phi_0) \tag{4}$$

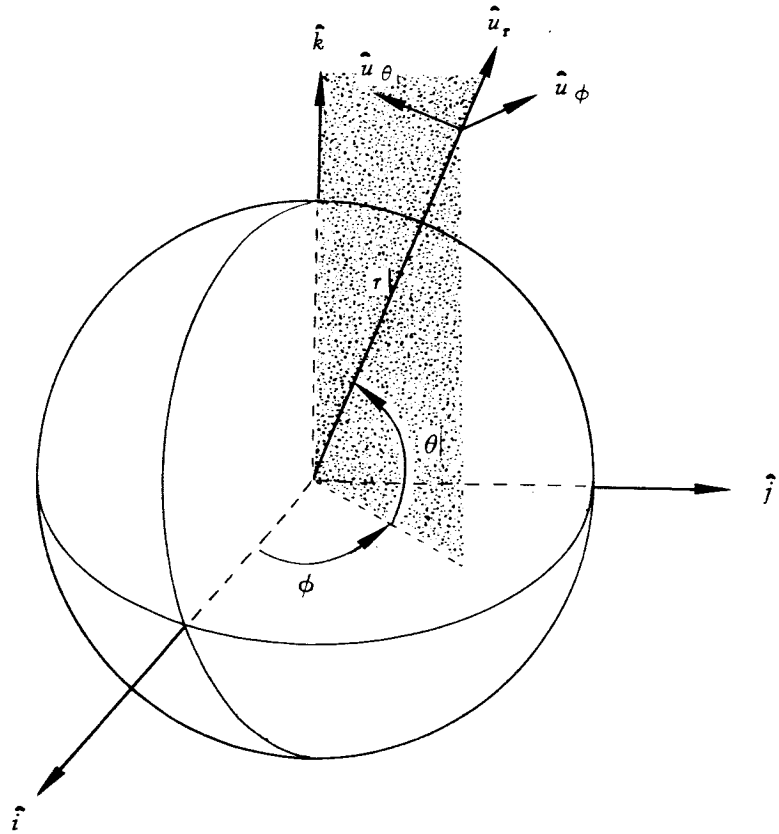

FIGURE 1. COORDINATE SYSTEM

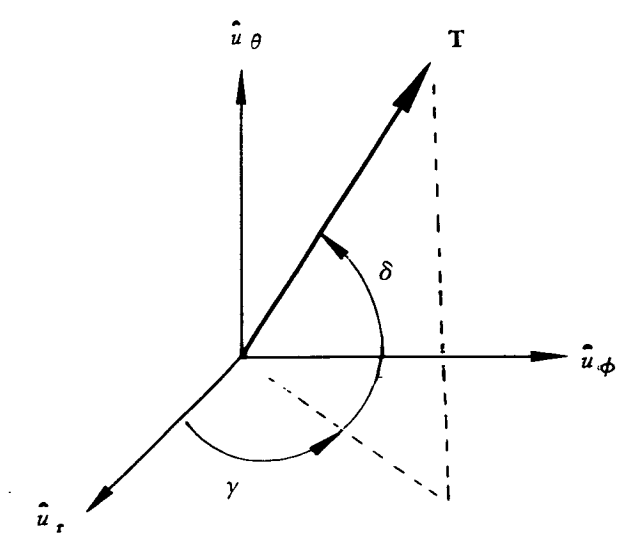

FIGURE 2. GIMBAL ANGLE COORDINATES

The equations governing the thrust orientation angles (γ and δ) during powered flight, such that the gross weight placed in orbit shall be a maximum, are*

$$\tan \gamma = \frac{\lambda_3}{\lambda_1 r \cos \theta} \tag{5}$$

$$\tan \delta = \frac{\lambda_2 \cos \theta}{\sqrt{\lambda_1^2 r^2 \cos^2 \theta + \lambda_3^2}} = \frac{\lambda_2}{\lambda_3} \cos \theta \sin \gamma \tag{6}$$

The equations of motion along the trajectory, which maximizes gross weight in orbit, are

$$\ddot{r} = \left[\frac{a (g_0)_\oplus (g_0)_\oplus I_{sp}}{(g_0)_\oplus I_{sp} - a (g_0)_\oplus t}\right] \frac{\lambda_1 r \cos \theta}{\sqrt{(\lambda_1^2 r^2 + \lambda_2^2) \cos^2 \theta + \lambda_3^2}} - \frac{GM}{r^2} + r (\dot{\theta}^2 + \dot{\phi}^2 \cos^2 \theta) \tag{7}$$

$$\ddot{\theta} = \left[\frac{a (g_0)_\oplus (g_0)_\oplus I_{sp}}{(g_0)_\oplus I_{sp} - a (g_0)_\oplus t}\right] \frac{\lambda_2 \cos \theta}{r \sqrt{(\lambda_1^2 r^2 + \lambda_2^2) \cos^2 \theta + \lambda_3^2}} - \frac{2 \dot{r} \dot{\theta}}{r} - \dot{\phi}^2 \sin \theta \cos \theta \tag{8}$$

$$\ddot{\phi} = \left[\frac{a (g_0)_\oplus (g_0)_\oplus I_{sp}}{(g_0)_\oplus I_{sp} - a (g_0)_\oplus t}\right] \frac{\lambda_3}{r \cos \theta \sqrt{(\lambda_1^2 r^2 + \lambda_2^2) \cos^2 \theta + \lambda_3^2}} + 2 \dot{\theta} \dot{\phi} \tan \theta - \frac{2 \dot{r} \dot{\phi}}{r} \tag{9}$$

$$\dot{\lambda}_1 - \frac{2}{r} (\lambda_2 \dot{\theta} + \lambda_3 \dot{\phi}) + \lambda_4 = 0 \tag{10}$$

$$\dot{\lambda}_2 + 2 (\lambda_1 r \dot{\theta} - \lambda_2 \frac{\dot{r}}{r} + \lambda_3 \dot{\phi} \tan \theta) + \lambda_5 = 0 \tag{11}$$

$$\dot{\lambda}_3 + 2 \left[(\lambda_1 r \cos \theta - \lambda_2 \sin \theta) \dot{\phi} \cos \theta + \lambda_3 (\dot{\theta} \tan \theta - \frac{\dot{r}}{r})\right] + C_1 = 0 \tag{12}$$

$$\dot{\lambda}_4 + \lambda_1 \left[2 \frac{GM}{r^3} + (\dot{\theta}^2 + \dot{\phi}^2 \cos^2 \theta)\right] + \frac{2 \dot{r}}{r^2} (\lambda_2 \dot{\theta} + \lambda_3 \dot{\phi})$$
$$- \left[\frac{a (g_0)_\oplus (g_0)_\oplus I_{sp}}{(g_0)_\oplus I_{sp} - a (g_0)_\oplus t}\right] \left[\frac{\lambda_2^2 \cos^2 \theta + \lambda_3^2}{r^2 \cos \theta \sqrt{(\lambda_1^2 r^2 + \lambda_2^2) \cos^2 \theta + \lambda_3^2}}\right] = 0 \tag{13}$$

$$\dot{\lambda}_5 - \dot{\phi}^2 (\lambda_1 r \sin 2\theta + \lambda_2 \cos 2\theta) + 2 \lambda_3 \dot{\phi} \dot{\theta} \sec^2 \theta$$
$$+ \left[\frac{a (g_0)_\oplus (g_0)_\oplus I_{sp}}{(g_0)_\oplus I_{sp} - a (g_0)_\oplus t}\right] \left[\frac{\lambda_3^2 \tan \theta \sec \theta}{r \sqrt{(\lambda_1^2 r^2 + \lambda_2^2) \cos^2 \theta + \lambda_3^2}}\right] = 0 \tag{14}$$

---

* The sign ambiguity discussed in Reference 1 is resolved by always considering that the vehicle is fired with the planetary rotation to the North.

Equations (7) through (14) constitute a set of three second-order and five first-order differential equations. Subject to initial and final conditions, they constitute a complete specification of the trajectory which maximizes gross weight in orbit (within the limits of variational calculus).

SECTION III. DERIVATION OF PLANAR EQUATIONS

Several methods are available for construction of the planar equations from the above set of three-dimensional equations.

The simplest procedure is to equate the non-planar components of equations (7) through (14) to zero, i.e., set θ, $\dot{\theta}$, $\ddot{\theta}$, λ_2, $\dot{\lambda}_2$, λ_5, and $\dot{\lambda}_5$ identically zero. This method has the disadvantage that physical significance is lost, and, what is worse, it is very difficult to insert a two-dimensional segment between three-dimensional segments (or vice-versa).

Another method of approach is a reformulation of the entire set of variational equations after incorporation of equation (4) in the form of a constraint as

$$\lambda_7 \left[\tan \theta - \tan I \sin (\phi + \phi_0) \right]$$

in the Eulerian fundamental function. This procedure is perfectly acceptable, but is much more cumbersome and complicated than necessary.

The simplest solution, which retains physical significance and allows a smooth transition between segments, is to incorporate equation (4) directly into the equations of interest.

We begin by solving (4) for

$$\sin \theta = \frac{\tan I \sin (\phi + \phi_0)}{\sqrt{1 + \tan^2 I \sin^2 (\phi + \phi_0)}} \tag{15}$$

and

$$\cos \theta = \frac{1}{\sqrt{1 + \tan^2 I \sin^2 (\phi + \phi_0)}} \tag{16}$$

Differentiating (4) with respect to time (requiring that the inclination remain constant) yields

$$\sec^2 \theta \, \dot{\theta} = \tan I \cos (\phi + \phi_0) \, \dot{\phi} \tag{17}$$

or

$$\dot{\theta} = \frac{\tan I \cos (\phi + \phi_0) \, \dot{\phi}}{1 + \tan^2 I \sin^2 (\phi + \phi_0)} \tag{18}$$

Differentiating (17)

$$\sec^2 \theta \, \ddot{\theta} + 2 \sec^2 \theta \tan \theta \, \dot{\theta}^2 = \tan I \cos (\phi + \phi_0) \, \ddot{\phi} - \tan I \sin (\phi + \phi_0) \, \dot{\phi}^2 \tag{19}$$

The second term of equation (19) may be written

$$2 \sec^2 \theta \tan \theta \dot{\theta}^2 = 2\dot{\theta} (\sec^2 \theta \, \dot{\theta}) \tan \theta \tag{20}$$

Substituting $\dot{\theta}$, $\sec^2\theta\dot{\theta}$, and $\tan\theta$ from (18), (17), and (4), respectively, we find

$$2\sec^2\theta\tan\theta\dot{\theta}^2 = 2\,\frac{\sin(\phi+\phi_0)\cos^2(\phi+\phi_0)\tan^3 I\,\dot{\phi}^2}{1+\tan^2 I\sin^2(\phi+\phi_0)} \tag{21}$$

Inserting (21) into (19) and solving for $\ddot{\theta}$ gives

$$\ddot{\theta} = \frac{\cos(\phi+\phi_0)\tan I\,\ddot{\phi}}{1+\tan^2 I\sin^2(\phi+\phi_0)} - \dot{\phi}^2\sin(\phi+\phi_0)\tan I\left\{\frac{1+\tan^2 I\,[1+\cos^2(\phi+\phi_0)]}{[1+\sin^2(\phi+\phi_0)\tan^2 I]^2}\right\} \tag{22}$$

Turning to equations (8) and (9), we eliminate $\dot{\theta}$ and the various trigonometric functions of θ via equations (18), (4), (15), and (16). (The θ terms involved in steering functions will not be eliminated until a more convenient grouping is obtained.) This gives

$$\ddot{\theta} = \left[\frac{a(g_0)_\oplus\,(g_0)_\oplus I_{sp}}{(g_0)_\oplus I_{sp} - a(g_0)_\oplus\,t}\right]\frac{\lambda_2\cos\theta}{r\sqrt{(\lambda_1^2 r^2+\lambda_2^2)\cos^2\theta+\lambda_3^2}}$$

$$-\frac{2\dot{r}\dot{\phi}}{r}\left[\frac{\cos(\phi+\phi_0)\tan I}{1+\sin^2(\phi+\phi_0)\tan^2 I}\right] - \frac{\dot{\phi}^2\sin(\phi+\phi_0)\tan I}{1+\sin^2(\phi+\phi_0)\tan^2 I} \tag{23}$$

$$\ddot{\phi} = \left[\frac{a(g_0)_\oplus\,(g_0)_\oplus I_{sp}}{(g_0)_\oplus I_{sp} - a(g_0)_\oplus\,t}\right]\frac{\lambda_3}{r\cos\theta\sqrt{(\lambda_1^2 r^2+\lambda_2^2)\cos^2\theta+\lambda_3^2}}$$

$$+\frac{2\dot{\phi}^2\sin(\phi+\phi_0)\cos(\phi+\phi_0)\tan^2 I}{1+\sin^2(\phi+\phi_0)\tan^2 I} - \frac{2\dot{r}\dot{\phi}}{r} \tag{24}$$

Inserting (23) and (24) into (22), expanding and collecting terms gives

$$\frac{1}{r}\left[\frac{a(g_0)_\oplus\,(g_0)_\oplus I_{sp}}{(g_0)_\oplus I_{sp} - a(g_0)_\oplus\,t}\right]\left\{\frac{\lambda_2\cos\theta}{\sqrt{(\lambda_1^2 r^2+\lambda_2^2)\cos^2\theta+\lambda_3^2}}\right.$$

$$\left.-\frac{\lambda_3\cos(\phi+\phi_0)\tan I}{\sqrt{(\lambda_1^2 r^2+\lambda_2^2)\cos^2\theta+\lambda_3^2}\,\cos\theta\,[1+\sin^2(\phi+\phi_0)\tan^2 I]}\right\} = 0 \tag{25}$$

The first bracket does not vanish for powered flight; thus the second term (within the braces) must be zero. This gives

$$\lambda_2\cos^2\theta\,[1+\sin^2(\phi+\phi_0)\tan^2 I] = \lambda_3\cos(\phi+\phi_0)\tan I \tag{26}$$

Substituting $\cos\theta$ from equation (16) yields

$$\lambda_2 = \lambda_3\cos(\phi+\phi_0)\tan I \tag{27}$$

Equation (27) expresses a relationship between the Lagrange multiplier governing plane changes (λ_2) and the multiplier involved in planar flight (λ_3). *This equation is valid if, and only if, equation* (4) *is valid.*

Our remaining task is to convert the other equations of interest to planar form. This may be accomplished by use of equations (4), (15), (16), (18), and (27).

Elimination of the terms involving θ and λ_2 from equation (7) gives

$$\ddot{r} = \left[\frac{a(g_0)_\oplus (g_0)_\oplus I_{sp}}{(g_0)_\oplus I_{sp} - a(g_0)_\oplus t}\right] \frac{\lambda_1 r}{\sqrt{\lambda_1^2 r^2 + \lambda_3^2 \sec^2 I}} - \frac{GM}{r^2} + \frac{r\dot{\phi}^2 \sec^2 I}{[1 + \sin^2(\phi + \phi_0)\tan^2 I]^2} \tag{28}$$

Equation (8) is replaced by equation (4) and equation (9) has been partially reduced to the form of equation (24). Inserting λ_2 from equation (27) into equation (24) gives

$$\ddot{\phi} = \left[\frac{a(g_0)_\oplus (g_0)_\oplus I_{sp}}{(g_0)_\oplus I_{sp} - a(g_0)_\oplus t}\right] \frac{\lambda_3 [1 + \sin^2(\phi + \phi_0)\tan^2 I]}{r\sqrt{\lambda_1^2 r^2 + \lambda_3^2 \sec^2 I}}$$

$$+ 2\dot{\phi}^2 \left[\frac{\sin(\phi - \phi_0)\cos(\phi + \phi_0)\tan^2 I}{1 + \sin^2(\phi + \phi_0)\tan^2 I}\right] - \frac{2\dot{r}\dot{\phi}}{r} \tag{29}$$

The equation for $\dot{\lambda}_1$, equation (10), becomes

$$\dot{\lambda}_1 - 2\lambda_3 \frac{\dot{\phi}}{r}\left[\frac{\sec^2 I}{1 + \sin^2(\phi + \phi_0)\tan^2 I}\right] + \lambda_4 = 0 \tag{30}$$

By passing equation (11) for the moment, we find the two-dimensional form of equation (12) is

$$\dot{\lambda}_3 + 2\left[\frac{\lambda_1 r\dot{\phi}}{1 + \tan^2 I \sin^2(\phi + \phi_0)} - \lambda_3 \frac{\dot{r}}{r}\right] + C_1 = 0 \tag{31}$$

In order to obtain an expression for $\dot{\lambda}_2$, we first take the time derivative of equation (27) which gives

$$\dot{\lambda}_2 = \dot{\lambda}_3 \cos(\phi + \phi_0)\tan I - \lambda_3 \dot{\phi}\sin(\phi + \phi_0)\tan I \tag{32}$$

and, after elimination of $\dot{\lambda}_3$ via (31), we find

$$\dot{\lambda}_2 = \lambda_3 \tan I \left[2\frac{\dot{r}}{r}\cos(\phi + \phi_0) - \dot{\phi}\sin(\phi + \phi_0)\right]$$

$$- 2\lambda_1 \dot{r}\dot{\phi}\left[\frac{\cos(\phi + \phi_0)\tan I}{1 + \sin^2(\phi + \phi_0)\tan^2 I}\right] - C_1 \cos(\phi + \phi_0)\tan I \tag{33}$$

Equation (33), along with the previously mentioned reduction formulas, now gives the planar form of equation (11) as

$$\lambda_5 = \tan I\,[C_1 \cos(\phi + \phi_0) - \lambda_3 \dot{\phi}\sin(\phi + \phi_0)] \tag{34}$$

Equation (34) is an analytical expression for the second "non-planar" Lagrange multiplier.

The planar form of equation (13) is

$$\dot{\lambda}_4 + \lambda_1 \left\{ 2 \frac{GM}{r^3} + \frac{\dot{\phi}^2 \sec^2 I}{[1 + \tan^2 I \sin^2 (\phi + \phi_0)]^2} \right\} + \frac{2 \dot{r} \dot{\phi}}{r^2} \left[\frac{\lambda_3 \sec^2 I}{1 + \tan^2 I \sin^2 (\phi + \phi_0)} \right]$$

$$- \left[\frac{a (g_0)_{\oplus} (g_0)_{\oplus} I_{sp}}{(g_0)_{\oplus} I_{sp} - a (g_0)_{\oplus} t} \right] \frac{\lambda_3^2 \sec^2 I}{r^2 \sqrt{\lambda_1^2 r^2 + \lambda_3^2 \sec^2 I}} = 0 \tag{35}$$

Similar reduction of equation (14) and the application of equation (34) yields an identity.

Equation (27) also provides an interesting relationship between the thrust orientation angles when applied to equation (6). From these we find

$$\tan \delta = \frac{[\lambda_3 \cos (\phi + \phi_0) \tan I]}{\lambda_3} \cos \theta \sin \gamma = \cos (\phi + \phi_0) \tan I \cos \theta \sin \gamma \tag{36}$$

Eliminating $\cos \theta$ from (36) gives

$$\tan \delta = \frac{\cos (\phi + \phi_0) \tan I}{\sqrt{1 + \tan^2 I \sin^2 (\phi + \phi_0)}} \sin \gamma \tag{37}$$

This is the relationship that must be maintained between the thrust orientation angles in order that a planar segment can be inserted into a three-dimensional trajectory.*

The previous development may be summarized by stating that equations (28), (29), (30), (31) and (34) are the equations of motion of a constant thrust rocket-powered vehicle along a two-dimensional trajectory. The trajectory has an inclination I with respect to a reference plane. Equations (4), (27), and (34) replace equations (8), (11), and (14), respectively. (Equations (4), (27), and (34) are carried during numerical computations so that an immediate transition to three-dimensional trajectories is possible.) The trajectory is now described by two first order and three second order equations. The loss of one degree of freedom has thus eliminated three variables.

SECTION IV. END CONDITIONS

The various end conditions of interest will now be investigated.

The first consideration will be of the initial conditions applicable to a direct ascent to escape or ascent from the lunar surface to a circular orbit. We have

$$t = t_0 = 0 \tag{38}$$

---

* Equation (37) is more generally applicable than our formulation has indicated. For, if the problem of constraining the equations of motion to a plane is formulated independently of the Lagrangian multipliers (that is, in terms of γ and δ) then the braces of equation (25) read

$$\left\{ \sin \delta - \frac{\cos \delta \sin \gamma \tan I \cos (\phi + \phi_0)}{\sqrt{1 + \tan^2 I \sin^2 (\phi + \phi_0)}} \right\}$$

which must be zero; equation (37) follows immediately showing that this equation is independent of considerations of optimality.

$$a = \frac{T}{W_0} = \frac{T}{m\,(g_0)_e} \tag{39}$$

$$r = r_0 = r_e \tag{40}$$

$$\dot{r} = \dot{r}_0 = 0 \tag{41}$$

$$\theta = \theta_0 \text{ (arbitrary, } \neq \pm \frac{\pi}{2}\text{)} \tag{42}$$

$$\dot{\theta} = \dot{\theta}_0 = 0 \tag{43}$$

$$\phi = \phi_0 = 0 \text{ (arbitrarily zero)} \tag{44}$$

$$\dot{\phi} = \dot{\phi}_0 = \Omega \text{ (angular velocity of the Moon)} \tag{45}$$

If the *first* end condition is a circular orbit zero radial velocity and circular energy must be specified; that is

$$\dot{r}_c = 0 \tag{46}$$

$$r_c^2\,(\dot{\theta}_c^2 + \dot{\phi}_c^2 \cos^2\theta_c) = \frac{GM}{r_c} \tag{47}$$

The orbital inclination is given by

$$\tan I = \frac{\sqrt{\sin^2(\theta_c - \theta_0) + 1/2\,[\sin 2\theta_0 \sin 2\theta_c\,(1 - \cos\phi_c)]}}{\cos\theta_0 \cos\theta_c \sin\phi_c} \tag{48}$$

If the trajectory does *not* pass through a circular condition but flies directly to escape, the radial velocity does not (necessarily) vanish at cutoff. Furthermore, minimum energy escape is defined by zero (parabolic) energy. From equation (3) comes

$$\frac{1}{2}\,[\dot{r}_p^2 + r_p^2\,(\dot{\theta}_p^2 + \dot{\phi}_p^2 \cos^2\theta_p)] - \frac{GM}{r_p} = 0 \tag{49}$$

Equation (48) is still valid for direct escape.

The remaining point of interest for direct escape or escape which is initiated via ascent to circular orbit is the inclusion of thrust-velocity alignment at cutoff in either of these conditions. This is equivalent to requiring that our optimal steering program terminate in a gravity turn.

To proceed with the formulation, unit vectors in the thrust and velocity direction are written from equations (1) and (2) as

$$\hat{u}_{\mathbf{v}} \equiv + \frac{\mathbf{v}}{v} = \frac{\dot{r}}{\sqrt{\dot{r}^2 + r^2(\dot{\theta}^2 + \dot{\phi}^2\cos^2\theta)}}\,\hat{u}_r + \frac{r\dot{\theta}}{\sqrt{\dot{r}^2 + r^2(\dot{\theta}^2 + \dot{\phi}^2\cos^2\theta)}}\,\hat{u}_\theta$$

$$+ \frac{r\dot{\phi}\cos\theta}{\sqrt{\dot{r}^2 + r^2(\dot{\theta}^2 + \dot{\phi}^2\cos^2\theta)}}\,\hat{u}_\phi \tag{50}$$

and

$$\hat{u}_{\mathbf{T}} \equiv \frac{\mathbf{T}}{T} = \cos\delta\cos\gamma\,\hat{u}_r + \sin\delta\,\hat{u}_\theta + \cos\delta\sin\gamma\,\hat{u}_\phi\,. \tag{51}$$

Equating components of these unit vectors, we can solve for

$$\tan\gamma = \frac{r\dot{\phi}\cos\theta}{\dot{r}} \tag{52}$$

and

$$\tan\delta = \frac{r\dot{\theta}}{\sqrt{\dot{r}^2 + r^2\dot{\phi}^2\cos^2\theta}} \tag{53}$$

It may be seen, from equation (52), that as the radial velocity vanishes along a gravity turn the angle γ approaches $\pm\,\pi/2$.

The end conditions applicable to escape from lunar orbit along a planar trajectory will now be considered. If the vehicle is in a circular orbit the radial velocity is zero. The planar form of equation (47), derived as usual, is

$$\frac{r_c^2\,\dot{\phi}_c^2\sec^2 I_c}{[1+\tan^2 I_c\sin^2(\phi_c+\phi_0)]^2} = \frac{GM}{r_c} \tag{54}$$

This equation may be conveniently inverted to give $\dot{\phi}_c$ for escape from orbit if r_c is specified. Thus

$$\dot{\phi}_c = \sqrt{\frac{MG}{r_c^3}}\;\cos I_c\,[1+\tan^2 I_c\,\sin^2(\phi_c+\phi_0)] \tag{55}$$

Escape occurs, as before, when the total energy is zero. The two-dimensional form of equation (49) is

$$\frac{1}{2}\left\{\dot{r}_p^2 + \frac{r_p^2\,\dot{\phi}_p^2\sec^2 I_c}{[1+\tan^2 I_c\sin^2(\phi_p+\phi_0)]^2}\right\} - \frac{MG}{r_p} = 0 \tag{56}$$

where the subscript denoting a circular condition has been retained on the inclination symbol since we are following a planar trajectory and no change occurs in the inclination.

The planar forms of equations (52) and (53) are

$$\tan\gamma = \frac{r\dot{\phi}}{\dot{r}\sqrt{1+\tan^2 I\sin^2(\phi+\phi_0)}} \tag{57}$$

and

$$\tan\delta = \frac{r\dot{\phi}\tan I\cos(\phi+\phi_0)}{\sqrt{1+\tan^2 I\sin^2(\phi+\phi_0)}\,\sqrt{\dot{r}^2[1+\tan^2 I\sin^2(\phi+\phi_0)] + r^2\dot{\phi}^2}} \tag{58}$$

If either of the above equations is fulfilled along a two-dimensional trajectory, the other is automatically satisfied. The insertion of the last two equations into equation (37) yields an identity.

Although the derivation will not be given here, it is possible to rewrite equations (52) and (53) or equations (57) and (58) in terms of Lagrange multipliers, rather than the thrust orientation angles by use of the equations of Sections II and III. These relationships are not as useful for numerical applications as those presented above since it is difficult to specify convergence tolerances on the final (unknown) values of the Lagrange multipliers.

SECTION V. NUMERICAL INTEGRATION PROCEDURE

The numerical integration procedure used in the preparation of the data presented in the following section was closely connected with the discussion in Section VII of Ref. 1. Only the differences between the procedure given in this reference and the techniques employed here will be discussed.

DIRECT ESCAPE

Consider, first, the problem of direct escape from the lunar surface (i.e., a circular orbit is not attained before escape conditions are reached). For this case a three-dimensional ascent trajectory is employed and equations (7) through (14) govern the time history of such a trajectory. At the lift-off site, equations (38) through (45) determine the initial conditions of the state variables and the specific impulse is assumed to be given.

The remaining initial conditions which must be specified are the Lagrangian multipliers λ_1°, λ_2°, λ_3°, λ_4°, λ_5°, and C_1. Since the set of equations governing these multipliers is homogeneous in the lambdas, one of the initial values is arbitrary; the chosen multiplier was $C_1(\lambda_6)$ and the value $C_1 = -10^5$ was found to be a convenient "scale factor" choice. (This value is used for all results given in this report.)

If we restrict our discussion to vertical lift-off, equations (5) and (6) show that λ_2° and λ_3° must be chosen equal to zero if λ_1° is to be finite.

We are left with three initial values, i.e., λ_1°, λ_4° and λ_5°. It was found convenient to iterate final inclination with λ_5° and final thrust and velocity vector alignment (with respect to γ) with λ_4°. This leaves a degree of freedom open, and it may be utilized in any of several ways. We may, for example, choose to determine an altitude at which escape occurs via λ_1°. This altitude may be defined as the altitude at which maximum payload may be injected into an escape trajectory. Alternatively, it may be an altitude which is matched against the altitude attained by the same vehicle (at escape) if the trajectory had passed through a given parking orbit. We could also utilize λ_1° to align thrust and velocity with respect to δ as λ_4° was used for this alignment with respect to γ.

The final parameter determining the escape, energy, can be determined directly from the burning time. The optimal steering program assures that the time necessary to attain escape energy is a minimum.

ESCAPE THROUGH ORBIT

Escape through orbit is a more practical operation than direct escape since the latter mode allows very little margin for error. On the other hand, the parking orbit trimming, plane matching, launch window alignment, etc.

The study of the trajectories which attain a parking orbit present a basically different situation than the problem mentioned above. In that case we had a surplus of degrees of freedom which enabled most end conditions of interest to be reached. In the present case we have no available freedom other than burning time from orbit to escape. The problem of initial values necessary to attain a circular orbit from ground launch, treated in Reference 1, need not concern us here; it is only necessary to note that all mathematical quantities have given values once an orbit has been attained. If we require any conditions (besides energy) to be prespecified when escape occurs we must allow a discontinuity in the state variables or the Lagrange multipliers. The first mentioned choice is physically unrealistic whereas the second choice amounts to a

reorientation of the thrust direction and/or its rate of direction change. This is physically justified by considering that we have nulled the thrust vector, reoriented the vehicle (or modified the vehicle rates) and reignited. This process may be considered to occur in an arbitrarily short time. We have, none the less, perturbed our overall optimum considerations.

To proceed with the discussion, the planar escape portion of the trajectory is mated to the three-dimensional ascent portion of the trajectory which was discussed in the above-mentioned reference. In practice, the vehicle was studied from ground launch to escape for convenience. Equations (7) through (14) were used until orbit was achieved and then equations (28), (29), (30), (31), and (35) were used. Equations (4), (18), (27), and (34) were used to keep track of $\theta, \dot{\theta}$, λ_2, and λ_5, respectively.

We can consider that all multipliers are known from cutoff conditions of the boost to orbit or reset various values. In resetting the values, it should be noted that thrust will be oriented along the velocity vector at orbital launch providing that λ_1 is given a value of zero at this point. Either λ_3 or λ_4 may be used to align thrust and velocity at the final point. The other of this pair may be used to specify an altitude at which escape occurs.

All state variables are known from cutoff conditions of the ascent maneuver (even if it is a "virtual" cutoff), but one point should be noted. The conversion between equations governing three-dimensional trajectories and circular trajectories usually is slightly in error since non-zero convergence tolerances on end conditions are necessary in practice. We may thus have a computed orbital inclination from the ascent that differs very slightly from a defined inclination that is put into the planar equations. Some state variables thus experience a discontinuity, but such errors are orders of magnitude lower than those resulting from the approximations used in construction of our mathematical model.

ESCAPE FROM ORBIT

The escape maneuver initiated from an orbit which has not been obtained via powered ascent directly to that orbit differs only very slightly from the above considerations of escape through orbit. The primary distinction between these situations is that certain state variables are interrelated by Kepler's laws. We may define the altitude of interest and assure a circular orbit by insisting that $\dot{r} = 0$ and $\dot{\phi}$ be given by equation (55). The angle ϕ may be chosen arbitrarily since we are not conducting a launch window study.

The various unspecified multipliers (λ_1, λ_3, λ_4) may be determined by the same considerations as given above for escape through orbit.

In practice, the initial value of λ_1 at orbit was always set equal to zero in order that the thrust and velocity vectors were initially aligned. The value of λ_3 at orbit was constant (10^8) and λ_4 was chosen to have such a value that thrust and velocity vectors were aligned at cutoff.

In order to check the validity of these restrictions, trajectories were calculated which isolated initial values of λ_1 and λ_3 in such a way that the mass fraction at escape was maximized. (This procedure amounts to determining an optimal initial angle of attack and an optimal final altitude.) The performance increase was so small that it affected only the last significant figure of the mass fraction. Such differences are totally useless from an engineering viewpoint.

SECTION VI. NUMERICAL RESULTS

The numerical data of this section present some of the more common results used in the study of ascent trajectories. The two basic parameters are specific impulse (300, 350, 400, and 450 sec.) and initial *lunar* thrust-to-weight ratio (1 through 7). The initial values of the Lagrangian multipliers for each case are given and allow extension of the results to other problems of interest, if computation facilities are available. (The present study was conducted using an IBM 7094 computer.)

Before proceeding to a discussion of specific results, a few general comments are in order. The lift-off site is always on the lunar equator and the longitude, ϕ, is always initially zero (since the moon is rotationally symmetric, by assumption, this is no restriction). The vehicle lifts off vertically ($\lambda_2^\circ = \lambda_3^\circ = 0$) and the trajectory is towards the North in the same sense as the lunar rotation. All three-dimensional trajectories have a final inclination (with respect to the lunar equator) of five degrees; all planar trajectories have a constant inclination of five degrees. The time increment used for numerical integration was four seconds. All altitudes are given in meters, angles in degrees, time and specific impulse in seconds, and all thrust-to-weight ratios are lunar referenced.

Those trajectories that pass through a circular orbit during ascent always involve some discontinuity in the variables. This is because the ascent trajectory never achieves an *exact* circular orbit.* The values were reset to zero tolerence figures before initiating the planar escape maneuver. In all cases the value of λ_1 at orbit is taken to be zero. In the trajectories which pass through orbit an alignment of the thrust and velocity vectors at escape is achieved by a discontinuity of either λ_3 or λ_4 at orbit. (The magnitude of this discontinuity is roughly 10 percent of the value achieved at orbit.)

For either of the two basic modes (direct or through orbit) two sets of data are presented. The first set fixes the altitude at which escape or orbit occurs at 15 kilometers and the second set requires that thrust and velocity be achieved at orbit and/or escape.

DIRECT ESCAPE

Tables 1 through 20 deal with trajectories which achieve parabolic escape energy without passing through a circular orbit. The first 10 of these tables provide data for vehicles which achieve an altitude of 15 kilometers, an inclination of 5 degrees, and an alignment of thrust and velocity vectors (with respect to γ) at escape. It may be noted that the mass fraction continually increases with increasing initial thrust-to-weight ratio, at least through a value of $T/W_0 = 7$. Another point of importance, in connection *only* with this set of 10 tables, is that *the radial velocity components are negative (for all values of specific impulse) if the initial thrust-to-weight ratio is less than 4* (with the actual crossover point being between 3 and 4).

The second set of tables, Tables 11 through 20, deals with direct escape and is similar to the first set, but does not achieve a uniform altitude of 15 kilometers. The altitudes of each case of these tables is matched against the altitude achieved by a vehicle with the same specific impulse and initial thrust-to-weight ratio that passed through circular orbit (specifically the cases listed in Tables 33 through 42). This altitude matching allows a direct comparison of the mass fraction achieved at escape between the two modes. It may be noted that the direct mode is better at low initial thrust-to-weight ratios, while just the reverse is true at intermediate

---

* The convergence tolerences (deviation from prespecified final values) were as follows:

$$\Delta\gamma = \pm .001^\circ, \quad \Delta I = \pm .001^\circ, \quad \Delta \dot{r} = \pm .001 \text{ meters/second}, \quad \Delta r = \pm 10 \text{ meters}.$$

values of this parameter. At the upper end of the thrust-to-weight values presented here, the comparison seems to depend upon specific impulse - but the differences are so small as to preclude any definite statement.

ESCAPE THROUGH ORBIT

Tables 21 through 86 deal with escape trajectories which attain a circular orbit as an intermediate condition. These tables are subdivided into three major catagories. It is assumed in Tables 21 through 42 that the vehicle does not achieve an alignment of thrust and velocity at escape; in Tables 43 through 64 such an alignment is achieved via a discontinuity in the multiplier λ_4 at orbit; such an alignment is also attained in Tables 65 through 86, but in these cases the discontinuity occurs in the multiplier λ_3 at orbit.

Each of these three sets are subdivided according to the altitude that is achieved *at orbit*. The first groups always pass through a 15-kilometer orbit and the escape maneuver is initiated from this point. (The thrust and velocity are not aligned at injection into this orbit since prespecification of inclination, radial velocity - zero, and altitude use up all degrees of freedom.) For these cases it may be seen that there apparently exist certain initial thrust-to-weight ratios that produce a maximum mass fraction at escape. The actual optimum was isolated by numerical iteration for each value of specific impulse, and is presented as the first table of each of these groups (Tables 21, 43, and 65).

The second halves of each of the three sets have varying altitudes. As noted in Reference 1, prespecification of inclination, radial velocity (zero), and thrust-velocity alignment yields a fixed (though *a priori* unknown) altitude. These trajectories, then, achieve the altitude predetermined by other requirements and escape from this altitude. It may be noted that the mass fraction continues to increase with increasing initial thrust-to-weight ratio; but the altitudes exhibit a peculiar maxima. These maxima were established by iteration and the results for each specific impulse are given in Tables 32, 54, and 76.*

ESCAPE FROM ORBIT

Tables 87 through 97 deal with escape trajectories which originate in an orbit rather than at the lunar surface. These trajectories are parameterized according to the altitude of the circular orbit in addition to thrust-to-weight ratios and specific impulse values. It may be noted that there exist optimum thrust-to-weight ratios (≈ 0.6) which maximize the mass fraction at escape, but the decrease from optimum is very small for thrusts higher than optimum. Because of this weak dependence the actual optima were not isolated. In all cases λ_4 was initially chosen in such a way that the thrust and velocity were aligned at escape. A few trial runs were made which determined an optimal value of λ_3 at orbit so that a maximum mass fraction resulted. (This procedure can be regarded as determining an optimal final altitude at escape.) The results showed such a small increase in mass fraction that it was not felt worthwhile to pursue the matter. A similar optimization with respect to λ_1 would be possible here (as well as in the escape through orbit cases) and such a procedure would essentially fix the initial thrust orientation angle at orbit.

---

* The trajectories are extremely difficult and slow to isolate due to their instability, long burning times, and the necessity of multiple trajectories for isolation.

Table 1. Direct Escape at 15 Kilometers

Initial Lunar Thrust-to-Weight Ratio = 1

I_{sp}	λ_1°	λ_4°	λ_5°	m_f/m_0	γ_{esc}	t_{esc}
300	83.15797	.1399788	-8766.8	.34894	88.903	1181.18
350	97.02905	.1582547	-8760.5	.39772	88.652	1274.80
400	110.55014	.1760349	-8754.7	.43948	88.424	1355.89
450	123.71187	.1933272	-8749.5	.47556	88.210	1427.19

Table 2. Direct Escape at 15 Kilometers

Initial Lunar Thrust-to-Weight Ratio = 1.1

I_{sp}	λ_1°	λ_4°	λ_5°	m_f/m_0	γ_{esc}	t_{esc}
300	55.40028	.1034617	-8775.8	.36701	90.322	1044.00
350	63.00272	.1136794	-8771.7	.41798	90.192	1119.91
400	70.01945	.1230203	-8768.1	.46151	90.066	1184.17
450	76.50384	.1315959	-8765.0	.49903	89.947	1239.38

Table 3. Direct Escape at 15 Kilometers
Initial Lunar Thrust-to-Weight Ratio = 1.3

I_{sp}	λ_1°	λ_4°	λ_5°	m_f/m_0	γ_{esc}	t_{esc}
300	30.25460	.0696072	-8783.9	.38772	91.570	854.48
350	33.61508	.0746207	-8781.4	.44041	91.536	911.10
400	36.57148	.0789407	-8779.4	.48512	91.493	958.06
450	39.18912	.0827062	-8777.7	.52342	91.448	997.65

Table 4. Direct Escape at 15 Kilometers
Initial Lunar Thrust-to-Weight Ratio = 1.5

I_{sp}	λ_1°	λ_4°	λ_5°	m_f/m_0	γ_{esc}	t_{esc}
300	19.16560	.0534579	-8787.2	.39935	91.972	726.48
350	21.06624	.0567533	-8785.3	.45270	91.982	772.28
400	22.70581	.0595187	-8783.9	.49777	91.975	809.92
450	24.13105	.0618718	-8782.7	.53622	91.962	841.41

Table 5. Direct Escape at 15 Kilometers
Initial Lunar Thrust-to-Weight Ratio = 2

I_{sp}	λ_1°	λ_4°	λ_5°	m_f/m_0	γ_{esc}	I_{esc}
300	8.36417	.0346039	-8789.7	.41433	91.839	531.27
350	9.08879	.0365069	-8788.5	.46825	91.917	562.76
400	9.70115	.0380611	-8787.6	.51353	91.967	588.38
450	10.22228	.0393434	-8786.8	.55197	91.994	609.63

Table 6. Direct Escape at 15 Kilometers
Initial Lunar Thrust-to-Weight Ratio = 3

I_{sp}	λ_1°	λ_4°	λ_5°	m_f/m_0	γ_{esc}	t_{esc}
300	2.87864	.0199489	-8790.2	.42635	90.607	346.91
350	3.10110	.0211377	-8789.2	.48058	90.767	366.47
400	3.28794	.0220956	-8788.5	.52590	90.882	382.28
450	3.44492	.0228727	-8787.9	.56421	90.962	395.31

Table 7. Direct Escape at 15 Kilometers
Initial Lunar Thrust-to-Weight Ratio = 4

I_{sp}	λ_1°	λ_4°	λ_5°	m_f/m_0	γ_{esc}	I_{esc}
300	1.40394	.0130653	-8789.9	.43170	89.317	257.76
350	1.50670	.0140269	-8789.0	.48604	89.545	271.96
400	1.59227	.0147890	-8788.3	.53136	89.710	283.41
450	1.66391	.0154008	-8787.8	.56960	89.829	292.82

Table 8. Direct Escape at 15 Kilometers
Initial Lunar Thrust-to-Weight Ratio = 5

I_{sp}	λ_1°	λ_4°	λ_5°	m_f/m_0	γ_{esc}	I_{esc}
300	.81644	.0087675	-8789.7	.43476	88.118	205.10
350	.87413	.0096319	-8788.8	.48916	88.411	216.25
400	.92187	.0103046	-8788.1	.53448	88.619	225.22
450	.96168	.0108428	-8787.6	.57268	88.775	232.58

Table 9. Direct Escape at 15 Kilometers
Initial Lunar Thrust-to-Weight Ratio = 6

I_{sp}	λ_1°	λ_4°	λ_5°	m_f/m_0	γ_{esc}	I_{esc}
300	.52876	.0056761	-8789.5	.43674	86.996	170.31
350	.56487	.0064998	-8788.6	.49118	87.352	179.49
400	.59480	.0071323	-8788.0	.53650	87.605	186.87
450	.61979	.0076331	-8787.5	.57466	87.792	192.92

Table 10. Direct Escape at 15 Kilometers

Initial Lunar Thrust-to-Weight Ratio = 7

I_{sp}	λ_1°	λ_4°	λ_5°	m_f/m_0	γ_{esc}	I_{esc}
300	.36782	.0032473	-8789.4	.43813	85.934	145.62
350	.39252	.0040622	-8788.5	.49260	86.351	153.42
400	.41280	.0046800	-8787.8	.53791	86.647	159.68
450	.42972	.0051652	-8787.4	.57606	86.866	164.81

Table 11. Direct Escape: Altitudes Matched with Corresponding Cases of Table 33

Initial Lunar Thrust-to-Weight Ratio = 1

I_{sp}	λ_1°	λ_4°	λ_5°	$(r_f - r_0)_{esc}$	m_f/m_0	γ_{esc}	t_{esc}
300	86.97878	.1425812	-8766.0	59213	.34289	85.718	1192.15
350	102.01591	.1623182	-8759.2	66037	.39098	85.314	1289.06
400	116.72450	.1816175	-8753.1	71871	.43226	84.960	1373.36
450	131.13195	.2005430	-8747.5	76881	.46800	84.658	1447.76

Table 12. Direct Escape: Altitudes Matched with Corresponding Cases of Table 34

Initial Lunar Thrust-to-Weight Ratio = 1.1

I_{sp}	λ°_1	λ°_4	λ°_5	$(r - r_0)_{esc}$	m_f/m_0	γ_{esc}	t_{esc}
300	58.28887	.1038685	-8775.2	67914	.36022	86.310	1055.19
350	66.67229	.1149451	-8770.8	76132	.41049	85.985	1134.34
400	74.40167	.1250686	-8766.9	83259	.45356	85.675	1201.66
450	81.64229	.1345390	-8763.5	89511	.49076	85.434	1259.83

Table 13. Direct Escape: Altitudes Matched with Corresponding Cases of Table 35

Initial Lunar Thrust-to-Weight Ratio = 1.3

I_{sp}	λ_1°	λ_4°	λ_5°	$(r_f - r_0)_{esc}$	m_f/m_0	γ_{esc}	t_{esc}
300	31.73147	.0674822	-8783.7	66899	.38160	87.162	863.01
350	35.39710	.0726495	-8781.1	74606	.43380	86.900	921.87
400	38.64153	.0771508	-8778.9	81248	.47821	86.679	970.92
450	41.52786	.0811066	-8777.1	87021	.51634	86.491	1012.47

Table 14. Direct Escape: Altitudes Matched with Corresponding Cases of Table 36

Initial Lunar Thrust-to-Weight Ratio = 1.5

I_{sp}	λ_1°	λ_4°	λ_5°	$(r_f - r_0)_{esc}$	m_f/m_0	γ_{esc}	t_{esc}
300	19.95861	.0504551	-8787.2	59506	.39439	87.736	732.48
350	22.00744	.0536951	-8785.2	66026	.44738	87.524	779.79
400	23.78100	.0564376	-8783.7	71596	.49225	87.347	818.83
450	25.32845	.0587885	-8782.5	76399	.53061	87.197	851.59

Table 15. Direct Escape: Altitudes Matched with Corresponding Cases of Table 37

Initial Lunar Thrust-to-Weight Ratio = 2

I_{sp}	λ_1°	λ_4°	λ_5°	$(r_f - r_0)_{esc}$	m_f/m_0	γ_{esc}	t_{esc}
300	8.58475	.0316955	-8789.8	41704	.41156	88.583	533.79
350	9.34691	.0334072	-8788.5	45914	.46527	88.441	565.90
400	9.99134	.0348141	-8787.5	49466	.51045	88.322	592.10
450	10.54239	.0359900	-8786.8	52497	.54885	88.222	613.87

Table 16. Direct Escape: Altitudes Matched with Corresponding Cases of Table 38
Initial Lunar Thrust-to-Weight Ratio = 3

I_{sp}	λ°_1	λ°_4	λ°_5	$(r_f - r_0)_{esc}$	m_f/m_0	γ_{esc}	t_{esc}
300	2.90426	.0186871	-8790.2	22384	.42562	89.301	347.35
350	3.13490	.0196417	-8789.2	24478	.47972	89.218	367.08
400	3.32690	.0204172	-8788.5	26215	.52496	89.150	383.04
450	3.48905	.0210567	-8787.9	27692	.56323	89.091	396.21

Table 17. Direct Escape: Altitudes Matched with Corresponding Cases of Table 39

Initial Lunar Thrust-to-Weight Ratio = 4

I_{sp}	λ_1°	λ_4°	λ_5°	$(r_f - r_0)_{esc}$	m_f / m_0	γ_{esc}	t_{esc}
300	1.40149	.0133399	-8789.9	13799	.43182	89.596	257.70
350	1.50711	.0140233	-8789.0	15040	.48604	89.541	271.96
400	1.59451	.0145751	-8788.3	16071	.53127	89.493	283.46
450	1.66792	.0150295	-8787.8	16940	.56945	89.452	292.92

Table 18. Direct Escape: Altitudes Matched with Corresponding Cases of Table 40

Initial Lunar Thrust-to-Weight Ratio = 5

I_{sp}	λ_1°	λ_4°	λ_5°	$(r_f - r_0)_{esc}$	m_f/m_0	γ_{esc}	t_{esc}
300	.80843	.0103761	-8789.6	9352	.43530	89.746	204.90
350	.86741	.0109119	-8788.7	10173	.48959	89.705	216.07
400	.91602	.0113437	-8788.1	10855	.53482	89.669	225.05
450	.95673	.0116989	-8787.6	11428	.57294	89.639	232.43

Table 19. Direct Escape: Altitudes Matched with Corresponding Cases of Table 41

Initial Lunar Thrust-to-Weight Ratio = 6

I_{sp}	λ_1°	λ_4°	λ_5°	$(r_f - r_0)_{esc}$	m_f/m_0	γ_{esc}	t_{esc}
300	.51954	.0084856	-8789.4	6754	.43754	89.833	170.07
350	.55660	.0089271	-8788.5	7340	.49186	89.800	179.26
400	.58707	.0092826	-8787.9	7825	.53708	89.772	186.63
450	.61252	.0095746	-8787.4	8232	.57518	89.748	192.68

Table 20. Direct Escape: Altitudes Matched with Corresponding Cases of Table 42

Initial Lunar Thrust-to-Weight Ratio = 7

I_{sp}	λ_1°	λ_4°	λ_5°	$(r_f - r_0)_{esc}$	m_f/m_0	γ_{esc}	t_{esc}
300	.35909	.0071739	-8789.2	5109	.43908	89.887	145.38
350	.38425	.0075496	-8788.3	5547	.49344	89.861	153.17
400	.40487	.0078517	-8787.7	5907	.53865	89.838	159.43
450	.42211	.0080998	-8787.2	6212	.57672	89.818	164.56

Table 21. Escape Through a 15 Kilometer Circular Orbit
m_{esc}/m_0 Maximized Via Choice of T/W_0

I_{sp}	T/W_0	λ_1°	λ_4°	λ_5°	$\left(\frac{m_f}{m_0}\right)_{orb}$	(γ_{orb})	$(r_f - r_0)_{esc}$	$\left(\frac{m_f}{m_0}\right)_{esc}$	γ_{esc}	t_{esc}
300	3.96543	1.39913	.0126811	-8805.6	.54633	91.013	15804	.43050	88.083	260.56
350	4.07906	1.34109	.0122489	-8804.6	.59580	90.795	15960	.48573	87.770	266.85
400	4.16864	1.29880	.0119387	-8803.8	.63577	90.633	16095	.53172	87.519	271.73
450	4.23908	1.26712	.0117014	-8803.3	.66867	90.502	16212	.57046	87.312	275.75

Table 22. Escape Through a 15 Kilometer Circular Orbit. Thrust and Velocity Vectors Not Aligned at Escape
Initial Lunar Thrust-to-Weight Ratio = 1

I_{sp}	λ_1°	λ_4°	λ_5°	$(m_f/m_0)_{orb}$	$(\gamma)_{orb}$	$(r_f - r_0)_{esc}$	$(m_f/m_0)_{esc}$	γ_{esc}	t_{esc}
300	65.09321	.1066509	-8792.8	.44723	80.106	22823	.35279	85.290	1174.19
350	75.01276	.1195080	-8787.7	.49268	79.155	24951	.40210	84.460	1265.52
400	84.84919	.1323969	-8783.0	.53053	78.409	26923	.44419	83.797	1344.49
450	94.59077	.1452506	-8778.7	.56258	77.813	28727	.48046	83.265	1413.86

Table 23. Escape Through a 15 Kilometer Circular Orbit. Thrust and Velocity Vectors Not Aligned at Escape

Initial Lunar Thrust-to-Weight Ratio = 1.1

I_{sp}	λ_1°	λ_4°	λ_5°	$(m_f/m_0)_{orb}$	$(\gamma)_{orb}$	$(r_f - r_0)_{esc}$	$(m_f/m_0)_{esc}$	γ_{esc}	t_{esc}
300	35.99196	.0628207	-8800.2	.47404	77.918	23202	.37384	82.886	1032.73
350	39.79936	.0674281	-8797.4	.52170	76.724	25456	.42566	81.663	1105.14
400	43.31592	.0717841	-8795.0	.56126	75.752	27562	.46976	80.629	1166.04
450	46.56987	.0758766	-8792.9	.59461	74.943	29507	.50764	79.745	1218.08

Table 24. Escape Through a 15 Kilometer Circular Orbit. Thrust and Velocity Vectors Not Aligned at Escape
Initial Lunar Thrust-to-Weight Ratio = 1.3

I_{sp}	λ_1°	λ_4°	λ_5°	$(m_f/m_0)_{orb}$	$(\gamma)_{orb}$	$(r_f - r_0)_{esc}$	$(m_f/m_9)_{esc}$	γ_{esc}	t_{esc}
300	16.15442	.0316771	-8804.4	.50289	77.621	22288	.39644	81.613	842.31
350	17.20222	.0325911	-8802.8	.55180	76.459	24242	.45003	80.279	895.44
400	18.11438	.0334556	-8801.5	.59202	75.518	26057	.49530	79.150	939.12
450	18.91465	.0342560	-8800.4	.62566	74.741	27724	.53391	78.185	975.68

Table 25. Escape Through a 15 Kilometer Circular Orbit. Thrust and Velocity Vectors Not Aligned at Escape
Initial Lunar Thrust-to-Weight Ratio = 1.5

I_{sp}	λ_1°	λ_4°	λ_5°	$(m_f/m_0)_{orb}$	$(\gamma)_{orb}$	$(r_f - r_0)_{esc}$	$(m_f/m_0)_{esc}$	γ_{esc}	t_{esc}
300	9.42197	.0207388	-8805.4	.51793	78.772	21019	.40822	81.841	715.76
350	9.84948	.0208316	-8804.0	.56710	77.727	22600	.46243	80.598	758.56
400	10.21344	.0209669	-8803.0	.60731	76.889	24058	.50801	79.552	793.42
450	10.52648	.0211175	-8802.2	.64077	76.202	25389	.54672	78.663	822.35

Table 26. Escape Through a 15 Kilometer Circular Orbit. Thrust and Velocity Vectors Not Aligned at Escape
Initial Lunar Thrust-to-Weight Ratio = 2.0

I_{sp}	λ_1°	λ_4°	λ_5°	$(m_f/m_0)_{orb}$	$(\gamma)_{orb}$	$(r_f - r_0)_{esc}$	$(m_f/m_0)_{esc}$	γ_{esc}	t_{esc}
300	4.11135	.0124421	-8805.6	.53503	82.191	18670	.42162	83.480	524.66
350	4.19652	.0120772	-8804.5	.58424	81.362	19614	.47634	82.500	554.19
400	4.26921	.0118226	-8803.7	.62423	80.708	20478	.52210	81.685	578.02
450	4.33149	.0116363	-8803.0	.65731	80.178	21259	.56078	80.998	597.64

Table 27. Escape Through a 15 Kilometer Circular Orbit. Thrust and Velocity Vectors Not Aligned at Escape
Initial Lunar Thrust-to-Weight Ratio = 3.0

I_{sp}	λ_1°	λ_4°	λ_5°	$(m_f/m_0)_{orb}$	$(\gamma)_{orb}$	$(r_f - r_0)_{esc}$	$(m_f/m_0)_{esc}$	γ_{esc}	t_{esc}
300	1.91021	.0109303	-8805.5	.54476	87.397	16587	.42927	86.255	345.15
350	1.90315	.0103782	-8804.4	.59403	86.751	17007	.48430	85.590	363.85
400	1.90020	.0099785	-8803.7	.63388	86.250	17389	.53015	85.040	378.85
450	1.89934	.0096760	-8803.1	.66672	85.849	17734	.56880	84.579	391.15

Table 28. Escape Through a 15 Kilometer Circular Orbit. Thrust and Velocity Vectors Not Aligned at Escape
Initial Lunar Thrust-to-Weight Ratio = 4.0

I_{sp}	λ_1°	λ_4°	λ_5°	$(m_f/m_0)_{orb}$	$(\gamma)_{orb}$	$(r_f - r_0)_{esc}$	$(m_f/m_0)_{esc}$	γ_{esc}	t_{esc}
300	1.38907	.0127624	-8805.6	.54633	91.127	15785	.43049	88.139	258.31
350	1.36368	.0120715	-8804.6	.59579	90.534	16010	.48573	87.635	272.13
400	1.34631	.0115732	-8803.8	.63574	90.079	16217	.53170	87.219	283.20
450	1.33379	.0111970	-8803.2	.66862	89.719	16403	.57042	86.871	292.26

Table 29. Escape Through a 15 Kilometer Circular Orbit. Thrust and Velocity Vectors Not Aligned at Escape
Initial Lunar Thrust-to-Weight Ratio = 5.0

I_{sp}	λ_1°	λ_4°	λ_5°	$(m_f/m_0)_{orb}$	$(\gamma)_{orb}$	$(r_f - r_0)_{esc}$	$(m_f/m_0)_{esc}$	γ_{esc}	t_{esc}
300	1.20759	.0154050	-8805.9	.54536	94.160	15402	.42972	89.566	206.93
350	1.17344	.0145543	-8804.8	.59511	93.569	15535	.48516	89.158	217.94
400	1.14949	.0139442	-8804.0	.63526	93.121	15658	.53129	88.821	226.76
450	1.13181	.0134852	-8803.5	.66828	92.768	15770	.57012	88.539	233.97

Table 30. Escape Through a 15 Kilometer Circular Orbit. Thrust and Velocity Vectors Not Aligned at Escape
Initial Lunar Thrust-to-Weight Ratio = 6.0

I_{sp}	λ_1°	λ_4°	λ_5°	$(m_f/m_0)_{orb}$	$(\gamma)_{orb}$	$(r_f - r_0)_{esc}$	$(m_f/m_0)_{esc}$	γ_{esc}	t_{esc}
300	1.14167	.0184201	-8806.3	.54323	96.824	15190	.42802	90.751	172.95
350	1.10105	.0173855	-8805.1	.59332	96.210	15273	.48368	90.405	182.14
400	1.07241	.0166474	-8804.4	.63372	95.747	15350	.52999	90.119	189.49
450	1.05117	.0160941	-8803.7	.66694	95.386	15422	.56896	89.879	195.50

Table 31. Escape Through a 15 Kilometer Circular Orbit. Thrust and Velocity Vectors Not Aligned at Escape
Initial Lunar Thrust-to-Weight Ratio = 7.0

I_{sp}	λ_1°	λ_4°	λ_5°	$(m_f/m_0)_{orb}$	$(\gamma)_{orb}$	$(r_f - r_0)_{esc}$	$(m_f/m_0)_{esc}$	γ_{esc}	t_{esc}
300	1.12683	.0216784	-8806.7	.54043	99.266	15061	.42579	91.793	148.82
350	1.08040	.0204370	-8805.5	.59089	98.615	15113	.48168	91.490	156.72
400	1.04766	.0195552	-8804.7	.63159	98.127	15163	.52819	91.239	163.04
450	1.02335	.0188964	-8804.1	.66505	97.749	15210	.56733	91.029	168.21

Table 32. Escape Through Orbit. Thrust and Velocity Vectors Aligned at Orbit: No Alignment at Escape
$r_{esc} - r_0$ Maximized Via Choice of T/W_0

I_{sp}	T/W_0	λ_1°	λ_4°	λ_5°	$(r_f - r_0)_{orb}$	$\left(\frac{m_f}{m_0}\right)_{orb}$	$(r_f - r_0)_{esc}$	$\left(\frac{m_f}{m_0}\right)_{esc}$	γ_{esc}	t_{esc}
300	1.17298	48.22915	.0920875	-8800.3	64328	.46435	69167	.36737	88.698	978.48
350	1.16857	55.29260	.101501	-8796.6	71331	.51075	77421	.41804	88.444	1054.09
400	1.16481	61.92562	.110269	-8793.3	77343	.54944	84590	.46128	88.244	1118.77
450	1.16168	68.13357	.118431	-8790.4	82568	.58222	90871	.49854	88.085	1174.72

Table 33. Escape Through Orbit. Thrust and Velocity Vectors Aligned at Orbit: No Alignment at Escape

Initial Lunar Thrust-to-Weight Ratio = 1

I_{sp}	λ_1°	λ_4°	λ_5°	$(r_f - r_0)_{orb}$	$(m_f/m_0)_{orb}$	$(r_f - r_0)_{esc}$	γ_{esc}	$(m_f/m_0)_{esc}$	t_{esc}
300	97.33660	.1603670	-8786.2	54154	.42877	59219	90.593	.33903	1199.16
350	114.60499	.1829909	-8778.7	59664	.47291	66040	90.557	.38686	1297.79
400	131.65260	.2053368	-8771.8	64282	.50999	71869	90.549	.42794	1383.81
450	148.46797	.2274060	-8765.3	68191	.54162	76885	90.562	.46353	1459.92

Table 34. Escape Through Orbit. Thrust and Velocity Vectors Aligned at Orbit: No Alignment at Escape
Initial Lunar Thrust-to-Weight Ratio = 1.1

I_{sp}	λ_1°	λ_4°	λ_5°	$(r_f - r_0)_{orb}$	$(m_f/m_0)_{orb}$	$(r_f - r_0)_{esc}$	γ_{esc}	$(m_f/m_0)_{esc}$	t_{esc}
300	62.95928	.1128095	-8796.3	62931	.45185	67924	89.332	.35747	1059.73
350	72.00603	.1246639	-8791.7	69847	.49814	76125	89.119	.40771	1139.68
400	80.44945	.1356819	-8787.7	75796	.53692	83259	88.951	.45076	1207.81
450	88.34058	.1459543	-8784.2	80968	.56990	89512	88.817	.48798	1266.71

Table 35. Escape Through Orbit. Thrust and Velocity Vectors Aligned at Orbit: No Alignment at Escape

Initial Lunar Thrust-to-Weight Ratio = 1.3

I_{sp}	λ_1°	λ_4°	λ_5°	$(r_f - r_0)_{orb}$	$(m_f/m_0)_{orb}$	$(r_f - r_0)_{esc}$	γ_{esc}	$(m_f/m_0)_{esc}$	t_{esc}
300	32.51963	.0693737	-8804.2	62420	.48068	66902	87.958	.38020	864.97
350	36.13233	.0743249	-8801.8	68994	.52859	74610	87.584	.43254	923.91
400	39.32520	.0786480	-8799.8	74597	.56840	81255	87.274	.47709	973.00
450	42.16431	.0824576	-8798.1	79426	.60199	87030	87.015	.51535	1014.55

Table 36. Escape Through Orbit. Thrust and Velocity Vectors Aligned at Orbit: No Alignment at Escape
Initial Lunar Thrust-to-Weight Ratio = 1.5

I_{sp}	λ_1°	λ_4°	λ_5°	$(r_f - r_0)_{orb}$	$(m_f/m_0)_{orb}$	$(r_f - r_0)_{esc}$	γ_{esc}	$(m_f/m_0)_{esc}$	t_{esc}
300	19.70747	.0497318	-8806.7	55626	.49807	59505	87.336	.39373	733.28
350	21.58605	.0525388	-8805.0	61178	.54649	66025	86.907	.44693	780.42
400	23.20294	.0549127	-8803.7	65863	.58648	71595	86.549	.49199	819.24
450	24.60780	.0569473	-8802.6	69864	.62003	76397	86.248	.53050	851.78

Table 37. Escape Through Orbit. Thrust and Velocity Vectors Aligned at Orbit: No Alignment at Escape
Initial Lunar Thrust-to-Weight Ratio = 2

I_{sp}	λ_1°	λ_4°	λ_5°	$(r_f - r_0)_{orb}$	$(m_f/m_0)_{orb}$	$(r_f - r_0)_{esc}$	γ_{esc}	$(m_f/m_0)_{esc}$	t_{esc}
300	7.99520	.0290282	-8807.6	39045	.52145	41703	86.952	.41167	533.69
350	8.61537	.0302629	-8806.4	42606	.57010	45913	86.518	.46565	565.51
400	9.13358	.0312711	-8805.6	45567	.60993	49465	86.156	.51103	591.40
450	9.57261	.0321097	-8804.9	48064	.64309	52496	85.850	.54959	612.87

Table 38. Escape Through Orbit. Thrust and Velocity Vectors Aligned at Orbit: No Alignment at Escape.
Initial Lunar Thrust-to-Weight Ratio = 3

I_{sp}	λ_1°	λ_4°	λ_5°	$(r_f - r_0)_{orb}$	$(m_f/m_0)_{orb}$	$(r_f - r_0)_{esc}$	γ_{esc}	$(m_f/m_0)_{esc}$	t_{esc}
300	2.55822	.0157716	-8806.3	20985	.54028	22379	87.290	.42593	347.17
350	2.72493	.0163452	-8805.4	22742	.58879	24469	86.935	.48026	366.69
400	2.86142	.0168046	-8804.7	24186	.62822	26215	86.639	.52569	382.45
450	2.97511	.0171806	-8804.2	25392	.66085	27692	86.391	.56409	395.42

Table 39. Escape Through Orbit. Thrust and Velocity Vectors Aligned at Orbit: No Alignment at Escape

Initial Lunar Thrust-to-Weight Ratio = 4

I_{sp}	λ_1°	λ_4°	λ°_5	$(r_f - r_0)_{orb}$	$(m_f/m_0)_{orb}$	$(r_f - r_0)_{esc}$	γ_{esc}	$(m_f/m_0)_{esc}$	t_{esc}
300	1.20225	.0107577	-8805.2	12954	.54828	13796	87.715	.43197	257.64
350	1.27440	.0111352	-8804.4	13995	.59665	15037	87.427	.48640	271.77
400	1.33297	.0114358	-8803.8	14847	.63586	16069	87.187	.53180	283.14
450	1.38143	.0116807	-8803.3	15555	.66822	16938	86.986	.57009	292.48

Table 40. Escape Through Orbit. Thrust and Velocity Vectors Aligned at Orbit: No Alignment at Escape
Initial Lunar Thrust-to-Weight Ratio = 5

I_{sp}	λ_1°	λ_4°	λ_5°	$(r_f - r_0)_{orb}$	$(m_f/m_0)_{orb}$	$(r_f - r_0)_{esc}$	γ_{esc}	$(m_f/m_0)_{esc}$	t_{esc}
300	.68292	.0081228	-8804.6	8784	.55266	9345	88.050	.43528	204.91
350	.72190	.0084052	-8803.8	9474	.60094	10167	87.809	.48975	216.00
400	.75340	.0086295	-8803.2	10036	.64001	10848	87.610	.53512	224.91
450	.77935	.0088118	-8802.7	10502	.67222	11421	87.442	.57335	232.21

Table 41. Escape Through Orbit. Thrust and Velocity Vectors Aligned at Orbit: No Alignment at Escape
Initial Lunar Thrust-to-Weight Ratio = 6

l_{ap}	λ_1°	λ_4°	λ_5°	$(r_f - r_0)_{orb}$	$(m_f/m_0)_{orb}$	$(r_f - r_0)_{esc}$	γ_{esc}	$(m_f/m_0)_{esc}$	t_{esc}
300	.43458	.0065027	-8804.1	6352	.55539	6752	88.307	.43735	170.13
350	.45855	.0067285	-8803.3	6843	.60361	7336	88.100	.49184	179.26
400	.47786	.0069076	-8802.7	7243	.64283	7820	87.930	.53719	186.59
450	.49373	.0070530	-8802.3	7573	.67470	8226	87.787	.57538	192.59

Table 42. Escape Through Orbit. Thrust and Velocity Vectors Aligned at Orbit: No Alignment at Escape
Initial Lunar Thrust-to-Weight Ratio = 7

I_{sp}	λ_1°	λ_4°	λ_5°	$(r_f - r_0)_{orb}$	$(m_f/m_0)_{orb}$	$(r_f - r_0)_{esc}$	γ_{esc}	$(m_f/m_0)_{esc}$	t_{esc}
300	.29831	.0054087	-8803.8	4811	.55726	5109	88.506	.43877	145.46
350	.31435	.0055967	-8803.0	5178	.60543	5547	88.326	.49327	153.22
400	.32724	.0057458	-8802.4	5477	.64435	5908	88.177	.53860	159.44
450	.33782	.0058667	-8801.9	5724	.67638	6212	88.052	.57676	164.54

Table 43. Escape Through a 15 Kilometer Circular Orbit. Thrust and Velocity Vectors Aligned at Escape Via λ_4 Discontinuity m_{esc}/m_0 Maximized Via Choice of T/W_0

I_{sp}	T/W_0	λ_1°	λ_4°	λ_5°	$\left(\frac{m_f}{m_0}\right)_{orb}$	γ_{orb}	$(\lambda_4)_{adj}$	$(r_f - r_0)_{esc}$	$\left(\frac{m_f}{m_0}\right)_{esc}$	γ_{esc}	t_{esc}
300	3.95880	1.40110	.01266562	-8805.5	.54633	90.991	.0235160	15701	.43050	88.957	260.99
350	4.07047	1.34346	.01222944	-8804.5	.59579	90.767	.0239285	15820	.48574	88.871	267.41
400	4.15618	1.30205	.01191114	-8803.8	.63577	90.592	.0242574	15923	.53173	88.802	272.54
450	4.22604	1.27037	.01167303	-8803.2	.66867	90.461	.0245140	16010	.57047	88.746	276.60

Table 44. Escape Through a 15 Kilometer Circular Orbit. Thrust and Velocity Vectors Aligned at Escape Via λ_4 Discontinuity
Initial Lunar Thrust-to-Weight Ratio = 1

I_{sp}	λ_1°	λ_4°	λ_5°	$(m_f/m_0)_{orb}$	γ_{orb}	$(\lambda_4)_{adj}$	$(r_f - r_0)_{esc}$	$(m_f/m_0)_{esc}$	γ_{esc}	t_{esc}
300	65.09321	.1066509	-8792.8	.44723	80.106	.0948049	22317	.35280	86.636	1174.17
350	75.01276	.1195080	-8787.7	.49268	79.155	.0998273	24200	.40212	86.237	1265.48
400	84.84919	.1323969	-8783.0	.53053	78.409	.1038764	25954	.44421	85.896	1344.44
450	94.59077	.1452506	-8778.7	.56258	77.813	.1072438	27568	.48048	85.605	1413.80

Table 45. Escape Through a 15 Kilometer Circular Orbit. Thrust and Velocity Vectors Aligned at Escape Via λ_4 Discontinuity
Initial Lunar Thrust-to-Weight Ratio = 1.1

I_{sp}	λ_1°	λ_4°	λ_5°	$(m_f/m_0)_{orb}$	γ_{orb}	$(\lambda_4)_{adj}$	$(r_f - r_0)_{esc}$	$(m_f/m_0)_{esc}$	γ_{esc}	t_{esc}
300	35.99196	.0628207	-8800.2	.47404	77.918	.0847933	21782	.37391	86.768	1032.62
350	39.79936	.0674281	-8797.4	.52170	76.724	.0889406	23515	.42576	86.379	1104.95
400	43.31592	.0717841	-8795.0	.56126	75.752	.0922670	25120	.46988	86.053	1165.77
450	46.56987	.0758766	-8792.9	.59461	74.943	.0949934	26591	.50778	85.776	1217.73

Table 46. Escape Through a 15 Kilometer Circular Orbit. Thrust and Velocity Vectors Aligned at Escape Via λ_4 Discontinuity
Initial Lunar Thrust-to-Weight Ratio = 1.3

I_{sp}	λ_1°	λ_4°	λ_5°	$(m_f/m_0)_{orb}$	γ_{orb}	$(\lambda_4)_{adj}$	$(r_f - r_0)_{esc}$	$(m_f/m_0)_{esc}$	γ_{esc}	t_{esc}
300	16.15442	.0316771	-8804.4	.50289	77.621	.0709060	20467	.39657	87.097	842.12
350	17.20222	.0325911	-8802.8	.55180	76.459	.0742109	21826	.45022	86.756	895.14
400	18.11438	.0334556	-8801.5	.59202	75.518	.0768395	23073	.49553	86.472	938.70
450	18.91465	.0342560	-8800.4	.62566	74.741	.0789782	24207	.53417	86.232	975.15

Table 47. Escape Through a 15 Kilometer Circular Orbit. Thrust and Velocity Vectors Aligned at Escape Via λ_4 Discontinuity
Initial Lunar Thrust-to-Weight Ratio = 1.5

I_{sp}	λ_1°	λ_4°	λ_5°	$(m_f/m_0)_{orb}$	γ_{orb}	$(\lambda_4)_{adj}$	$(r_f - r_0)_{esc}$	$(m_f/m_0)_{esc}$	γ_{esc}	t_{esc}
300	9.42197	.0207388	-8805.4	.51793	78.772	.0613059	19361	.40836	87.407	715.58
350	9.84948	.0208316	-8804.0	.56710	77.727	.0641268	20425	.46261	87.107	758.29
400	10.21344	.0209669	-8803.0	.60731	76.889	.0663673	21395	.50823	86.858	793.05
450	10.52648	.0211175	-8802.2	.64077	76.202	.0681881	22273	.54698	86.649	821.89

Table 48. Escape Through a 15 Kilometer Circular Orbit. Thrust and Velocity Vectors Aligned at Escape Via λ_4 Discontinuity
Initial Lunar Thrust-to-Weight Ratio = 2

I_{sp}	λ_1°	λ_4°	λ_5°	$(m_f/m_0)_{orb}$	γ_{orb}	$(\lambda_4)_{adj}$	$(r_f - r_0)_{esc}$	$(m_f/m_0)_{esc}$	γ_{esc}	t_{esc}
300	4.11135	.0124421	-8805.6	.53503	82.191	.0460564	17625	.42172	87.987	524.57
350	4.19652	.0120772	-8804.5	.58424	81.362	.0481631	18251	.47647	87.758	554.06
400	4.26921	.0118226	-8803.7	.62423	80.708	.0498358	18817	.52225	87.570	577.84
450	4.33149	.0116363	-8803.0	.65731	80.178	.0511950	19326	.56095	87.413	597.41

Table 49. Escape Through a 15 Kilometer Circular Orbit. Thrust and Velocity Vectors Aligned at Escape Via λ_4 Discontinuity
Initial Lunar Thrust-to-Weight Ratio = 3

I_{sp}	λ_1°	λ_4°	λ_5°	$(m_f/m_0)_{orb}$	γ_{orb}	$(\lambda_4)_{adj}$	$(r_f - r_0)_{esc}$	$(m_f/m_0)_{esc}$	γ_{esc}	t_{esc}
300	1.91021	.0109303	-8805.5	.54476	87.397	.0308575	16213	.42930	88.626	345.13
350	1.90315	.0103782	-8804.4	.59403	86.751	.0322599	16500	.48434	88.470	363.82
400	1.90020	.0099785	-8803.7	.63388	86.250	.0333716	16758	.53020	88.342	378.81
450	1.89934	.0096760	-8803.1	.66672	85.849	.0342737	16989	.56886	88.234	391.10

Table 50. Escape Through a 15 Kilometer Circular Orbit. Thrust and Velocity Vectors Aligned at Escape Via λ_4 Discontinuity
Initial Lunar Thrust-to-Weight Ratio = 4

I_{sp}	λ_1°	λ_4°	λ_5°	$(m_f/m_0)_{orb}$	γ_{orb}	$(\lambda_4)_{adj}$	$(r_f - r_0)_{esc}$	$(m_f/m_0)_{esc}$	γ_{esc}	t_{esc}
300	1.38907	.0127624	-8805.6	.54633	91.127	.0232792	15687	.43050	88.968	258.30
350	1.36368	.0120715	-8804.6	.59579	90.534	.0243401	15849	.48573	88.851	272.13
400	1.34631	.0115732	-8803.8	.63574	90.079	.0251815	15996	.53171	88.755	283.20
450	1.33379	.0111970	-8803.2	.66862	89.719	.0258646	16127	.57043	88.675	292.25

Table 51. Escape Through a 15 Kilometer Circular Orbit. Thrust and Velocity Vectors Aligned at Escape Via λ_4 Discontinuity
Initial Lunar Thrust-to-Weight Ratio = 5

I_{sp}	λ_1°	λ_4°	λ_5°	$(m_f/m_0)_{orb}$	γ_{orb}	$(\lambda_4)_{adj}$	$(r_f - r_0)_{esc}$	$(m_f/m_0)_{esc}$	γ_{esc}	t_{esc}
300	1.20759	.0154050	-8805.9	.54536	94.160	.0187288	15439	.42972	89.176	206.93
350	1.17344	.0145543	-8804.8	.59511	93.569	.0195844	15543	.48516	89.083	217.94
400	1.14949	.0139442	-8804.0	.63526	93.121	.0202630	15637	.53129	89.006	226.76
450	1.13181	.0134852	-8803.5	.66828	92.768	.0208139	15721	.57012	88.942	233.97

Table 52. Escape Through a 15 Kilometer Circular Orbit. Thrust and Velocity Vectors Aligned at Escape Via λ_4 Discontinuity
Initial Lunar Thrust-to-Weight Ratio = 6

I_{sp}	λ_1°	λ_4°	λ_5°	$(m_f/m_0)_{orb}$	γ_{orb}	$(\lambda_4)_{adj}$	$(r_f - r_0)_{esc}$	$(m_f/m_0)_{esc}$	γ_{esc}	t_{esc}
300	1.14167	.0184201	-8806.3	.54323	96.824	.0156938	15303	.42803	89.315	172.95
350	1.10105	.0173855	-8805.1	.59332	96.210	.0164131	15375	.48369	89.237	182.14
400	1.07241	.0166474	-8804.4	.63372	95.747	.0169835	15440	.52999	89.173	189.49
450	1.05117	.0160941	-8803.7	.66694	95.386	.0174465	15499	.56897	89.119	195.50

Table 53. Escape Through a 15 Kilometer Circular Orbit. Thrust and Velocity Vectors Aligned at Escape Via λ_4 Discontinuity
Initial Lunar Thrust-to-Weight Ratio = 7

I_{sp}	λ_1°	λ_4°	λ_5°	$(m_f/m_0)_{orb}$	γ_{orb}	$(\lambda_4)_{adj}$	$(r_f - r_0)_{esc}$	$(m_f/m_0)_{esc}$	γ_{esc}	t_{esc}
300	1.12683	.0216784	-8806.7	.54043	99.266	.0135218	15220	.42581	89.412	148.82
350	1.08040	.0204370	-8805.5	.59089	98.615	.0141447	15274	.48170	89.346	156.72
400	1.04766	.0195552	-8804.7	.63159	98.127	.0146385	15322	.52820	89.291	163.04
450	1.02335	.0188964	-8804.1	.66505	97.749	.0150393	15365	.56734	89.245	168.20

Table 54. Escape Through Orbit. Thrust and Velocity Aligned at Orbit: Alignment at Escape Via λ_4 Discontinuity $r_{esc} - r_0$ Maximized Via Choice of T/W_0

I_{sp}	(T/W_0)	λ_1°	λ_4°	λ_5°	$(r_f - r_0)_{orb}$	$\left(\frac{m_f}{m_0}\right)_{orb}$	$(\lambda_4)_{adj}$	$(r_f - r_0)_{esc}$	$\left(\frac{m_f}{m_0}\right)_{esc}$	γ_{esc}	t_{esc}
300	1.16739	49.16537	.093416	-8800.1	64309	.46349	.0819072	69674	.36669	87.161	984.23
350	1.15928	57.19099	.104149	-8796.1	71285	.50920	.0869468	78023	.41679	86.824	1064.83
400	1.15561	64.13471	.113315	-8792.7	77293	.54783	.0985838	85284	.45994	86.547	1130.47
450	1.15175	70.87809	.122183	-8789.6	82499	.58042	.0942018	91646	.49701	86.312	1188.46

Table 55. Escape Through Orbit. Thrust and Velocity Aligned at Orbit: Alignment at Escape Via λ_4 Discontinuity

Initial Lunar Thrust-to-Weight Ratio = 1

I_{sp}	λ_1°	λ_4°	λ_5°	$(r_f - r_0)_{orb}$	$(m_f/m_0)_{orb}$	$(\lambda_4)_{adj}$	$(r_f - r_0)_{esc}$	γ_{esc}	$(m_f/m_0)_{esc}$	t_{esc}
300	97.33660	.1603670	-8786.2	54154	.42877	.0971743	60510	86.903	.33907	1199.09
350	114.60499	.1829909	-8778.7	59664	.47291	.1026799	67615	86.542	.38690	1297.69
400	131.65260	.2053368	-8771.8	64282	.50999	.1071933	73711	86.240	.42799	1383.69
450	148.46797	.2274060	-8765.3	68191	.54162	.1109596	78981	85.984	.46359	1459.77

Table 56. Escape Through Orbit. Thrust and Velocity Aligned at Orbit: Alignment at Escape Via λ_4 Discontinuity
Initial Lunar Thrust-to-Weight Ratio = 1.1

I_{sp}	λ_1°	λ_4°	λ_5°	$(r_f - r_0)_{orb}$	$(m_f/m_0)_{orb}$	$(\lambda_4)_{adj}$	$(r_f - r_0)_{esc}$	γ_{esc}	$(m_f/m_0)_{esc}$	$t_{esc.}$
300	62.95928	.1128095	-8796.3	62931	.45185	.0873622	68686	87.059	.35748	1059.71
350	72.00603	.1246639	-8791.7	69847	.49814	.0921228	77024	86.722	.40772	1139.65
400	80.44945	.1356819	-8787.7	75796	.53692	.0960009	84284	86.441	.45078	1207.78
450	88.34058	.1459543	-8784.2	80968	.56990	.0992210	90655	86.204	.48800	1266.67

Table 57. Escape Through Orbit. Thrust and Velocity Aligned at Orbit: Alignment at Escape Via λ_4 Discontinuity
Initial Lunar Thrust-to-Weight Ratio = 1.3

I_{sp}	λ_1°	λ_4°	λ_5°	$(r_f - r_0)_{orb}$	$(m_f/m_0)_{orb}$	$(\lambda_4)_{adj}$	$(r_f - r_0)_{esc}$	γ_{esc}	$(m_f/m_0)_{esc}$	t_{esc}
300	32.51963	.0693737	-8804.2	62420	.48068	.0730556	67087	87.349	.38020	864.97
350	36.13233	.0743249	-8801.8	68994	.52859	.0768649	74792	87.050	.43254	923.91
400	39.32520	.0786480	-8799.8	74597	.56840	.0799465	81430	86.802	.47709	973.00
450	42.16431	.0824576	-8798.1	79426	.60199	.0824902	87196	86.595	.51535	1014.55

Table 58. Escape Through Orbit. Thrust and Velocity Aligned at Orbit: Alignment at Escape Via λ_4 Discontinuity
Initial Lunar Thrust-to-Weight Ratio = 1.5

I_{sp}	λ_1°	λ_4°	λ_5°	$(r_f - r_0)_{orb}$	$(m_f/m_0)_{orb}$	$(\lambda_4)_{adj}$	$(r_f - r_0)_{esc}$	γ_{esc}	$(m_f/m_0)_{esc}$	t_{esc}
300	19.70747	.0497318	-8806.7	55626	.49807	.0629618	59431	87.603	.39373	733.28
350	21.58605	.0525388	-8805.0	61178	.54649	.0661635	65893	87.335	.44694	780.41
400	23.20294	.0549127	-8803.7	65863	.58648	.0687434	71406	87.113	.49199	819.24
450	24.60780	.0569473	-8802.6	69864	.62003	.0708658	76155	86.928	.53050	851.78

Table 59. Escape Through Orbit. Thrust and Velocity Aligned at Orbit: Alignment at Escape Via λ_4 Discontinuity
Initial Lunar Thrust-to-Weight Ratio = 2

I_{sp}	λ_1°	λ_4°	λ_5°	$(r_f - r_0)_{orb}$	$(m_f/m_0)_{orb}$	$(\lambda_4)_{adj}$	$(r_f - r_0)_{esc}$	γ_{esc}	$(m_f/m_0)_{esc}$	t_{esc}
300	7.99520	.0290282	-8807.6	39045	.52145	.0468977	41454	88.082	.41167	533.68
350	8.61537	.0302629	-8806.4	42606	.57010	.0492043	45581	87.869	.46566	565.50
400	9.13358	.0312711	-8805.6	45567	.60993	.0510539	49055	87.693	.51105	591.39
450	9.57261	.0321097	-8804.9	48064	.64309	.0525691	52013	87.546	.54960	612.85

Table 60. Escape Through Orbit. Thrust and Velocity Aligned at Orbit: Alignment at Escape Via λ_4 Discontinuity
Initial Lunar Thrust-to-Weight Ratio = 3

I_{sp}	λ_1°	λ_4°	λ_5°	$(r_f - r_0)_{orb}$	$(m_f/m_0)_{orb}$	$(\lambda_4)_{adj}$	$(r_f - r_0)_{esc}$	γ_{esc}	$(m_f/m_0)_{esc}$	t_{esc}
300	2.55822	.0157716	-8806.3	20985	.54028	.0310671	22168	88.648	.42594	347.16
350	2.72493	.0163452	-8805.4	22742	.58879	.0325521	24199	88.500	.48028	366.68
400	2.86142	.0168046	-8804.7	24186	.62822	.0337385	25889	88.377	.52571	382.44
450	2.97511	.0171806	-8804.2	25392	.66085	.0347074	27316	88.275	.56411	395.41

Table 61. Escape Through Orbit. Thrust and Velocity Aligned at Orbit: Alignment at Escape Via λ_4 Discontinuity
Initial Lunar Thrust-to-Weight Ratio = 4

I_{ep}	λ_1°	λ_4°	λ_5°	$(r_f - r_0)_{orb}$	$(m_f/m_0)_{orb}$	$(\lambda_4)_{adj}$	$(r_f - r_0)_{esc}$	γ_{esc}	$(m_f/m_0)_{esc}$	t_{esc}
300	1.20225	.0107577	-8805.2	12954	.54828	.0232117	13648	88.962	.43198	257.63
350	1.27440	.0111352	-8804.4	13995	.59665	.0243056	14848	88.849	.48641	271.77
400	1.33297	.0114358	-8803.8	14847	.63586	.0251780	15843	88.755	.53181	283.14
450	1.38143	.0116807	-8803.3	15555	.66822	.0258896	16679	88.678	.57011	292.47

Table 62. Escape Through Orbit. Thrust and Velocity Aligned at Orbit: Alignment at Escape Via λ_4 Discontinuity
Initial Lunar Thrust-to-Weight Ratio = 5

I_{sp}	λ_1°	λ_4°	λ_5°	$(r_f - r_0)_{orb}$	$(m_f/m_0)_{orb}$	$(\lambda_4)_{adj}$	$(r_f - r_0)_{esc}$	γ_{esc}	$(m_f/m_0)_{esc}$	t_{esc}
300	.68292	.0081228	-8804.6	8784	.55266	.0185197	9238	89.160	.43528	204.91
350	.72190	.0084052	-8803.8	9474	.60094	.0193848	10032	89.068	.48975	216.00
400	.75340	.0086295	-8803.2	10036	.64001	.0200741	10687	88.993	.53513	224.90
450	.77935	.0088118	-8802.7	10502	.67222	.0206358	11236	88.930	.57336	232.21

Table 63. Escape Through Orbit. Thrust and Velocity Aligned at Orbit: Alignment at Escape Via λ_4 Discontinuity
Initial Lunar Thrust-to-Weight Ratio = 6

I_{sp}	λ_1°	λ_4°	λ_5°	$(r_f - r_0)_{orb}$	$(m_f/m_0)_{orb}$	$(\lambda_4)_{adj}$	$(r_f - r_0)_{esc}$	γ_{esc}	$(m_f/m_0)_{esc}$	t_{esc}
300	.43458	.0065027	-8804.1	6352	.55539	.0154026	6672	89.295	.43735	170.13
350	.45855	.0067285	-8803.3	6843	.60361	.0161177	7235	89.218	.49185	179.26
400	.47786	.0069076	-8802.7	7243	.64283	.0166870	7700	89.155	.53720	186.59
450	.49373	.0070530	-8802.3	7573	.67470	.0171508	8089	89.102	.57539	192.59

Table 64. Escape Through Orbit. Thrust and Velocity Aligned at Orbit: Alignment at Escape Via λ_4 Discontinuity
Initial Lunar Thrust-to-Weight Ratio = 7

I_{sp}	λ_1°	λ_4°	λ_5°	$(r_f - r_0)_{orb}$	$(m_f/m_0)_{orb}$	$(\lambda_4)_{adj}$	$(r_f - r_0)_{esc}$	γ_{esc}	$(m_f/m_0)_{esc}$	t_{esc}
300	.29831	.0054087	-8803.8	4811	.55726	.0131820	5048	89.392	.43877	145.46
350	.31435	.0055967	-8803.0	5178	.60543	.0137913	5469	89.327	.49327	153.22
400	.32724	.0057458	-8802.4	5477	.64435	.0142762	5816	89.272	.53861	159.44
450	.33782	.0058667	-8801.9	5724	.67638	.0146710	6107	89.227	.57677	164.54

Table 65. Escape Through a 15 Kilometer Circular Orbit. Thrust and Velocity Vectors Aligned at Escape Via λ_3 Discontinuity m_{esc}/m_0 Maximized Via Choice of T/W_0

I_{sp}	T/W_0	λ_1°	λ_4°	λ_5°	$\left(\frac{m_f}{m_0}\right)_{orb}$	γ_{orb}	$(\lambda_3)_{adj}$	$(r_f - r_0)_{esc}$	$\left(\frac{m_f}{m_0}\right)_{esc}$	γ_{esc}	t_{esc}
300	3.95889	1.40109	.0126659	-8805.6	.54633	90.991	16529896	15692	.43050	88.977	260.98
350	4.07028	1.34351	.0122290	-8804.6	.59580	90.766	15911499	15808	.48574	88.889	267.42
400	4.15608	1.30207	.0119109	-8803.8	.63577	90.592	15478395	15907	.53173	88.809	272.55
450	4.22554	1.27050	.0116719	-8803.3	.66868	90.459	15044504	15988	.57047	88.774	276.63

Table 66. Escape Through a 15 Kilometer Circular Orbit. Thrust and Velocity Vectors Aligned at Escape Via λ_3 Discontinuity
Initial Lunar Thrust-to-Weight Ratio = 1

I_{sp}	λ_1°	λ_4°	λ_5°	$(m_f/m_0)_{orb}$	γ_{orb}	$(\lambda_3)_{adj}$	$(r_f - r_0)_{esc}$	$(m_f/m_0)_{esc}$	γ_{esc}	t_{esc}
300	65.09321	.1066509	-8792.8	.44723	80.106	78392237	22291	.35280	86.645	1174.17
350	75.01276	.1195080	-8787.7	.49268	79.155	80427294	24159	.40212	86.247	1265.48
400	84.84919	.1323969	-8783.0	.53053	78.409	82360332	25898	.44421	85.905	1344.44
450	94.59077	.1452506	-8778.7	.56258	77.813	84157260	27499	.48048	85.614	1413.79

Table 67. Escape Through a 15 Kilometer Circular Orbit. Thrust and Velocity Vectors Aligned at Escape Via λ_3 Discontinuity
Initial Lunar Thrust-to-Weight Ratio = 1.1

I_{sp}	λ_1°	λ_4°	λ_5°	$(m_f/m_0)_{orb}$	γ_{orb}	$(\lambda_3)_{adj}$	$(r_f - r_0)_{esc}$	$(m_f/m_0)_{esc}$	γ_{esc}	t_{esc}
300	35.99196	.0628207	-8800.2	.47404	77.918	55124840	21689	.37391	86.788	1032.62
350	39.79936	.0674281	-8797.4	.52170	76.724	55158485	23364	.42576	86.428	1104.95
400	43.31592	.0717841	-8795.0	.56126	75.752	55255215	24915	.46988	86.114	1165.77
450	46.56987	.0758766	-8792.9	.59461	74.943	55344178	26332	.50778	85.848	1217.73

Table 68. Escape Through a 15 Kilometer Circular Orbit. Thrust and Velocity Vectors Aligned at Escape Via λ_3 Discontinuity
Initial Lunar Thrust-to-Weight Ratio = 1.3

I_{sp}	λ_1°	λ_4°	λ_5°	$(m_f/m_0)_{orb}$	γ_{orb}	$(\lambda_3)_{adj}$	$(r_f - r_0)_{esc}$	$(m_f/m_0)_{esc}$	γ_{esc}	t_{esc}
300	16.15442	.0316771	-8804.4	.50289	77.621	35031137	20295	.39657	87.160	842.12
350	17.20222	.0325911	-8802.8	.55180	76.459	34314216	21575	.45022	86.828	895.14
400	18.11438	.0334556	-8801.5	.59202	75.518	33645234	22728	.49553	86.575	938.70
450	18.91465	.0342560	-8800.4	.62566	74.741	33137631	23779	.53417	86.340	975.14

Table 69. Escape Through a 15 Kilometer Circular Orbit. Thrust and Velocity Vectors Aligned at Escape Via λ_3 Discontinuity
Initial Lunar Thrust-to-Weight Ratio = 1.5

I_{sp}	λ_1°	λ_4°	λ_5°	$(m_f/m_0)_{orb}$	γ_{orb}	$(\lambda_3)_{adj}$	$(r_f - r_0)_{esc}$	$(m_f/m_0)_{esc}$	γ_{esc}	t_{esc}
300	9.42197	.0207388	-8805.4	.51793	78.772	26619899	19185	.40836	87.467	715.58
350	9.84948	.0208316	-8804.0	.56710	77.727	25726087	20157	.46262	87.206	758.29
400	10.21344	.0209669	-8803.0	.60731	76.889	25081451	21046	.50823	86.956	793.05
450	10.52648	.0211175	-8802.2	.64077	76.202	24431143	21821	.54698	86.790	821.89

Table 70. Escape Through a 15 Kilometer Circular Orbit. Thrust and Velocity Vectors Aligned at Escape Via λ_3 Discontinuity
Initial Lunar Thrust-to-Weight Ratio = 2

I_{sp}	λ_1°	λ_4°	λ_5°	$(m_f/m_0)_{orb}$	γ_{orb}	$(\lambda_3)_{adj}$	$(r_f - r_0)_{esc}$	$(m_f/m_0)_{esc}$	γ_{esc}	t_{esc}
300	4.11135	.0124421	-8805.6	.53503	82.191	18718418	17499	.42172	88.054	524.57
350	4.19652	.0120772	-8804.5	.58424	81.362	17936237	18066	.47647	87.845	554.06
400	4.26921	.0118226	-8803.7	.62423	80.708	17309248	18570	.52225	87.675	577.84
450	4.33149	.0116363	-8803.0	.65731	80.178	16835640	19023	.56095	87.516	597.41

Table 71. Escape Through a 15 Kilometer Circular Orbit. Thrust and Velocity Vectors Aligned at Escape Via λ_3 Discontinuity
Initial Lunar Thrust-to-Weight Ratio = 3

I_{sp}	λ_1°	λ_4°	λ_5°	$(m_f/m_0)_{orb}$	γ_{orb}	$(\lambda_3)_{adj}$	$(r_f - r_0)_{esc}$	$(m_f/m_0)_{esc}$	γ_{esc}	t_{esc}
300	1.91021	.0109303	-8805.5	.54476	87.397	15804692	16175	.42930	88.662	345.13
350	1.90315	.0103782	-8804.4	.59403	86.751	15068421	16441	.48434	88.517	363.82
400	1.90020	.0099785	-8803.7	.63388	86.250	14501600	16677	.53020	88.400	378.81
450	1.89934	.0096760	-8803.1	.66672	85.849	14069437	16887	.56886	88.296	391.10

Table 72. Escape Through a 15 Kilometer Circular Orbit. Thrust and Velocity Vectors Aligned at Escape Via λ_3 Discontinuity
Initial Lunar Thrust-to-Weight Ratio = 4

I_{sp}	λ_1°	λ_4°	λ_5°	$(m_f/m_0)_{orb}$	γ_{orb}	$(\lambda_3)_{adj}$	$(r_f - r_0)_{esc}$	$(m_f/m_0)_{esc}$	γ_{esc}	t_{esc}
300	1.38907	.0127624	-8805.6	.54633	91.127	16606926	15679	.43050	88.983	258.30
350	1.36368	.0120715	-8804.6	.59579	90.534	15786343	15834	.48573	88.876	272.13
400	1.34631	.0115732	-8803.8	.63574	90.079	15262824	15977	.53171	88.762	283.20
450	1.33379	.0111970	-8803.2	.66862	89.719	14719845	16097	.57043	88.708	292.25

Table 73. Escape Through a 15 Kilometer Circular Orbit. Thrust and Velocity Vectors Aligned at Escape Via λ_3 Discontinuity
Initial Lunar Thrust-to-Weight Ratio = 5

I_{sp}	λ_1°	λ_4°	λ_5°	$(m_f/m_0)_{orb}$	γ_{orb}	$(\lambda_3)_{adj}$	$(r_f - r_0)_{esc}$	$(m_f/m_0)_{esc}$	γ_{esc}	t_{esc}
300	1.20759	.0154050	-8805.9	.54536	94.160	18605897	15440	.42972	89.176	206.93
350	1.17344	.0145543	-8804.8	.59511	93.569	17650474	15543	.48516	89.089	217.94
400	1.14949	.0139442	-8804.0	.63526	93.121	17029513	15636	.53129	88.999	226.76
450	1.13181	.0134852	-8803.5	.66828	92.768	16469441	15717	.57012	88.944	233.97

Table 74. Escape Through a 15 Kilometer Circular Orbit. Thrust and Velocity Vectors Aligned at Escape Via λ_3 Discontinuity
Initial Lunar Thrust-to-Weight Ratio = 6

I_{sp}	λ_1°	λ_4°	λ_5°	$(m_f/m_0)_{orb}$	γ_{orb}	$(\lambda_3)_{adj}$	$(r_f - r_0)_{esc}$	$(m_f/m_0)_{esc}$	γ_{esc}	t_{esc}
300	1.14167	.0184201	-8806.3	.54323	96.824	21134610	15307	.42803	89.316	172.95
350	1.10105	.0173855	-8805.1	.59332	96.210	20023013	15379	.48369	89.240	182.14
400	1.07241	.0166474	-8804.4	.63372	95.747	19228236	15444	.52999	89.177	189.49
450	1.05117	.0160941	-8803.7	.66694	95.386	18650386	15503	.56897	89.119	195.50

Table 75. Escape Through a 15 Kilometer Circular Orbit. Thrust and Velocity Vectors Aligned at Escape Via λ_3 Discontinuity
Initial Lunar Thrust-to-Weight Ratio = 7

I_{sp}	λ_1°	λ_4°	λ_5°	$(m_f/m_0)_{orb}$	γ_{orb}	$(\lambda_3)_{adj}$	$(r_f - r_0)_{esc}$	$(m_f/m_0)_{esc}$	γ_{esc}	t_{esc}
300	1.12683	.0216784	-8806.7	.54043	99.266	24010765	15224	.42581	89.419	148.82
350	1.08040	.0204370	-8805.5	.59089	98.615	22739501	15278	.48170	89.350	156.72
400	1.04766	.0195552	-8804.7	.63159	98.127	21831820	15327	.52820	89.292	163.04
450	1.02335	.0188964	-8804.1	.66505	97.749	21102384	15371	.56734	89.250	168.20

Table 76. Escape Through Orbit. Thrust and Velocity Vectors Aligned at Orbit: Alignment at Escape Via λ_3 Discontinuity $r_{esc} - r_0$ Maximized Via Choice of T/W_0

I_{sp}	T/W_0	λ_1°	λ_4°	λ_5°	$(r_f - r_0)_{orb}$	$\left(\frac{m_f}{m_0}\right)_{orb}$	$(\lambda_3)_{adj}$	$(r_f - r_0)_{esc}$	$\left(\frac{m_f}{m_0}\right)_{esc}$	γ_{esc}	t_{esc}
300	1.16539	49.50698	.0939008	-8799.1	64301	.46317	91136628	69696	.36645	87.155	986.30
350	1.15869	57.31591	.1043232	-8796.0	71282	.50910	96828493	78050	.41670	86.818	1065.52
400	1.15562	64.13471	.1133156	-8792.7	77293	.54783	101348480	85314	.45994	86.541	1130.47
450	1.15161	70.91796	.1222379	-8789.6	82499	.58039	105523640	91683	.49699	86.304	1188.65

Table 77. Escape Through Orbit. Thrust and Velocity Vectors Aligned at Orbit: Alignment at Escape Via λ_3 Discontinuity
Initial Lunar Thrust-to-Weight Ratio = 1

I_{sp}	λ_1°	λ_4°	λ_5°	$(r_f - r_0)_{orb}$	$(m_f/m_0)_{orb}$	$(\lambda_3)_{orb}^{adj}$	$(r_f - r_0)_{esc}$	γ_f	$(m_f/m_0)_{esc}$	t_{esc}
300	97.33660	.1603670	-8786.2	54154	.42877	120781899	60550	86.900	.33907	1199.09
350	114.60499	.1829909	-8778.7	59664	.47291	127789755	67666	86.536	.38690	1297.69
400	131.65260	.2053368	-8771.8	64282	.50999	133795945	73775	86.231	.42799	1383.69
450	148.46797	.2274060	-8765.3	68191	.54162	139006034	79057	85.972	.46359	1459.77

Table 78. Escape Through Orbit. Thrust and Velocity Vectors Aligned at Orbit: Alignment at Escape Via λ_3 Discontinuity
Initial Lunar Thrust-to-Weight Ratio = 1.1

I_{sp}	λ_1°	λ_4°	λ_5°	$(r_f - r_0)_{orb}$	$(m_f/m_0)_{orb}$	$(\lambda_3)_{orb}^{adj}$	$(r_f - r_0)_{esc}$	γ_f	$(m_f/m_0)_{esc}$	t_{esc}
300	62.95928	.1128095	-8796.3	62931	.45185	101227050	68712	87.057	.35748	1059.71
350	72.00603	.1246639	-8791.7	69847	.49814	106682760	77058	86.717	.40772	1139.65
400	80.44945	.1356819	-8787.7	75796	.53692	111326360	84325	86.435	.45078	1207.78
450	88.34058	.1459543	-8784.2	80968	.56990	115334908	90702	86.196	.48800	1266.67

Table 79. Escape Through Orbit. Thrust and Velocity Vectors Aligned at Orbit: Alignment at Escape Via λ_3 Discontinuity
Initial Lunar Thrust-to-Weight Ratio = 1.3

I_{sp}	λ_1°	λ_4°	λ_5°	$(r_f - r_0)_{orb}$	$(m_f/m_0)_{orb}$	$(\lambda_3)_{orb}^{adj}$	$(r_f - r_0)_{esc}$	γ_f	$(m_f/m_0)_{esc}$	t_{esc}
300	32.51963	.0693737	-8804.2	62420	.48068	75084796	67095	87.349	.38020	864.97
350	36.13233	.0743249	-8801.8	68994	.52859	78592094	74801	87.046	.43254	923.91
400	39.32520	.0786480	-8799.8	74597	.56840	81515197	81440	86.796	.47709	973.00
450	42.16431	.0824576	-8798.1	79426	.60199	83993856	87206	86.587	.51534	1014.55

Table 80. Escape Through Orbit. Thrust and Velocity Vectors Aligned at Orbit: Alignment at Escape Via λ_3 Discontinuity
Initial Lunar Thrust-to-Weight Ratio = 1.5

I_{sp}	λ_1°	λ_4°	λ_5°	$(r_f - r_0)_{orb}$	$(m_f/m_0)_{orb}$	$(\lambda_3)_{orb}^{adj}$	$(r_f - r_0)_{esc}$	γ_f	$(m_f/m_0)_{esc}$	t_{esc}
300	19.70747	.0497318	-8806.7	55626	.49807	58933646	59428	87.603	.39373	733.28
350	21.58605	.0525388	-8805.0	61178	.54649	61356534	65887	87.334	.44694	780.41
400	23.20294	.0549127	-8803.7	65863	.58648	63357534	71397	87.111	.49199	819.24
450	24.60780	.0569473	-8802.6	69864	.62003	65039613	76143	86.924	.53050	851.78

Table 81. Escape Through Orbit. Thrust and Velocity Vectors Aligned at Orbit: Alignment at Escape Via λ_3 Discontinuity
Initial Lunar Thrust-to-Weight Ratio = 2

I_{sp}	λ_1°	λ_4°	λ_5°	$(r_f - r_0)_{orb}$	$(m_f/m_0)_{orb}$	$(\lambda_3)_{orb}^{adj}$	$(r_f - r_0)_{esc}$	γ_f	$(m_f/m_0)_{esc}$	t_{esc}
300	7.99520	.0290282	-8807.6	39045	.52145	37532545	41440	88.083	.41167	533.68
350	8.61537	.0302629	-8806.4	42606	.57010	38707427	45557	87.885	.46566	565.50
400	9.13358	.0312711	-8805.6	45567	.60993	39691166	49023	87.714	.51105	591.39
450	9.57261	.0321097	-8804.9	48064	.64309	40500162	51974	87.572	.54960	612.85

Table 82. Escape Through Orbit. Thrust and Velocity Vectors Aligned at Orbit: Alignment at Escape Via λ_3 Discontinuity
Initial Lunar Thrust-to-Weight Ratio = 3

I_{sp}	λ_1°	λ_4°	λ_5°	$(r_f - r_0)_{orb}$	$(m_f/m_0)_{orb}$	$(\lambda_3)_{orb}^{adj}$	$(r_f - r_0)_{esc}$	γ_f	$(m_f/m_0)_{esc}$	t_{esc}
300	2.55822	.0157716	-8806.3	20985	.54028	21079295	22150	88.669	.42594	347.16
350	2.72493	.0163452	-8805.4	22742	.58879	21686902	24178	88.506	.48028	366.68
400	2.86142	.0168046	-8804.7	24186	.62822	22040633	25859	88.406	.52571	382.44
450	2.97511	.0171806	-8804.2	25392	.66085	22448927	27284	88.288	.56411	395.41

Table 83. Escape Through Orbit. Thrust and Velocity Vectors Aligned at Orbit: Alignment at Escape Via λ_3 Discontinuity
Initial Lunar Thrust-to-Weight Ratio = 4

I_{sp}	λ_1°	λ_4°	λ_5°	$(r_f - r_0)_{orb}$	$(m_f/m_0)_{orb}$	$(\lambda_3)_{orb}^{adj}$	$(r_f - r_0)_{esc}$	γ_f	$(m_f/m_0)_{esc}$	t_{esc}
300	1.20225	.0107577	-8805.2	12954	.54828	14459485	13634	88.987	.43198	257.63
350	1.27440	.0111352	-8804.4	13995	.59665	14829265	14832	88.863	.48641	271.77
400	1.33297	.0114358	-8803.8	14847	.63586	15080678	15822	88.772	.53181	283.14
450	1.38143	.0116807	-8803.3	15555	.66822	15281284	16654	88.696	.57011	292.47

Table 84. Escape Through Orbit. Thrust and Velocity Vectors Aligned at Orbit: Alignment at Escape Via λ_3 Discontinuity
Initial Lunar Thrust-to-Weight Ratio = 5

I_{sp}	λ_1°	λ_4°	λ_5°	$(r_f - r_0)_{orb}$	$(m_f/m_0)_{orb}$	$(\lambda_3)_{orb}^{adj}$	$(r_f - r_0)_{esc}$	γ_f	$(m_f/m_0)_{esc}$	t_{esc}
300	.68292	.0081228	-8804.6	8784	.55266	10992657	9229	89.169	.43528	204.91
350	.72190	.0084052	-8803.8	9474	.60094	11218249	10019	89.079	.48976	216.00
400	.75340	.0086295	-8803.2	10036	.64001	11386967	10671	89.007	.53513	224.90
450	.77935	.0088118	-8802.7	10502	.67222	11515095	11217	88.948	.57336	232.21

Table 85. Escape Through Orbit. Thrust and Velocity Vectors Aligned at Orbit: Alignment at Escape Via λ_3 Discontinuity
Initial Lunar Thrust-to-Weight Ratio = 6

I_{sp}	λ_1°	λ_4°	λ_5°	$(r_f - r_0)_{orb}$	$(m_f/m_0)_{orb}$	$(\lambda_3)_{orb}^{adj}$	$(r_f - r_0)_{esc}$	γ_f	$(m_f/m_0)_{esc}$	t_{esc}
300	.43458	.0065027	-8804.1	6352	.55539	8813234	6664	89.305	.43735	170.13
350	.45855	.0067285	-8803.3	6843	.60361	8957997	7225	89.238	.49185	179.26
400	.47786	.0069076	-8802.7	7243	.64283	9101654	7687	89.173	.53720	186.59
450	.49373	.0070530	-8802.3	7573	.67470	9194145	8074	89.125	.57539	192.59

Table 86. Escape Through Orbit. Thrust and Velocity Vectors Aligned at Orbit: Alignment at Escape Via λ_3 Discontinuity
Initial Lunar Thrust-to-Weight Ratio = 7

I_{sp}	λ_1°	λ_4°	λ_5°	$(r_f - r_0)_{orb}$	$(m_f/m_0)_{orb}$	$(\lambda_3)_{orb}^{adj}$	$(r_f - r_0)_{esc}$	γ_f	$(m_f/m_0)_{esc}$	t_{esc}
300	.29831	.0054087	-8803.3	4811	.55726	7336970	5042	89.404	.43877	145.46
350	.31435	.0055967	-8803.0	5178	.60543	7458153	5461	89.345	.49327	153.22
400	.32724	.0057458	-8802.4	5477	.64435	7571865	5806	89.289	.53861	159.44
450	.33782	.0058667	-8801.9	5724	.67638	7646217	6094	89.247	.57677	164.54

Table 87. Escape From Orbit
Initial Lunar Thrust-to-Weight Ratio = .2

I_{sp}	$r_{orb} - r_0$	λ_4°	$r_{esc} - r_0$	γ_{esc}	m_{esc}/m_0	t_{esc}
300	50000	.204807	646682	64.069	.78012	1994.62
350	50000	.207696	670348	63.643	.80775	2034.58
400	50000	.209944	688883	63.309	.82922	2065.51
450	50000	.211764	703765	63.046	.84639	2090.19
300	100000	.187214	656635	65.058	.78430	1956.68
350	100000	.189569	678379	64.637	.81154	1994.48
400	100000	.191419	695363	64.316	.83268	2023.73
450	100000	.192912	708990	64.063	.84956	2047.03
300	150000	.171913	670080	65.992	.78815	1921.74
350	150000	.173894	690047	65.588	.81502	1957.65
400	150000	.175444	705627	65.280	.83585	1985.40
450	150000	.176691	718121	65.038	.85246	2007.48
300	200000	.158490	686699	66.878	.79170	1889.51
350	200000	.160195	705042	66.496	.81822	1923.74
400	200000	.161514	719357	66.201	.83876	1950.14
450	200000	.162537	730880	65.956	.85514	1971.09
300	250000	.146660	706123	67.734	.79499	1859.71
350	250000	.148118	723047	67.362	.82119	1892.41
400	250000	.149223	736278	67.067	.84146	1917.57
450	250000	.150135	746827	66.846	.85760	1937.59
300	300000	.136099	728183	68.532	.79804	1832.00
350	300000	.137396	743766	68.188	.82393	1863.36
400	300000	.138356	755977	67.905	.84395	1887.46
450	300000	.139148	765702	67.693	.85988	1906.60

Table 88. Escape From Orbit
Initial Lunar Thrust-to-Weight Ratio = .4

I_{sp}	$r_{orb} - r_0$	λ_4°	$r_{esc} - r_0$	γ_{esc}	m_{esc}/m_0	t_{esc}
300	50000	.140763	229089	74.467	.79002	952.40
350	50000	.141483	235946	74.187	.81703	968.20
400	50000	.141987	241326	73.950	.83790	980.30
450	50000	.142457	245551	73.796	.85450	989.87
300	100000	.130734	266862	75.149	.79269	940.27
350	100000	.131344	273217	74.864	.81941	955.59
400	100000	.131824	278140	74.653	.84004	967.33
450	100000	.132238	282038	74.503	.85645	976.60
300	150000	.121655	305740	75.778	.79524	928.73
350	150000	.122217	311595	75.512	.82167	943.62
400	150000	.122683	316103	75.327	.84208	955.02
450	150000	.123036	319720	75.174	.85830	964.02
300	200000	.113460	345550	76.382	.79766	917.72
350	200000	.113978	350956	76.134	.82383	932.21
400	200000	.114368	355157	75.942	.84402	943.29
450	200000	.114692	358496	75.798	.86006	952.04
300	250000	.106007	386229	76.946	.79999	907.18
350	250000	.106492	391223	76.717	.82589	921.30
400	250000	.106863	395097	76.542	.84587	932.09
450	250000	.107139	398208	76.396	.86174	940.61
300	300000	.099234	427662	77.485	.80221	897.07
350	300000	.099662	432313	77.259	.82787	910.84
400	300000	.099989	435920	77.086	.84764	921.37
450	300000	.100249	438797	76.951	.86335	929.67

Table 89. Escape From Orbit
Initial Lunar Thrust-to-Weight Ratio = .6

I_{sp}	$r_{orb} - r_0$	λ_4°	$r_{esc} - r_0$	γ_{esc}	m_{esc}/m_0	t_{esc}
300	50000	.124952	136653	78.892	.79037	633.87
350	50000	.125380	140062	78.676	.81739	644.20
400	50000	.125708	142712	78.511	.83825	652.10
450	50000	.125968	144830	78.381	.85485	658.33
300	100000	.116254	180533	79.410	.79290	626.22
350	100000	.116640	183668	79.205	.81963	636.28
400	100000	.116936	186105	79.048	.84027	643.97
450	100000	.117171	188053	78.925	.85668	650.04
300	150000	.108378	224965	79.895	.79533	618.86
350	150000	.108728	227854	79.700	.82179	628.67
400	150000	.108997	230099	79.552	.84221	636.17
450	150000	.109209	231892	79.434	.85843	642.08
300	200000	.101200	269904	80.339	.79768	611.77
350	200000	.101515	272574	80.152	.82387	621.35
400	200000	.101790	274627	80.024	.84407	628.66
450	200000	.101983	276282	79.913	.86012	634.44
300	250000	.094698	315264	80.769	.79994	604.94
350	250000	.094987	317732	80.592	.82586	614.29
400	250000	.095208	319648	80.457	.84586	621.44
450	250000	.095382	321177	80.351	.86175	627.07
300	300000	.088762	361020	81.171	.80212	598.35
350	300000	.089027	363304	81.004	.82779	607.49
400	300000	.089230	365078	80.876	.84759	614.47
450	300000	.089390	366493	80.775	.86331	619.97

Table 90. Escape From Orbit
Initial Lunar Thrust-to-Weight Ratio = .8

I_{sp}	$r_{orb} - r_0$	λ_4°	$r_{esc} - r_0$	γ_{esc}	m_{esc}/m_0	t_{esc}
300	50000	.117392	100911	81.383	.79022	475.73
350	50000	.117697	102954	81.209	.81726	483.48
400	50000	.117930	104542	81.076	.83815	489.40
450	50000	.118115	105813	80.971	.85476	494.07
300	100000	.109301	147235	81.799	.79274	470.01
350	100000	.109577	149109	81.634	.81950	477.57
400	100000	.109788	150566	81.509	.84015	483.34
450	100000	.109955	151732	81.410	.85657	487.89
300	150000	.101966	193899	82.186	.79517	464.51
350	150000	.102217	195622	82.031	.82165	471.87
400	150000	.102409	196962	81.912	.84208	477.50
450	150000	.102561	198032	81.819	.85832	481.94
300	200000	.095300	240867	82.548	.79751	459.20
350	200000	.095528	242453	82.401	.82372	466.39
400	200000	.095703	243687	82.289	.84394	471.88
450	200000	.095841	244672	82.201	.86001	476.22
300	250000	.089225	288104	82.887	.79978	454.07
350	250000	.089434	289568	82.748	.82572	461.10
400	250000	.089593	290705	82.642	.84573	466.46
450	250000	.089720	291614	82.558	.86163	470.69
300	300000	.083677	335583	83.203	.80196	449.11
350	300000	.083868	336936	83.072	.82766	455.98
400	300000	.084014	337986	82.971	.84746	461.23
450	300000	.084129	338826	82.892	.86320	465.36

Table 91. Escape From Orbit

Initial Lunar Thrust-to-Weight Ratio = 1

I_{sp}	$r_{orb} - r_0$	λ_4°	$r_{esc} - r_0$	γ_{esc}	m_{esc}/m_0	t_{esc}
300	50000	.112887	83431	82.964	.79009	380.82
350	50000	.113119	84789	82.818	.81715	387.03
400	50000	.113296	85846	82.707	.83804	391.77
450	50000	.113437	86692	82.619	.85466	395.51
300	100000	.105156	130984	83.311	.79262	376.24
350	100000	.105366	132228	83.174	.81939	382.29
400	100000	.105527	133196	83.069	.84005	386.91
450	100000	.105655	133970	82.987	.85648	390.56
300	150000	.098143	178768	83.634	.79506	371.82
350	150000	.098335	179910	83.505	.82154	377.72
400	150000	.098481	180798	83.406	.84199	382.24
450	150000	.098597	181508	83.328	.85823	385.79
300	200000	.091766	226757	83.935	.79740	367.56
350	200000	.091940	227807	83.813	.82362	373.32
400	200000	.092073	228623	83.720	.84385	377.73
450	200000	.092179	229276	83.646	.85992	381.20
300	250000	.085951	274928	84.215	.79967	363.44
350	250000	.086110	275895	84.100	.82563	369.08
400	250000	.086232	276647	84.012	.84565	373.38
450	250000	.086328	277248	83.943	.86155	376.77
300	300000	.080637	323261	84.476	.80186	359.47
350	300000	.080782	324154	84.368	.82757	364.97
400	300000	.080894	324847	84.285	.84738	369.18
450	300000	.080983	325402	84.219	.86312	372.49

Table 92. Escape From Orbit
Initial Lunar Thrust-to-Weight Ratio = 2

I_{sp}	$r_{orb} - r_0$	λ_4°	$r_{esc} - r_0$	γ_{esc}	m_{esc}/m_0	t_{esc}
300	50000	.104016	58765	86.355	.78985	190.63
350	50000	.104109	59129	86.277	.81693	193.75
400	50000	.104181	59413	86.217	.83784	196.13
450	50000	.104238	59640	86.170	.85448	198.01
300	100000	.096981	108109	86.541	.79240	188.32
350	100000	.097065	108442	86.468	.81918	191.36
400	100000	.097130	108700	86.412	.83987	193.68
450	100000	.097182	108908	86.367	.85631	195.51
300	150000	.090527	157521	86.702	.79485	186.09
350	150000	.090600	157826	86.632	.82136	189.06
400	150000	.090728	158058	86.591	.84181	191.32
450	150000	.090775	158248	86.550	.85808	193.11
300	200000	.084723	206985	86.863	.79722	183.95
350	200000	.084789	207264	86.797	.82345	186.84
400	200000	.084841	207481	86.748	.84369	189.05
450	200000	.084882	207655	86.708	.85978	190.80
300	250000	.079424	256498	87.012	.79950	181.88
350	250000	.079485	256755	86.951	.82547	184.70
400	250000	.079532	256955	86.904	.84550	186.86
450	250000	.079570	257114	86.867	.86142	188.56
300	300000	.074577	306056	87.151	.80171	179.88
350	300000	.074633	306292	87.093	.82742	182.64
400	300000	.074676	306476	87.049	.84725	184.75
450	300000	.074710	306623	87.014	.86300	186.41

Table 93. Escape From Orbit
Initial Lunar Thrust-to-Weight Ratio = 3

I_{sp}	$r_{orb} - r_0$	λ_4°	$r_{esc} - r_0$	γ_{esc}	m_{esc}/m_0	t_{esc}
300	50000	.101070	53953	87.544	.78980	127.12
350	50000	.101118	54118	87.491	.81688	129.20
400	50000	.101154	54246	87.450	.83780	130.79
450	50000	.101184	54350	87.418	.85443	132.05
300	100000	.094267	103655	87.670	.79235	125.58
350	100000	.094309	103806	87.620	.81914	127.60
400	100000	.094342	103923	87.582	.83982	129.15
450	100000	.094369	104017	87.552	.85627	130.38
300	150000	.088086	153387	87.786	.79481	124.09
350	150000	.088125	153525	87.740	.82132	126.07
400	150000	.088154	153632	87.704	.84178	127.58
450	150000	.088178	153718	87.676	.85804	128.77
300	200000	.082457	203144	87.894	.79718	122.66
350	200000	.082492	203270	87.851	.82342	124.59
400	200000	.082519	203369	87.817	.84366	126.06
450	200000	.082541	203448	87.791	.85975	127.22
300	250000	.077319	252924	87.995	.79947	121.27
350	250000	.077350	253040	87.954	.82544	123.16
400	250000	.077375	253131	87.922	.84547	124.60
450	250000	.077394	253203	87.897	.86139	125.73
300	300000	.072616	302725	88.088	.80167	119.94
350	300000	.072645	302831	88.049	.82740	121.78
400	300000	.072667	302914	88.019	.84723	123.19
450	300000	.072685	302981	87.996	.86298	124.30

Table 94. Escape From Orbit

Initial Lunar Thrust-to-Weight Ratio = 4

I_{sp}	$r_{orb} - r_0$	λ_4^0	$r_{esc} - r_0$	γ_{esc}	m_{esc}/m_0	t_{esc}
300	50000	.099614	52239	88.149	.78978	95.35
350	50000	.099639	52332	88.109	.81686	96.91
400	50000	.099658	52405	88.078	.83778	98.10
450	50000	.099674	52464	88.054	.85442	99.04
300	100000	.092923	102070	88.245	.79233	94.19
350	100000	.092945	102155	88.207	.81912	95.71
400	100000	.092963	102222	88.178	.83981	96.87
450	100000	.092977	102275	88.155	.85626	97.79
300	150000	.086844	151917	88.333	.79479	93.07
350	150000	.086864	151996	88.297	.82130	94.56
400	150000	.086880	152057	88.270	.84177	95.69
450	150000	.086893	152105	88.249	.85803	96.59
300	200000	.081307	201780	88.414	.79716	92.00
350	200000	.081325	201852	88.381	.82340	93.45
400	200000	.081339	201907	88.356	.84365	94.55
450	200000	.081350	201952	88.336	.85974	95.43
300	250000	.076251	251655	88.490	.79945	90.96
350	250000	.076267	251721	88.459	.82543	92.37
400	250000	.076280	251772	88.435	.84546	93.45
450	250000	.076290	251813	88.416	.86138	94.31
300	300000	.071624	301542	88.560	.80166	89.96
350	300000	.071639	301603	88.531	.82739	91.34
400	300000	.071650	301650	88.508	.84722	92.40
450	300000	.071659	301687	88.491	.86297	93.23

Table 95. Escape From Orbit

Initial Lunar Thrust-to-Weight Ratio = 5

I_{sp}	$r_{orb} - r_0$	λ_4°	$r_{esc} - r_0$	γ_{esc}	m_{esc}/m_0	t_{esc}
300	50000	.098738	51438	88.515	.78977	76.28
350	50000	.098750	51499	88.483	.81685	77.53
400	50000	.098759	51546	88.458	.83777	78.49
450	50000	.098767	51583	88.439	.85441	79.24
300	100000	.092116	101330	88.592	.79232	75.35
350	100000	.092126	101385	88.562	.81912	76.57
400	100000	.092134	101428	88.539	.83980	77.50
450	100000	.092141	101462	88.520	.85625	78.24
300	150000	.086098	151232	88.663	.79479	74.46
350	150000	.086107	151282	88.634	.82130	75.65
400	150000	.086114	151321	88.613	.84176	76.56
450	150000	.086120	151353	88.595	.85803	77.27
300	200000	.080616	201143	88.728	.79716	73.60
350	200000	.080624	201189	88.701	.82340	74.76
400	200000	.080630	201225	88.681	.84364	75.65
450	200000	.080635	201254	88.665	.85973	76.34
300	250000	.075610	251063	88.789	.79945	72.77
350	250000	.075617	251106	88.764	.82542	73.90
400	250000	.075622	251139	88.745	.84546	74.77
450	250000	.075627	251165	88.730	.86138	75.45
300	300000	.071028	300990	88.845	.80166	71.97
350	300000	.071034	301029	88.822	.82738	73.07
400	300000	.071039	301060	88.804	.84721	73.92
450	300000	.071043	301084	88.790	.86297	74.58

Table 96. Escape From Orbit
Initial Lunar Thrust-to-Weight Ratio = 6

I_{sp}	$r_{orb} - r_0$	λ_4°	$r_{esc} - r_0$	γ_{esc}	m_{esc}/m_0	t_{esc}
300	50000	.098154	51002	88.761	.78976	63.57
350	50000	.098157	51044	88.734	.81685	64.61
400	50000	.098159	51076	88.713	.83777	65.41
450	50000	.098162	51103	88.697	.85441	66.03
300	100000	.091577	100926	88.824	.79232	62.80
350	100000	.091579	100964	88.799	.81911	63.81
400	100000	.091581	100994	88.780	.83980	64.59
450	100000	.091583	101018	88.765	.85625	65.20
300	150000	.085601	150858	88.884	.79478	62.05
350	150000	.085602	150893	88.860	.82129	63.04
400	150000	.085604	150920	88.842	.84176	63.80
450	150000	.085605	150942	88.827	.85802	64.39
300	200000	.080156	200796	88.938	.79715	61.33
350	200000	.080157	200828	88.916	.82340	62.30
400	200000	.080158	200853	88.899	.84364	63.04
450	200000	.080159	200873	88.886	.85973	63.62
300	250000	.075183	250740	88.989	.79944	60.64
350	250000	.075184	250770	88.968	.82542	61.59
400	250000	.075184	250793	88.952	.84546	62.31
450	250000	.075185	250811	88.939	.86138	62.87
300	300000	.070631	300689	89.036	.80166	59.97
350	300000	.070632	300717	89.016	.82738	60.90
400	300000	.070632	300738	89.001	.84721	61.60
450	300000	.070633	300755	88.990	.86296	62.15

Table 97. Escape From Orbit

Initial Lunar Thrust-to-Weight Ratio = 7

I_{sp}	$r_{orb} - r_0$	λ_4°	$r_{esc} - r_0$	γ_{esc}	m_{esc}/m_0	t_{esc}
300	50000	.097737	50737	88.936	.78976	54.49
350	50000	.097733	50768	88.913	.81684	55.38
400	50000	.097731	50792	88.895	.83776	56.06
450	50000	.097730	50812	88.881	.85441	56.60
300	100000	.091193	100681	88.991	.79232	53.83
350	100000	.091189	100710	88.969	.81911	54.70
400	100000	.091186	100732	88.953	.83980	55.36
450	100000	.091185	100749	88.940	.85625	55.89
300	150000	.085245	150631	89.042	.79478	53.19
350	150000	.085241	150657	89.022	.82129	54.04
400	150000	.085239	150677	89.006	.84175	54.68
450	150000	.085237	150693	88.994	.85802	55.20
300	200000	.079826	200586	89.089	.79715	52.57
350	200000	.079823	200609	89.070	.82339	53.40
400	200000	.079820	200628	89.055	.84364	54.03
450	200000	.079818	200643	89.044	.85973	54.53
300	250000	.074878	250545	89.132	.79944	51.98
350	250000	.074874	250566	89.114	.82542	52.79
400	250000	.074871	250583	89.101	.84546	53.41
450	250000	.074870	250597	89.090	.86137	53.89
300	300000	.070348	300507	89.173	.80165	51.41
350	300000	.070344	300527	89.156	.82738	52.20
400	300000	.070341	300543	89.143	.84721	52.80
450	300000	.070339	300555	89.133	.86296	53.28

SECTION VII. GRAPHICAL PRESENTATION OF RESULTS

The following graphs present the numerical data of the previous section in a form which aids interpolation and allows a direct comparison of the various modes of escape. These graphs are presented in order corresponding to the tables of the preceding section.

A few general remarks about the graphs may be made. The initial lunar thrust-to-weight ratio is usually chosen as the independent variable for FIG 3 through 61 since most quantities exhibit strong dependence upon this quantity. These graphs are parameterized by four values of the specific impulse so that dependence of the dependent variable upon the two basic variables is immediately apparent.

The graphs which deviate from this format (FIG 17, 18, 23, 24, 30, 31, 37, 38, 45, and 53) are those in which the initial value of thrust-to-weight has been chosen to obtain a specific end condition, i.e., maximum mass fraction or maximum altitude at orbit. For a specified mode, the only remaining independent variable to be chosen is specific impulse and this parameter is used as the abscissa in these cases.

For each set of graphs the mass fraction, final value of gamma, and burning time are plotted as a function of the initial thrust-to-weight ratio. In all cases except the graphs corresponding to Tables 1 through 10 and 11 through 20* the escape altitude is also shown in a similar manner. In both sets of graphs dealing with direct escape the initial values of the Lagrangian multipliers necessary to achieve orbit are also plotted against initial lunar thrust-to-weight ratio. These types of graphs are not shown for the ascent-to-orbit phase of the trajectory since they are available in Reference 1. For those modes which involve a discontinuity in either of the multipliers λ_3 or λ_4 at circular orbit, graphical presentation shows the adjusted value which was necessary to attain alignment of the thrust and velocity vectors at escape.

FIG 62 through 97 deal with the escape-from-orbit maneuver. Since this involves the additional parameter of initial orbital altitude it is, naturally, more difficult to adequately graph the data. The initial thrust-to-weight ratios do not exert such strong influence as in the preceding cases, and the initial orbital altitude is usually a more convenient independent variable. A further complication that arises is that for certain plots the variation in specific impulse makes so little difference in certain other quantities that it becomes necessary to plot separate graphs for various values of I_{sp}. In FIG 92 through 97 the variation in mass fraction with initial thrust-to-weight ratio is continued only through $T/W_0 = 2.5$. Beyond this point the curves are too flat to be of interest.

---

* For Tables 1 through 10 the escape altitude is a constant, 15 km: Tables 11 through 20 have altitudes which correspond to Tables 33 through 42 on a case-by-case basis. FIG 26 and 27 thus correspond to the altitude plots for both sets of Tables, 11 through 20 and 33 through 42.

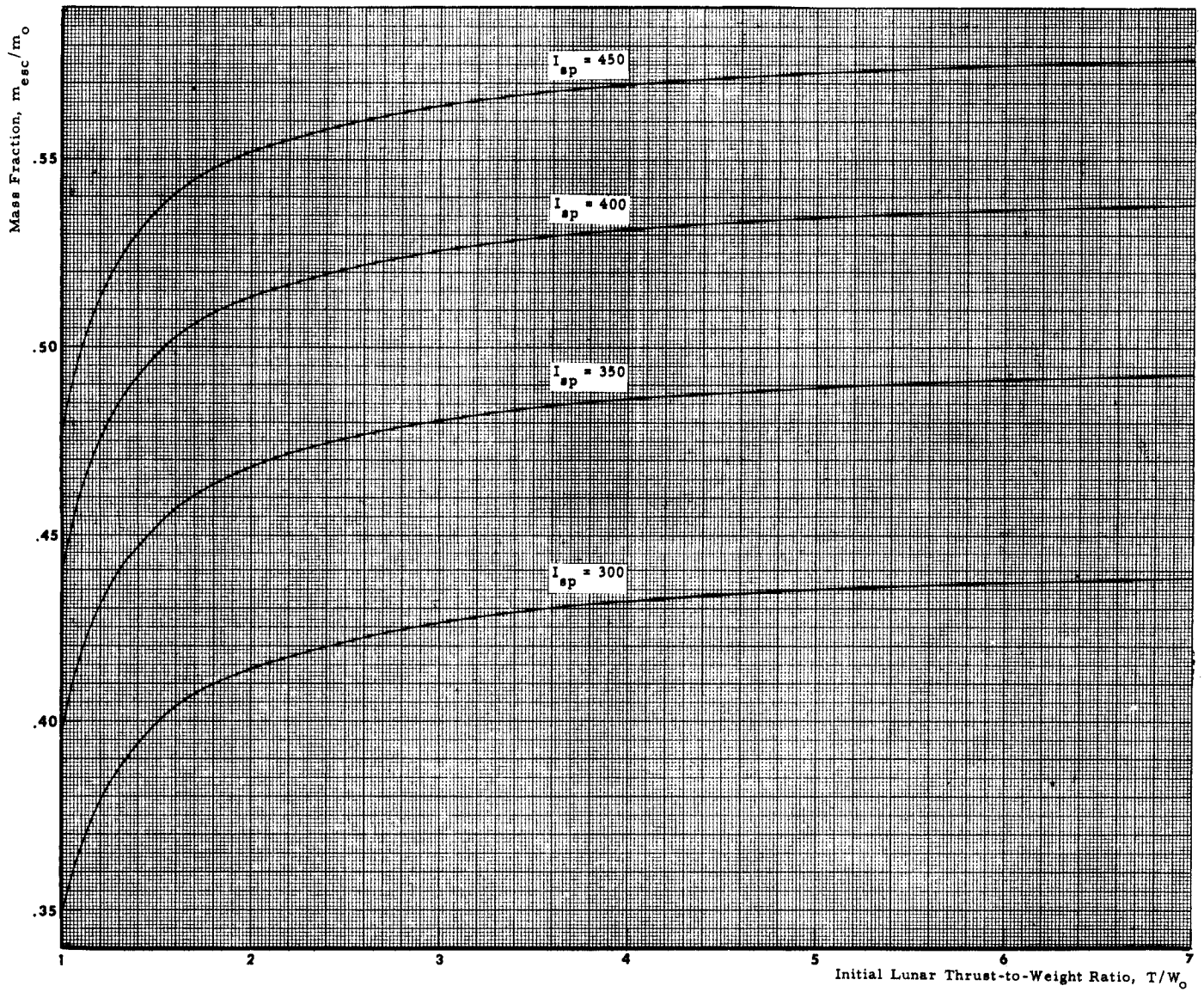

FIGURE 3. MASS FRACTION AT ESCAPE VS INITIAL LUNAR THRUST-TO-WEIGHT RATIO FOR DIRECT ESCAPE AT 15 Km.

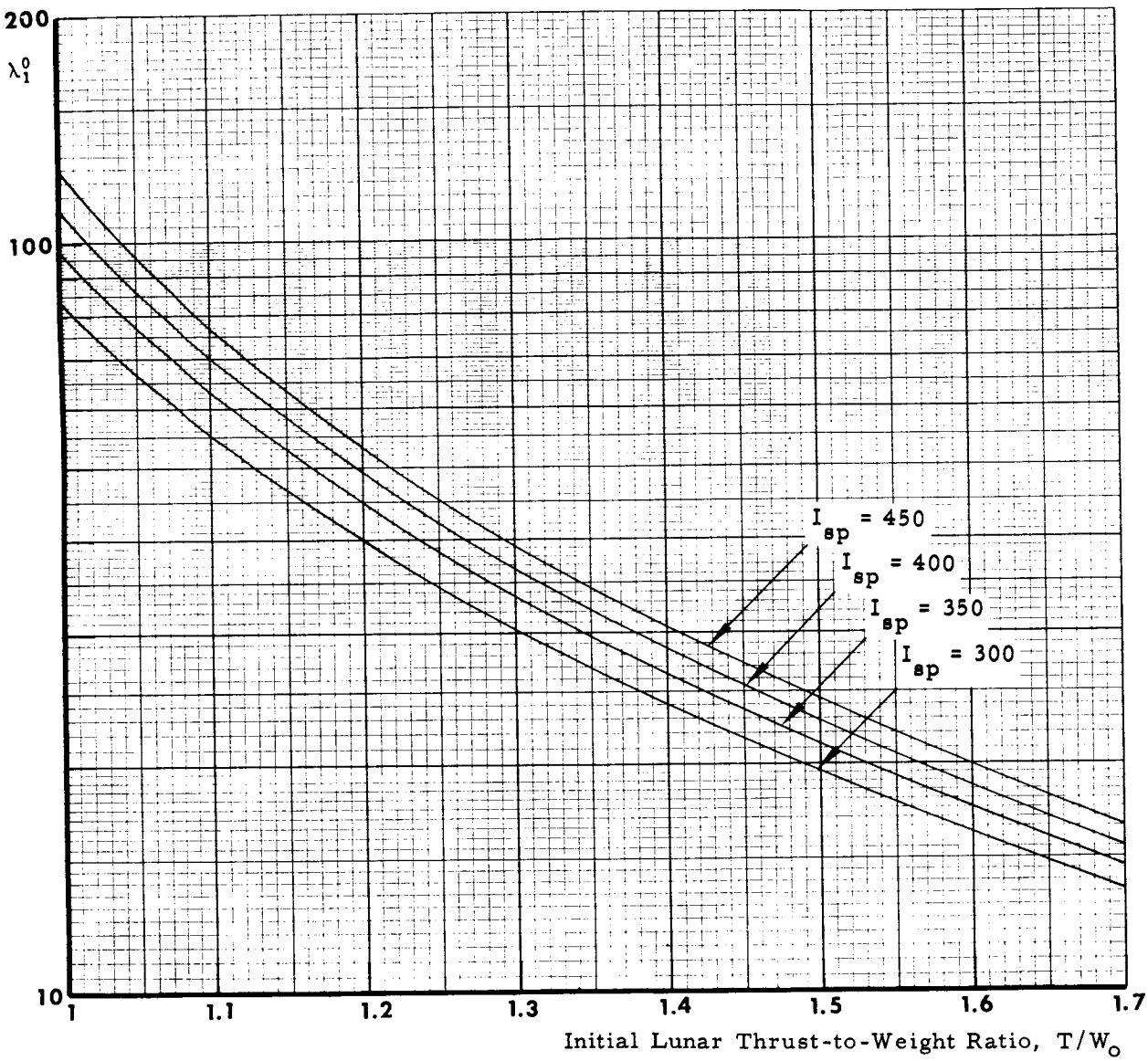

FIGURE 4. λ_1 VS INITIAL LUNAR THRUST-TO-WEIGHT RATIO FOR DIRECT ESCAPE AT 15 Km.

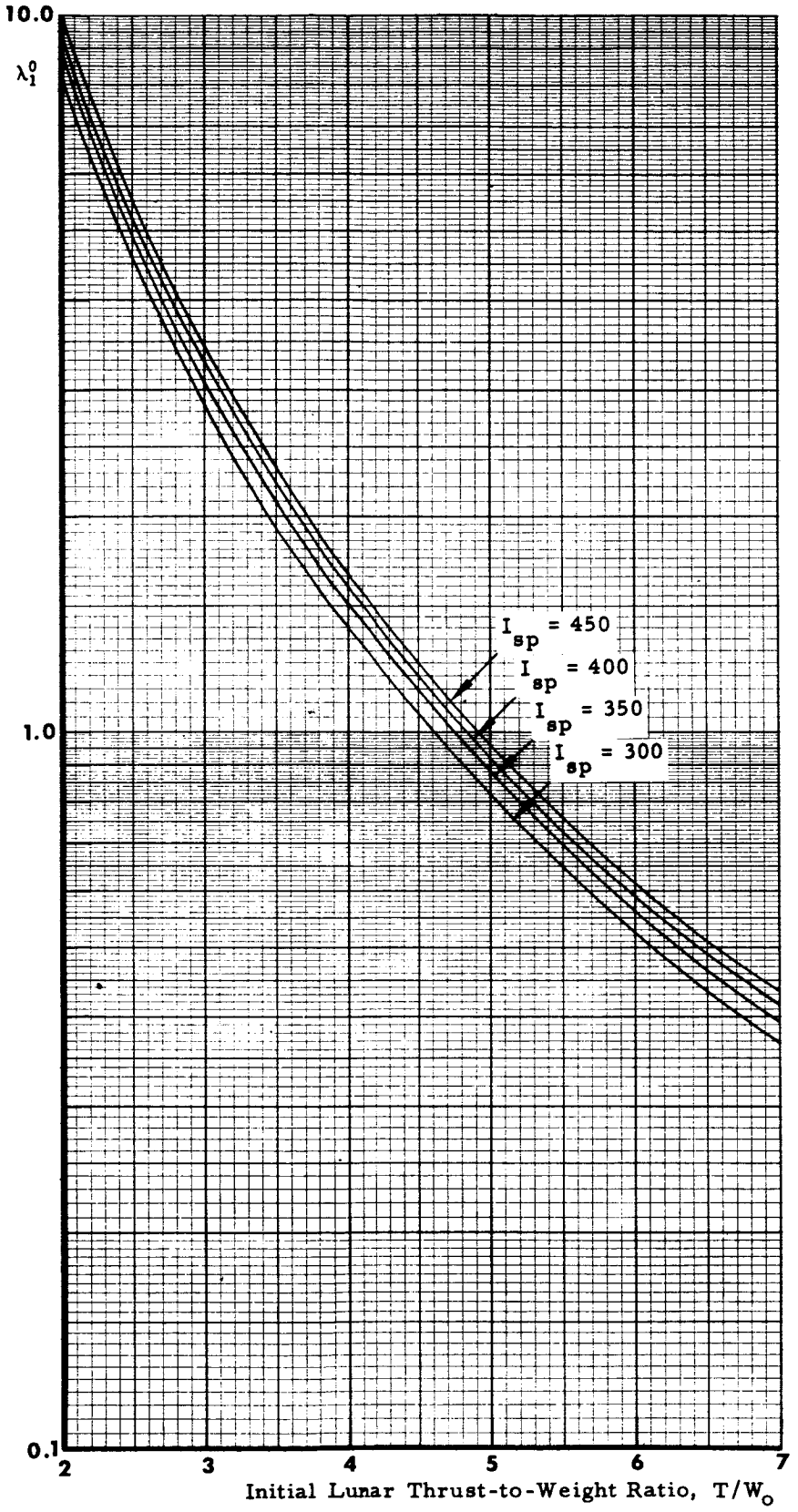

FIGURE 5. λ_1 VS INITIAL LUNAR THRUST-TO-WEIGHT RATIO FOR DIRECT ESCAPE AT 15 Km.

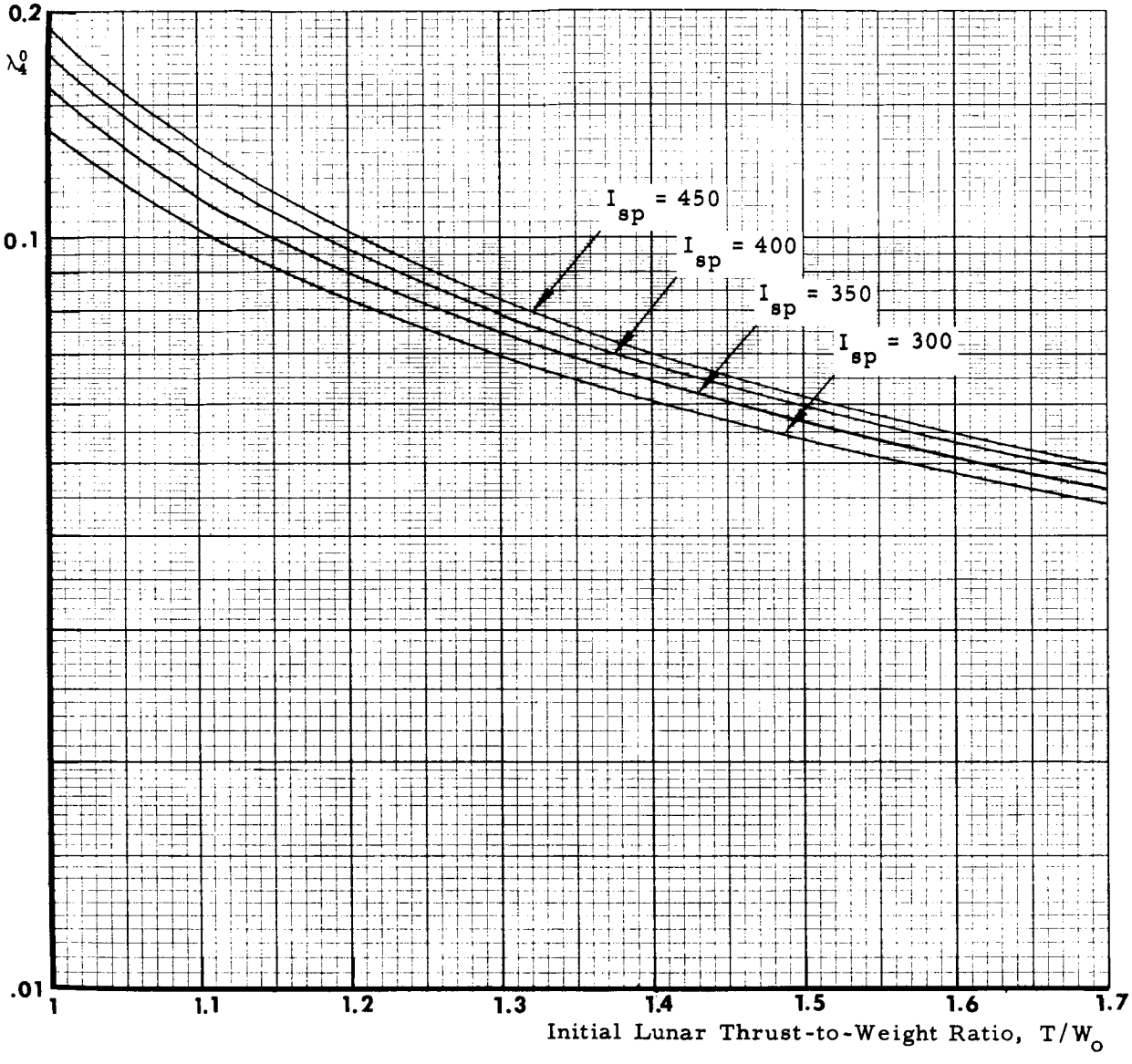

FIGURE 6. λ_4 VS INITIAL LUNAR THRUST-TO-WEIGHT RATIO FOR DIRECT ESCAPE AT 15 Km.

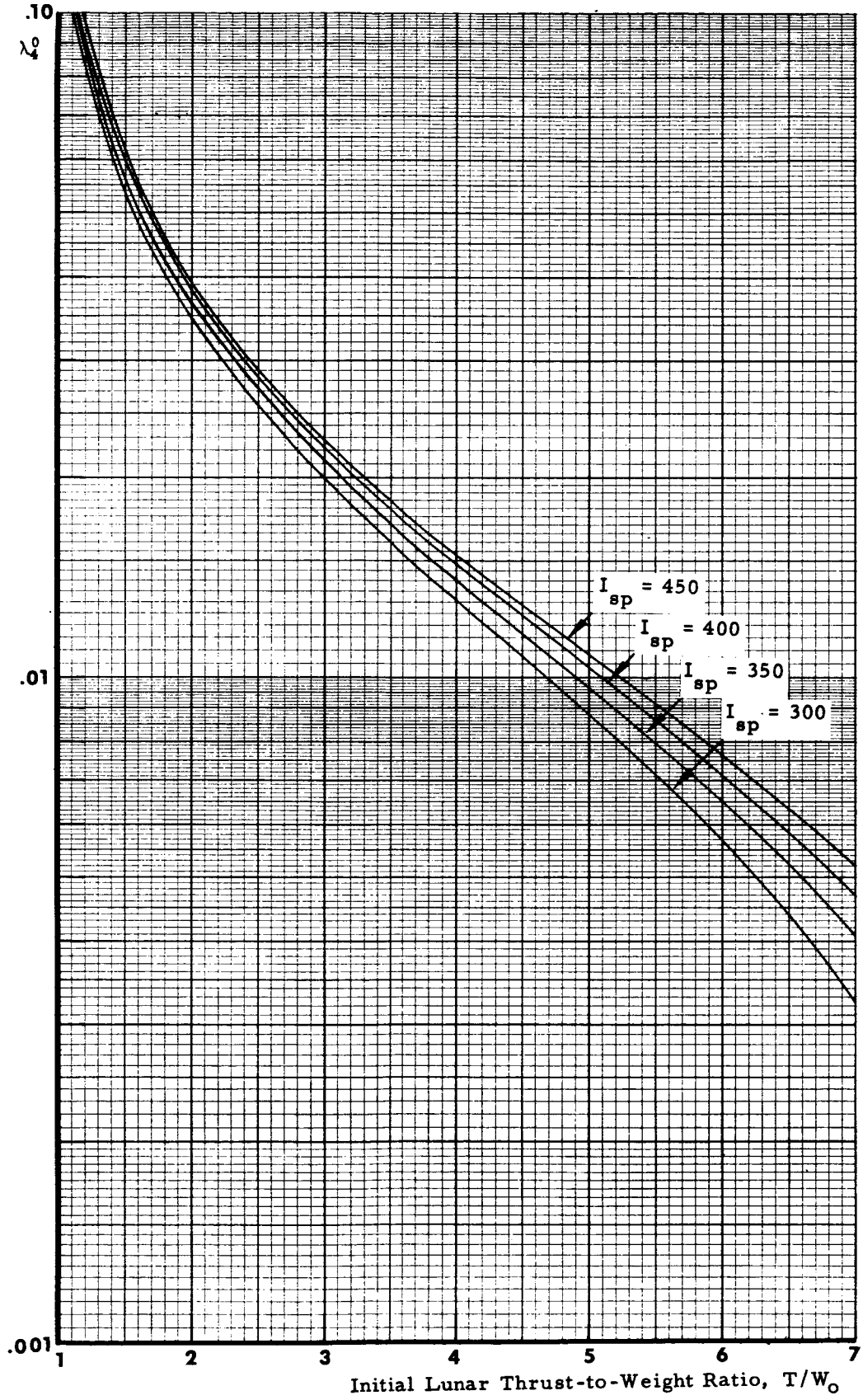

FIGURE 7. λ_4 VS INITIAL LUNAR THRUST-TO-WEIGHT RATIO FOR DIRECT ESCAPE AT 15 Km.

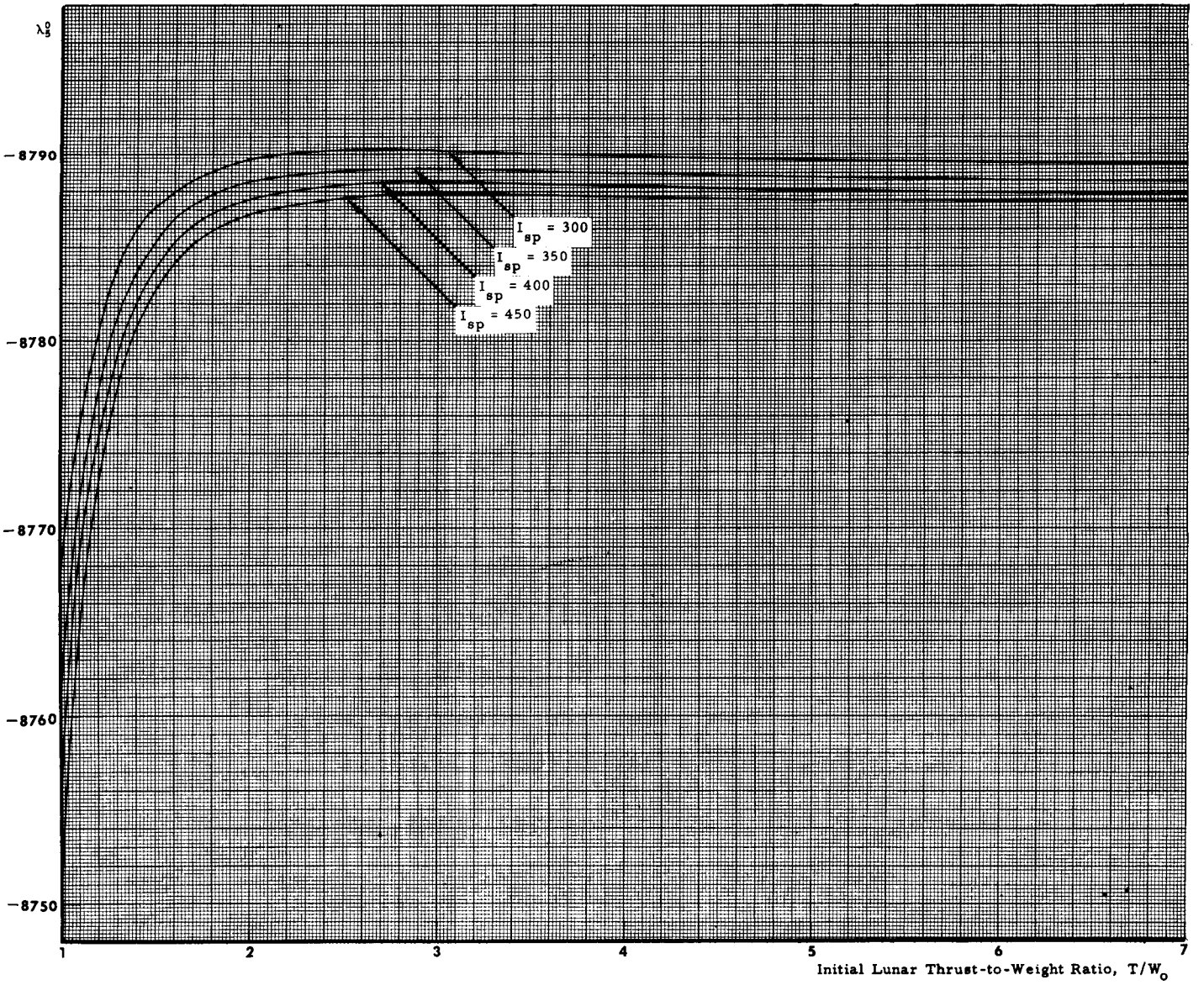

FIGURE 8. λ_5 VS INITIAL LUNAR THRUST-TO-WEIGHT RATIO FOR DIRECT ESCAPE AT 15 Km.

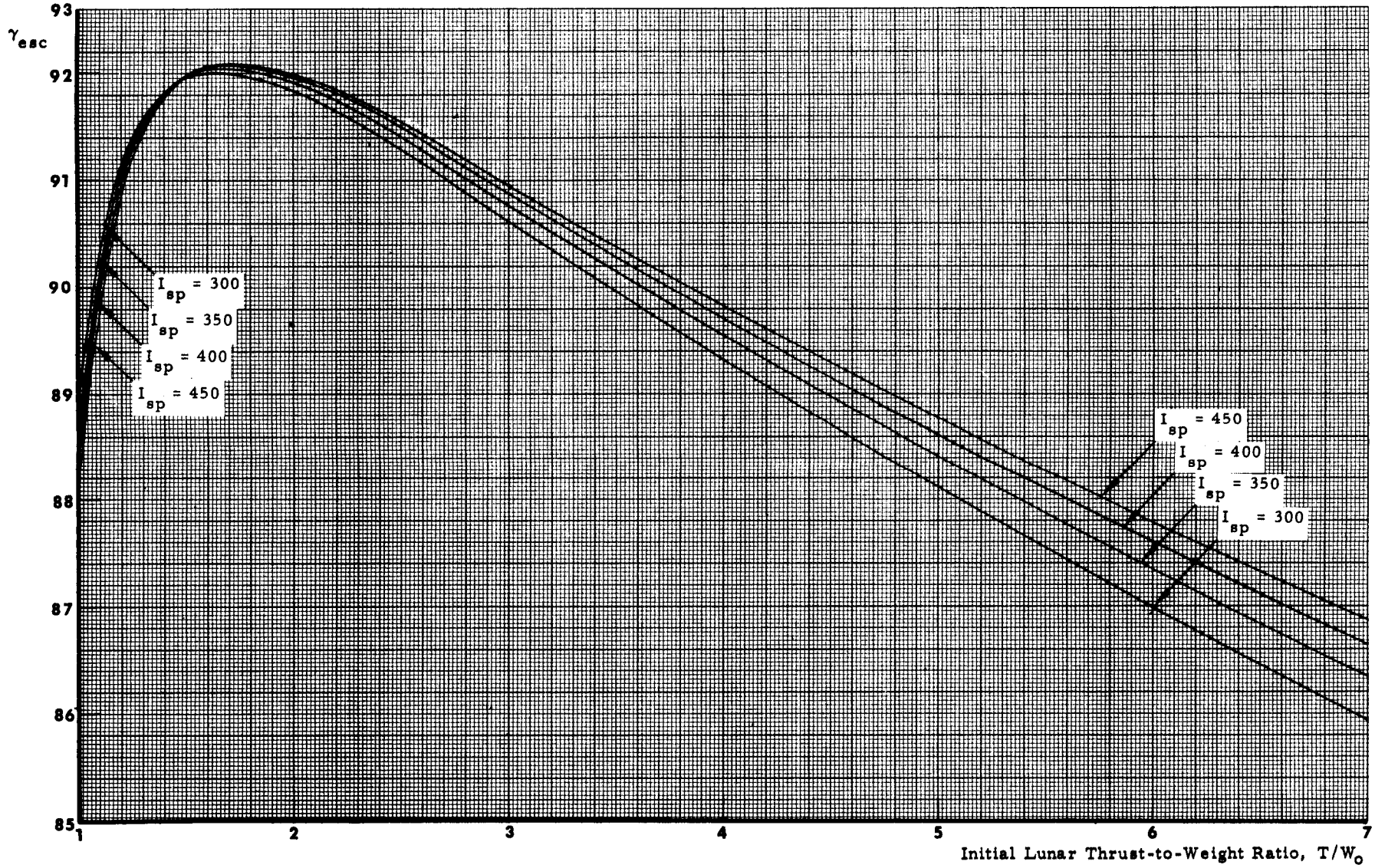

FIGURE 9. GAMMA AT ESCAPE VS INITIAL LUNAR THRUST-TO-WEIGHT RATIO FOR DIRECT ESCAPE AT 15 Km.

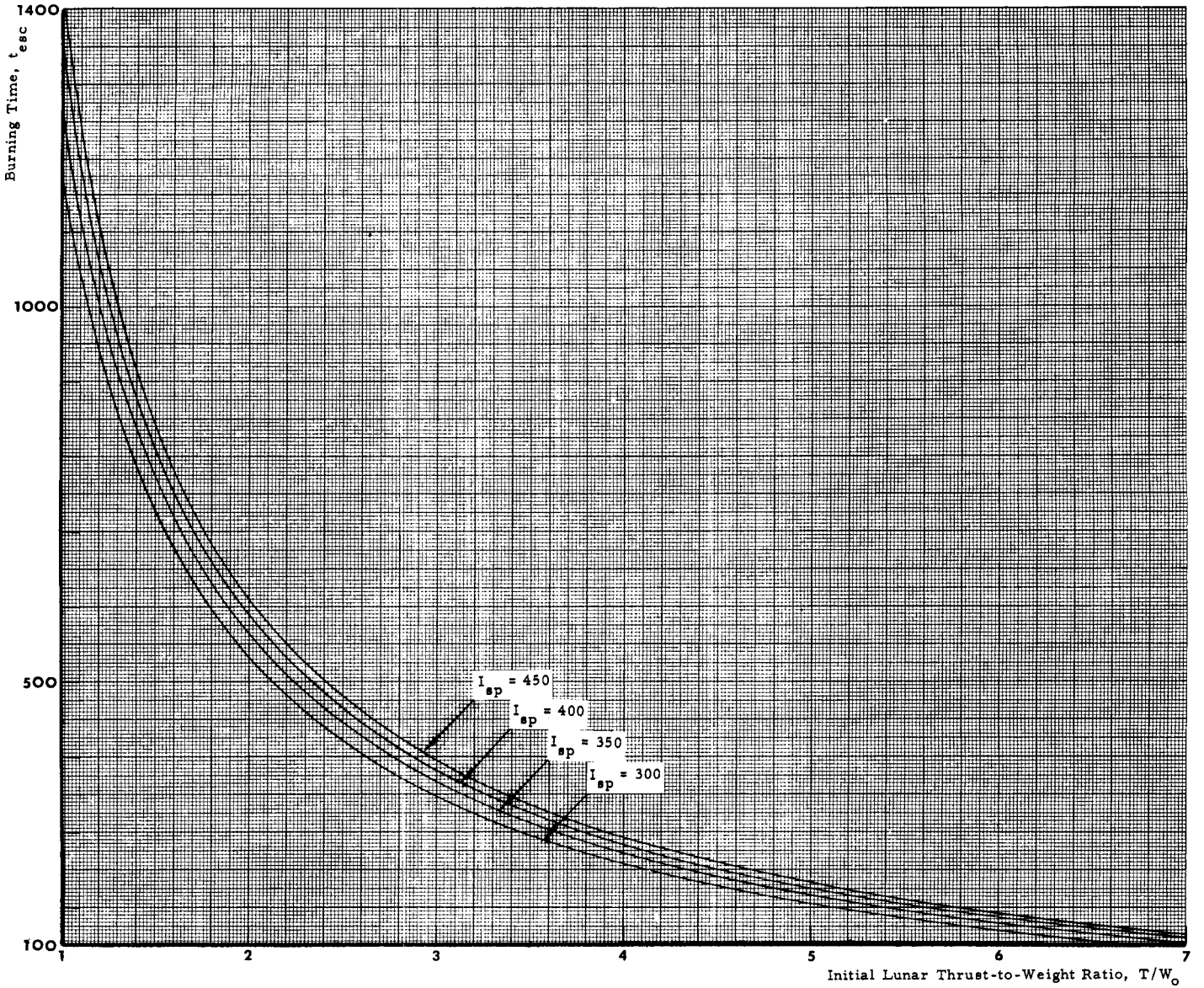

FIGURE 10. BURNING TIME TO ESCAPE VS INITIAL LUNAR THRUST-TO-WEIGHT RATIO FOR DIRECT ESCAPE AT 15 Km.

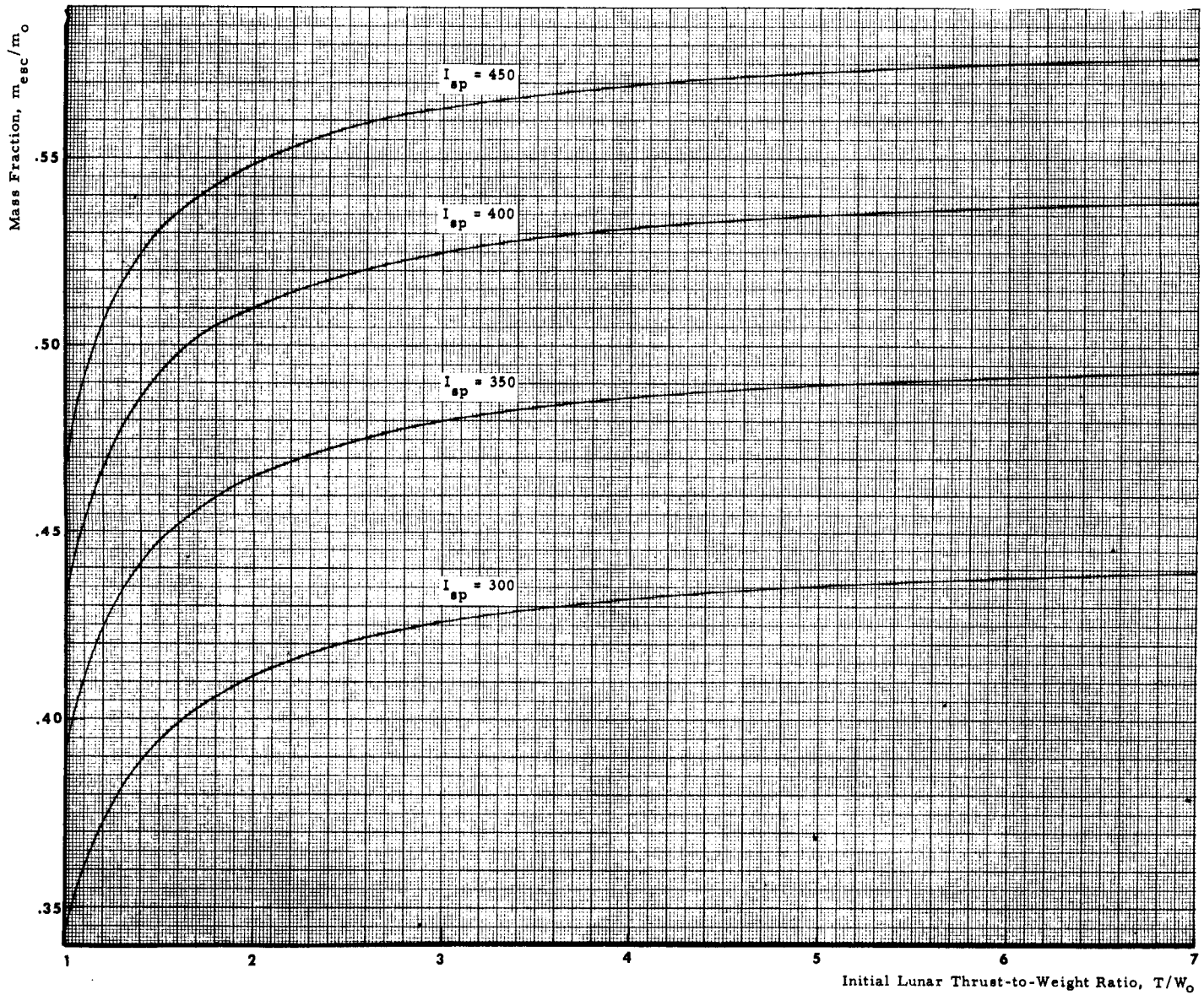

FIGURE 11. MASS FRACTION AT ESCAPE VS INITIAL LUNAR THRUST-TO-WEIGHT RATIO FOR DIRECT ESCAPE. ALTITUDES MATCHED WITH CORRESPONDING SPECIFIC IMPULSES AND THRUST-TO-WEIGHT RATIOS OF TABLES 33 THROUGH 42.

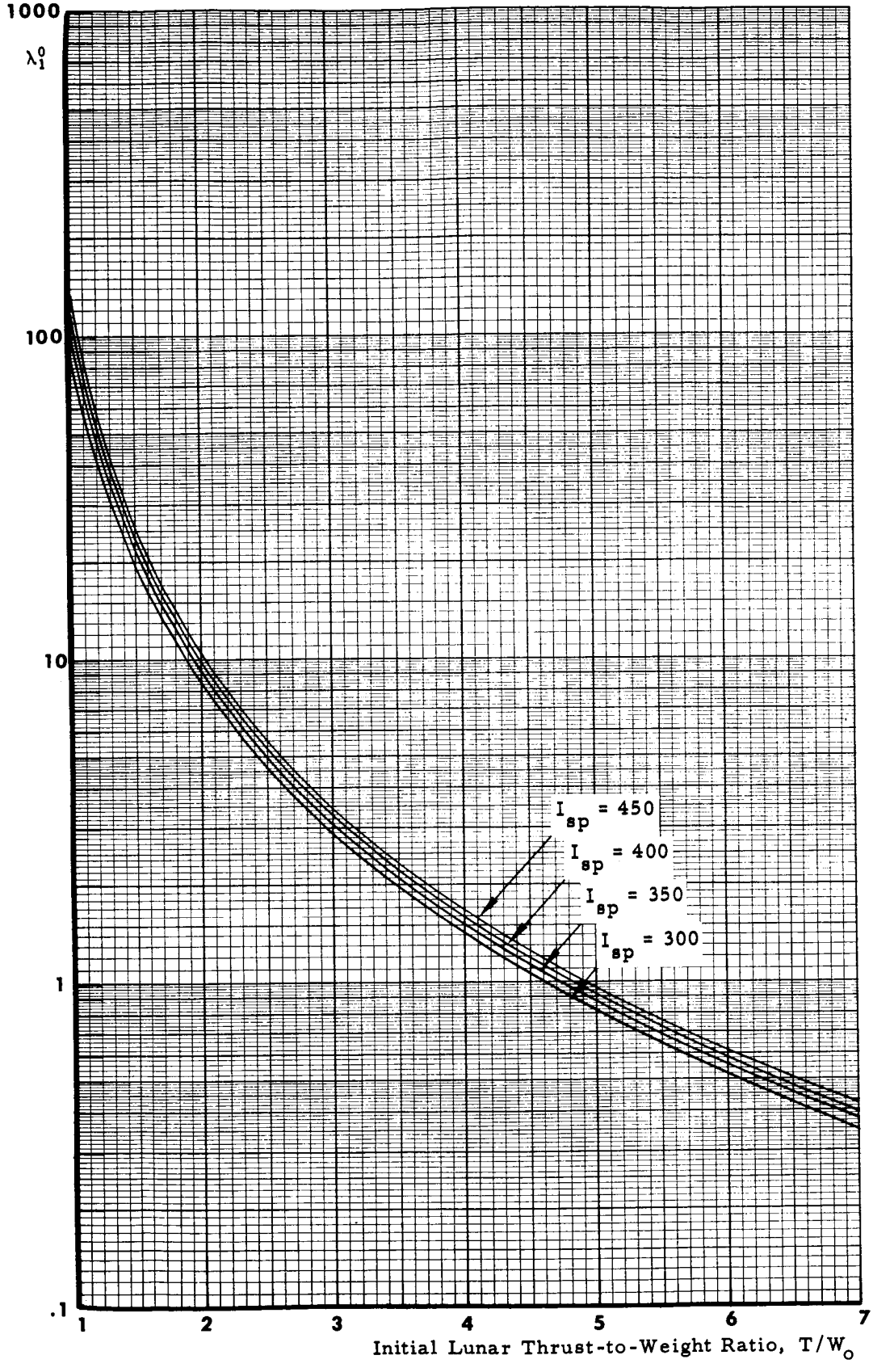

FIGURE 12. λ_1 VS INITIAL LUNAR THRUST-TO-WEIGHT RATIO FOR DIRECT ESCAPE. ALTITUDES MATCHED WITH CORRESPONDING SPECIFIC IMPULSES AND THRUST-TO-WEIGHT RATIOS OF TABLES 33 THROUGH 42.

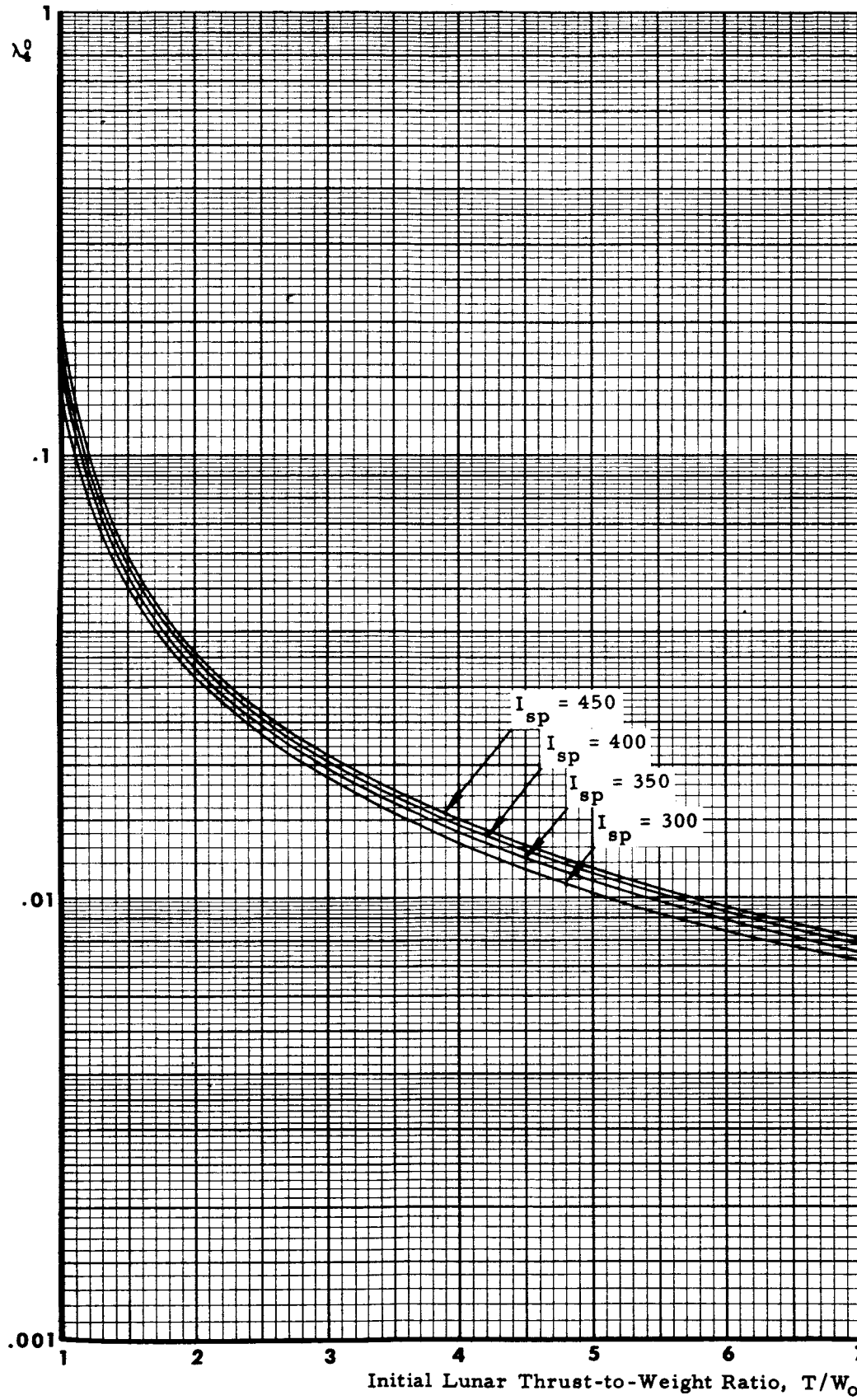

FIGURE 13. λ_4 VS INITIAL LUNAR THRUST-TO-WEIGHT RATIO FOR DIRECT ESCAPE. ALTITUDES MATCHED WITH CORRESPONDING SPECIFIC IMPULSES AND THRUST-TO-WEIGHT RATIOS OF TABLES 33 THROUGH 42.

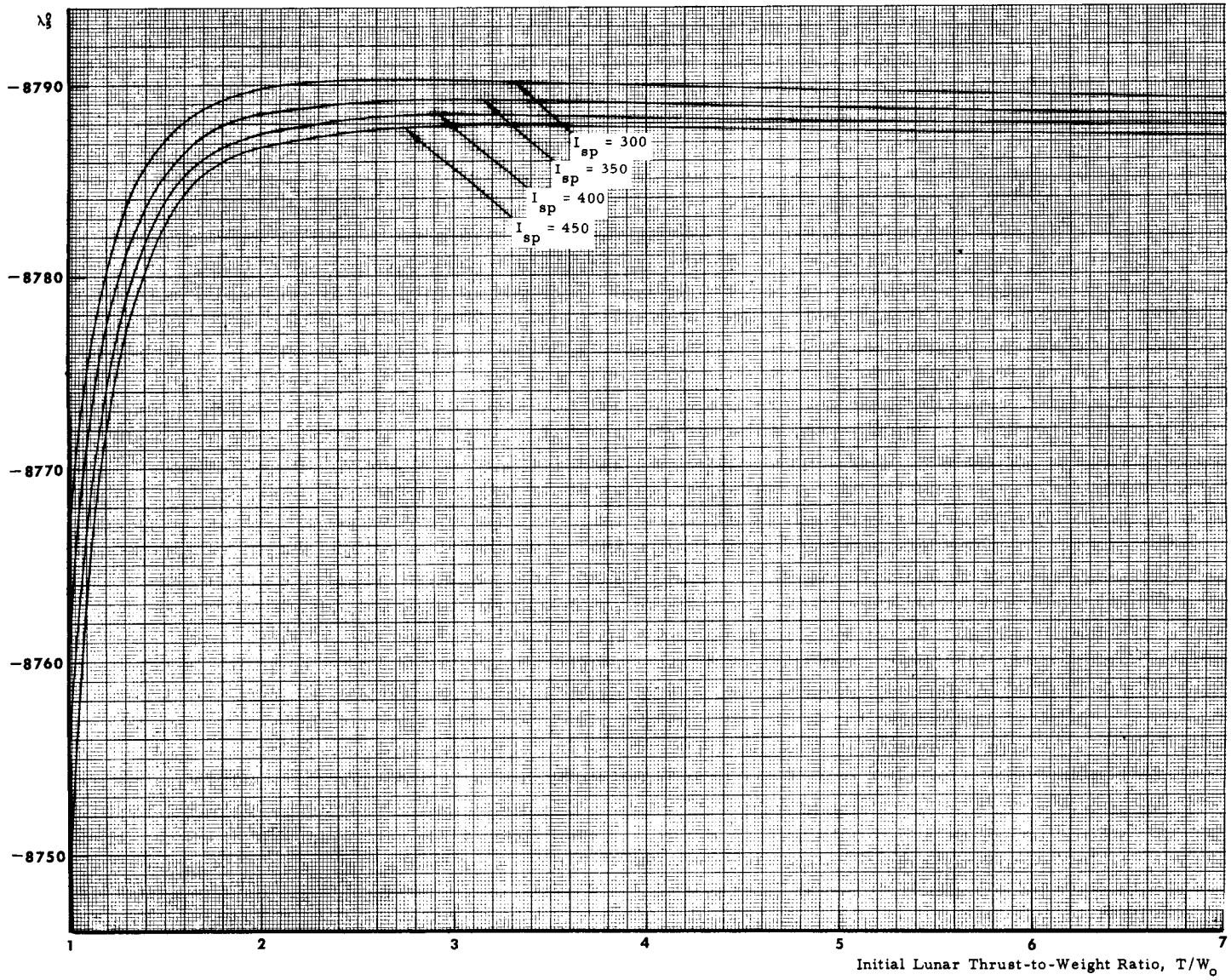

FIGURE 14. λ_ξ VS INITIAL LUNAR THRUST-TO-WEIGHT RATIO FOR DIRECT ESCAPE. ALTITUDES MATCHED WITH CORRESPONDING SPECIFIC IMPULSES AND THRUST-TO-WEIGHT RATIOS OF TABLES 33 THROUGH 42.

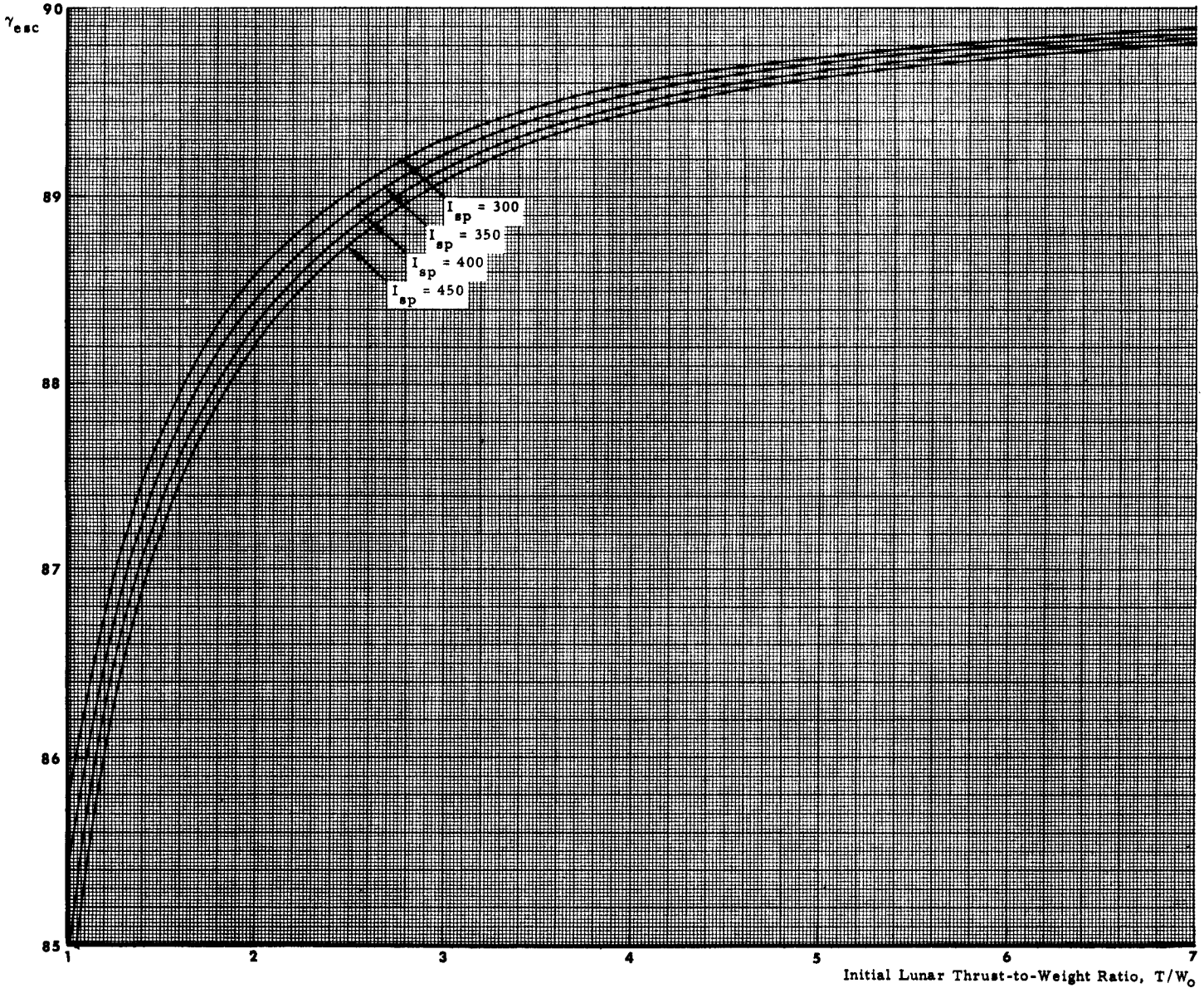

FIGURE 15. GAMMA AT ESCAPE VS INITIAL LUNAR THRUST-TO-WEIGHT RATIO FOR DIRECT ESCAPE. ALTITUDES MATCHED WITH CORRESPONDING SPECIFIC IMPULSES AND THRUST-TO-WEIGHT RATIOS OF TABLES 33 THROUGH 42.

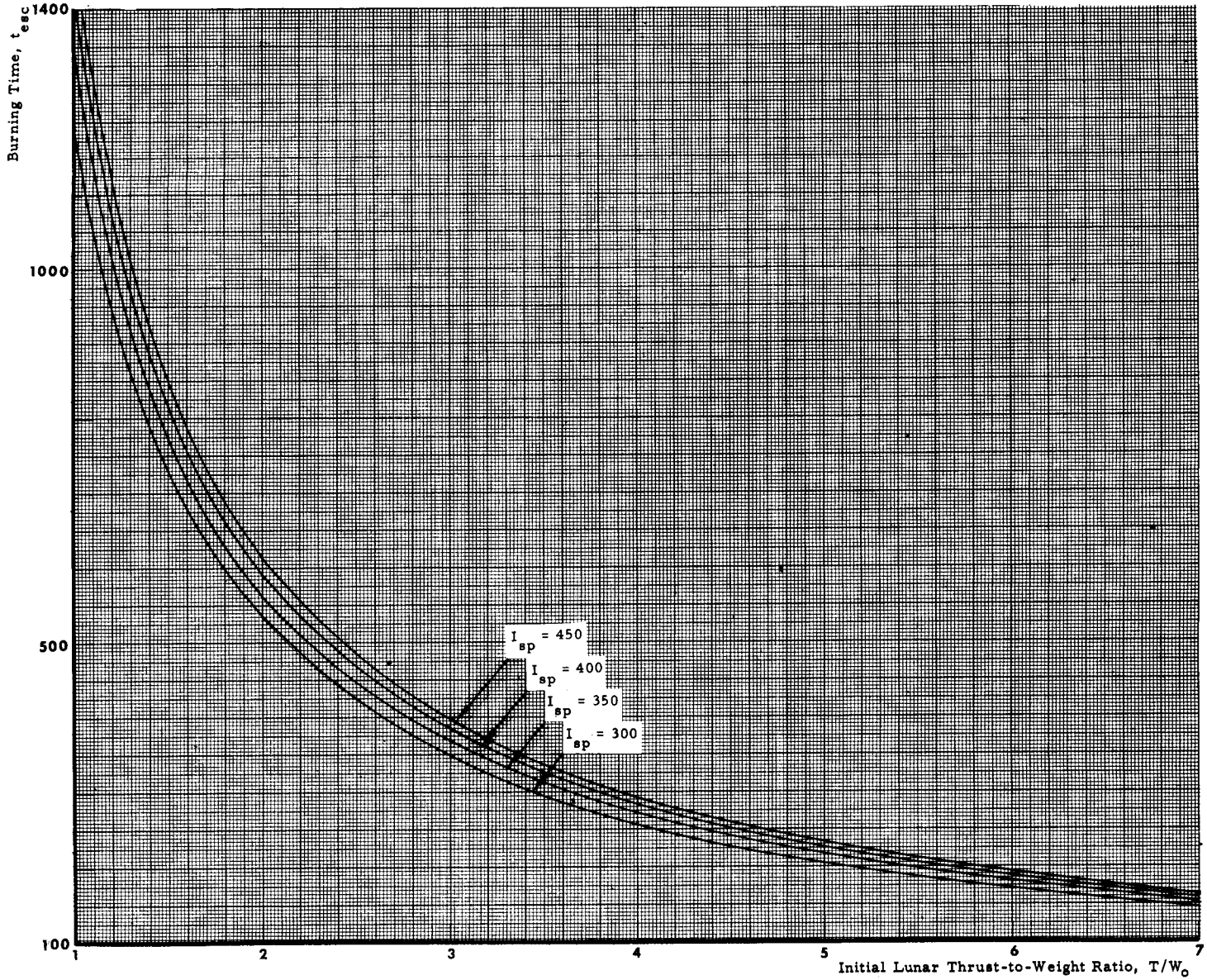

FIGURE 16. BURNING TIME TO ESCAPE VS INITIAL LUNAR THRUST-TO-WEIGHT RATIO FOR DIRECT ESCAPE. ALTITUDES MATCHED WITH CORRESPONDING SPECIFIC IMPULSES AND THRUST-TO-WEIGHT RATIOS OF TABLES 33 THROUGH 42.

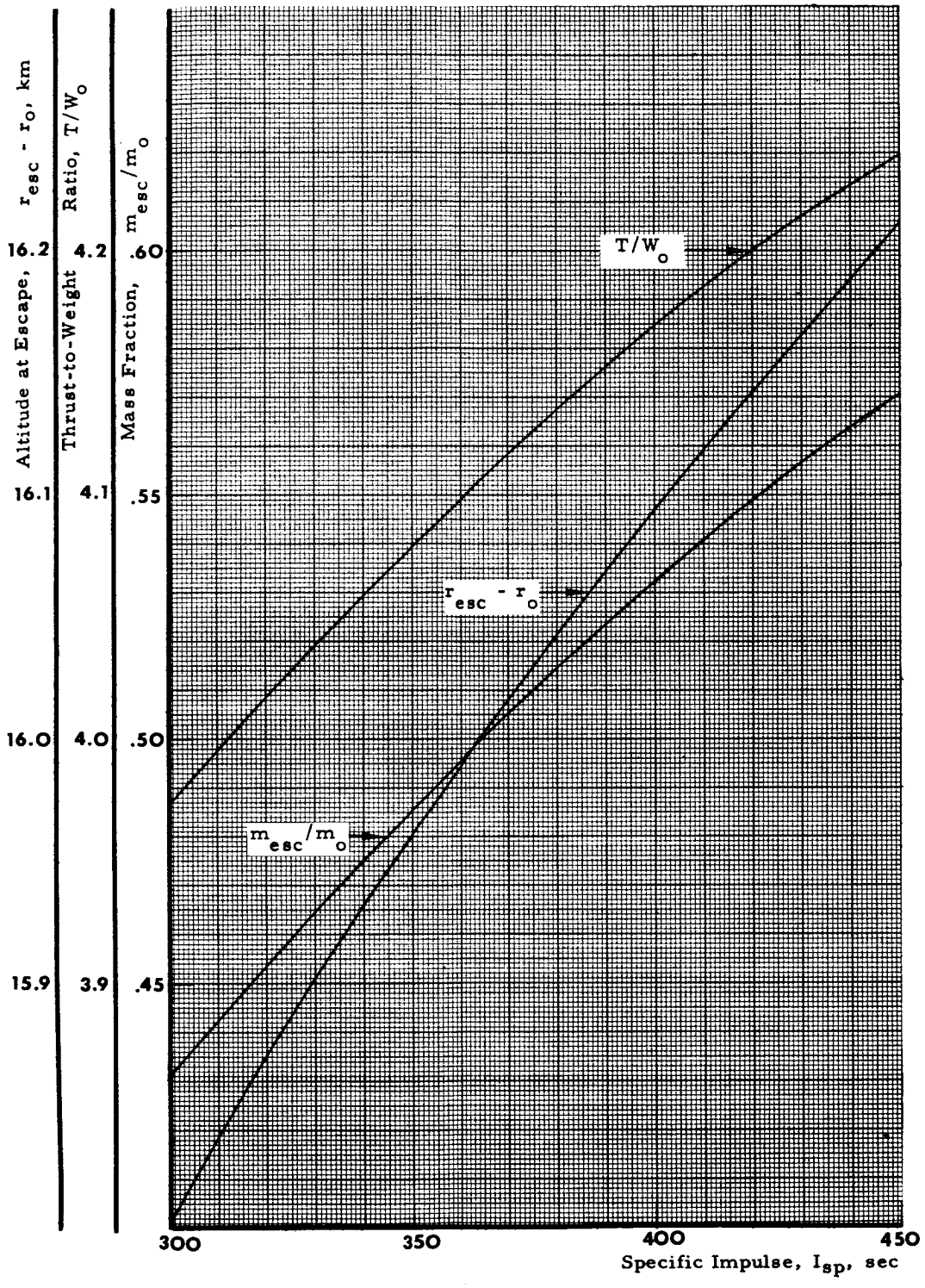

FIGURE 17. ALTITUDE, INITIAL LUNAR THRUST-TO-WEIGHT RATIO, AND MASS FRACTION VS SPECIFIC IMPULSE FOR ESCAPE THROUGH A 15 Km. CIRCULAR ORBIT. m_{esc}/m_o MAXIMIZED WITH RESPECT TO T/W_o. THRUST AND VELOCITY VECTORS NOT ALIGNED AT ESCAPE.

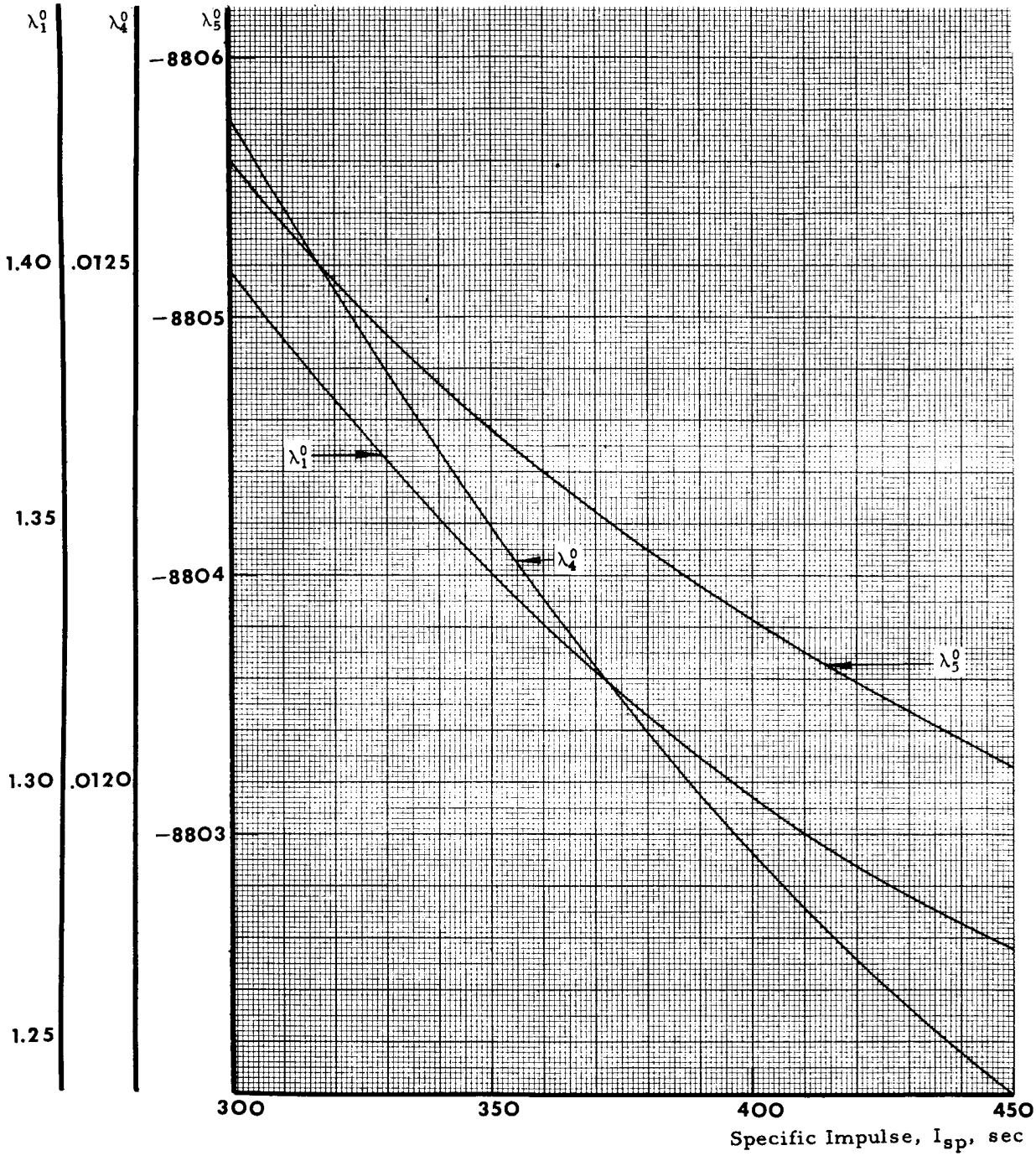

FIGURE 18. INITIAL VALUES OF λ_1, λ_4, AND λ_5 VS SPECIFIC IMPULSE FOR ESCAPE THROUGH A 15 Km. CIRCULAR ORBIT. m_{esc}/m_o MAXIMIZED WITH RESPECT TO T/W_o. THRUST AND VELOCITY VECTORS NOT ALIGNED AT ESCAPE.

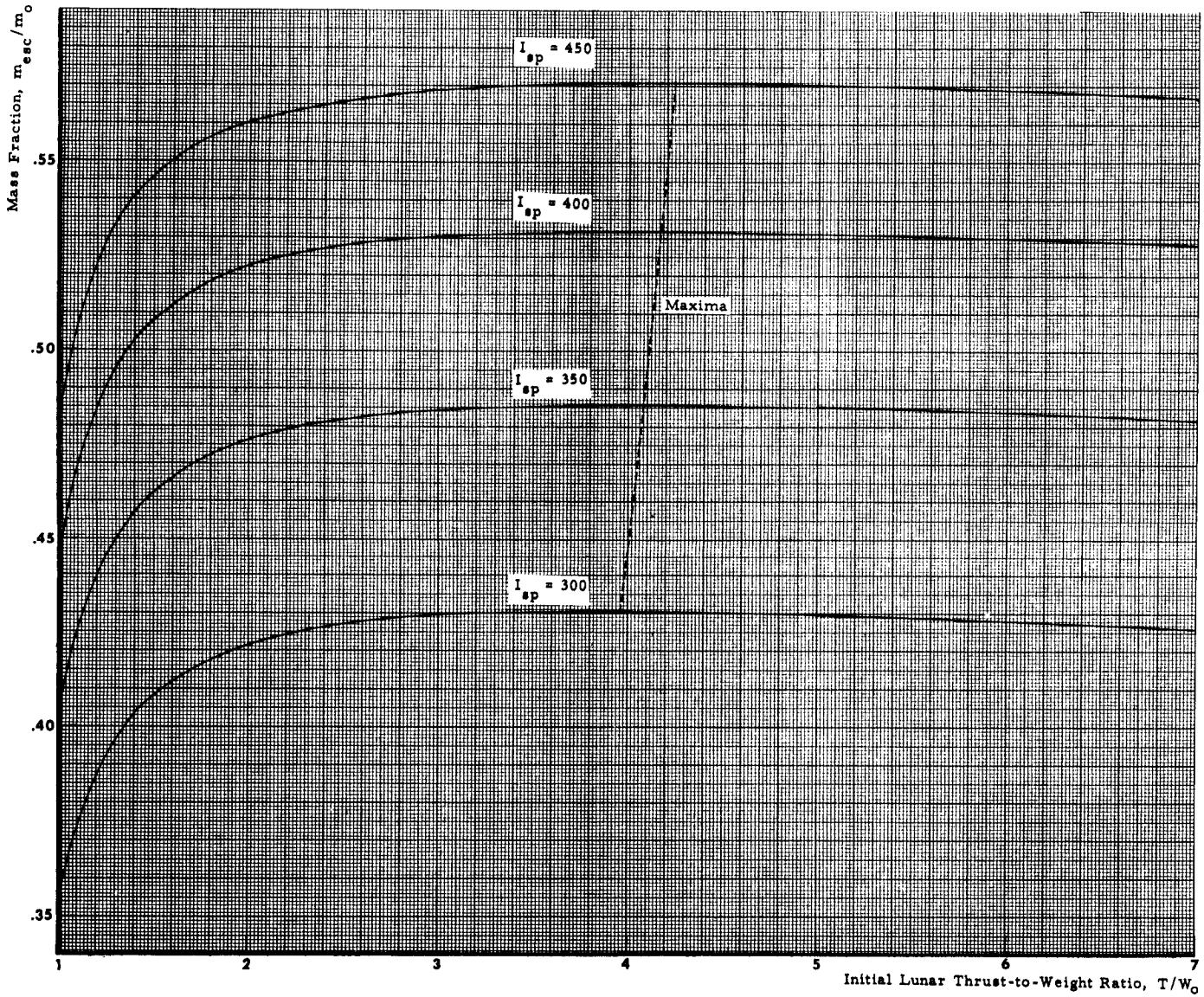

FIGURE 19. MASS FRACTION VS INITIAL LUNAR THRUST-TO-WEIGHT RATIO FOR ESCAPE THROUGH A 15-Km. CIRCULAR ORBIT. THRUST AND VELOCITY VECTORS NOT ALIGNED AT ESCAPE.

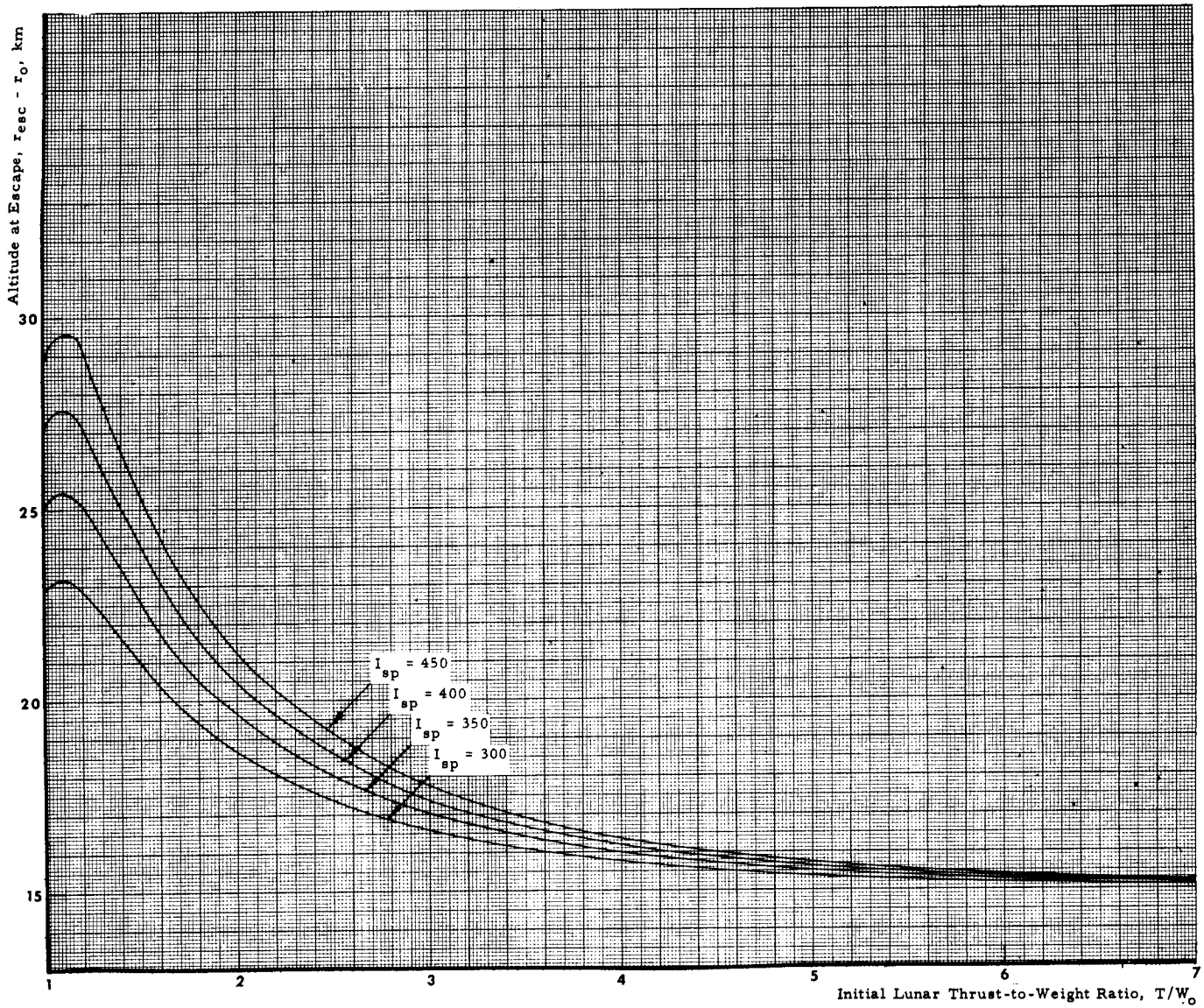

FIGURE 20. ALTITUDE AT ESCAPE VS INITIAL LUNAR THRUST-TO-WEIGHT RATIO FOR ESCAPE THROUGH A 15 Km. CIRCULAR ORBIT. THRUST AND VELOCITY VECTORS NOT ALIGNED AT ESCAPE.

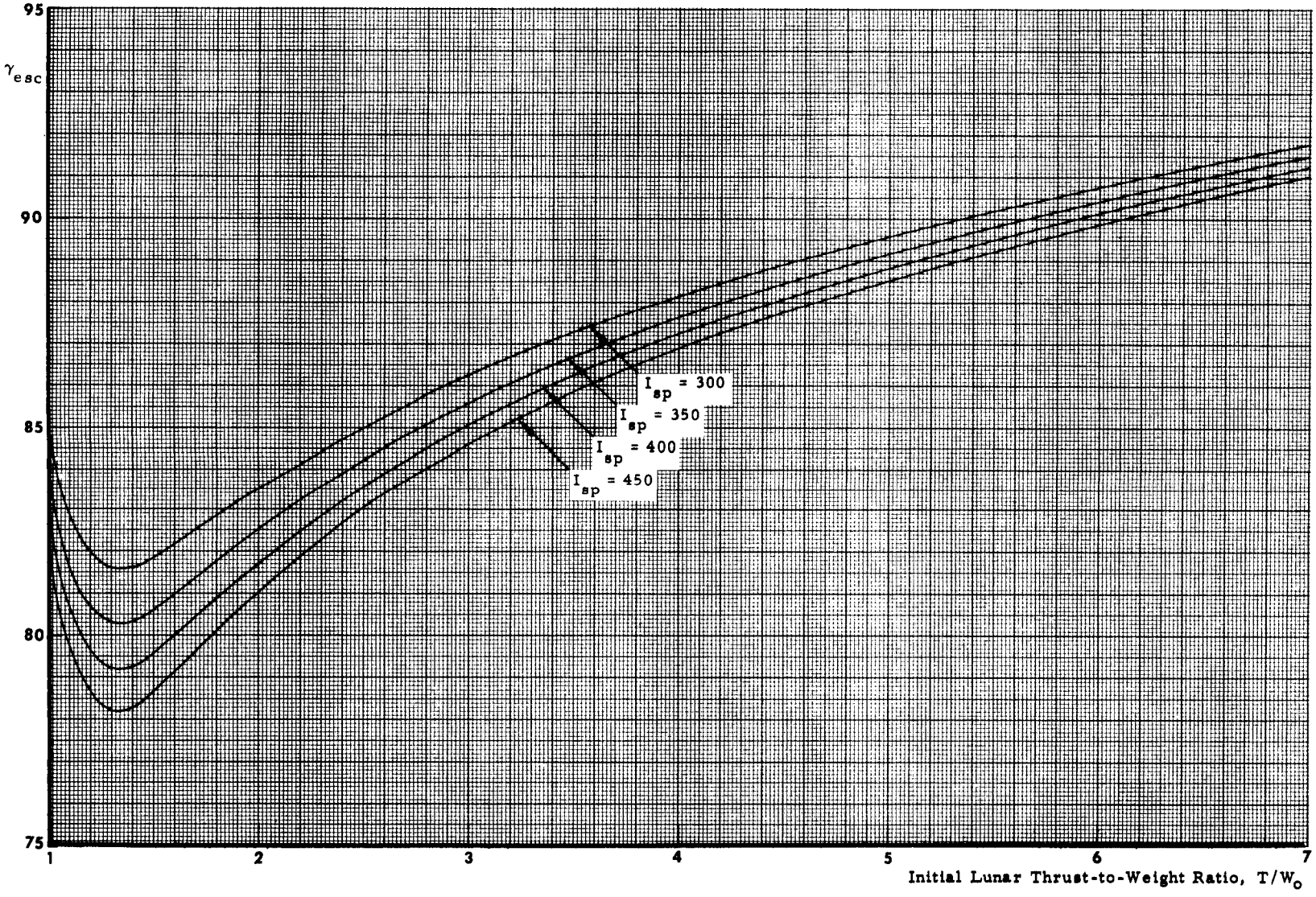

FIGURE 21. GAMMA AT ESCAPE VS INITIAL LUNAR THRUST-TO-WEIGHT RATIO FOR ESCAPE THROUGH A 15 Km. CIRCULAR ORBIT. THRUST AND VELOCITY VECTORS NOT ALIGNED AT ESCAPE.

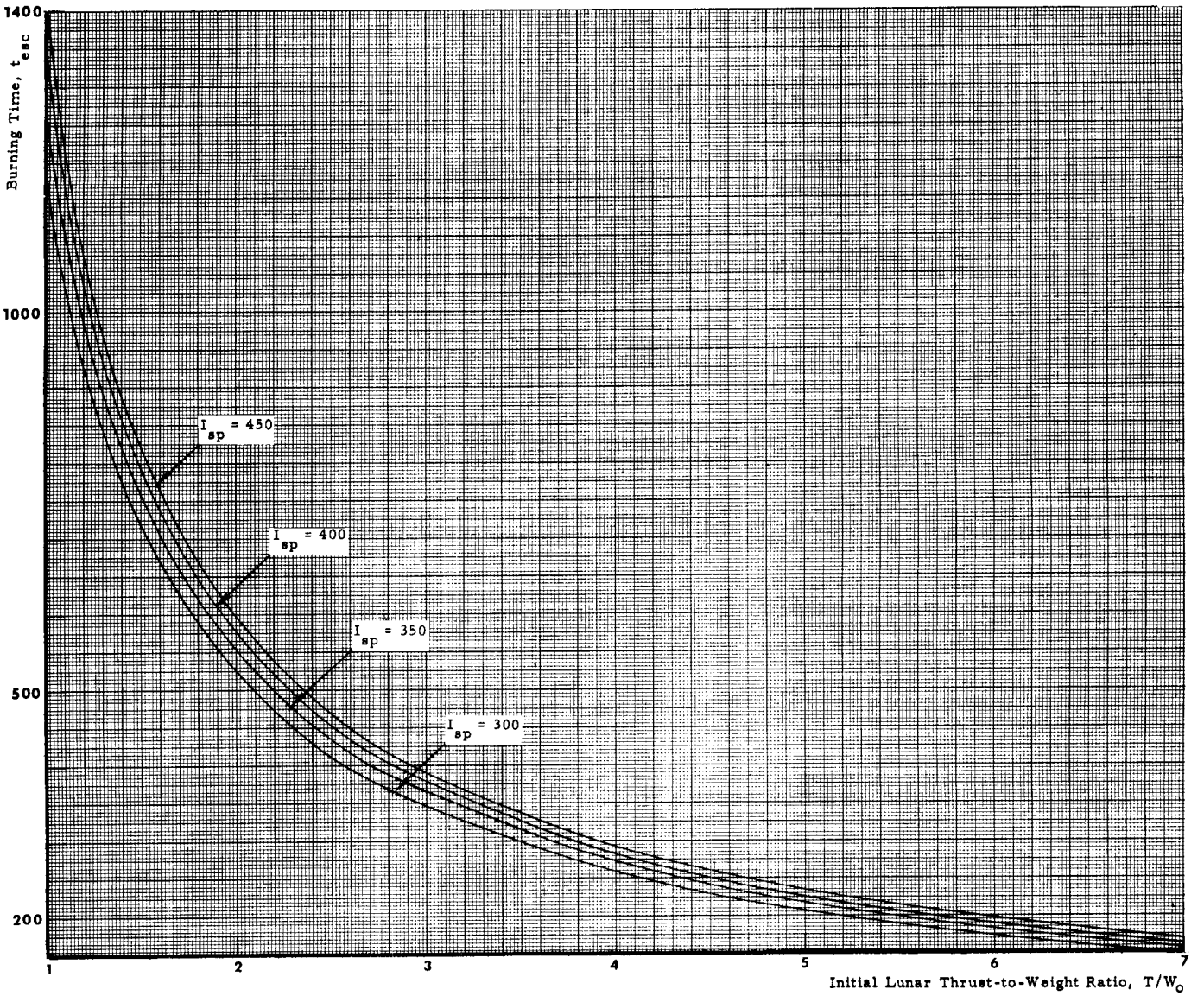

FIGURE 22. BURNING TIME TO ESCAPE VS INITIAL LUNAR THRUST-TO-WEIGHT RATIO FOR ESCAPE THROUGH A 15-Km. CIRCULAR ORBIT. THRUST AND VELOCITY VECTORS NOT ALIGNED AT ESCAPE.

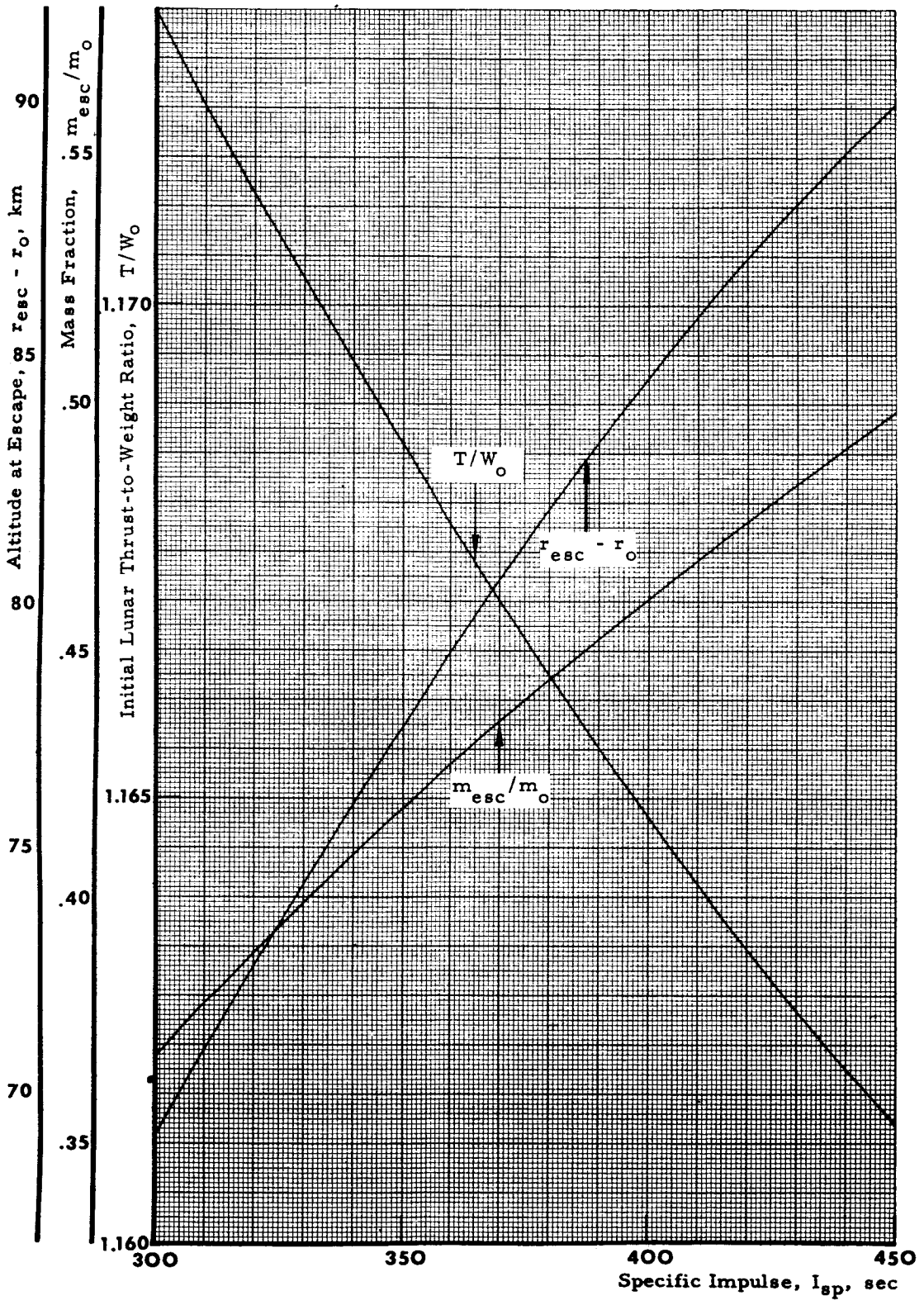

FIGURE 23. ALTITUDE, INITIAL LUNAR THRUST-TO-WEIGHT RATIO, AND MASS FRACTION VS SPECIFIC IMPULSE. $r_{esc}-r_o$ MAXIMIZED WITH RESPECT TO T/W_o. THRUST AND VELOCITY VECTORS ALIGNED AT CIRCULAR ORBIT BUT NOT ALIGNED AT ESCAPE.

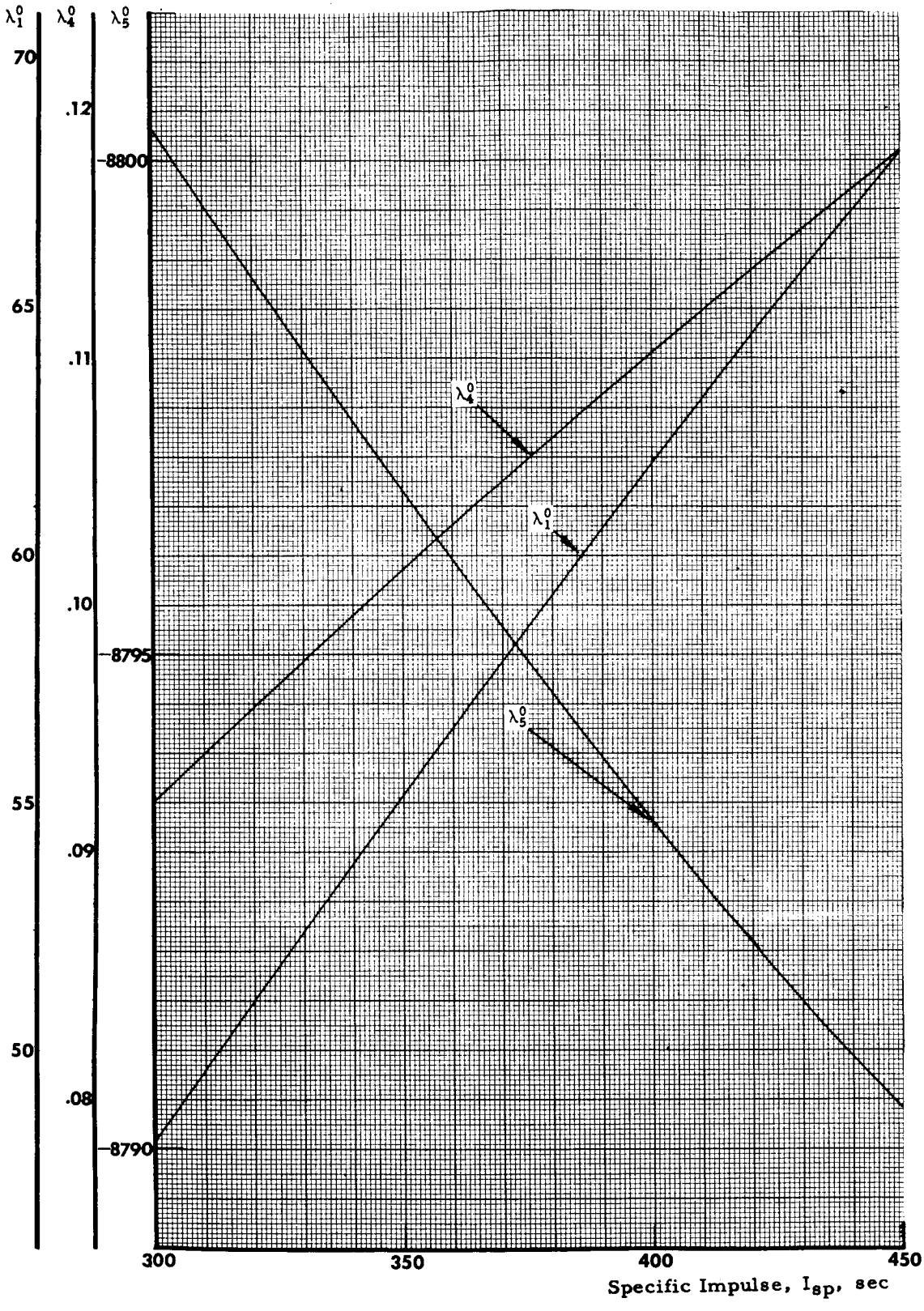

FIGURE 24. INITIAL VALUES OF λ_1, λ_4 and λ_5 VS SPECIFIC IMPULSE, $r_{esc}-r_o$ MAXIMIZED WITH RESPECT TO T/W_o. THRUST AND VELOCITY VECTORS ALIGNED AT CIRCULAR ORBIT BUT NOT ALIGNED AT ESCAPE.

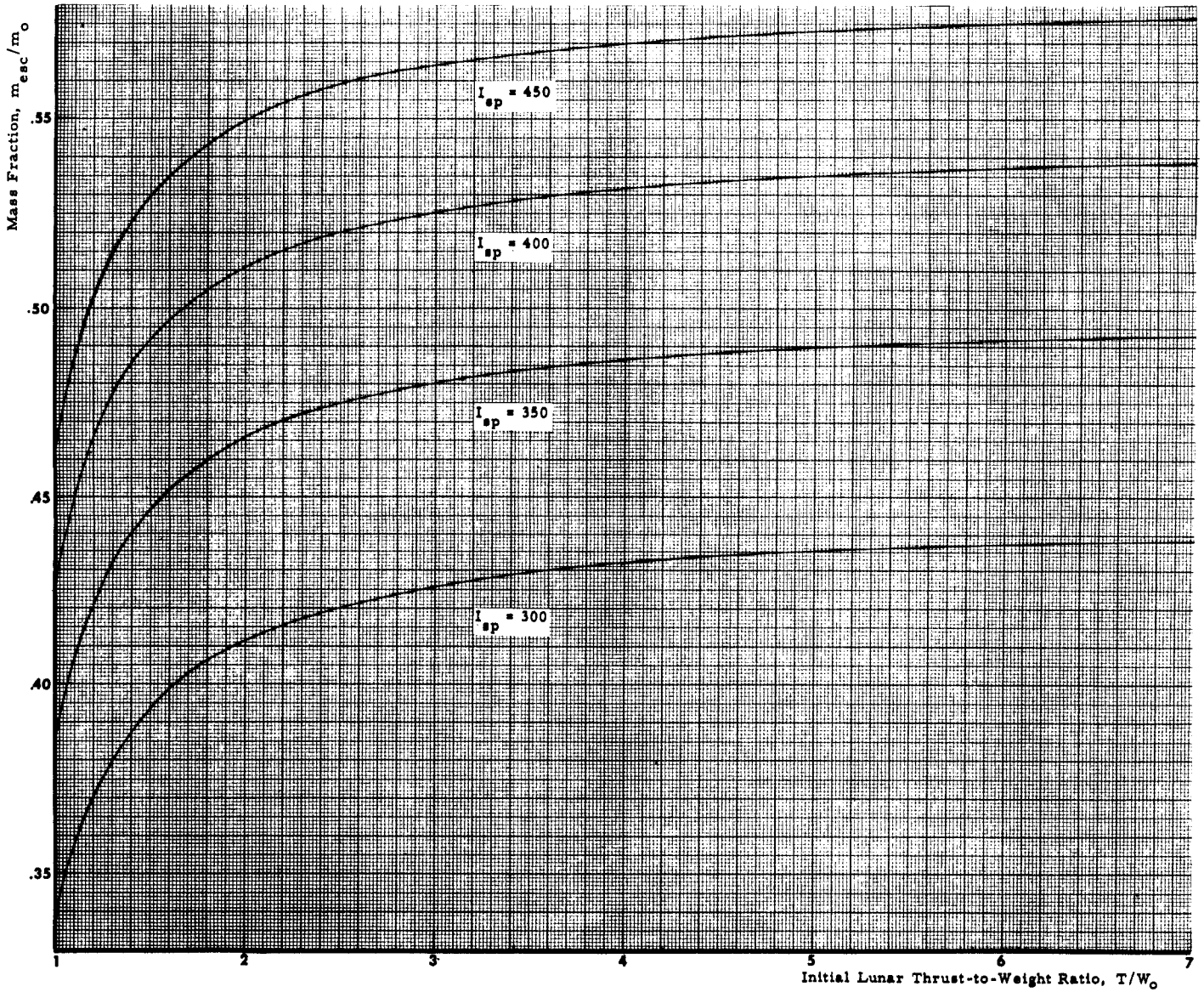

FIGURE 25. MASS FRACTION VS INITIAL LUNAR THRUST-TO-WEIGHT RATIO. THRUST AND VELOCITY VECTORS ALIGNED AT CIRCULAR ORBIT BUT NOT ALIGNED AT ESCAPE.

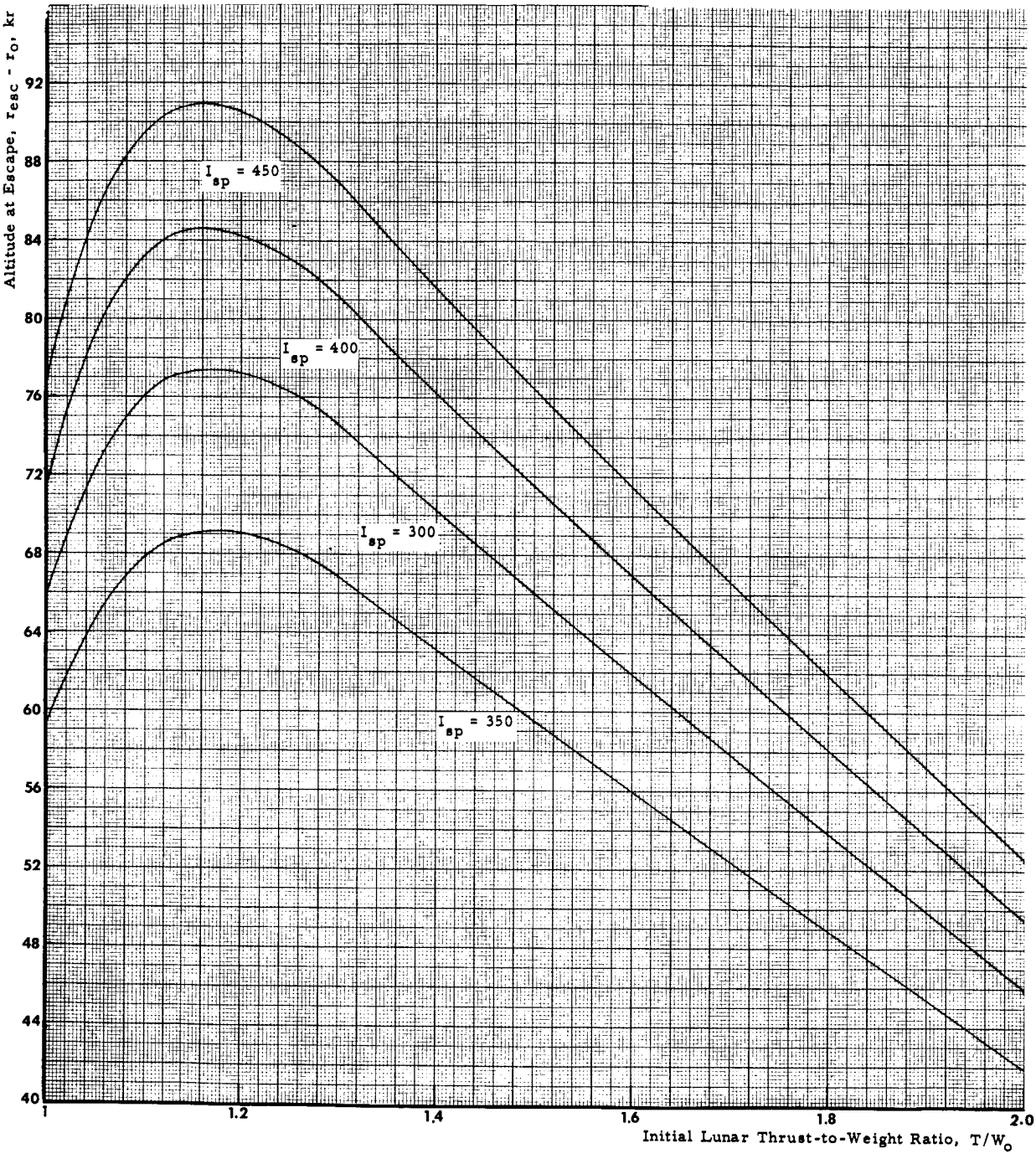

FIGURE 26. ALTITUDE VS INITIAL LUNAR THRUST-TO-WEIGHT RATIO. THRUST AND VELOCITY VECTORS ALIGNED AT CIRCULAR ORBIT BUT NOT ALIGNED AT ESCAPE.

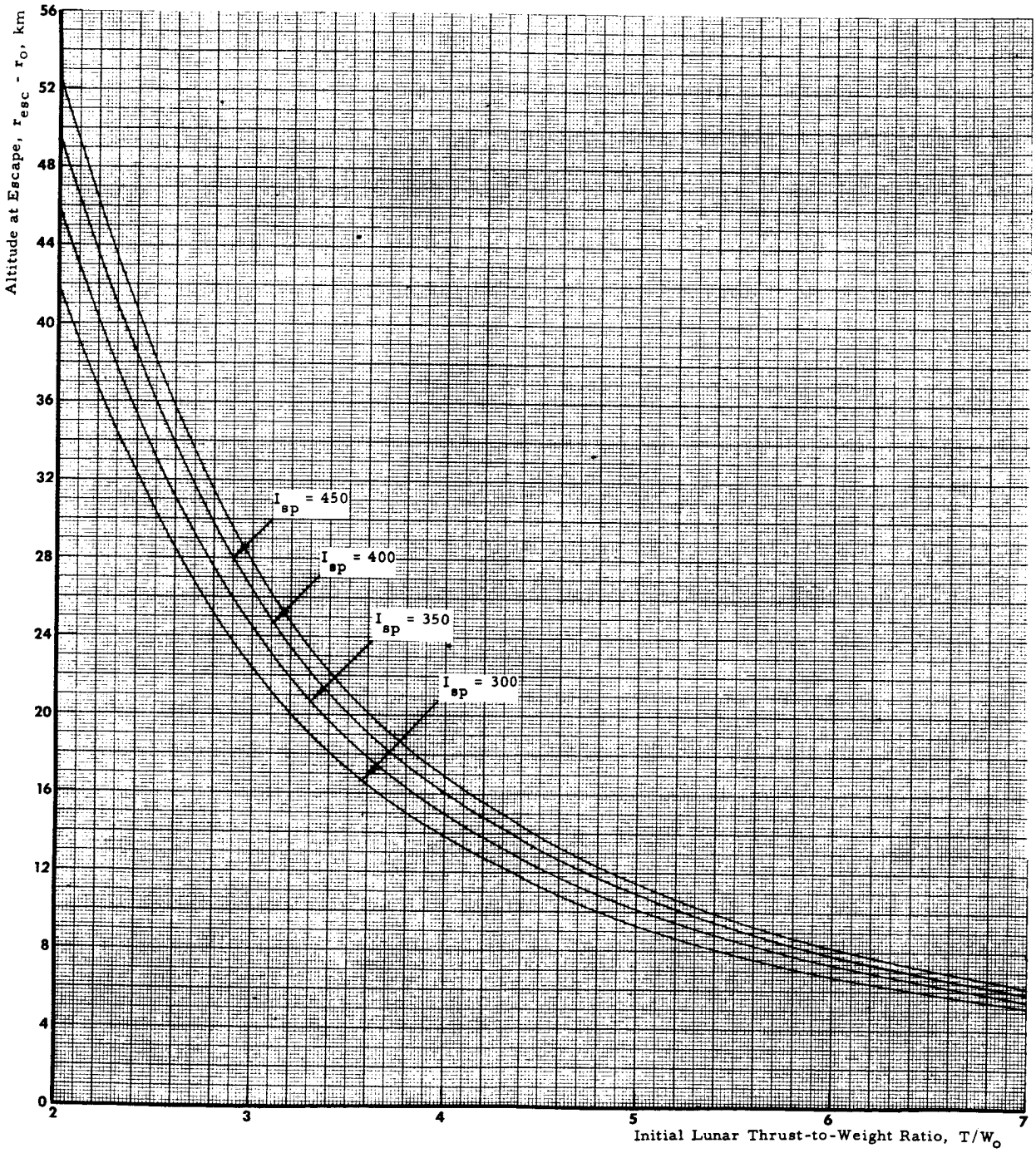

FIGURE 27. ALTITUDE VS INITIAL LUNAR THRUST-TO-WEIGHT RATIO. THRUST AND VELOCITY VECTORS ALIGNED AT CIRCULAR ORBIT BUT NOT ALIGNED AT ESCAPE.

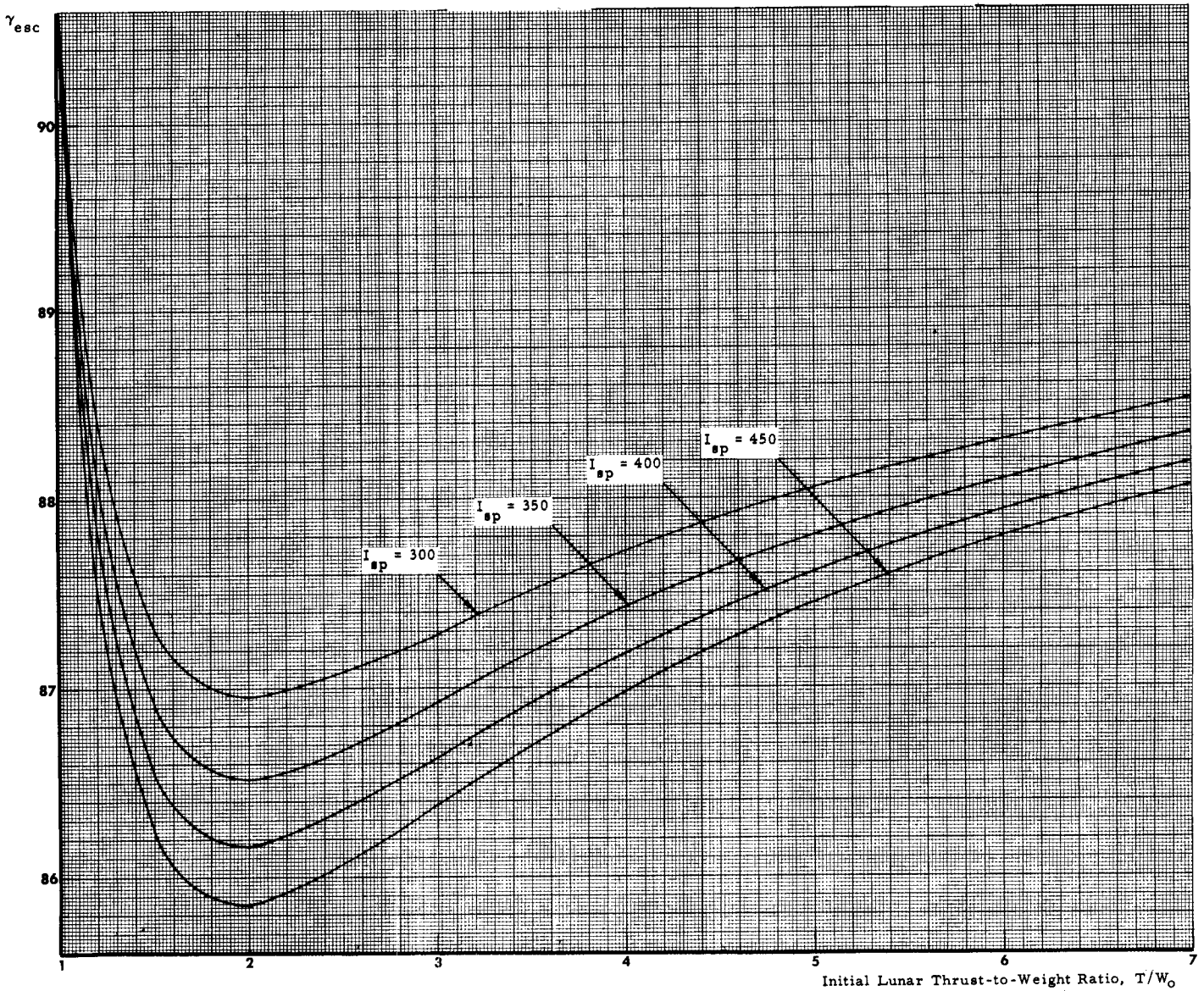

FIGURE 28. GAMMA AT ESCAPE VS INITIAL LUNAR THRUST-TO-WEIGHT RATIO. THRUST AND VELOCITY VECTORS ALIGNED AT CIRCULAR ORBIT BUT NOT ALIGNED AT ESCAPE.

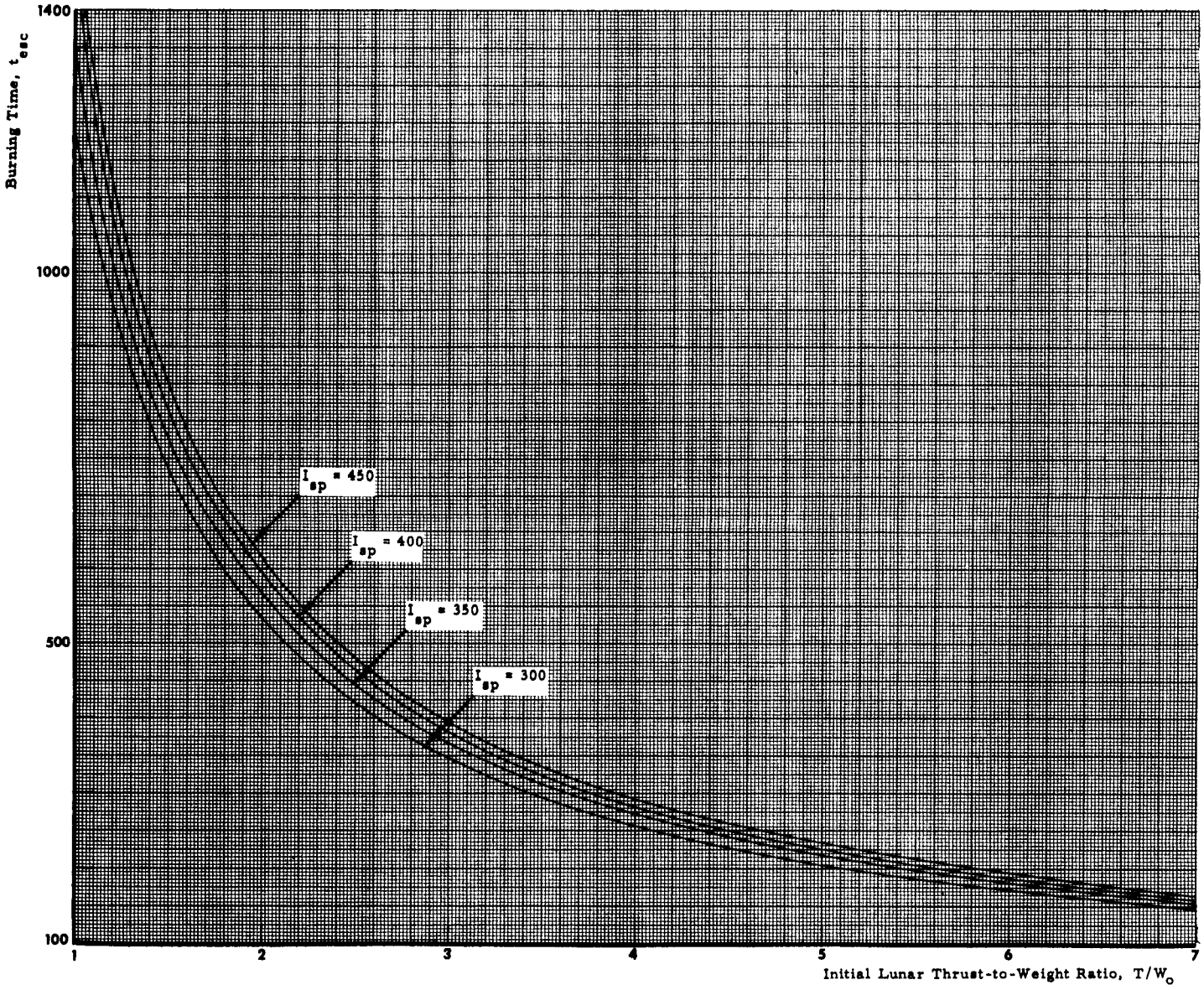

FIGURE 29. BURNING TIME TO ESCAPE VS INITIAL LUNAR THRUST-TO-WEIGHT RATIO. THRUST AND VELOCITY VECTORS ALIGNED AT CIRCULAR ORBIT BUT NOT ALIGNED AT ESCAPE.

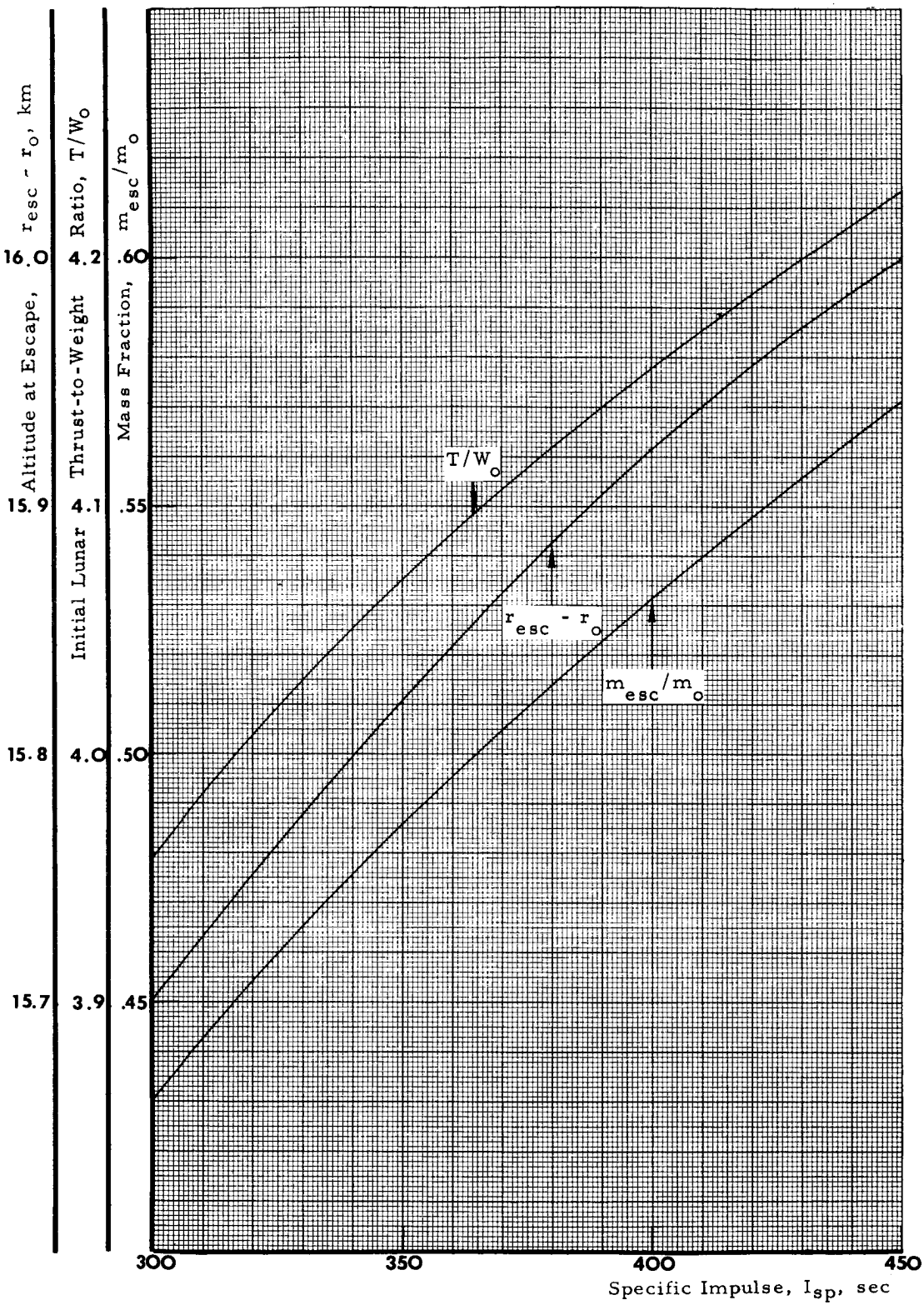

FIGURE 30. ALTITUDE, INITIAL LUNAR THRUST-TO-WEIGHT RATIO, AND MASS FRACTION VS SPECIFIC IMPULSE FOR ESCAPE THROUGH A 15-Km. CIRCULAR ORBIT. m_{esc}/m_o MAXIMIZED WITH RESPECT TO T/W_o. THRUST AND VELOCITY VECTORS ALIGNED AT ESCAPE VIA λ_4 DISCONTINUITY AT CIRCULAR ORBIT.

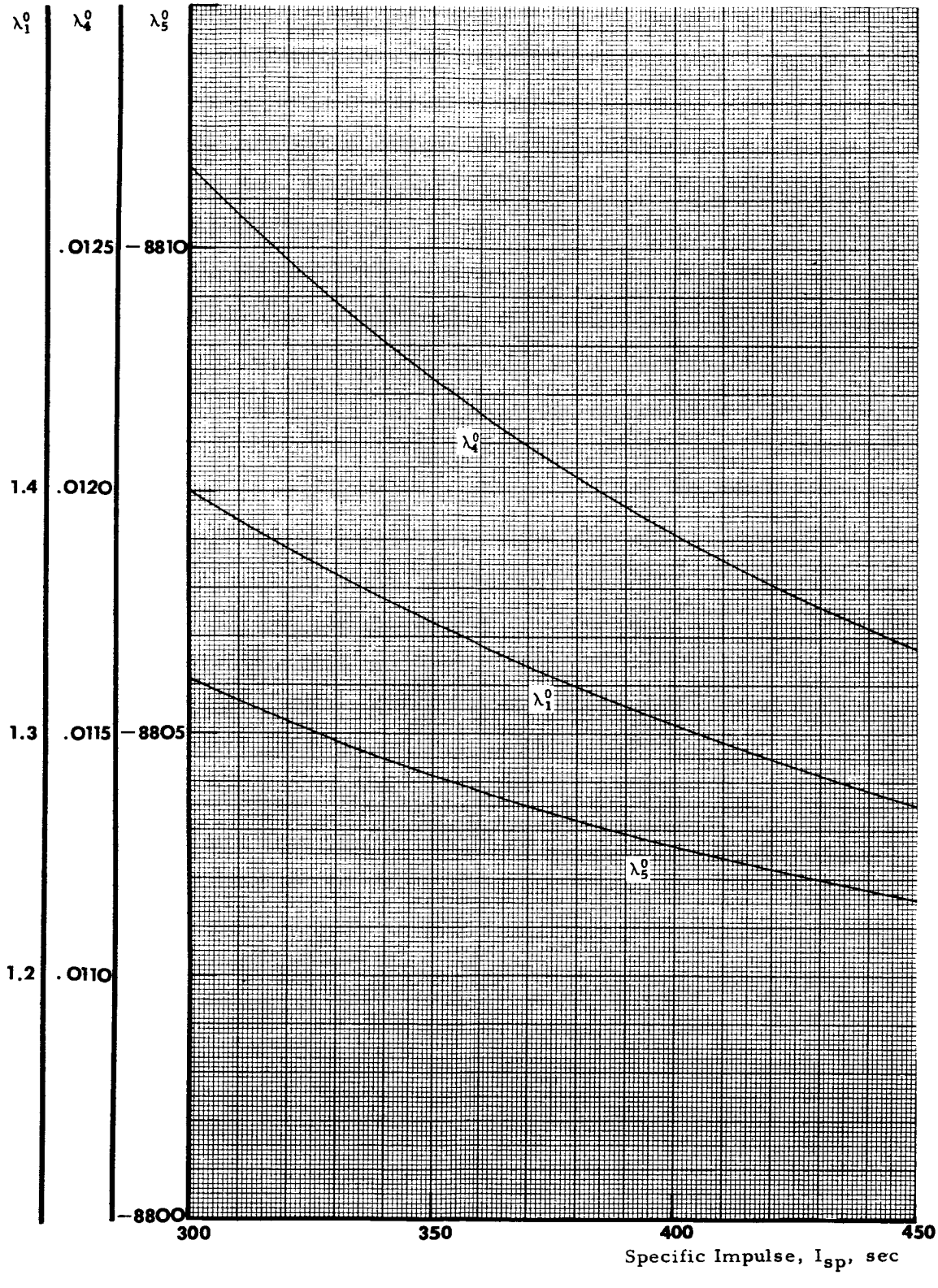

FIGURE 31. INITIAL VALUES OF λ_1, λ_4, AND λ_5 VS SPECIFIC IMPULSE FOR ESCAPE THROUGH A 15-Km. CIRCULAR ORBIT. m_{esc}/m_o MAXIMIZED WITH RESPECT TO T/W_o. THRUST AND VELOCITY VECTORS ALIGNED AT ESCAPE VIA λ_4 DISCONTINUITY AT CIRCULAR ORBIT.

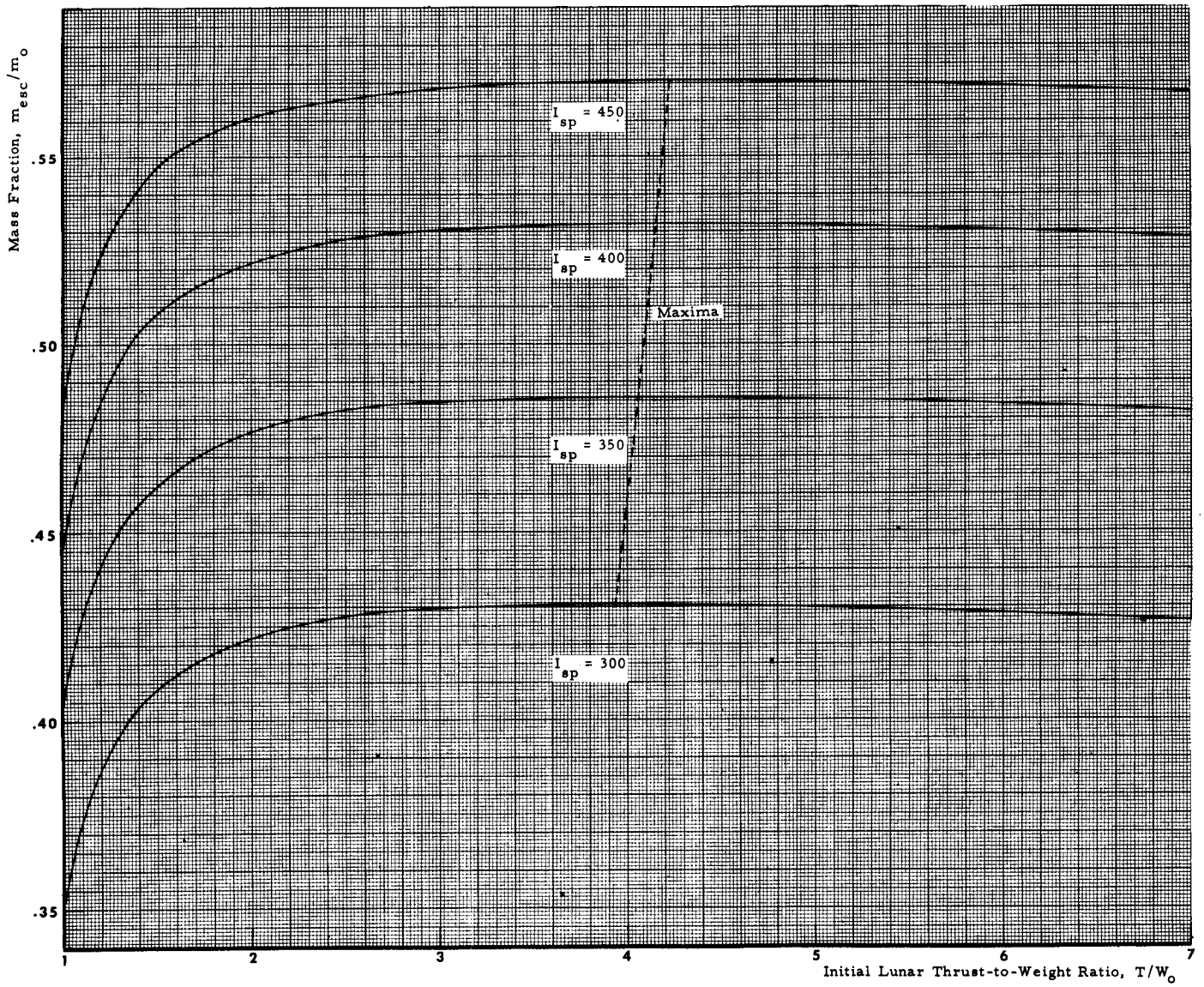

FIGURE 32. MASS FRACTION VS INITIAL LUNAR THRUST-TO-WEIGHT RATIO FOR ESCAPE THROUGH A 15-Km. CIRCULAR ORBIT. THRUST AND VELOCITY VECTORS ALIGNED AT ESCAPE VIA λ_4 DISCONTINUITY AT CIRCULAR ORBIT.

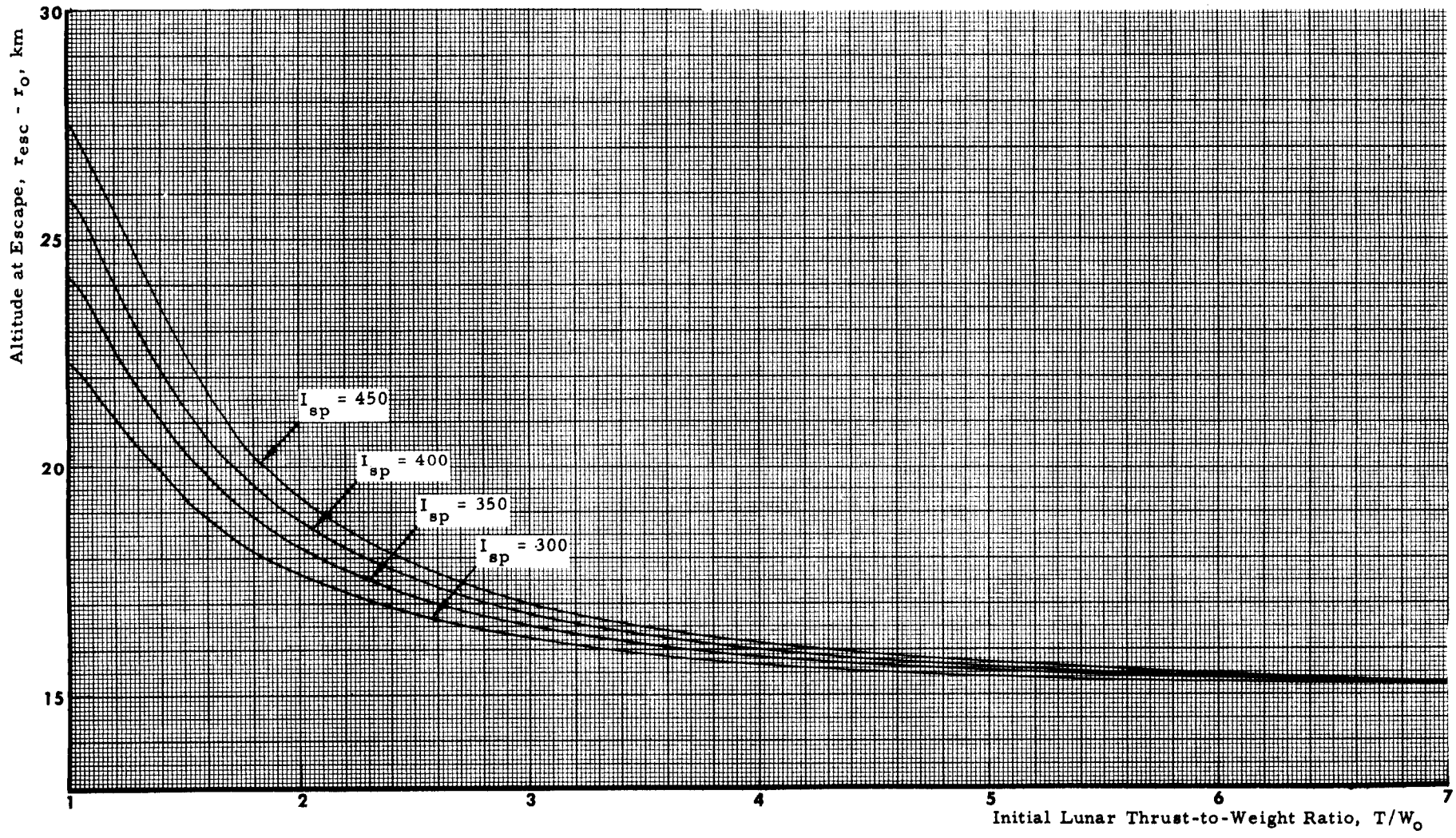

FIGURE 33. ALTITUDE VS INITIAL LUNAR THRUST-TO-WEIGHT RATIO FOR ESCAPE THROUGH A 15 Km. CIRCULAR ORBIT. THRUST AND VELOCITY VECTORS ALIGNED AT ESCAPE VIA λ_4 DISCONTINUITY AT CIRCULAR ORBIT.

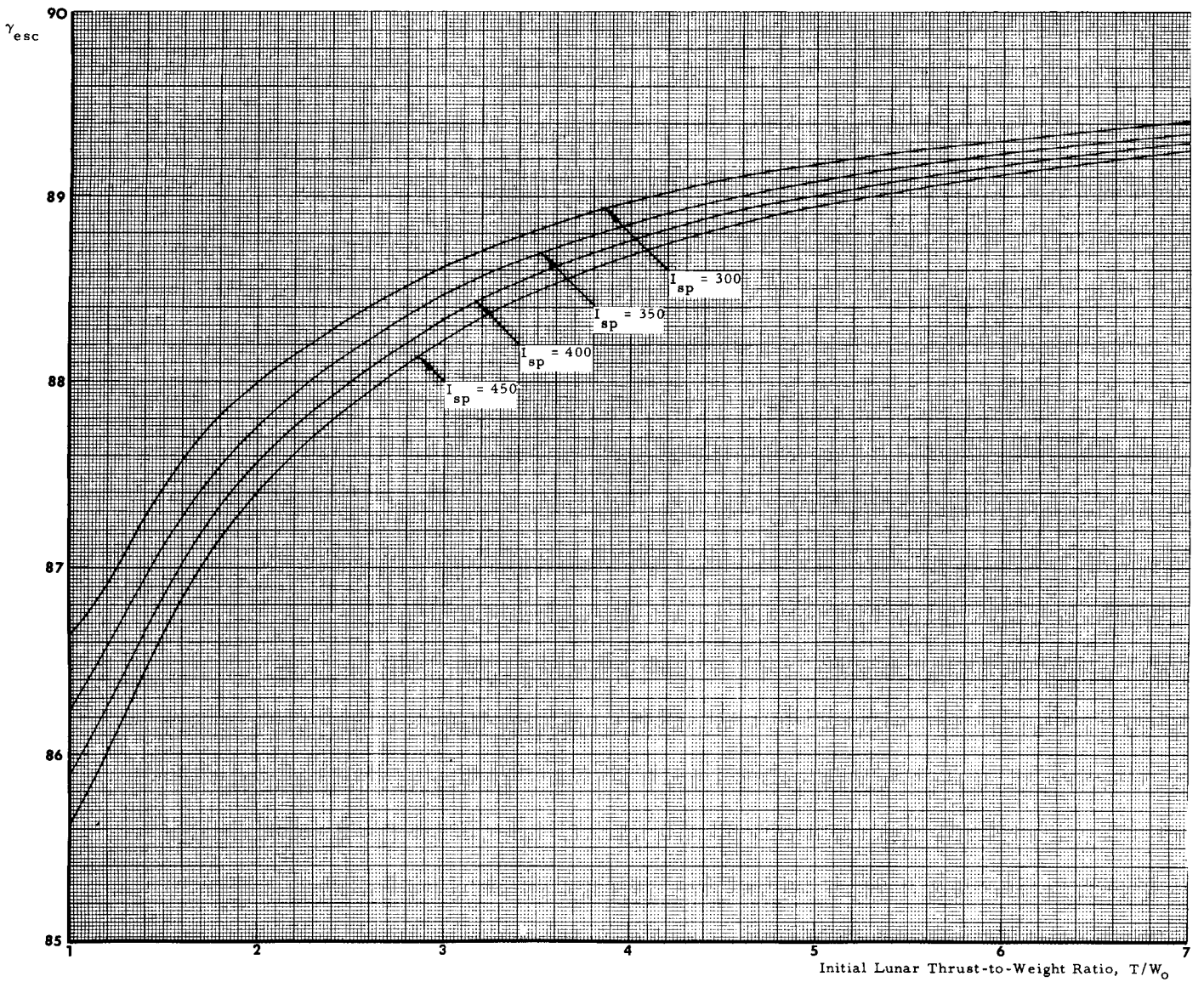

FIGURE 34. GAMMA AT ESCAPE VS INITIAL LUNAR THRUST-TO-WEIGHT RATIO FOR ESCAPE THROUGH A 15 Km. CIRCULAR ORBIT. THRUST AND VELOCITY VECTORS ALIGNED AT ESCAPE VIA λ_4 DISCONTINUITY AT CIRCULAR ORBIT.

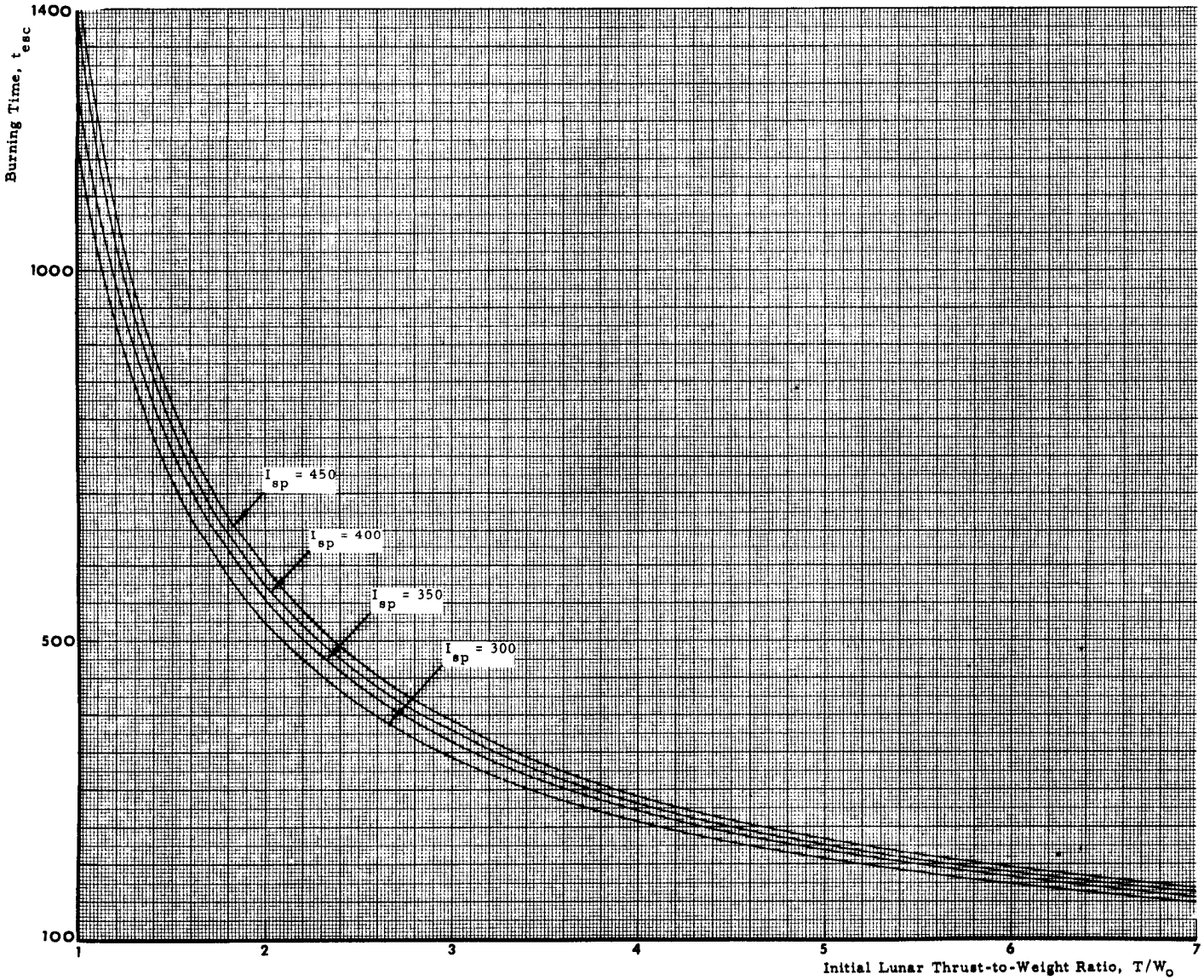

FIGURE 35. BURNING TIME TO ESCAPE VS INITIAL LUNAR THRUST-TO-WEIGHT RATIO FOR ESCAPE THROUGH A 15 Km. CIRCULAR ORBIT. THRUST AND VELOCITY VECTORS ALIGNED AT ESCAPE VIA λ_4 DISCONTINUITY AT CIRCULAR ORBIT.

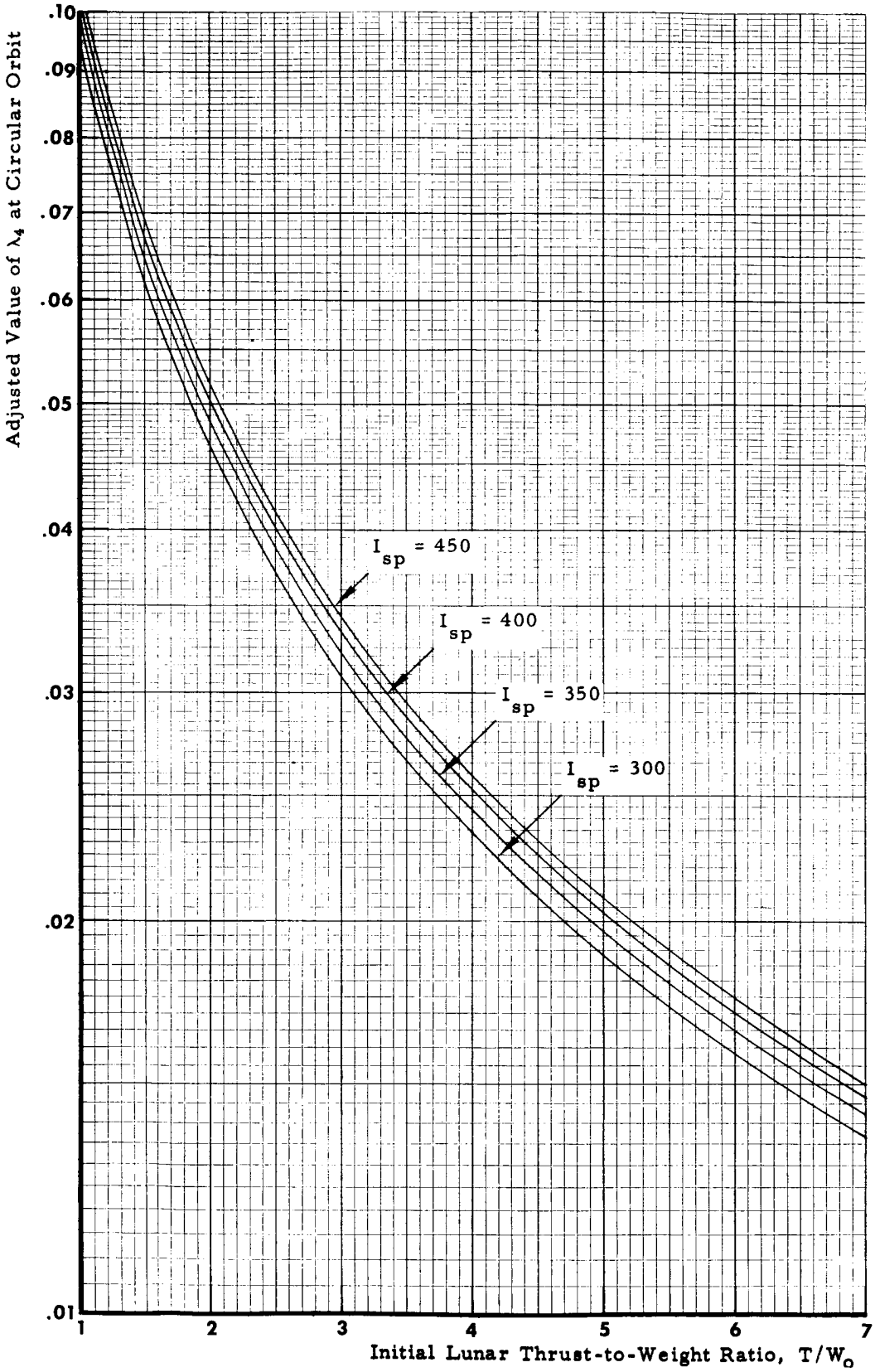

FIGURE 36. ADJUSTED VALUE OF λ_4 AT CIRCULAR ORBIT VS INITIAL LUNAR THRUST-TO-WEIGHT RATIO

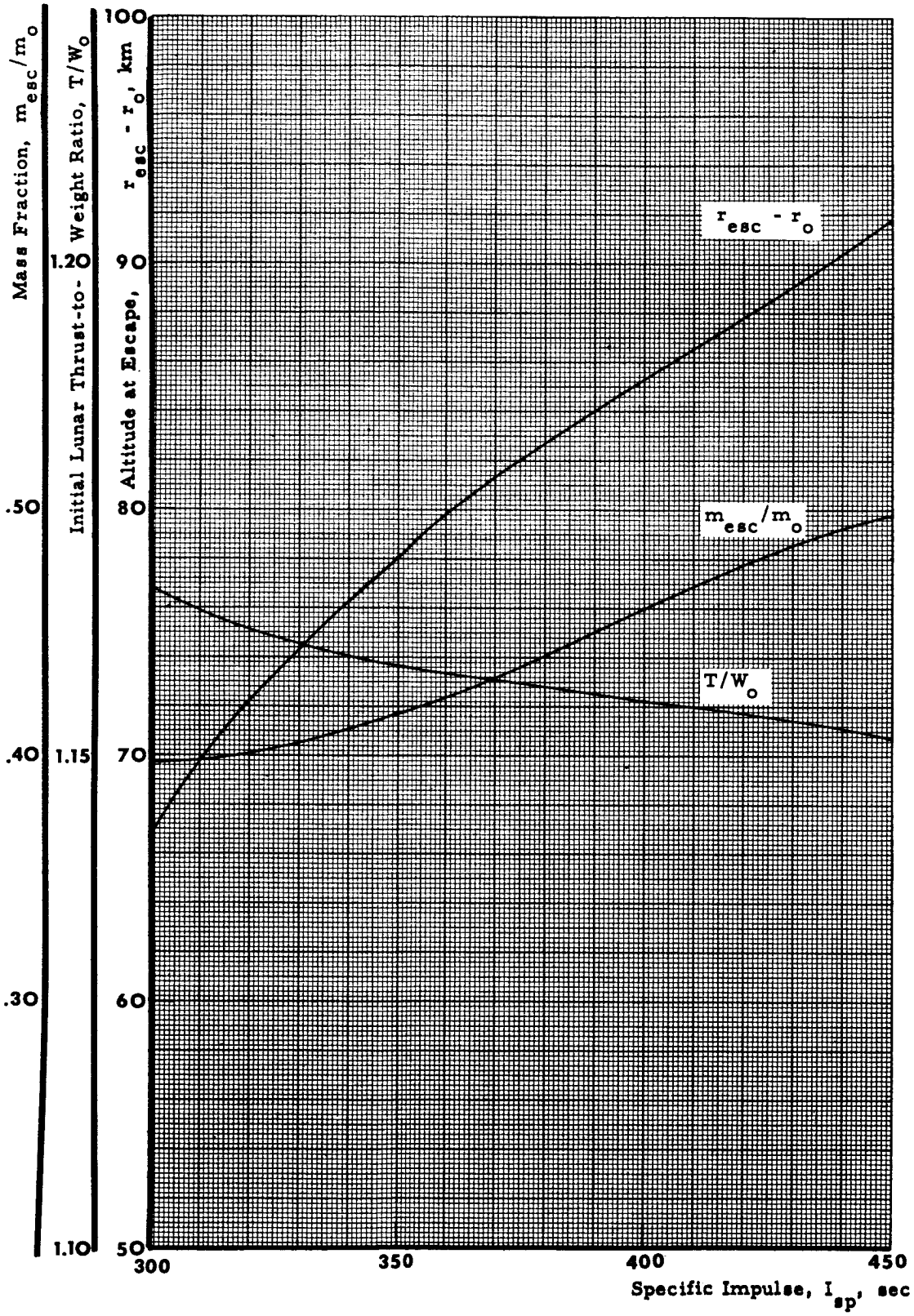

FIGURE 37. MASS FRACTION, INITIAL LUNAR THRUST-TO-WEIGHT RATIO, AND ALTITUDE VS SPECIFIC IMPULSE. $r_{esc}-r_o$ MAXIMIZED WITH RESPECT TO T/W_o. THRUST AND VELOCITY VECTORS ALIGNED AT ORBIT; ALIGNMENT AT ESCAPE VIA λ_4 DISCONTINUITY AT ORBIT.

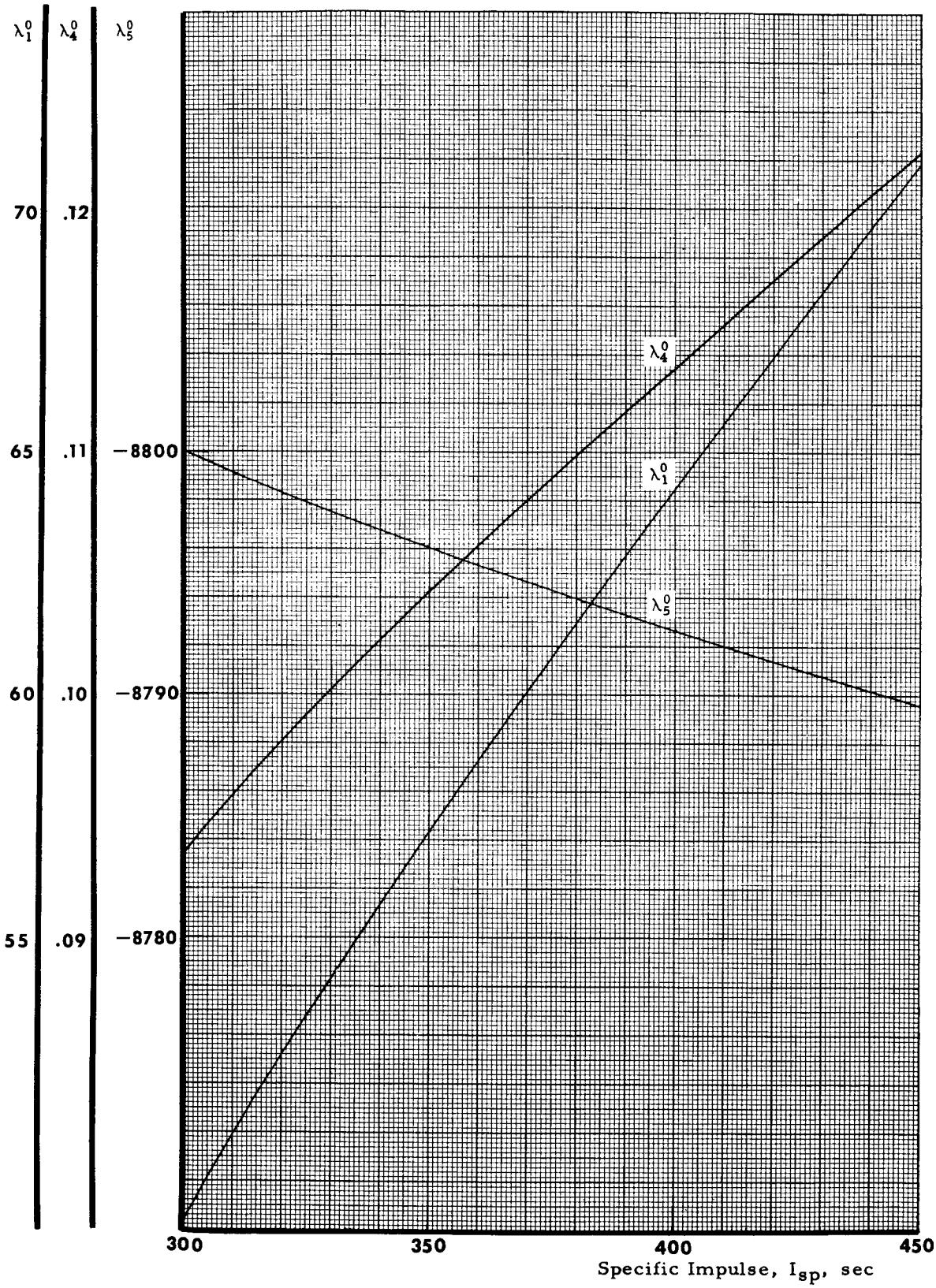

FIGURE 38. INITIAL VALUES OF λ_1, λ_4, AND λ_5 VS SPECIFIC IMPULSE. $r_{esc}-r_0$ MAXIMIZED WITH RESPECT TO T/W_0. THRUST AND VELOCITY VECTORS ALIGNED AT ORBIT: ALIGNMENT AT ESCAPE VIA λ_4 DISCONTINUITY AT ORBIT.

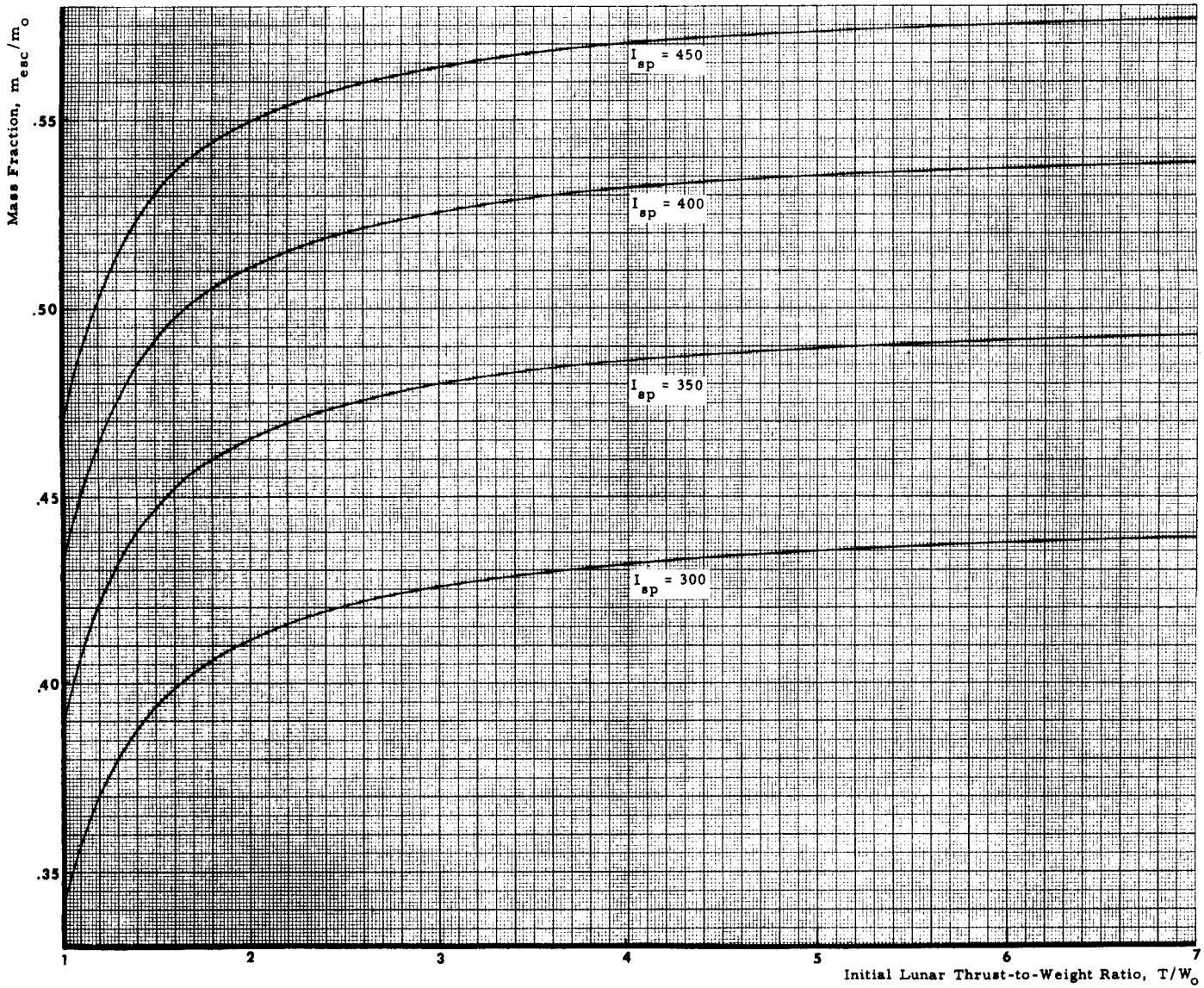

FIGURE 39. MASS FRACTION VS INITIAL LUNAR THRUST-TO-WEIGHT RATIO. THRUST AND VELOCITY VECTORS ALIGNED AT ORBIT: ALIGNMENT AT ESCAPE VIA λ_4 DISCONTINUITY AT ORBIT.

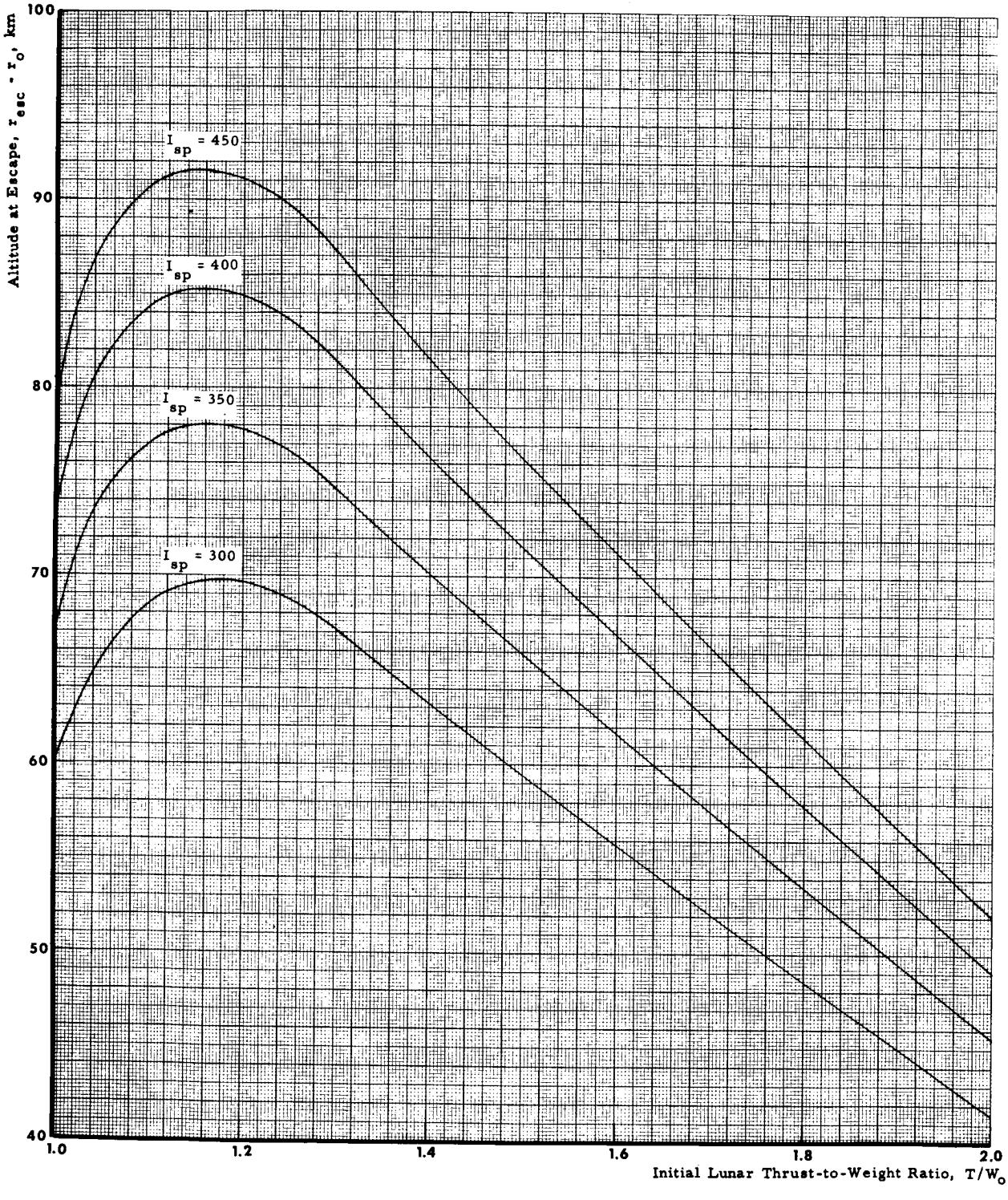

FIGURE 40. ALTITUDE VS INITIAL LUNAR THRUST-TO-WEIGHT RATIO. THRUST AND VELOCITY VECTORS ALIGNED AT ORBIT: ALIGNMENT AT ESCAPE VIA λ_4 DISCONTINUITY AT ORBIT.

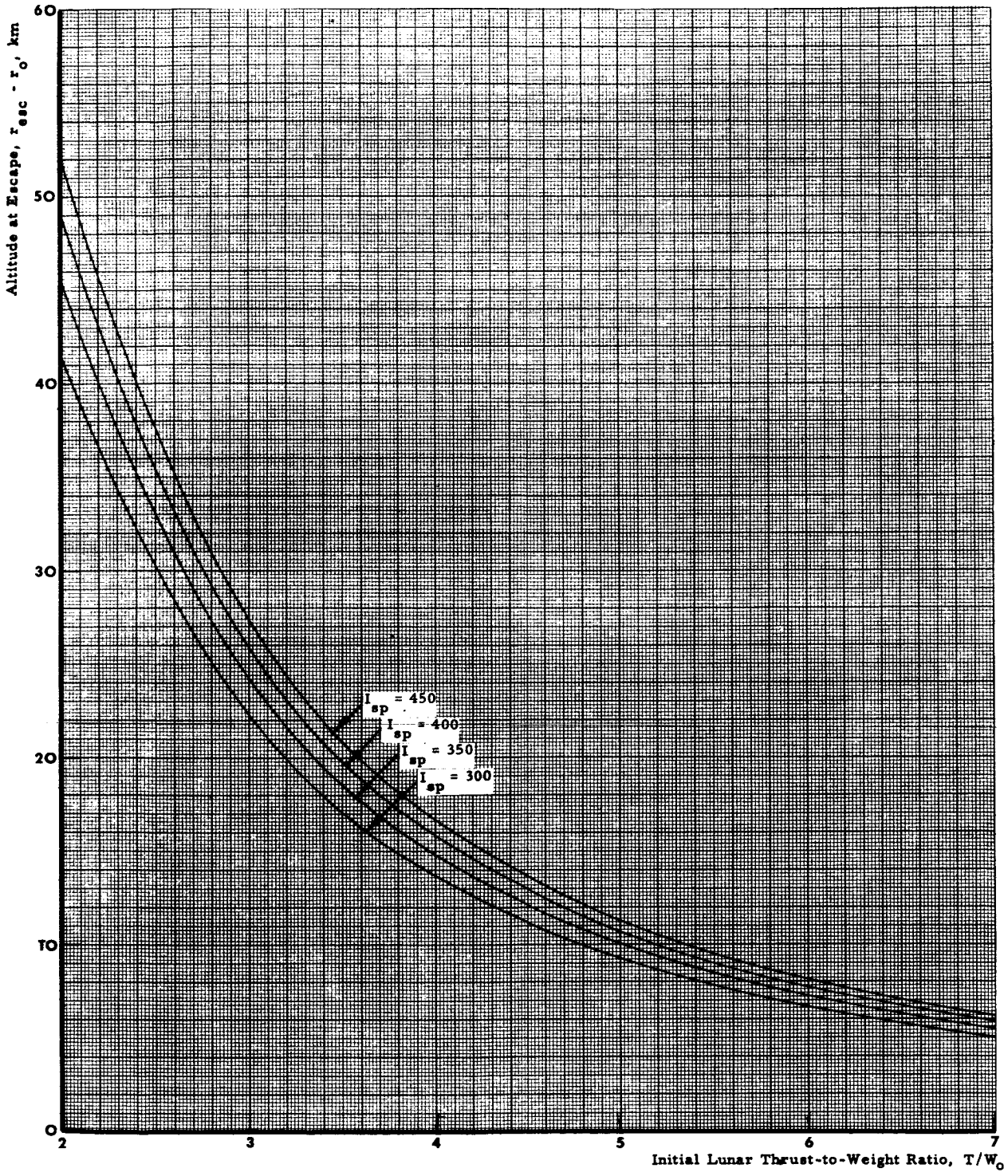

FIGURE 41. ALTITUDE VS INITIAL LUNAR THRUST-TO-WEIGHT RATIO. THRUST AND VELOCITY VECTORS ALIGNED AT ORBIT: ALIGNMENT AT ESCAPE VIA λ_4 DISCONTINUITY AT ORBIT.

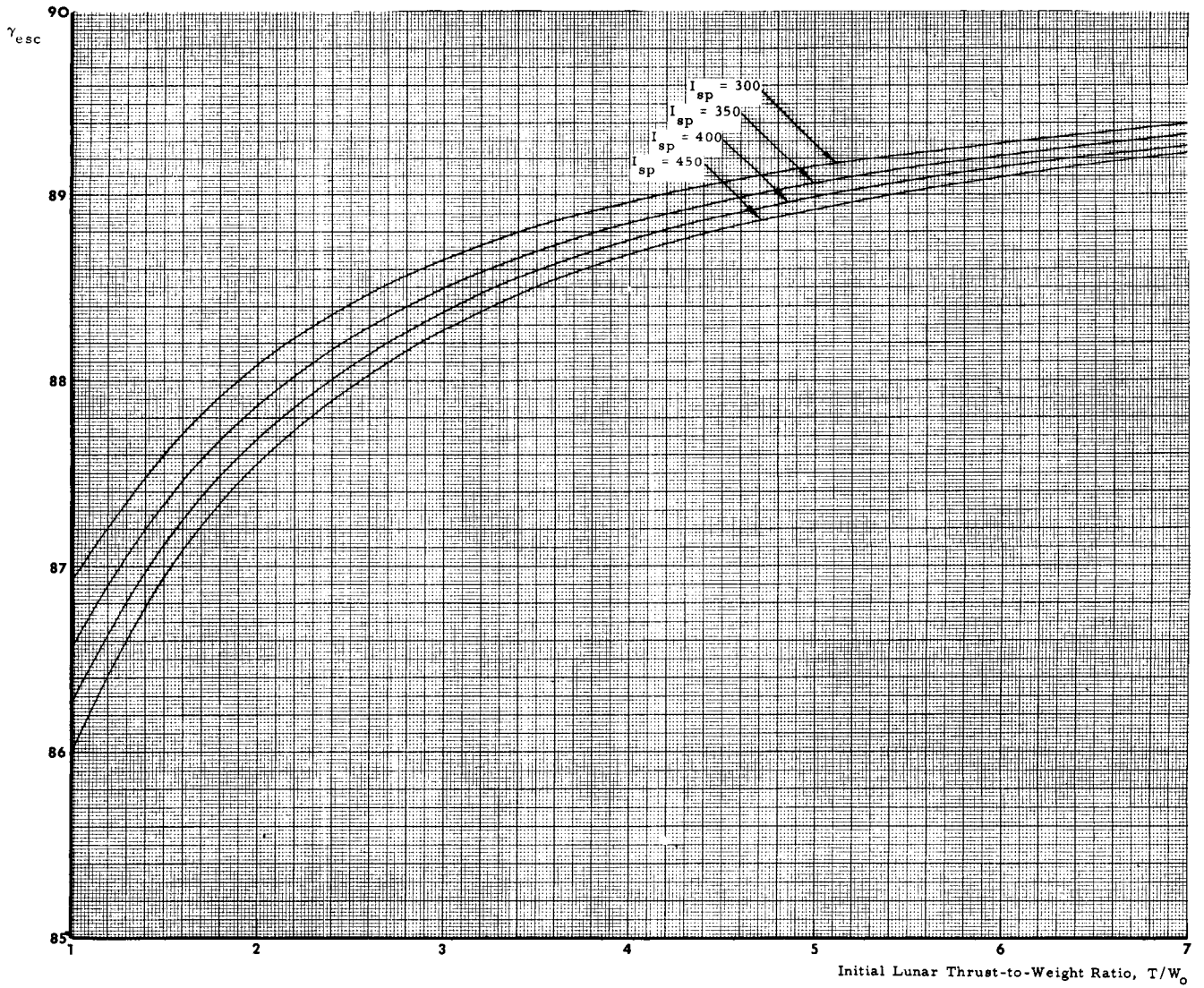

FIGURE 42. GAMMA AT ESCAPE VS INITIAL LUNAR THRUST-TO-WEIGHT RATIO. THRUST AND VELOCITY VECTORS ALIGNED AT ORBIT: ALIGNMENT AT ESCAPE VIA λ_4 DISCONTINUITY AT ORBIT.

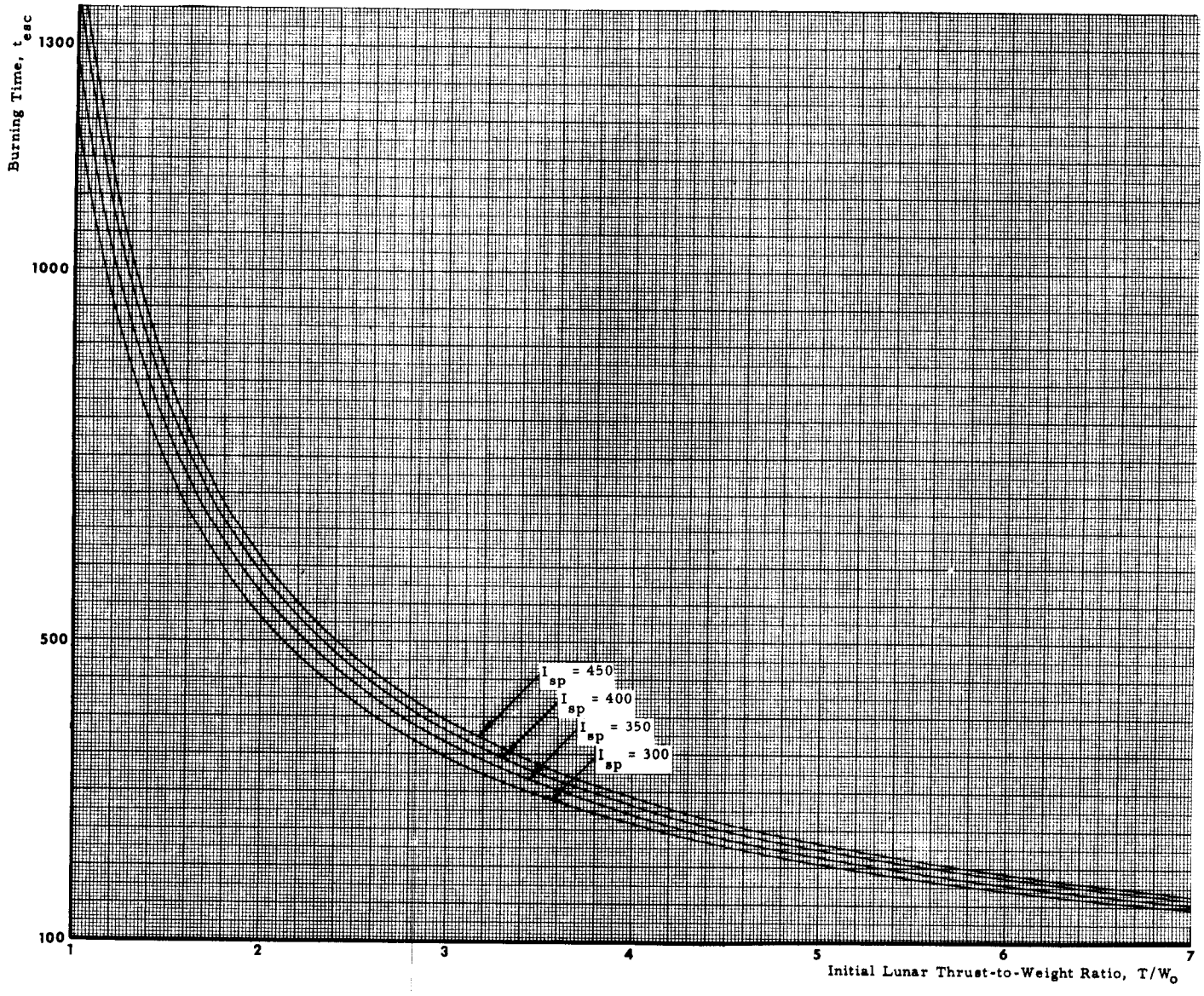

FIGURE 43. BURNING TIME TO ESCAPE VS INITIAL LUNAR THRUST-TO-WEIGHT RATIO. THRUST AND VELOCITY VECTORS ALIGNED AT ORBIT: ALIGNMENT AT ESCAPE VIA λ_4 DISCONTINUITY AT ORBIT.

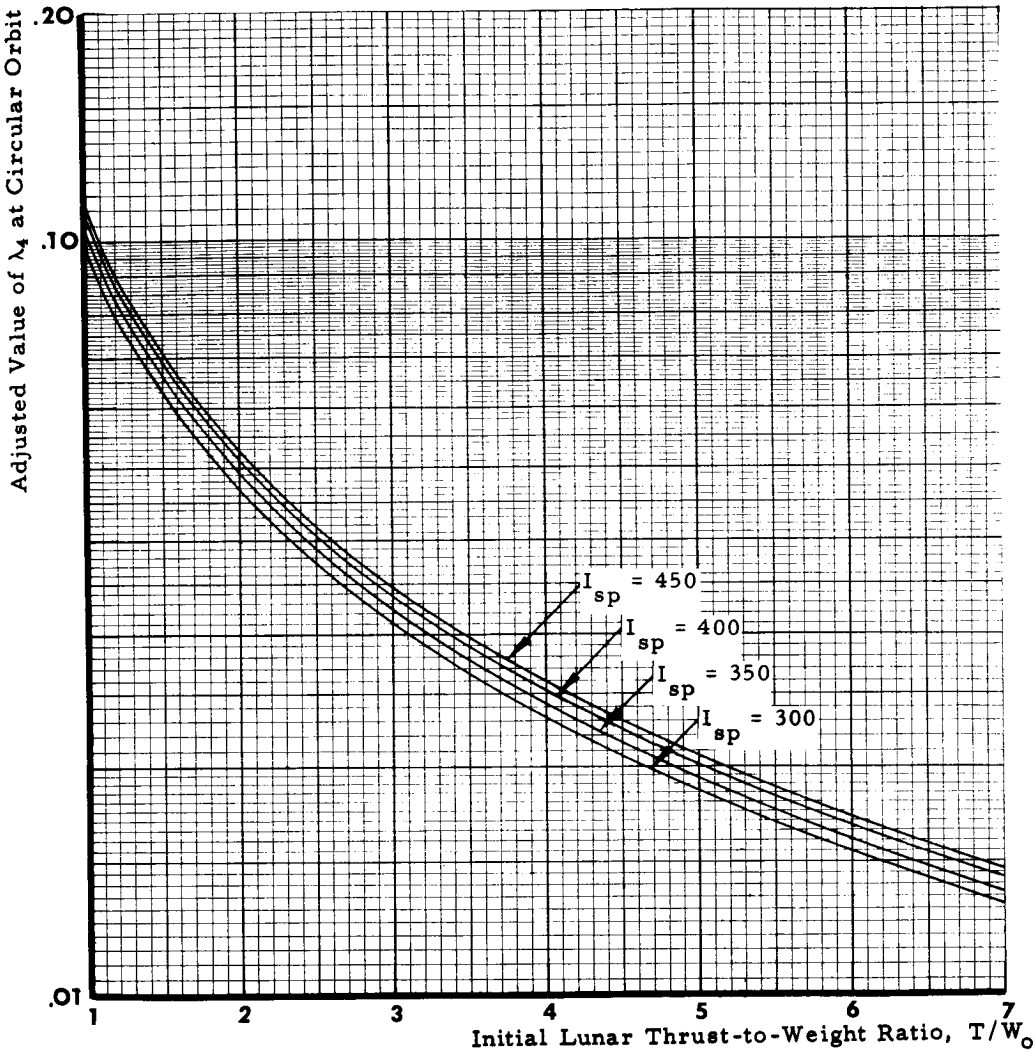

FIGURE 44. ADJUSTED VALUE OF λ_4 AT CIRCULAR ORBIT VS INITIAL LUNAR THRUST-TO-WEIGHT RATIO.

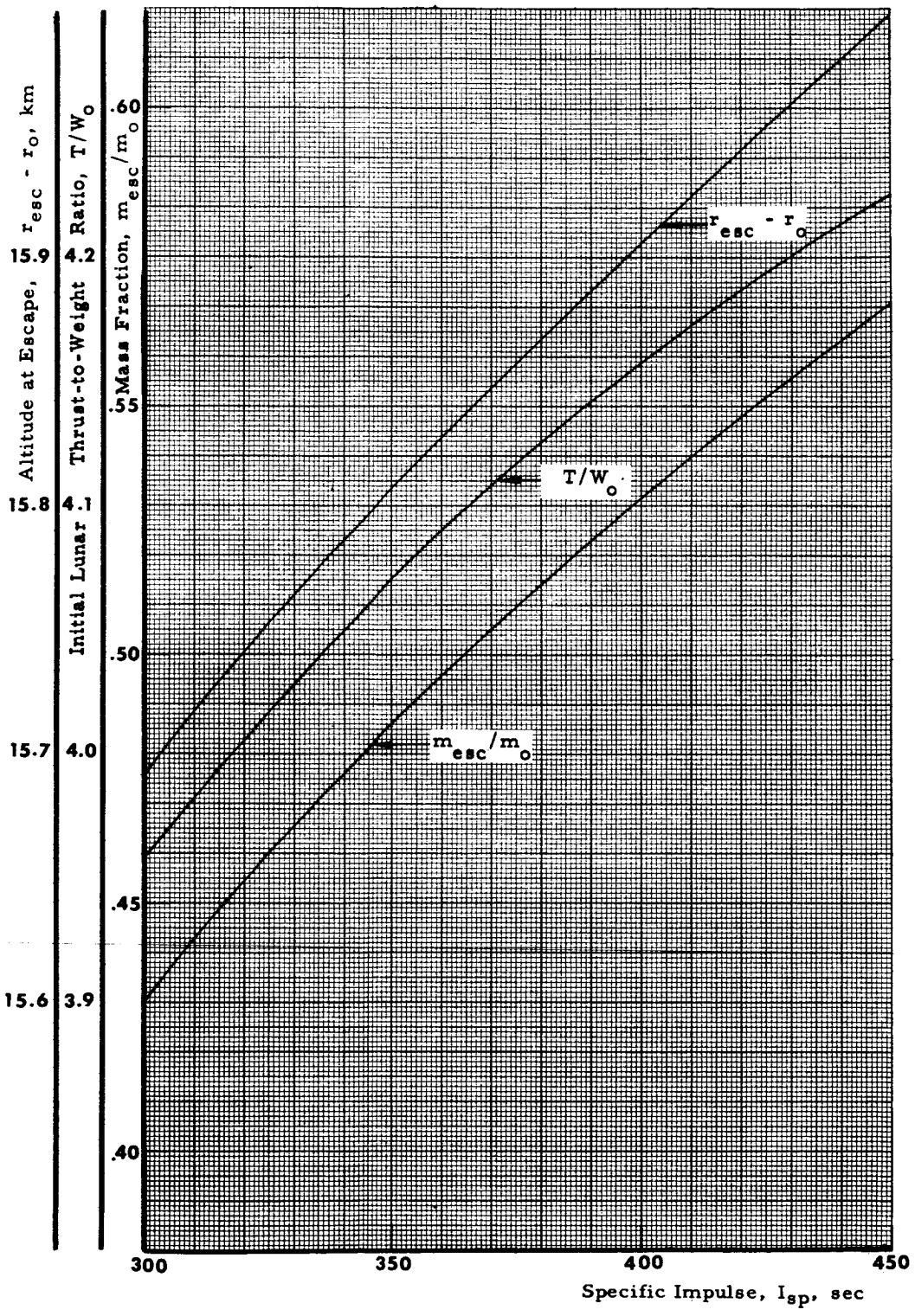

FIGURE 45. ALTITUDE, INITIAL LUNAR THRUST-TO-WEIGHT RATIO, AND MASS FRACTION VS SPECIFIC IMPULSE FOR ESCAPE THROUGH A 15 Km. CIRCULAR ORBIT. m_{esc}/m_o MAXIMIZED WITH RESPECT TO T/W_o. THRUST AND VELOCITY VECTORS ALIGNED AT ESCAPE VIA λ_3 DISCONTINUITY AT CIRCULAR ORBIT.

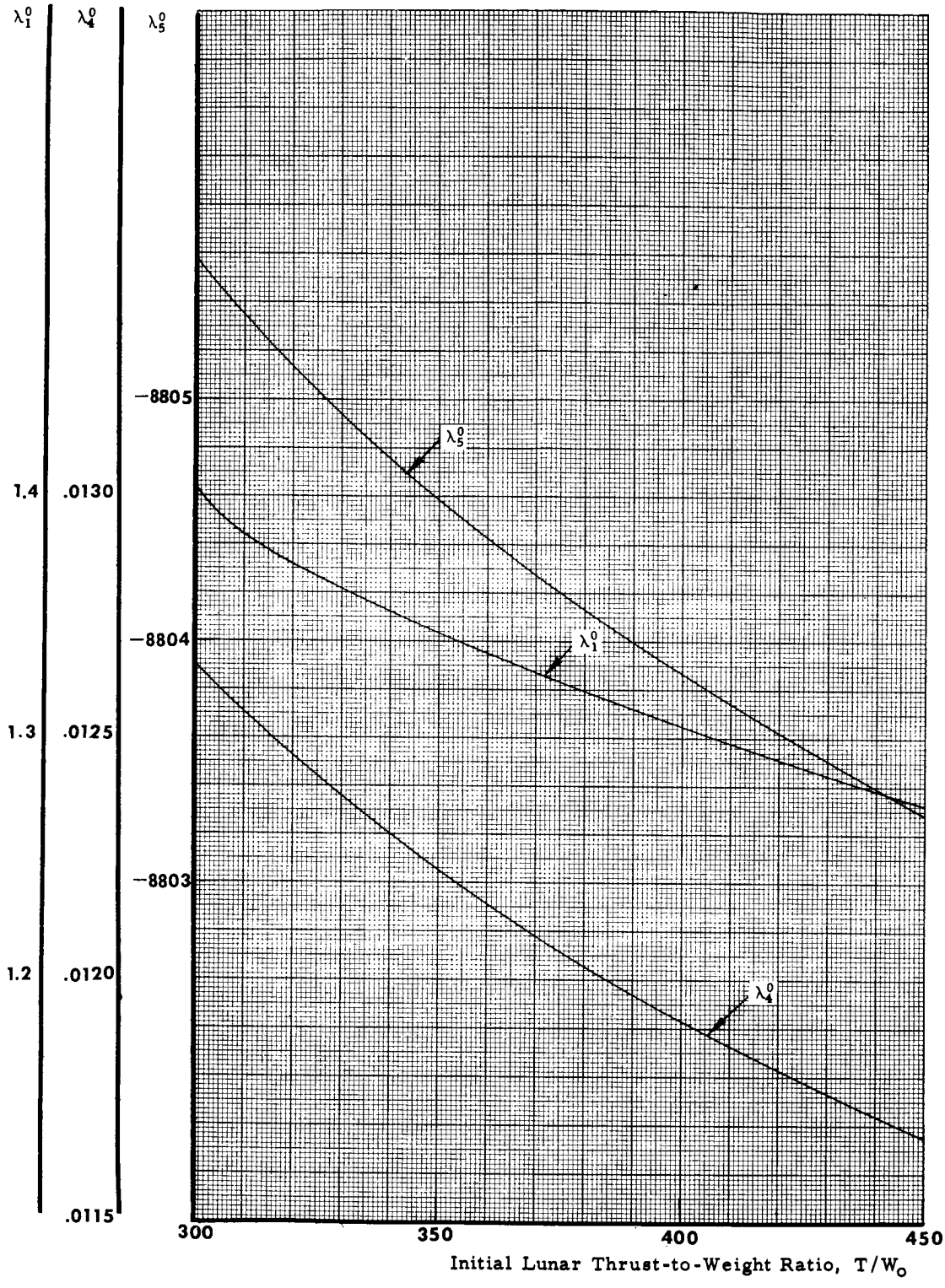

FIGURE 46. INITIAL VALUES OF λ_1, λ_4, and λ_5 VS SPECIFIC IMPULSE FOR ESCAPE THROUGH A 15 Km. CIRCULAR ORBIT. m_{esc}/m_o MAXIMIZED WITH RESPECT TO T/W_o. THRUST AND VELOCITY VECTORS ALIGNED AT ESCAPE VIA λ_3 DISCONTINUITY AT CIRCULAR ORBIT.

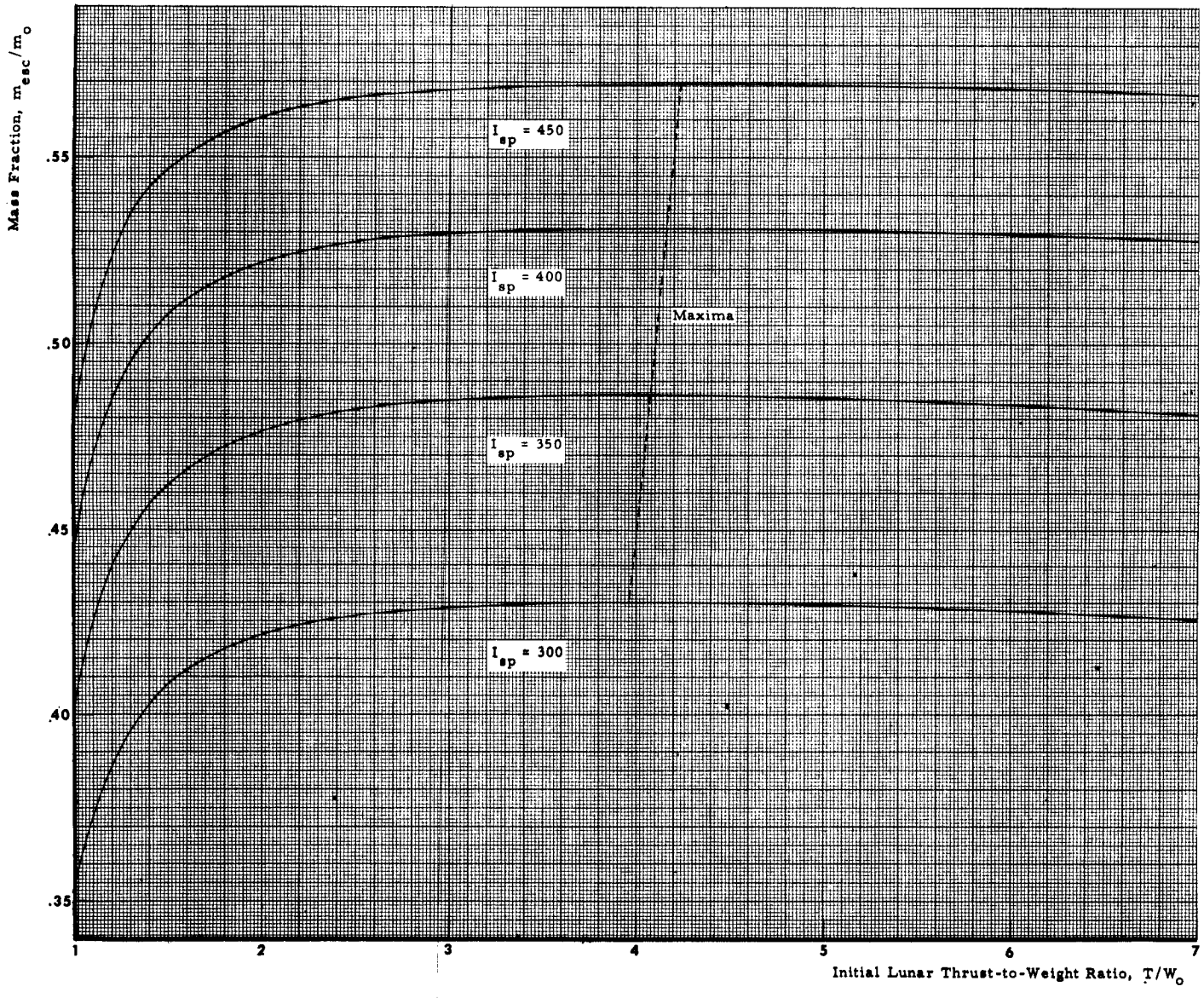

FIGURE 47. MASS FRACTION VS INITIAL LUNAR THRUST-TO-WEIGHT RATIO FOR ESCAPE THROUGH A 15-Km. CIRCULAR ORBIT. THRUST AND VELOCITY VECTORS ALIGNED AT ESCAPE VIA λ_3 DISCONTINUITY AT CIRCULAR ORBIT.

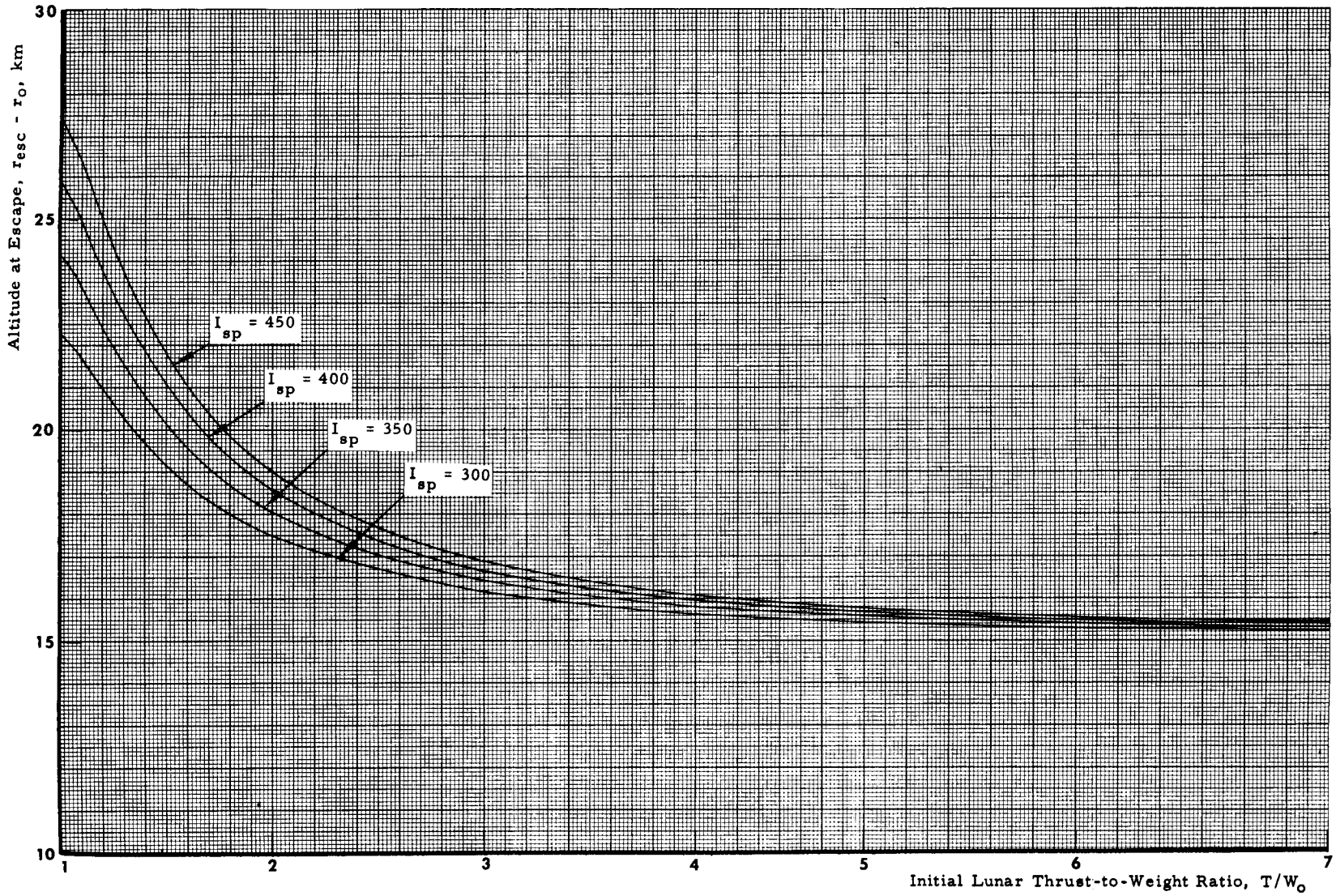

FIGURE 48. ALTITUDE VS INITIAL LUNAR THRUST-TO-WEIGHT RATIO FOR ESCAPE THROUGH A 15 Km. CIRCULAR ORBIT. THRUST AND VELOCITY VECTORS ALIGNED AT ESCAPE VIA λ_3 DISCONTINUITY AT CIRCULAR ORBIT.

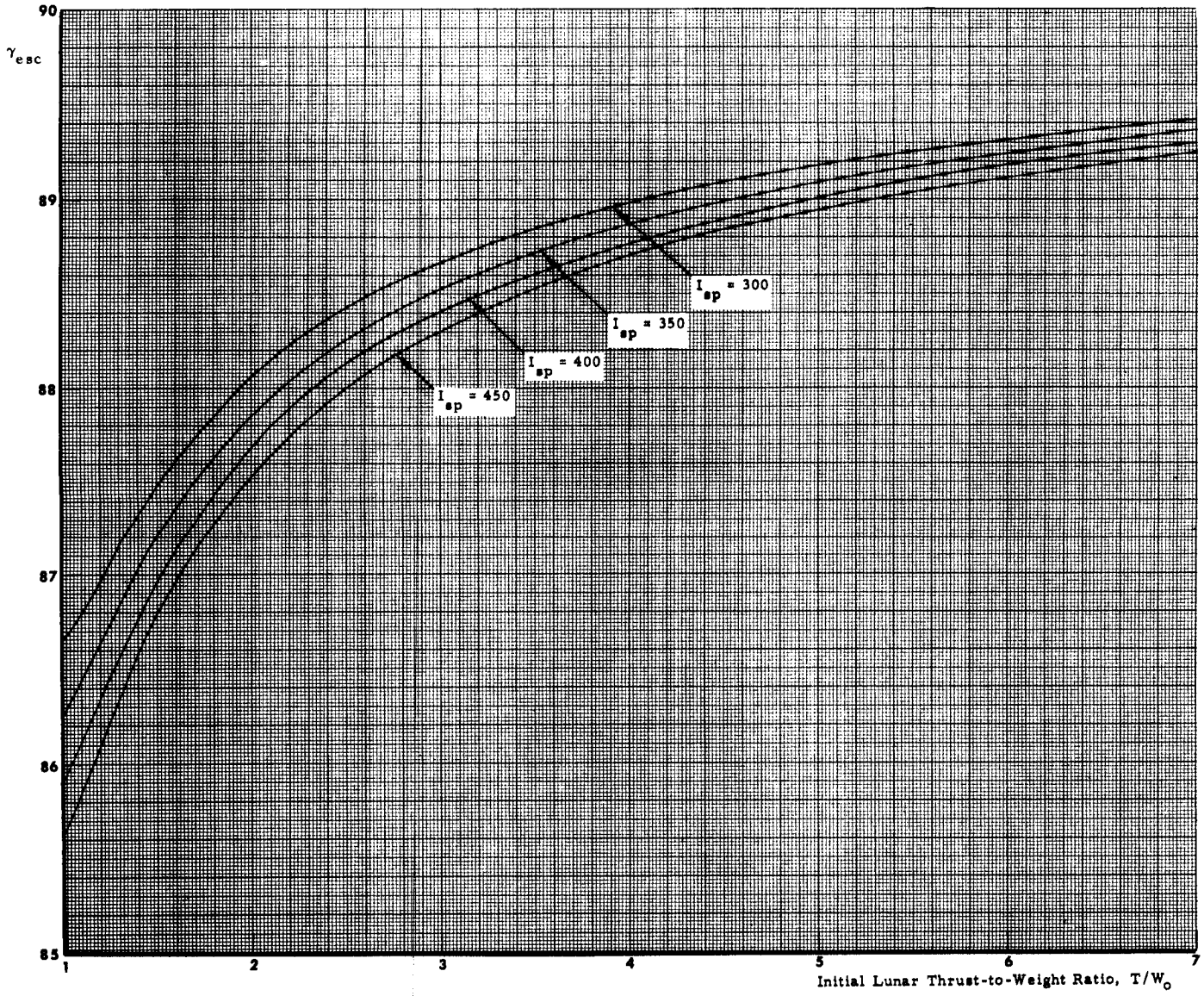

FIGURE 49. GAMMA AT ESCAPE VS INITIAL LUNAR THRUST-TO-WEIGHT RATIO FOR ESCAPE THROUGH A 15-Km. CIRCULAR ORBIT. THRUST AND VELOCITY VECTORS ALIGNED AT ESCAPE VIA λ_3 DISCONTINUITY AT CIRCULAR ORBIT.

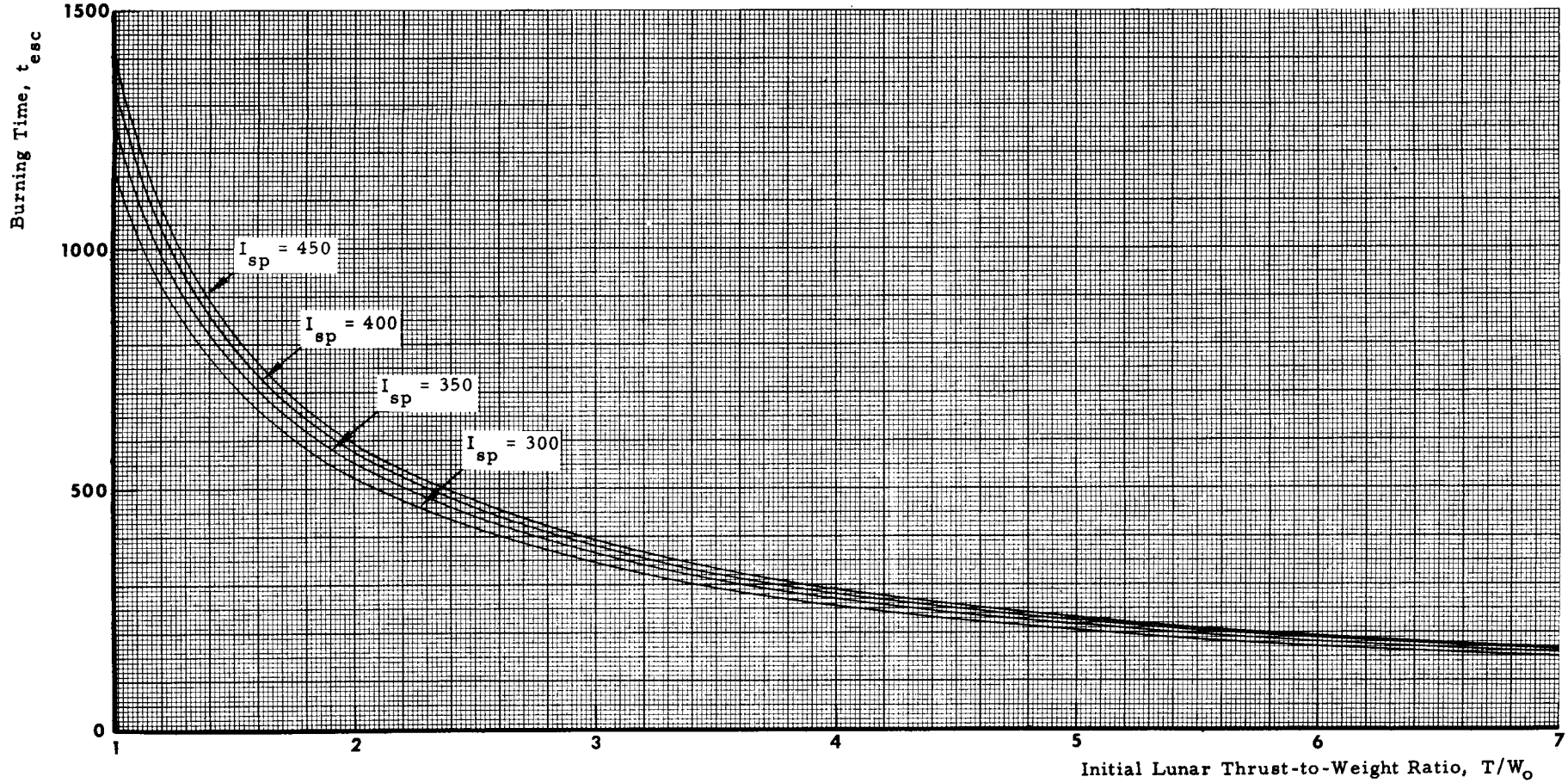

FIGURE 50. BURNING TIME TO ESCAPE VS INITIAL LUNAR THRUST-TO-WEIGHT RATIO FOR ESCAPE THROUGH A 15-Km. CIRCULAR ORBIT. THRUST AND VELOCITY VECTORS ALIGNED AT ESCAPE VIA λ_3 DISCONTINUITY AT CIRCULAR ORBIT.

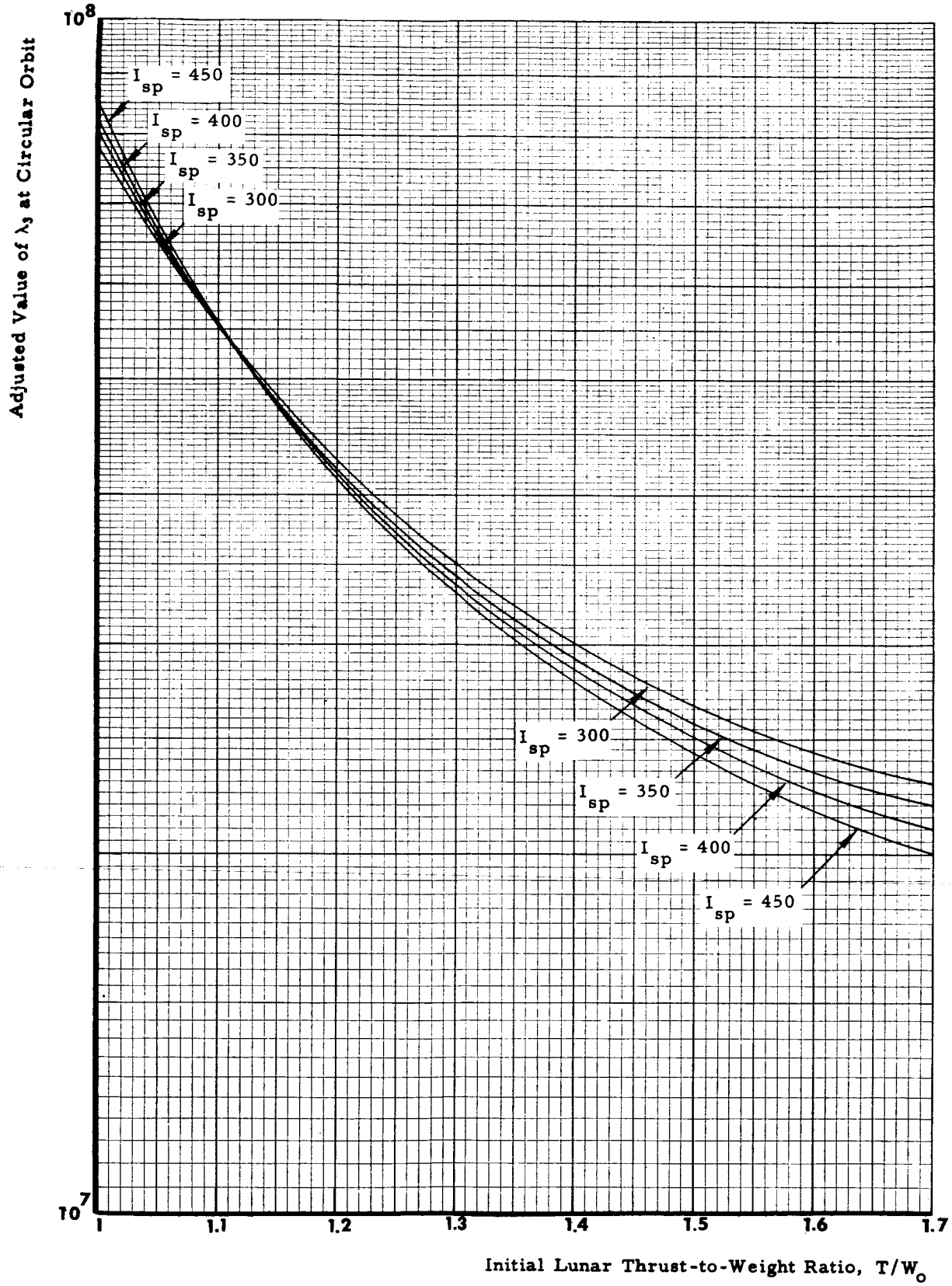

FIGURE 51. ADJUSTED VALUE OF λ_3 AT CIRCULAR ORBIT VS INITIAL LUNAR THRUST-TO-WEIGHT RATIO.

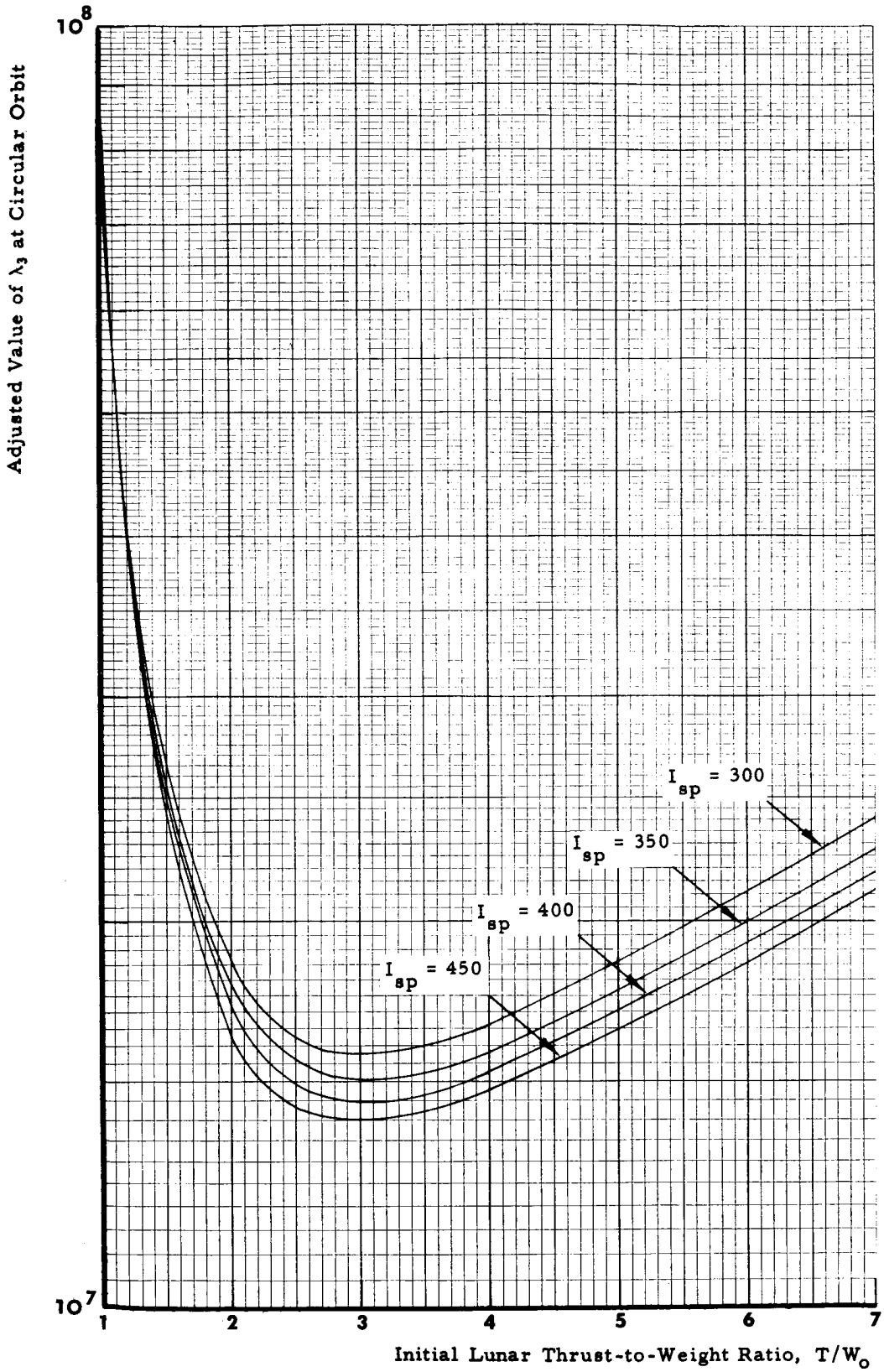

FIGURE 52. ADJUSTED VALUE OF λ_3 AT CIRCULAR ORBIT VS INITIAL LUNAR THRUST-TO-WEIGHT RATIO.

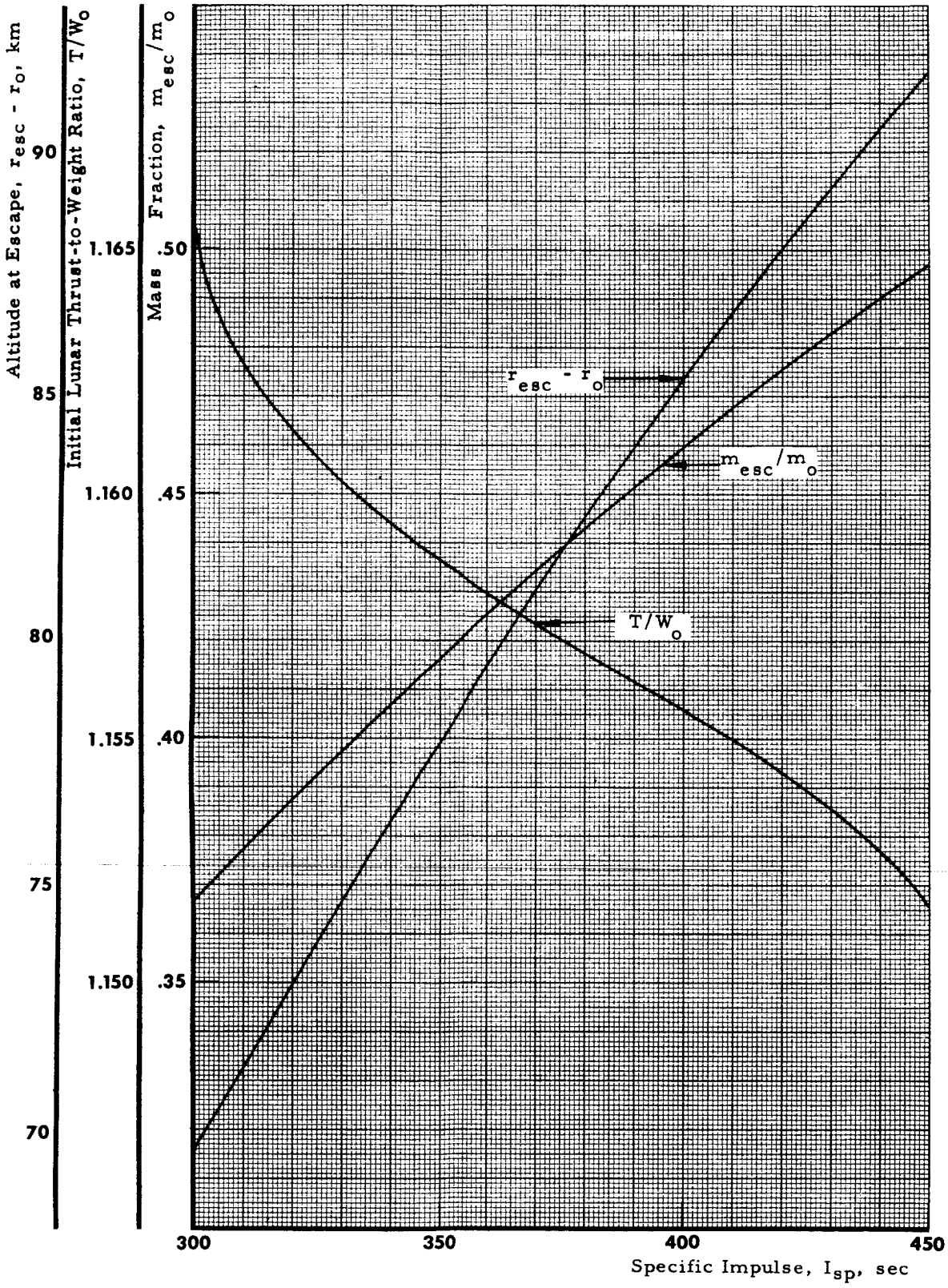

FIGURE 53. MASS FRACTION, INITIAL LUNAR THRUST-TO-WEIGHT RATIO, AND ALTITUDE VS SPECIFIC IMPULSE. $r_{esc} - r_o$ MAXIMIZED WITH RESPECT TO T/W_o. THRUST AND VELOCITY VECTORS ALIGNED AT ORBIT: ALIGNMENT AT ESCAPE VIA λ_3 DISCONTINUITY AT ORBIT.

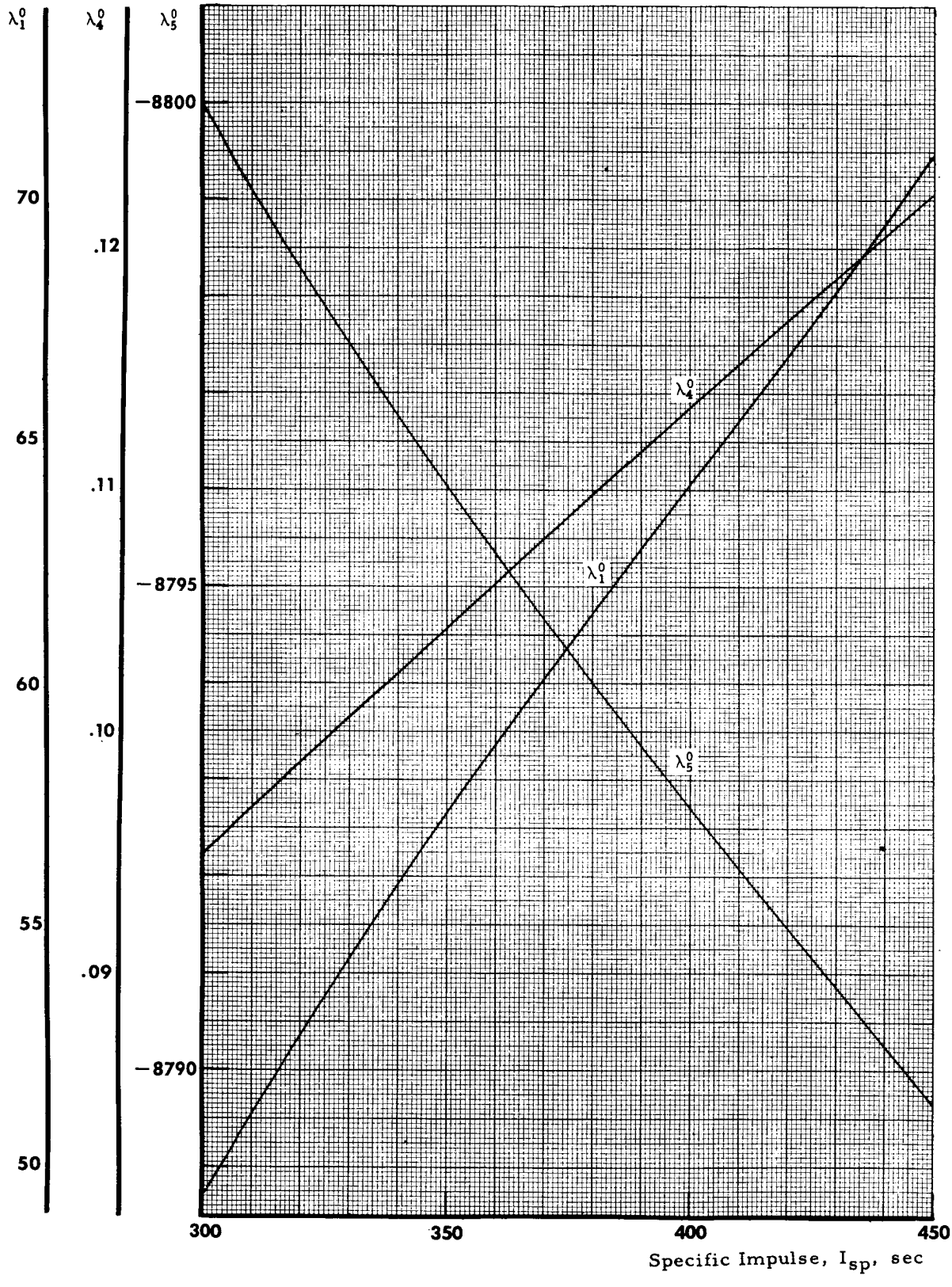

FIGURE 54. INITIAL VALUES OF λ_1, λ_4, AND λ_5 VS SPECIFIC IMPULSE. $r_{esc} - r_o$ MAXIMIZED WITH RESPECT TO T/W_o. THRUST AND VELOCITY VECTORS ALIGNED AT ORBIT: ALIGNMENT AT ESCAPE VIA λ_3 DISCONTINUITY AT ORBIT.

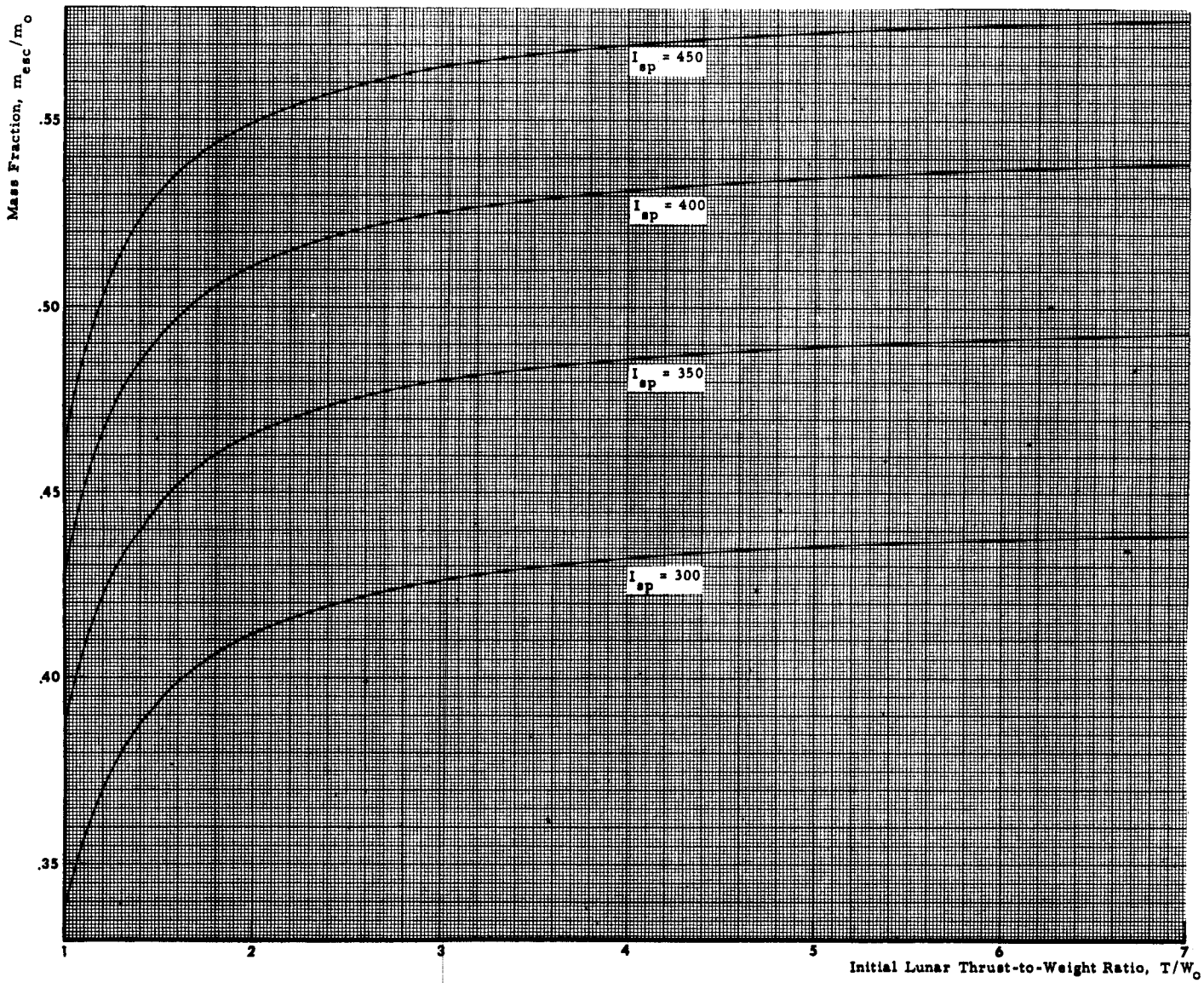

FIGURE 55. MASS FRACTION VS INITIAL LUNAR THRUST-TO-WEIGHT RATIO. THRUST AND VELOCITY VECTORS ALIGNED AT ORBIT: ALIGNMENT AT ESCAPE VIA λ_3 DISCONTINUITY AT ORBIT.

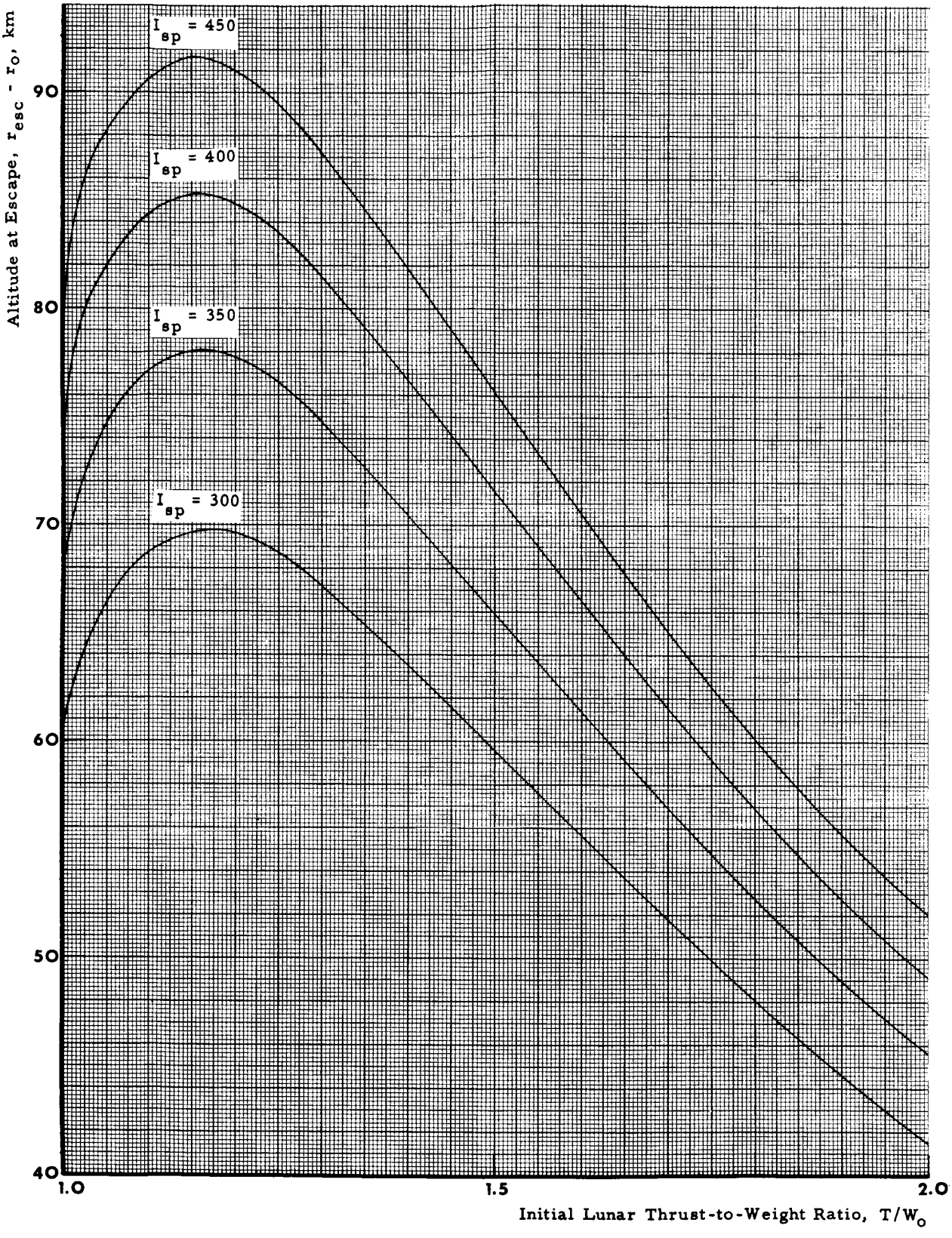

FIGURE 56. ALTITUDE VS INITIAL LUNAR THRUST-TO-WEIGHT RATIO. THRUST AND VELOCITY VECTORS ALIGNED AT ORBIT: ALIGNMENT AT ESCAPE VIA λ_3 DISCONTINUITY AT ORBIT.

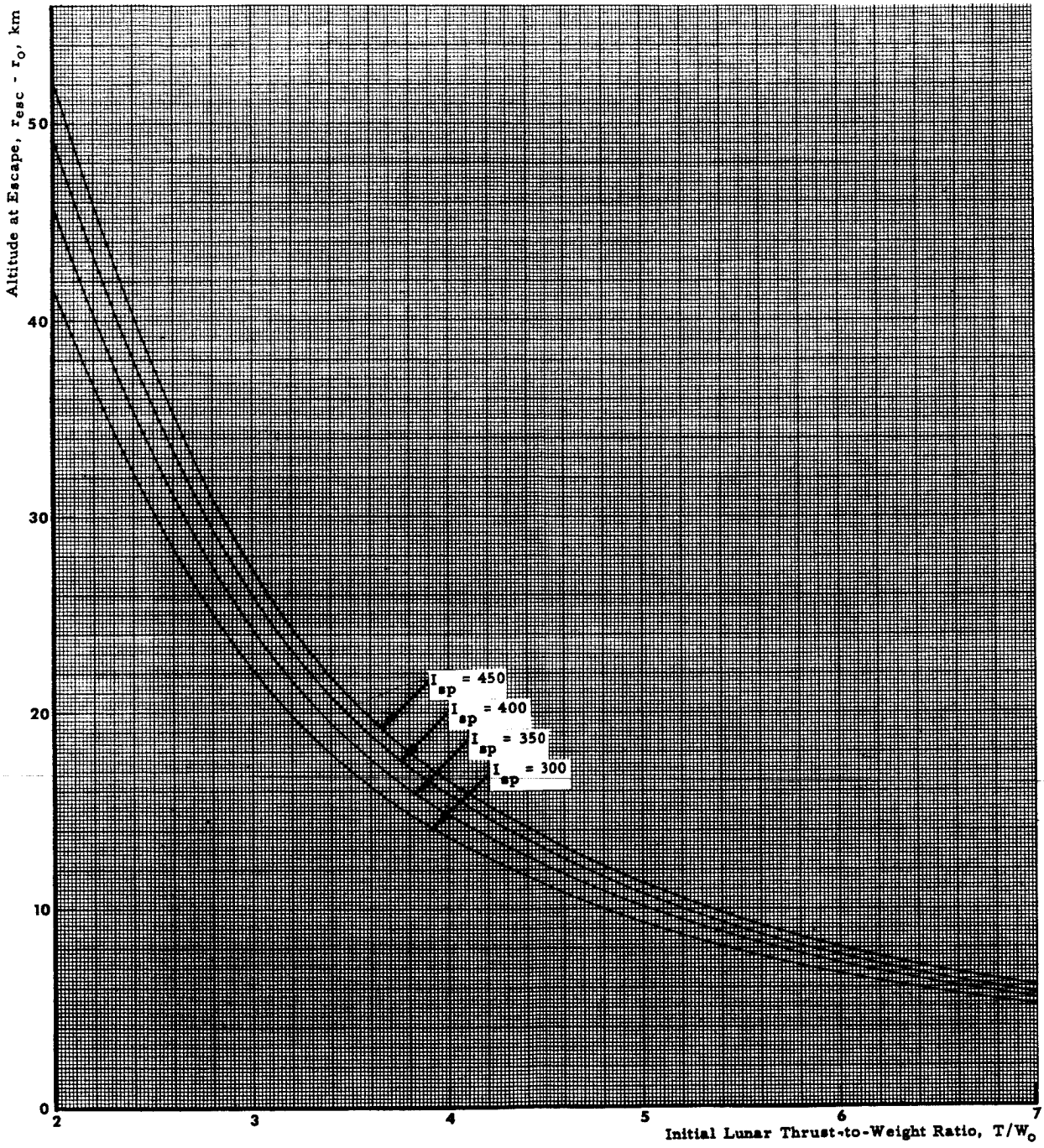

FIGURE 57. ALTITUDE VS INITIAL LUNAR THRUST-TO-WEIGHT RATIO. THRUST AND VELOCITY VECTORS ALIGNED AT ORBIT: ALIGNMENT AT ESCAPE VIA λ_3 DISCONTINUITY AT ORBIT.

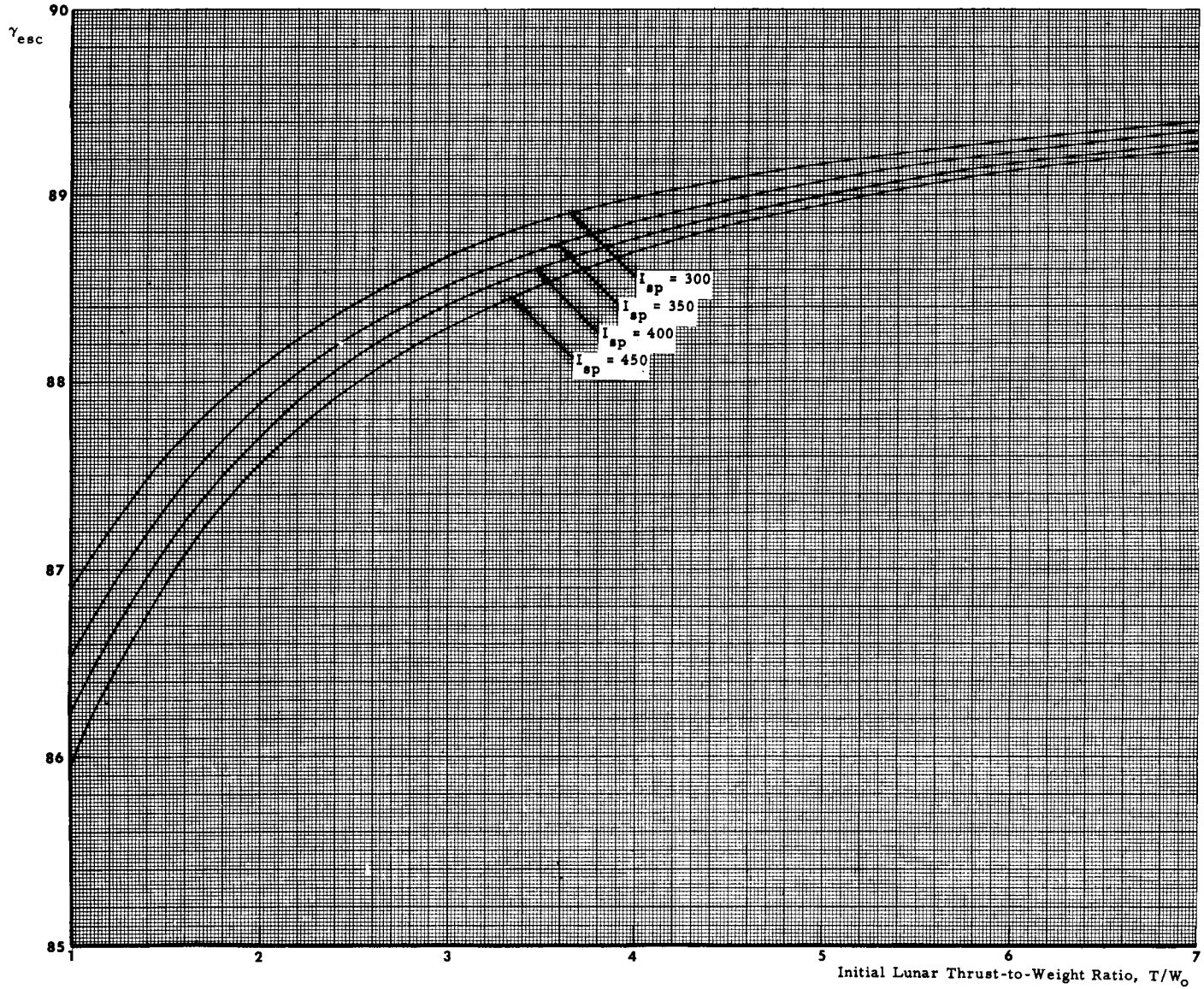

FIGURE 58. GAMMA AT ESCAPE VS INITIAL LUNAR THRUST-TO-WEIGHT RATIO. THRUST AND VELOCITY VECTORS ALIGNED AT ORBIT: ALIGNMENT AT ESCAPE VIA λ_3 DISCONTINUITY AT ORBIT.

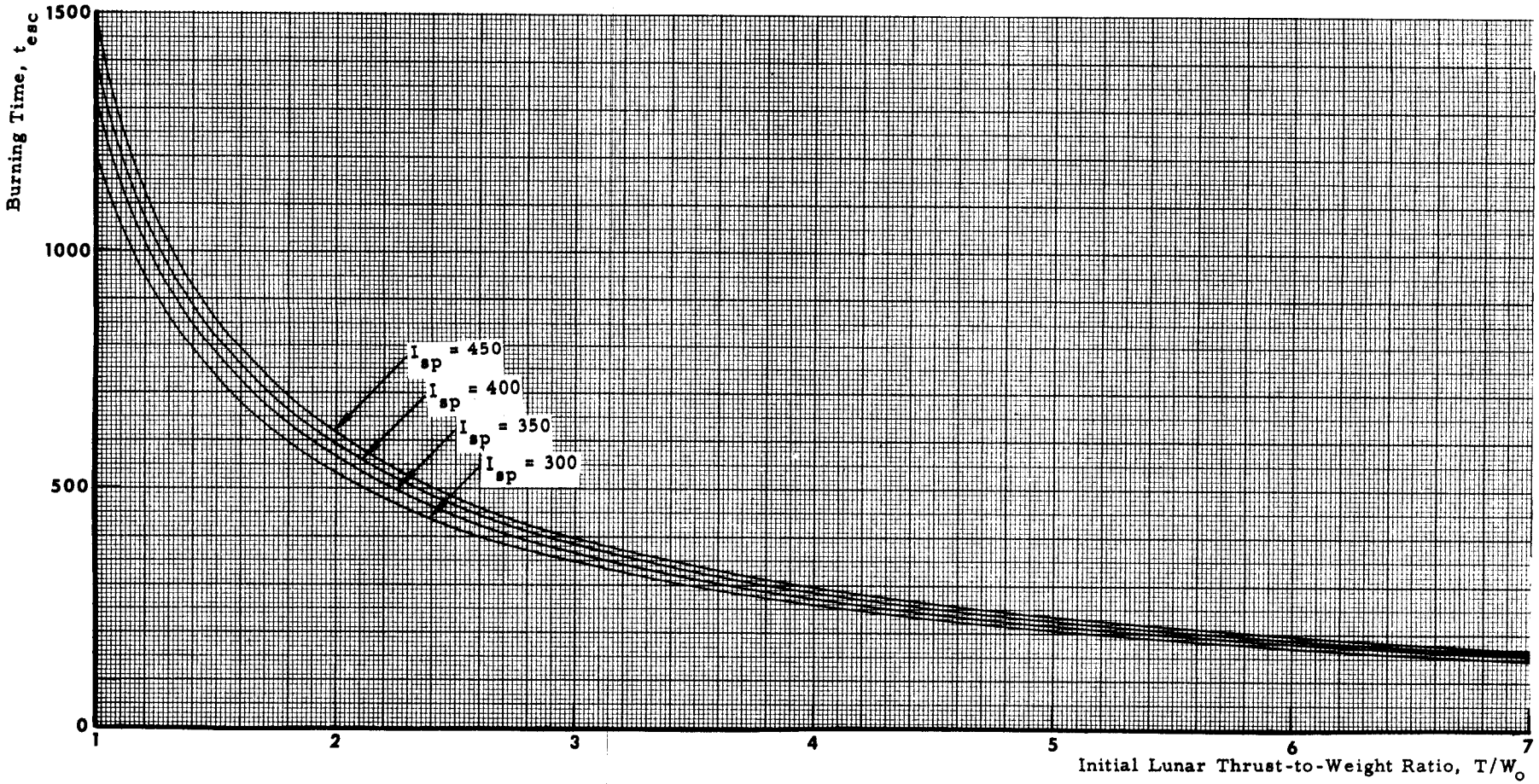

FIGURE 59. BURNING TIME TO ESCAPE VS INITIAL LUNAR THRUST-TO-WEIGHT RATIO. THRUST AND VELOCITY VECTORS ALIGNED AT ORBIT: ALIGNMENT AT ESCAPE VIA λ_3 DISCONTINUITY AT ORBIT.

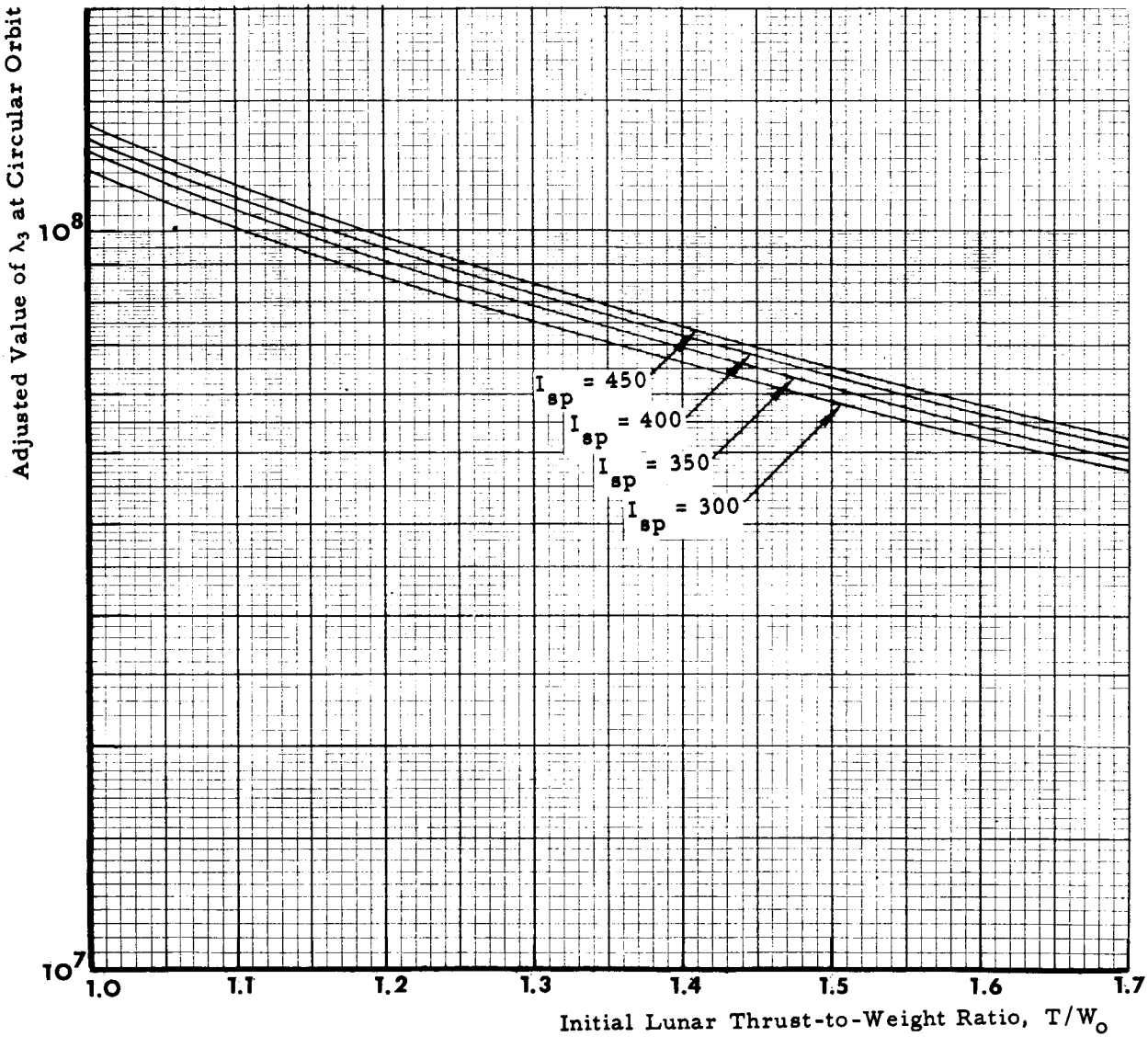

FIGURE 60. ADJUSTED VALUE OF λ_3 AT CIRCULAR ORBIT VS INITIAL LUNAR THRUST-TO-WEIGHT RATIO.

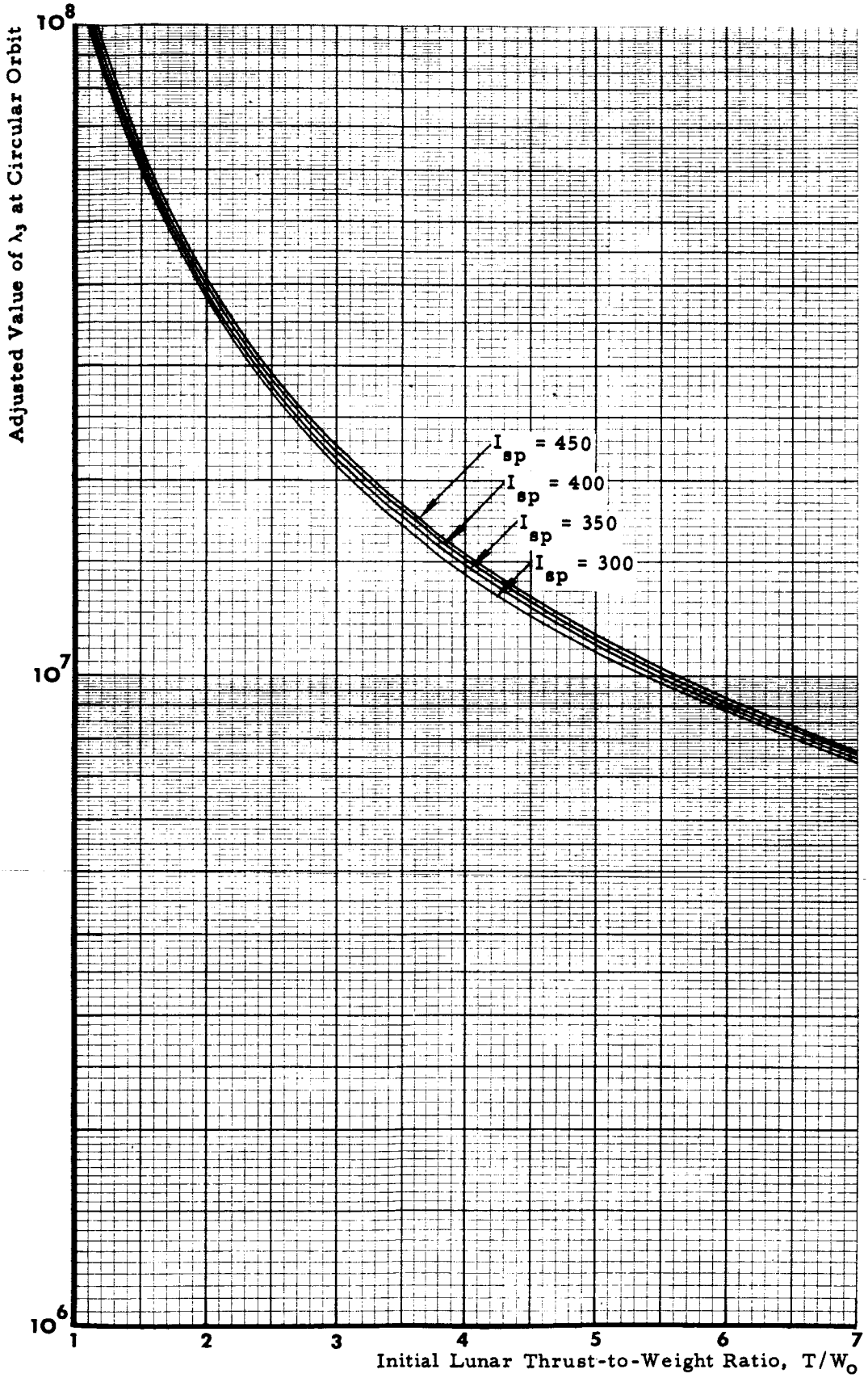

FIGURE 61. ADJUSTED VALUE OF λ_3 AT CIRCULAR ORBIT VS INITIAL LUNAR THRUST-TO-WEIGHT RATIO

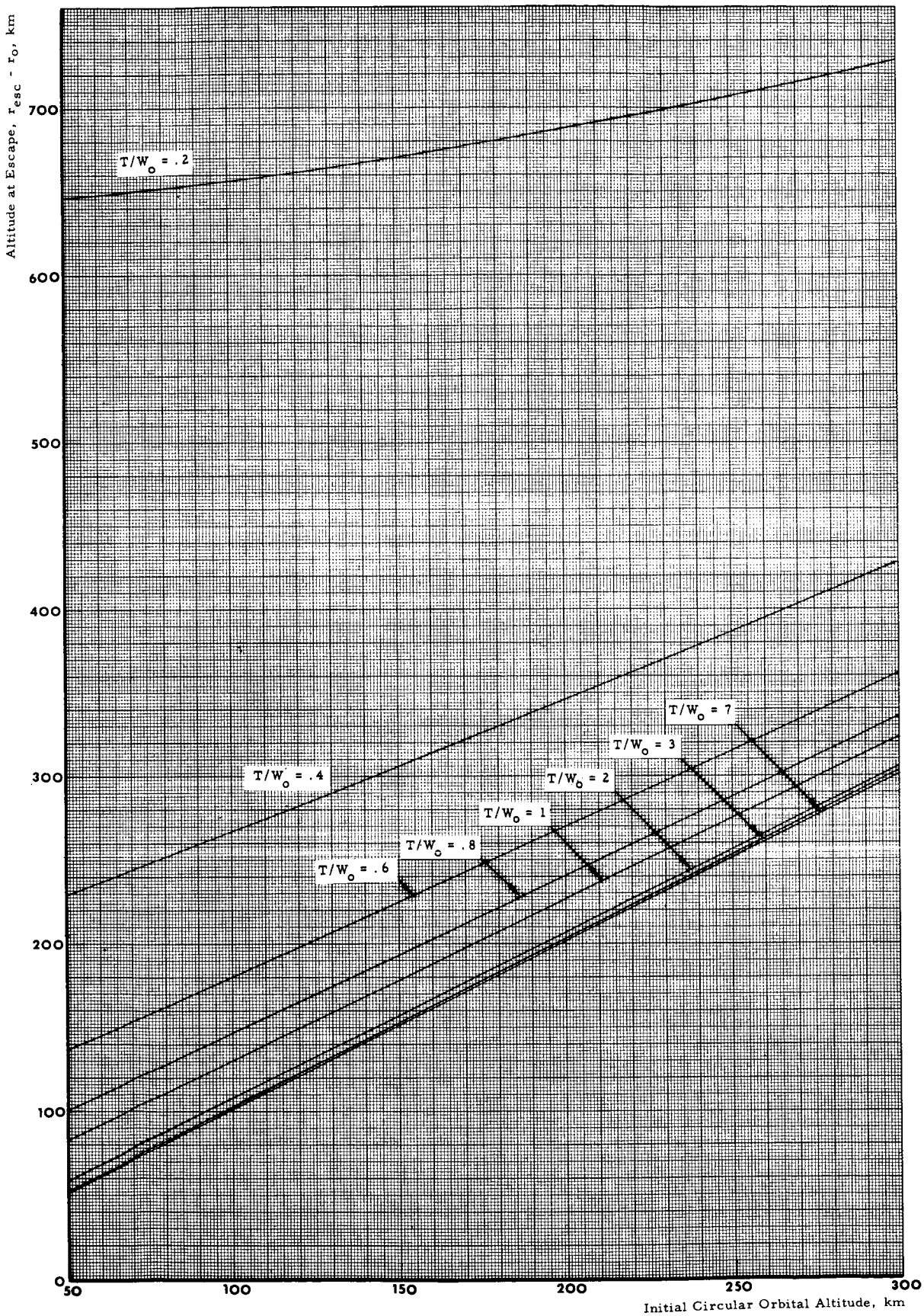

FIGURE 62. ESCAPE ALTITUDE VS INITIAL ORBITAL ALTITUDE FOR SPECIFIC IMPULSE OF 300 SEC.

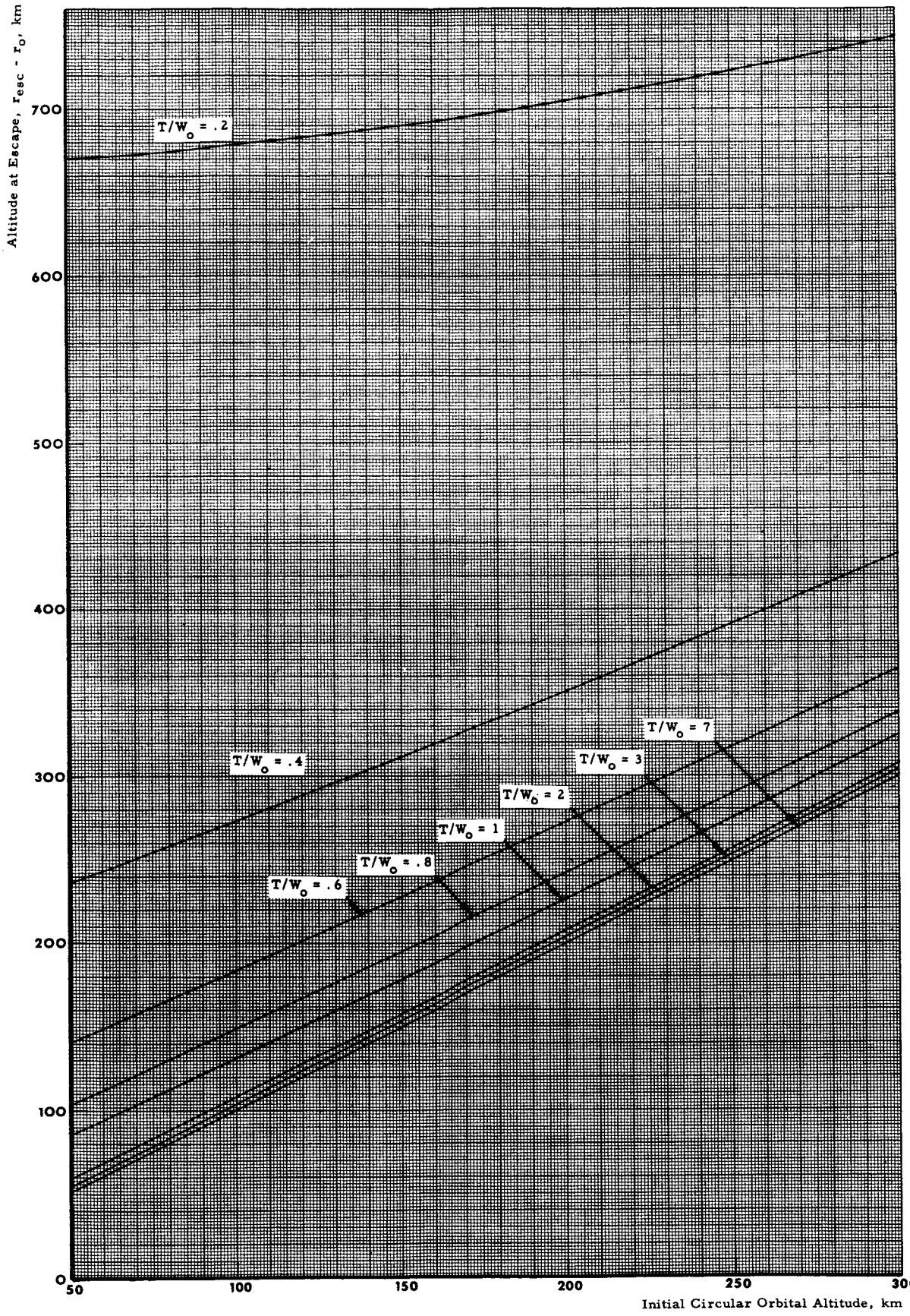

FIGURE 63. ESCAPE ALTITUDE VS INITIAL ORBITAL ALTITUDE FOR SPECIFIC IMPULSE OF 350 SEC.

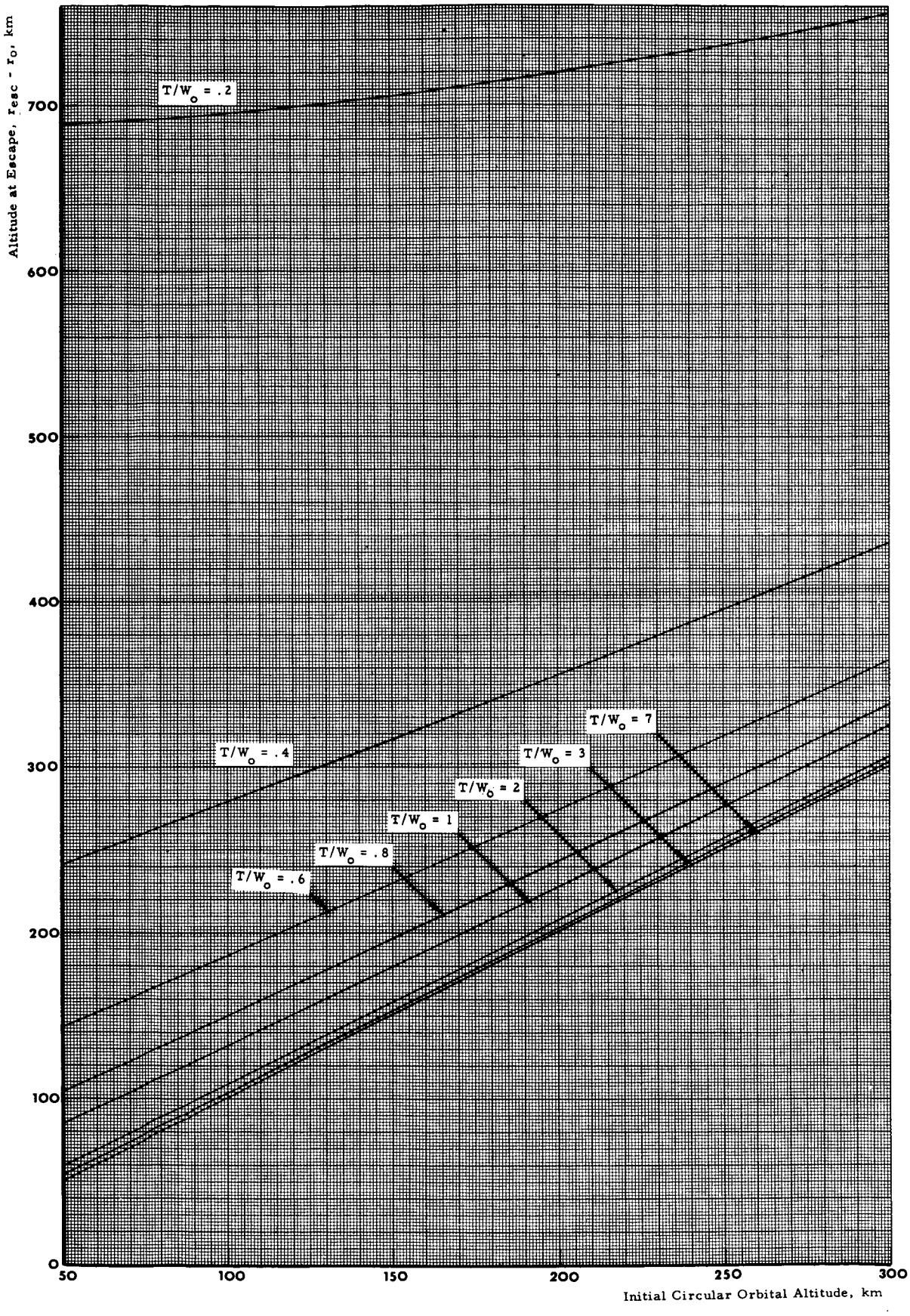

FIGURE 64. ESCAPE ALTITUDE VS INITIAL ORBITAL ALTITUDE FOR SPECIFIC IMPULSE OF 400 SEC.

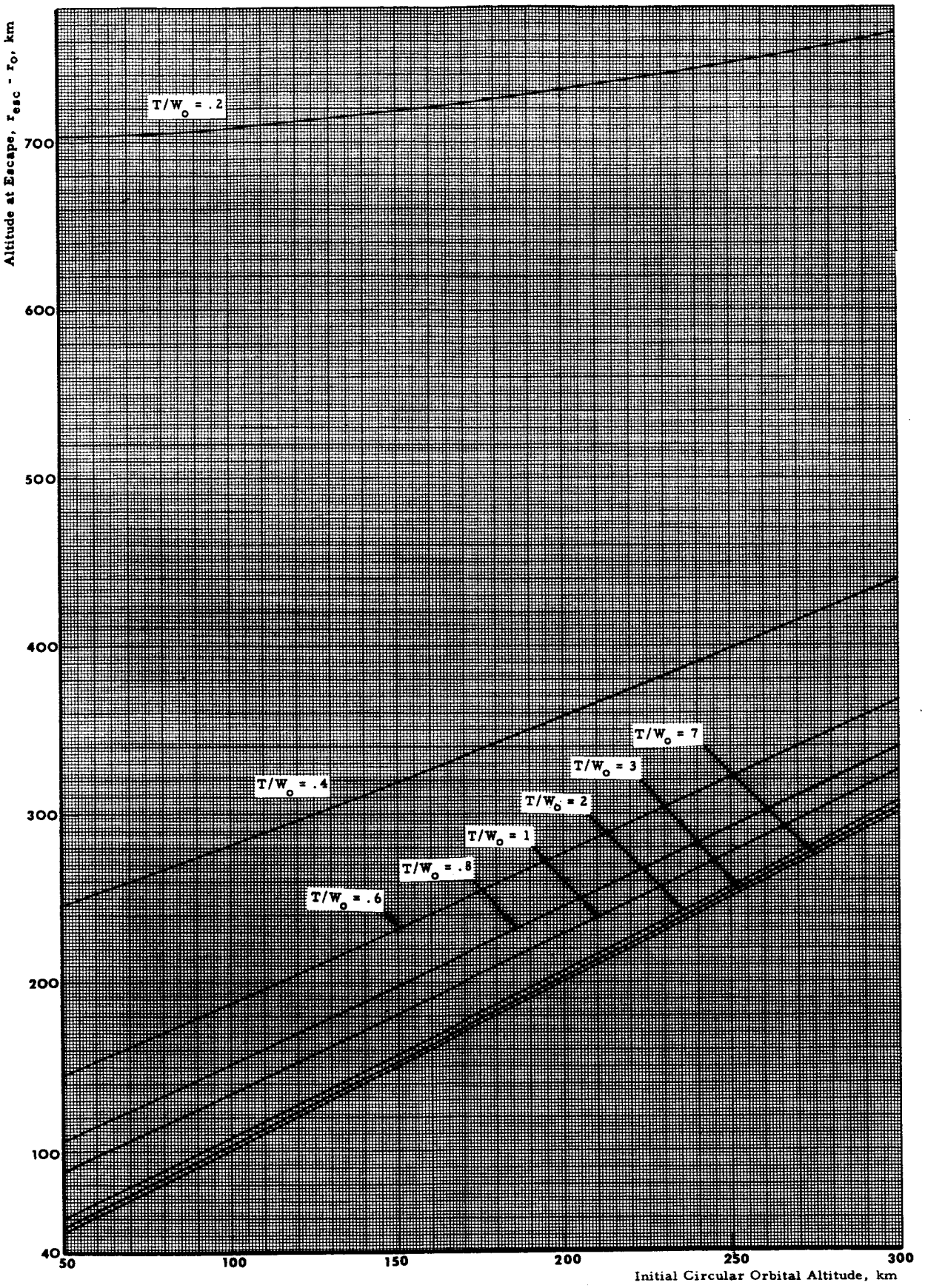

FIGURE 65. ESCAPE ALTITUDE VS INITIAL ORBITAL ALTITUDE FOR SPECIFIC IMPULSE OF 450 SEC.

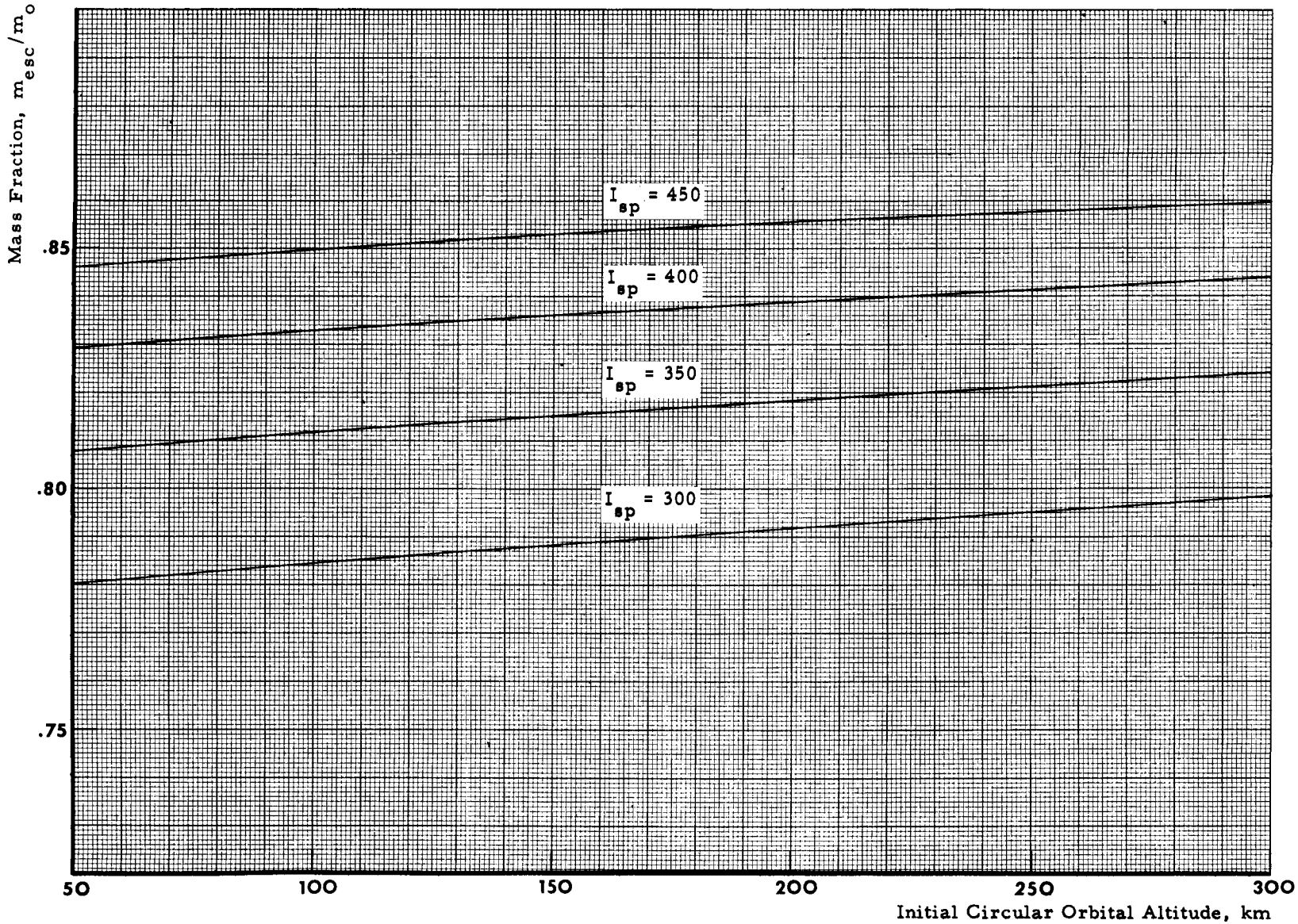

FIGURE 66. MASS FRACTION VS INITIAL ORBITAL ALTITUDE FOR INITIAL LUNAR THRUST-TO-WEIGHT RATIO = 0.2

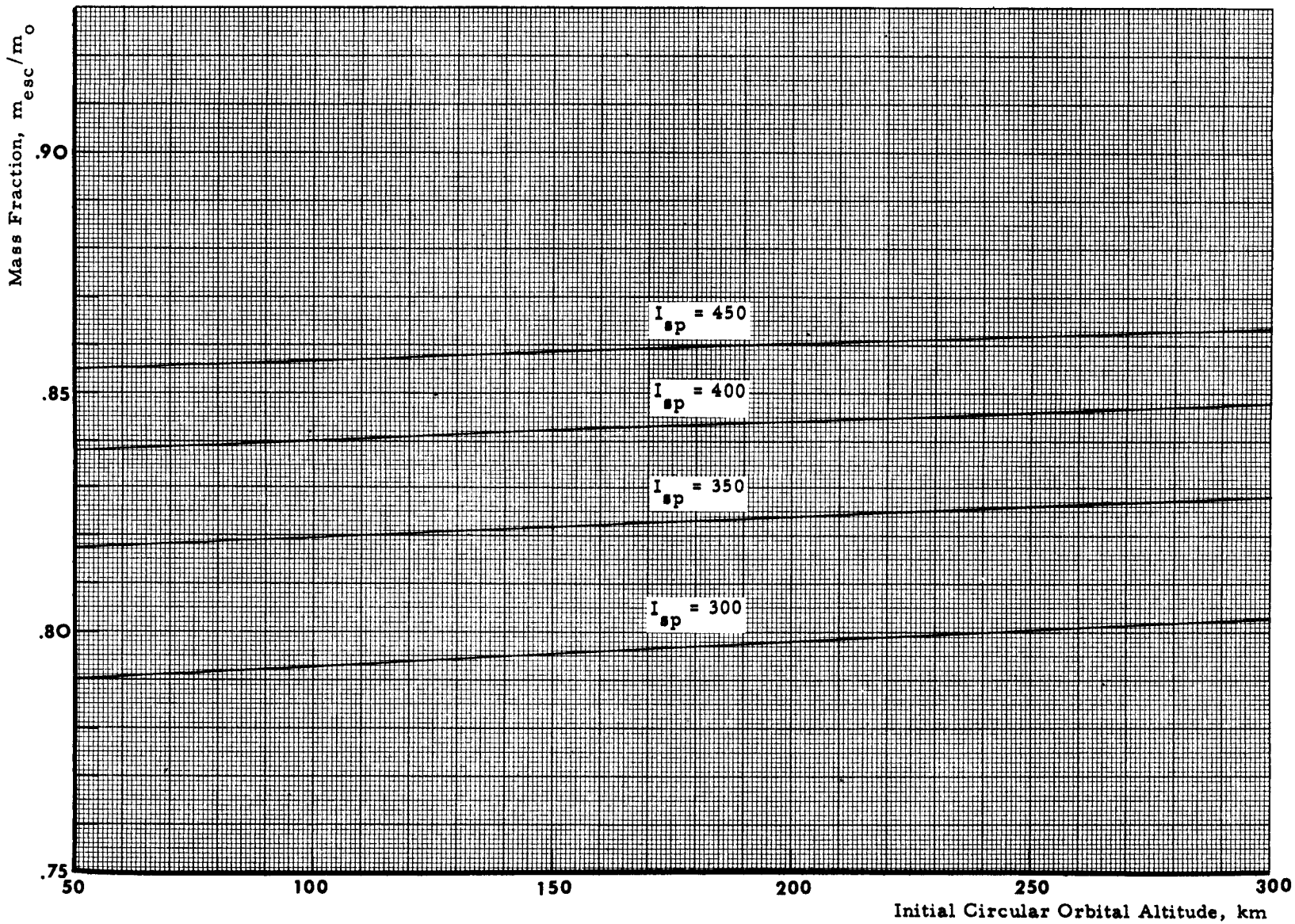

FIGURE 67. MASS FRACTION VS INITIAL ORBITAL ALTITUDE FOR INITIAL LUNAR THRUST-TO-WEIGHT RATIO = 0.4

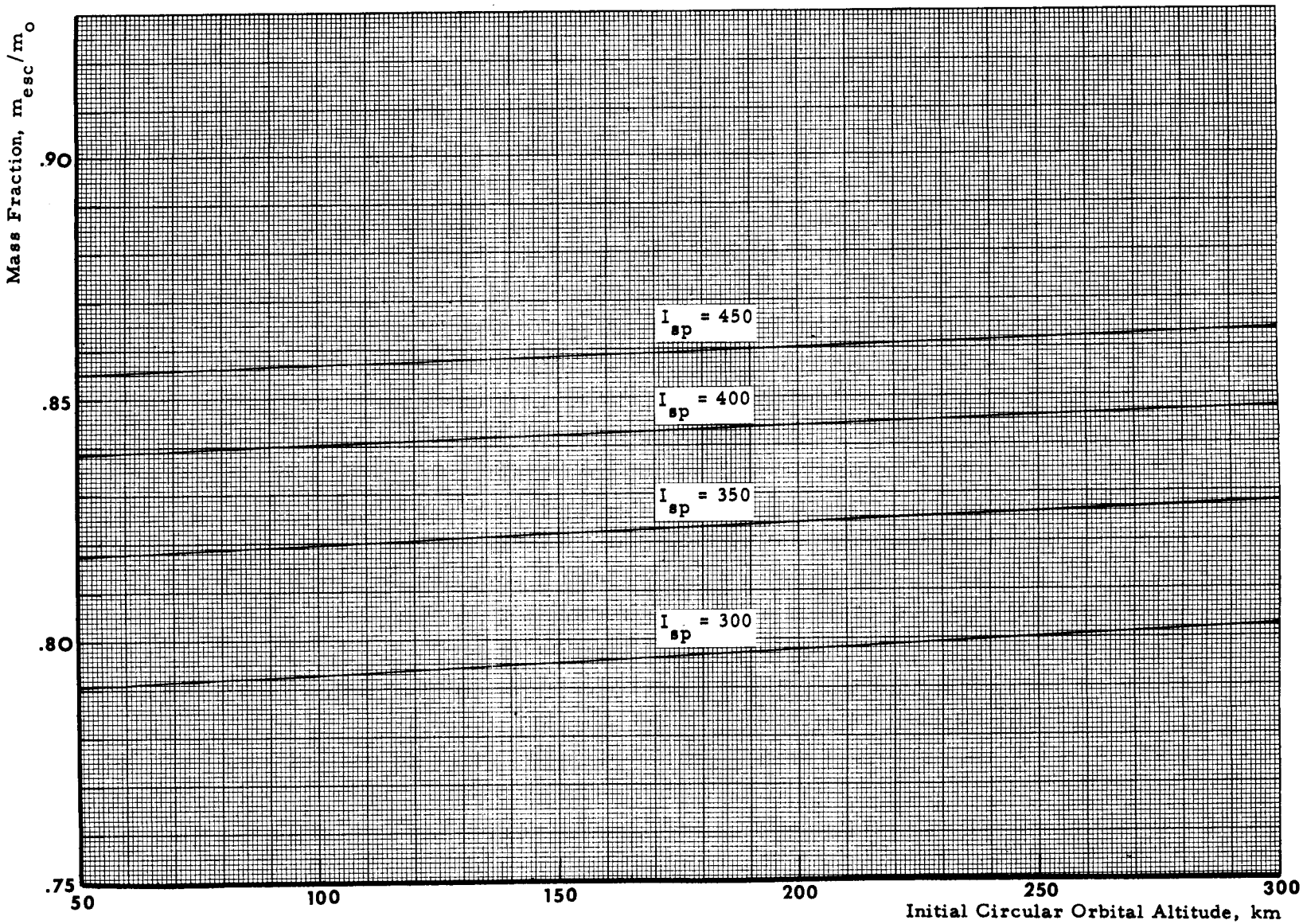

FIGURE 68. MASS FRACTION VS INITIAL ORBITAL ALTITUDE FOR INITIAL LUNAR THRUST-TO-WEIGHT RATIO = 0.6.

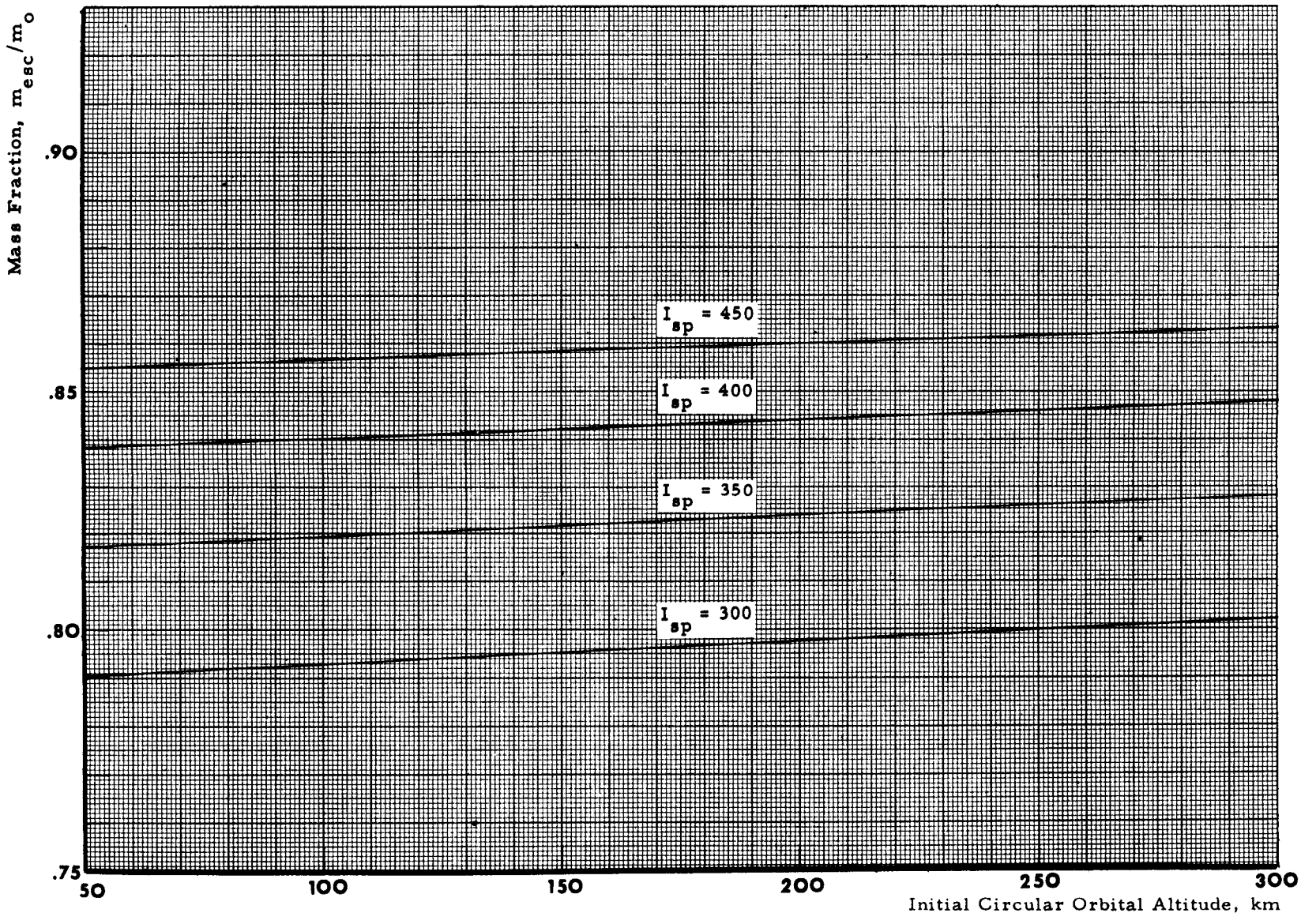

FIGURE 69. MASS FRACTION VS INITIAL ORBITAL ALTITUDE FOR INITIAL LUNAR THRUST-TO-WEIGHT RATIO = 0.8

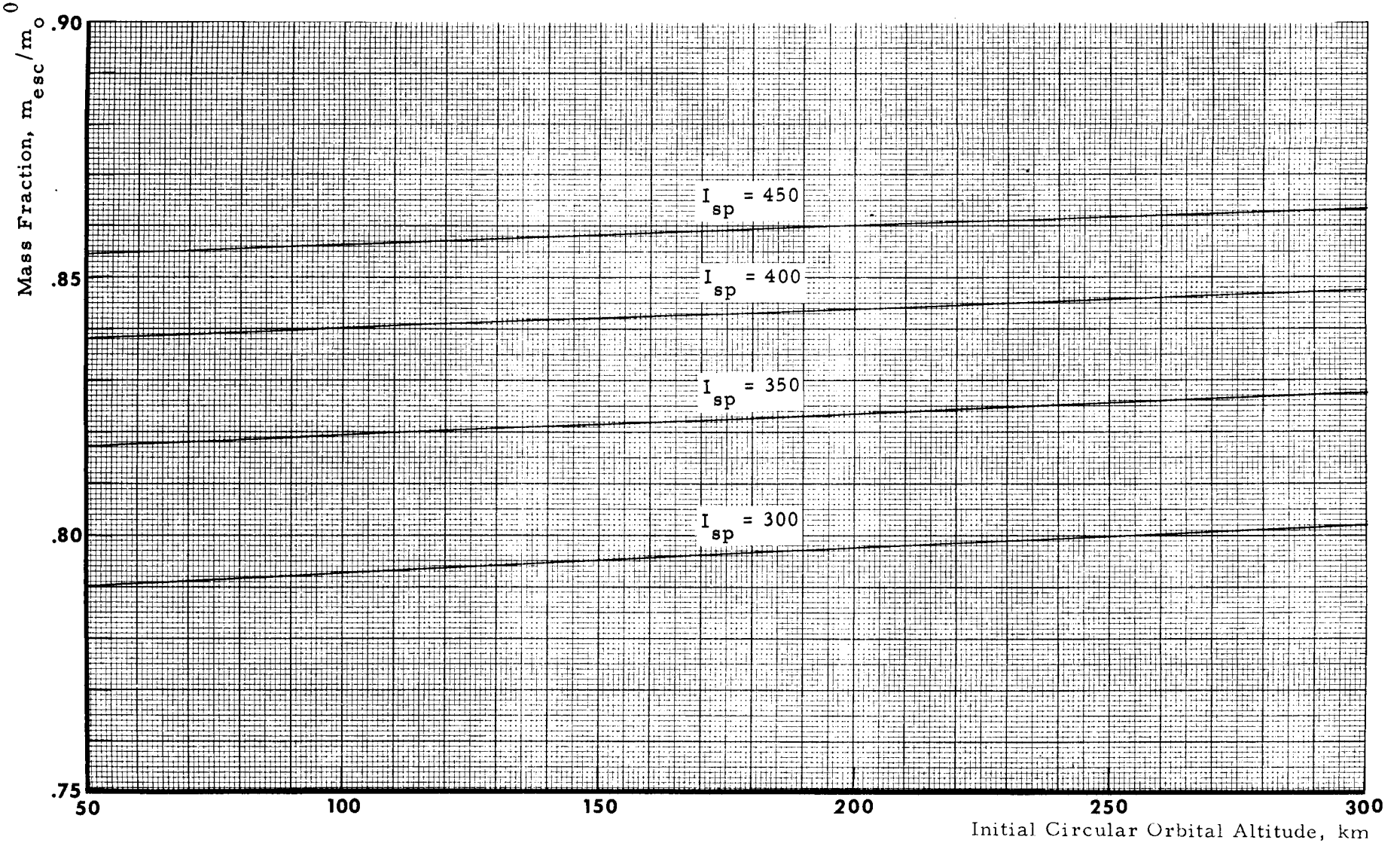

FIGURE 70. MASS FRACTION VS INITIAL ORBITAL ALTITUDE FOR INITIAL LUNAR THRUST-TO-WEIGHT RATIO = 1.0

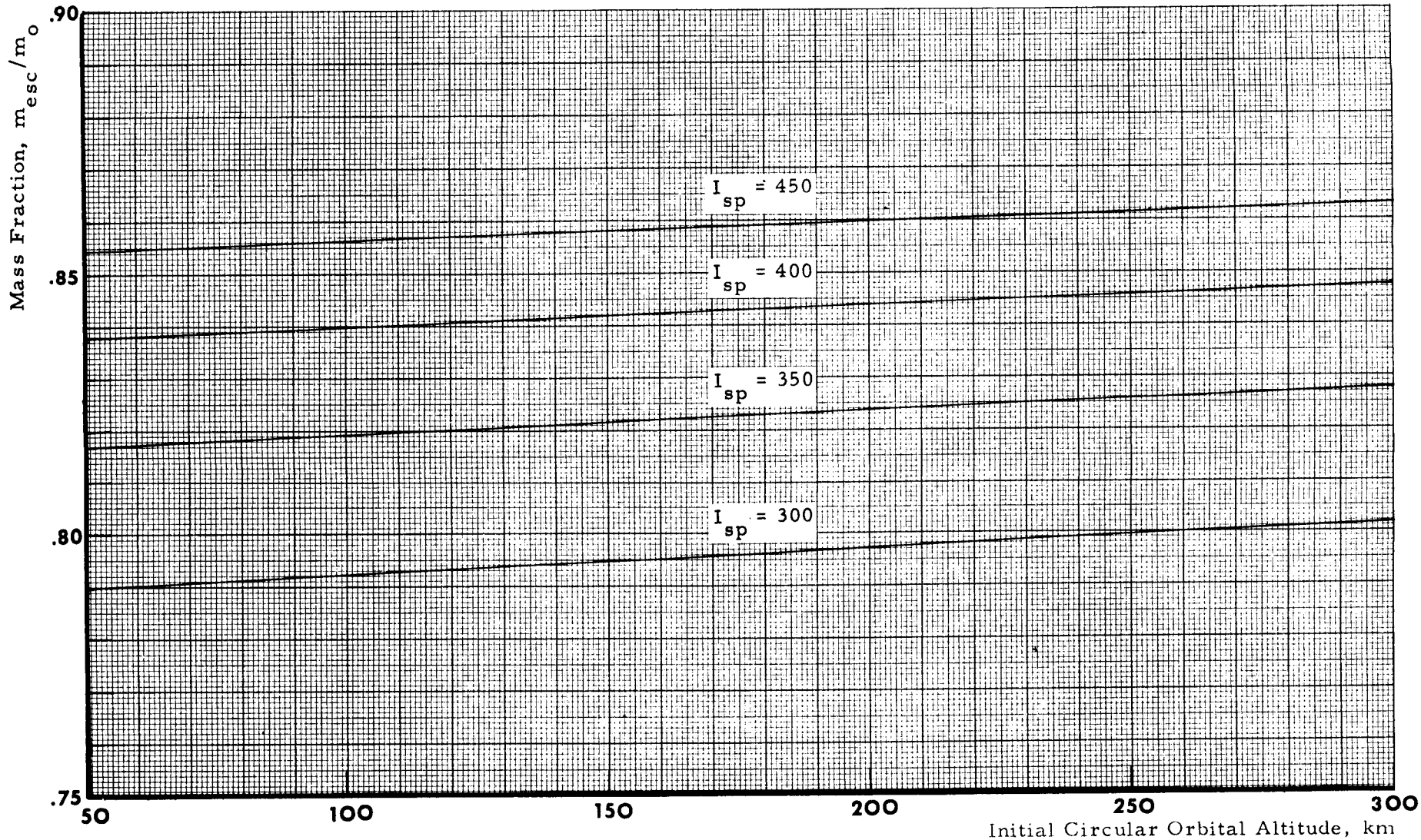

FIGURE 71. MASS FRACTION VS INITIAL ORBITAL ALTITUDE FOR INITIAL LUNAR THRUST-TO-WEIGHT RATIO = 2.0.

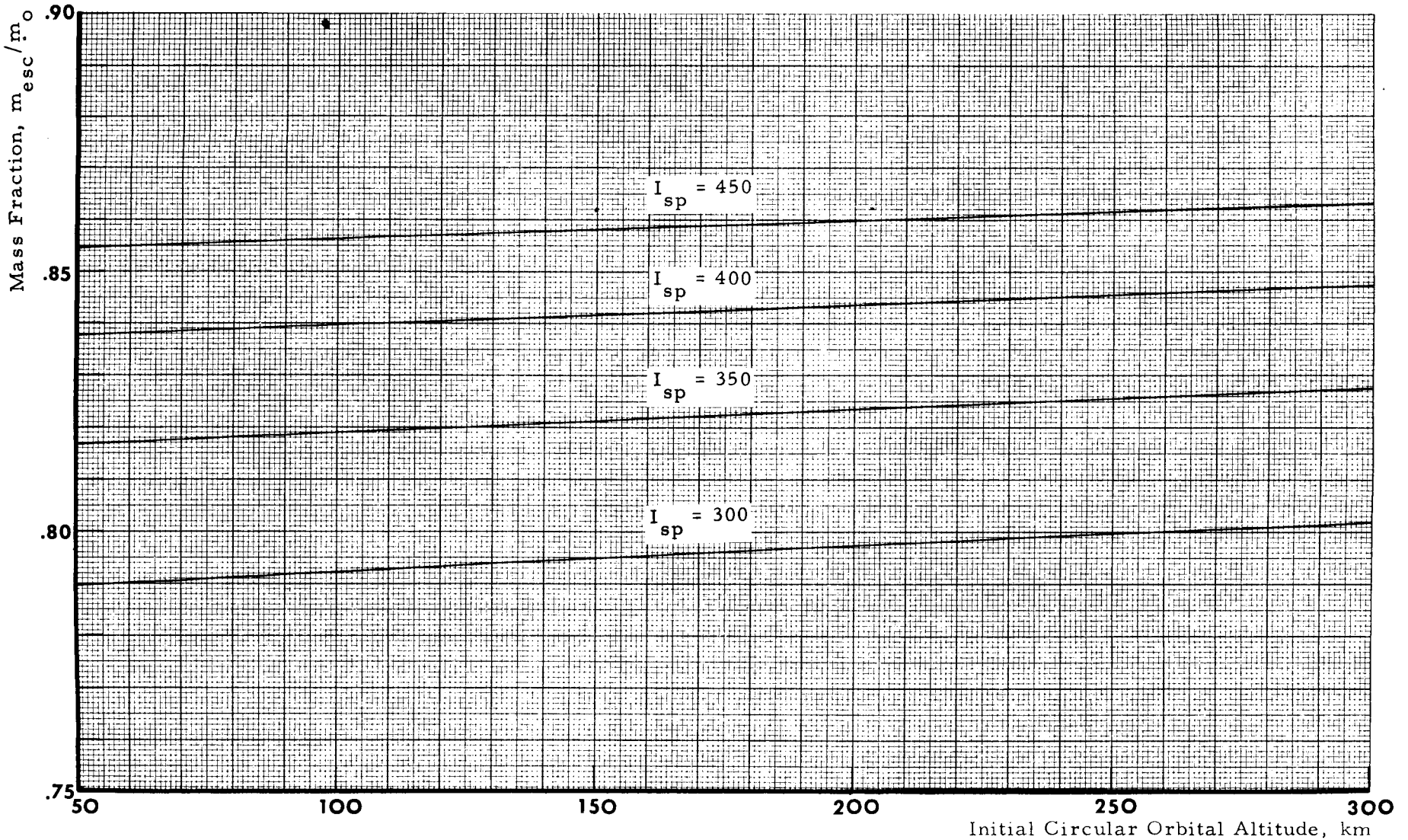

FIGURE 72. MASS FRACTION VS INITIAL ORBITAL ALTITUDE FOR INITIAL LUNAR THRUST-TO-WEIGHT RATIO = 3.0.

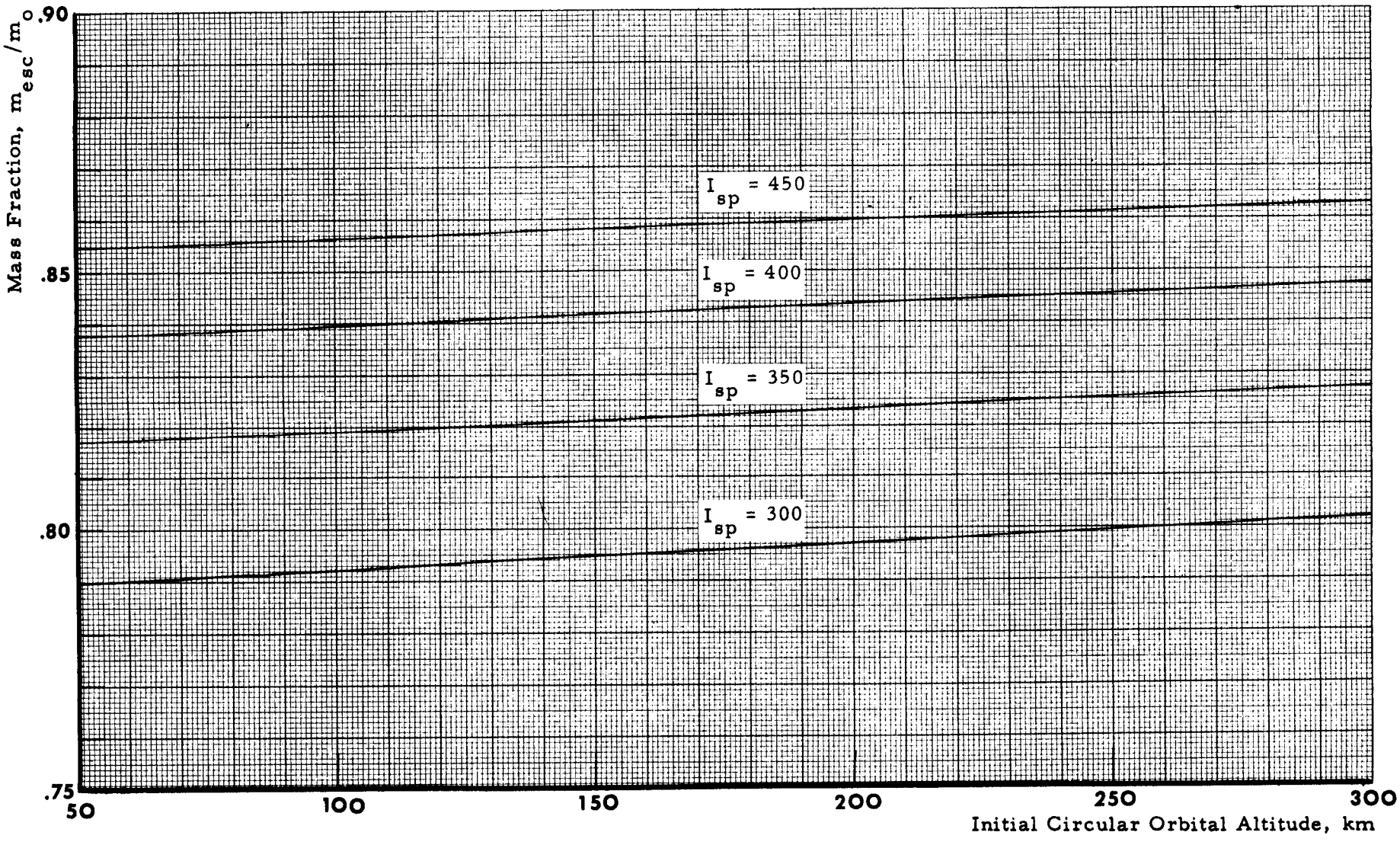

FIGURE 73. MASS FRACTION VS INITIAL ORBITAL ALTITUDE FOR INITIAL LUNAR THRUST-TO-WEIGHT RATIO = 4.0.

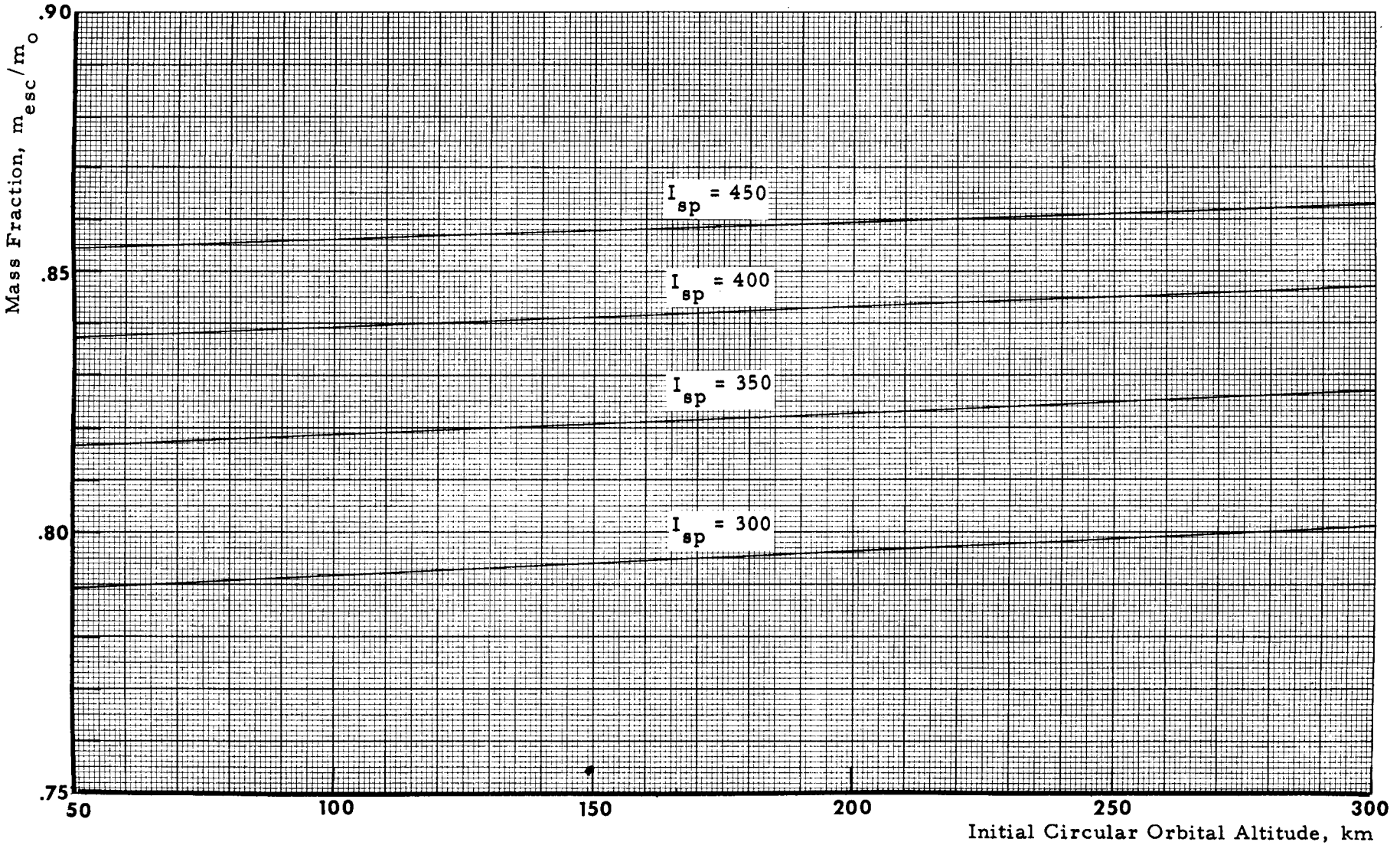

FIGURE 74. MASS FRACTION VS INITIAL ORBITAL ALTITUDE FOR INITIAL LUNAR THRUST-TO-WEIGHT RATIO = 5.0.

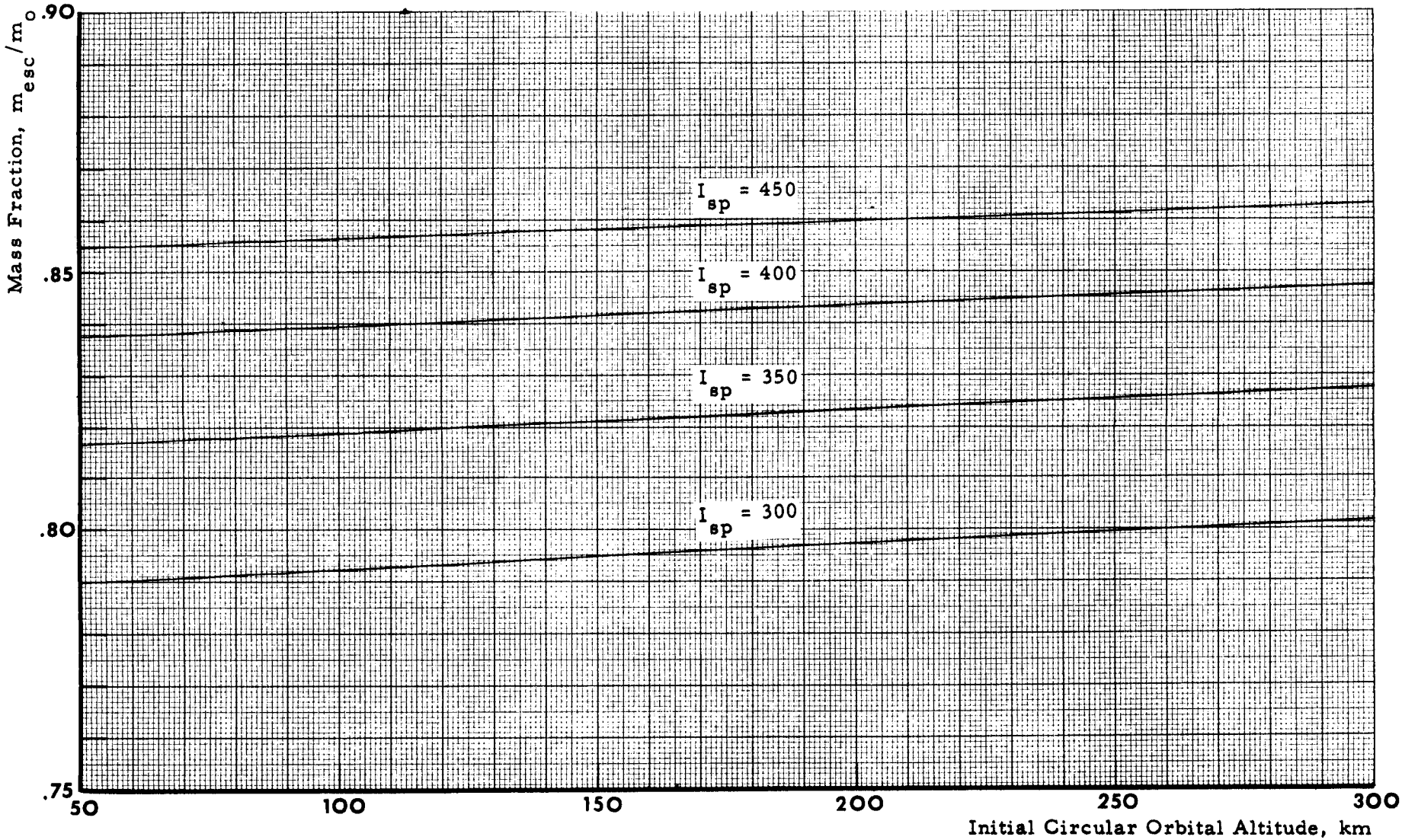

FIGURE 75. MASS FRACTION VS INITIAL ORBITAL ALTITUDE FOR INITIAL LUNAR THRUST-TO-WEIGHT RATIO = 6.0.

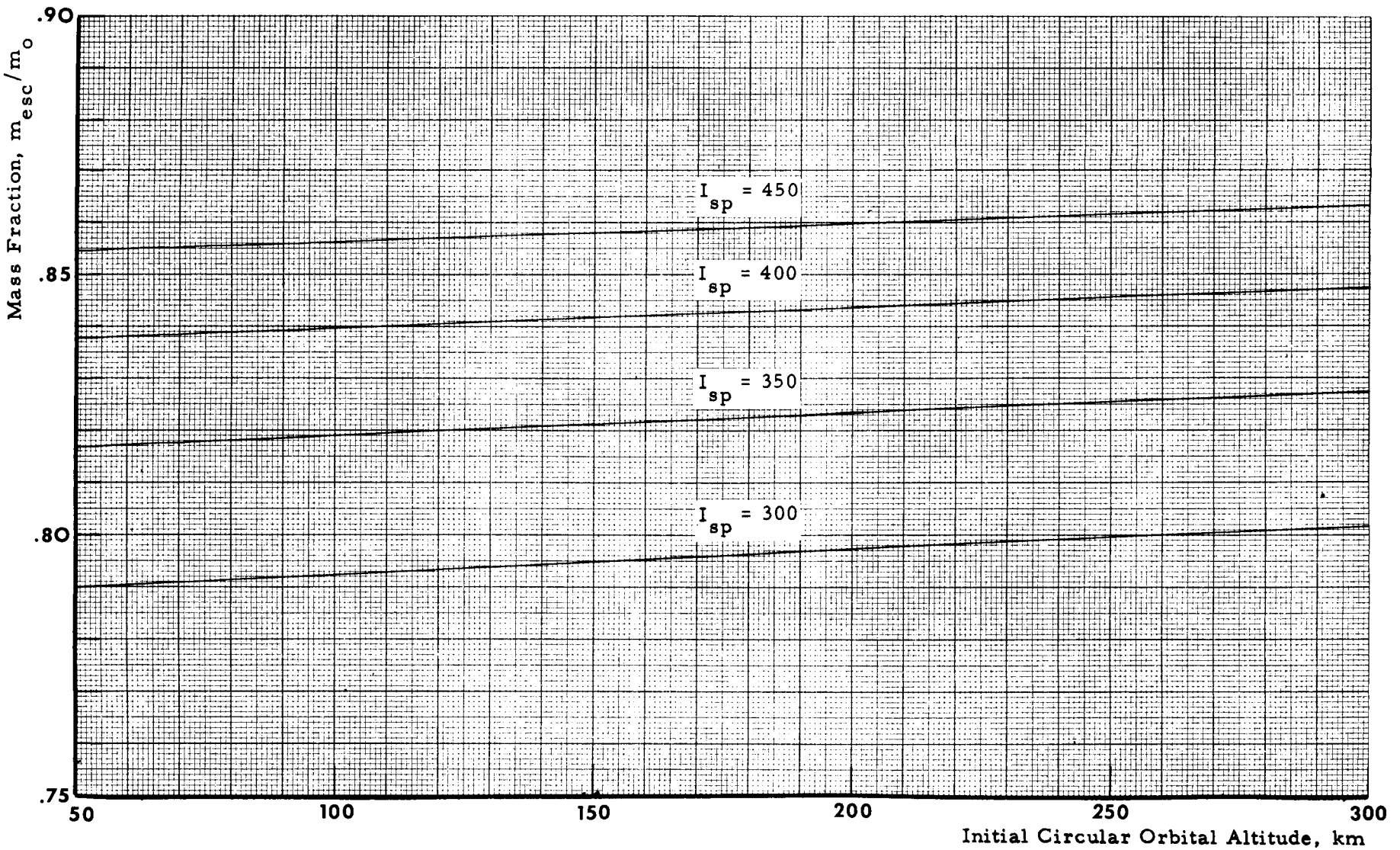

FIGURE 76. MASS FRACTION VS INITIAL ORBITAL ALTITUDE FOR INITIAL LUNAR THRUST-TO-WEIGHT RATIO = 7.0.

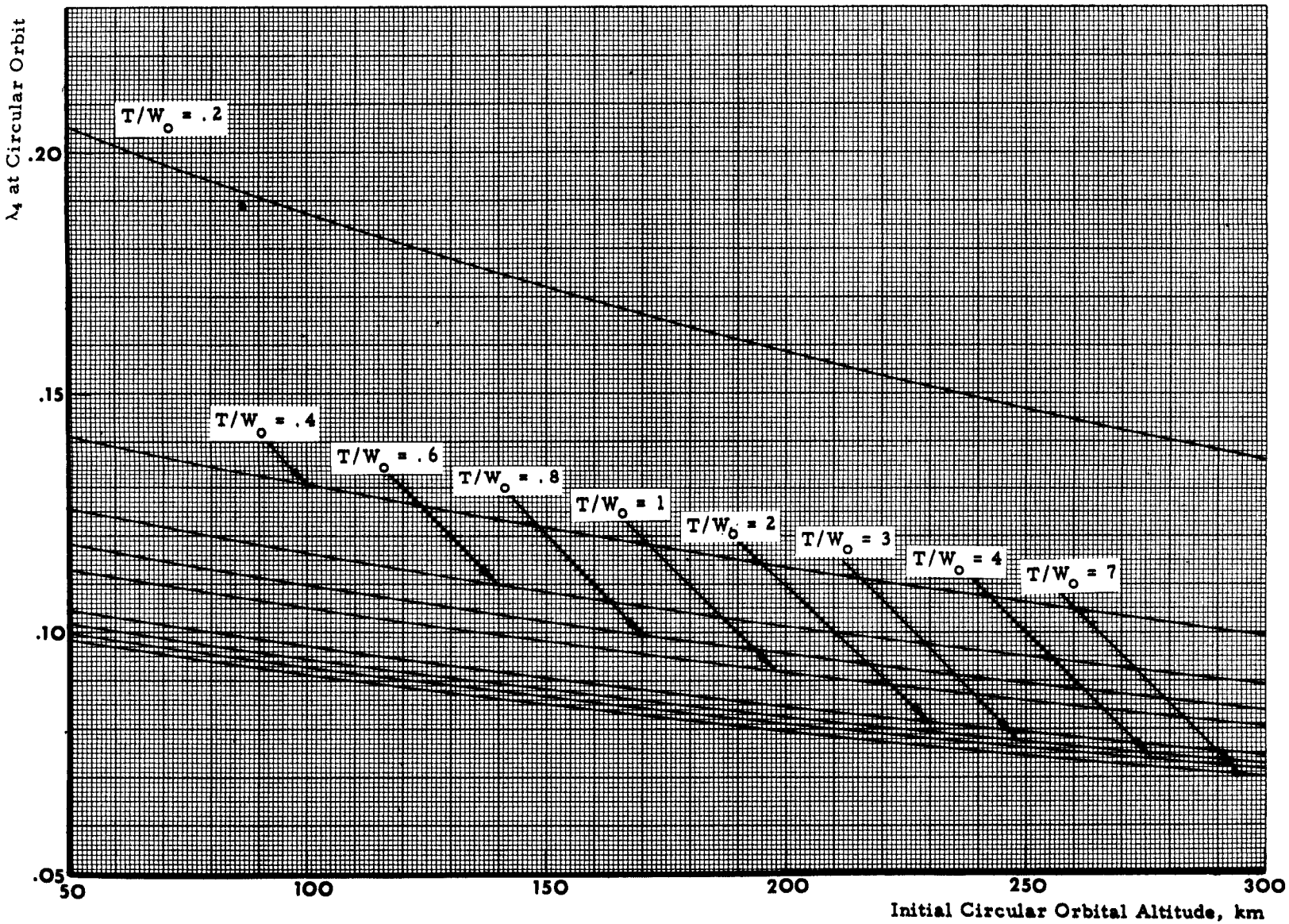

FIGURE 77. VALUE OF λ_4 AT CIRCULAR ORBIT VS INITIAL ORBITAL ALTITUDE FOR SPECIFIC IMPULSE OF 300 SEC.

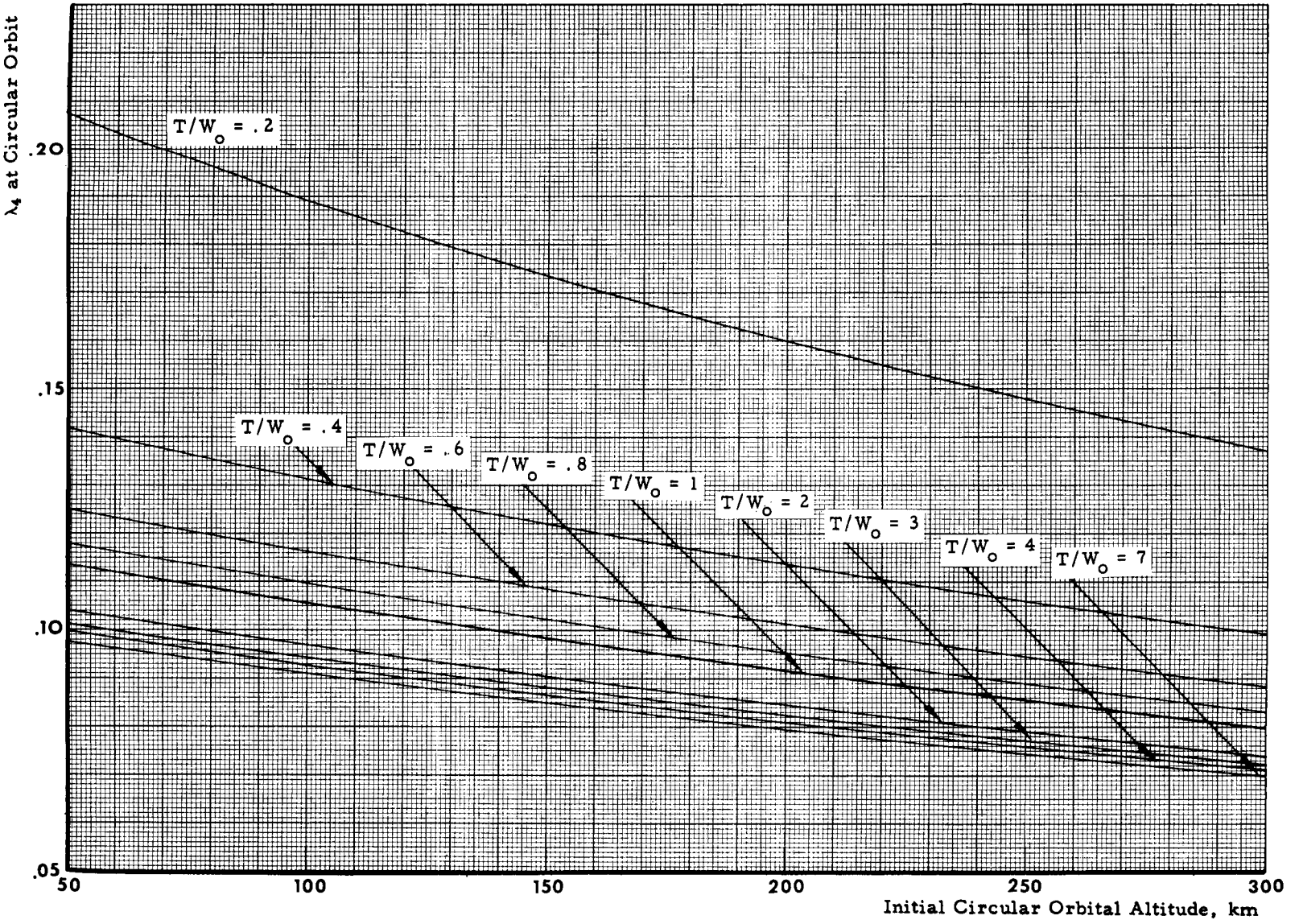

FIGURE 78. VALUE OF λ_4 AT CIRCULAR ORBIT VS INITIAL ORBITAL ALTITUDE FOR SPECIFIC IMPULSE OF 350 SEC.

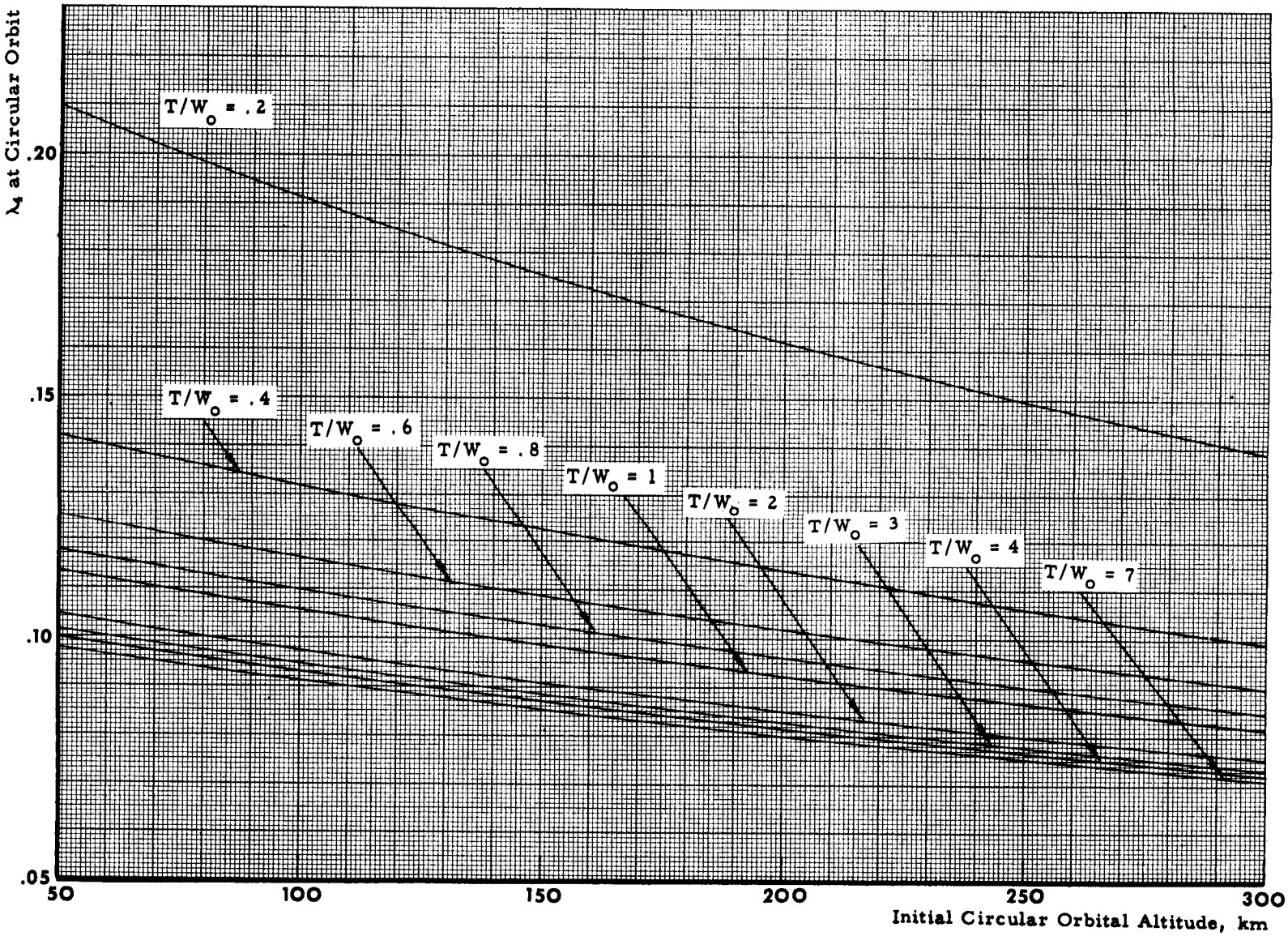

FIGURE 79. VALUE OF λ_4 AT CIRCULAR ORBIT VS INITIAL ORBITAL ALTITUDE FOR SPECIFIC IMPULSE OF 400 SEC.

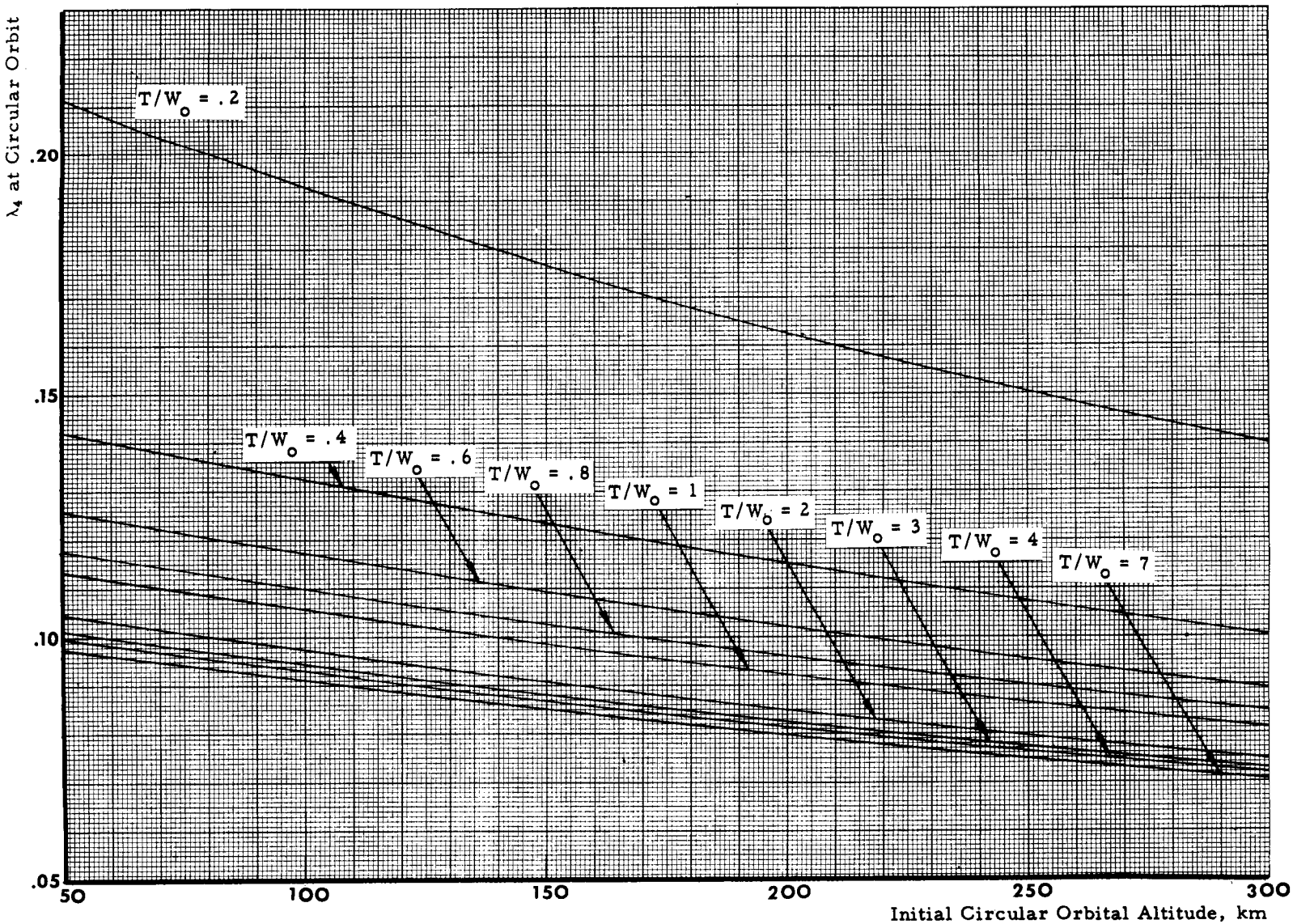

FIGURE 80. VALUE OF λ_4 AT CIRCULAR ORBIT VS INITIAL ORBITAL ALTITUDE FOR SPECIFIC IMPULSE OF 450 SEC.

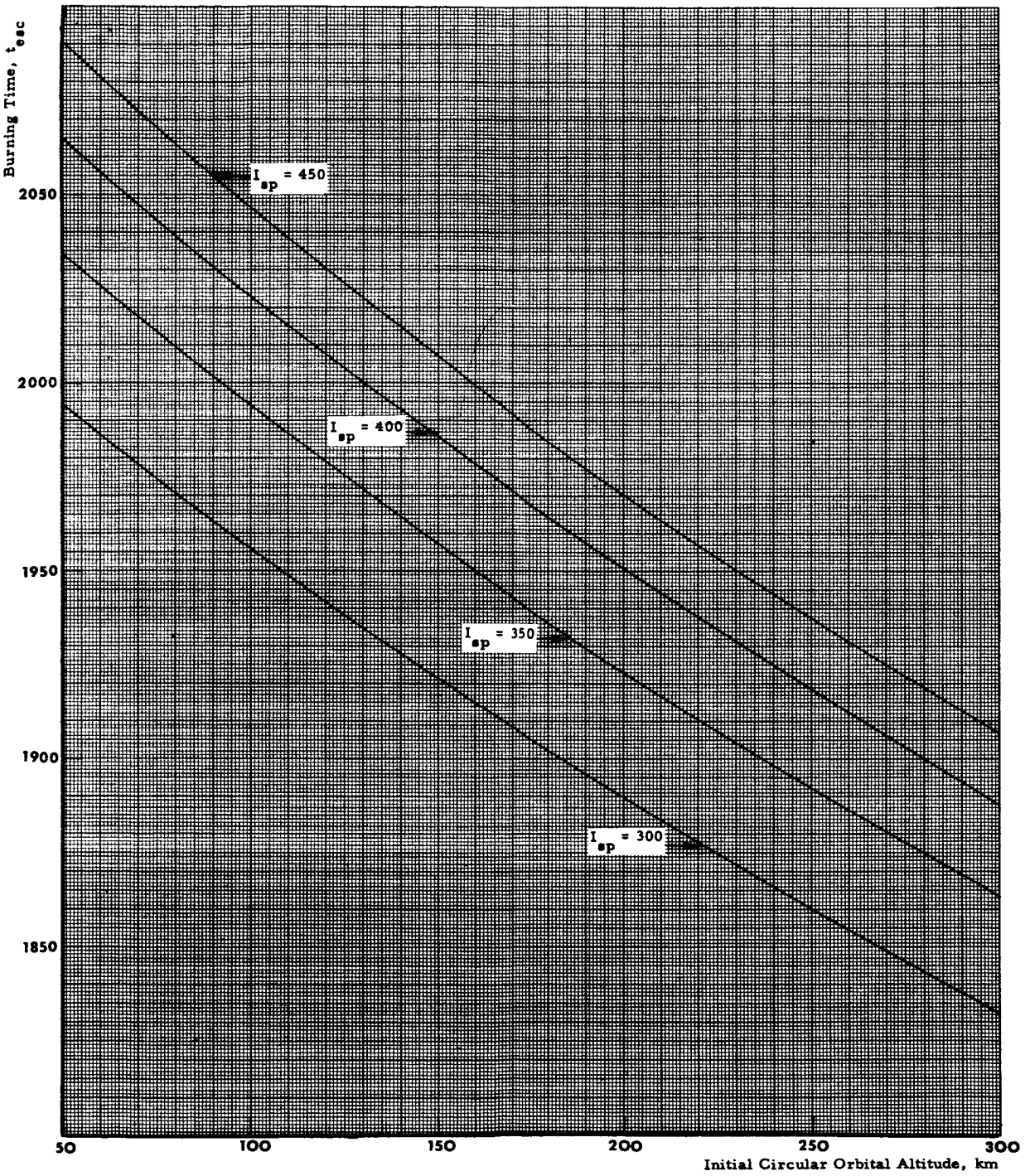

FIGURE 81. BURNING TIME TO ESCAPE VS INITIAL ORBITAL ALTITUDE FOR INITIAL LUNAR THRUST-TO-WEIGHT RATIO = 0.2.

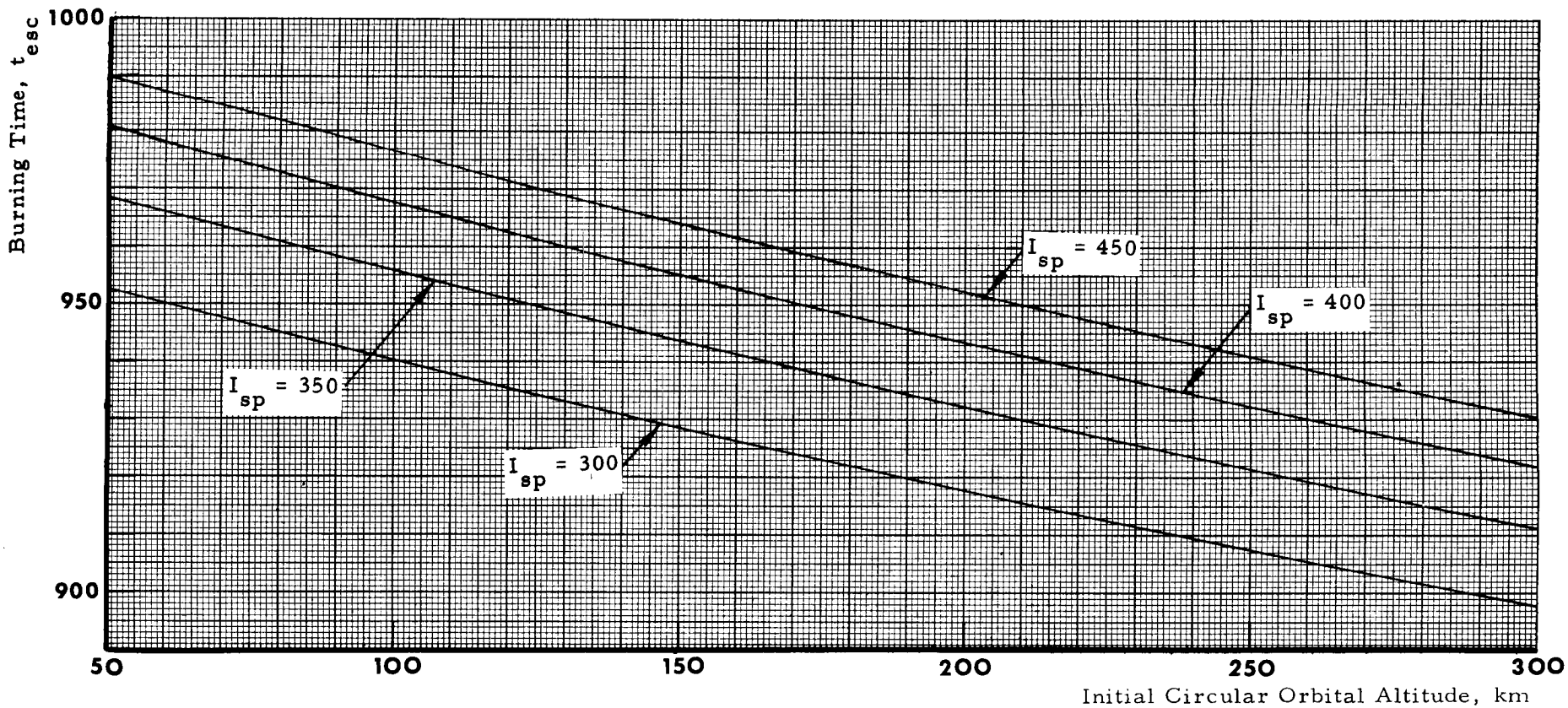

FIGURE 82. BURNING TIME TO ESCAPE VS INITIAL ORBITAL ALTITUDE FOR INITIAL LUNAR THRUST-TO-WEIGHT RATIO = 0.4.

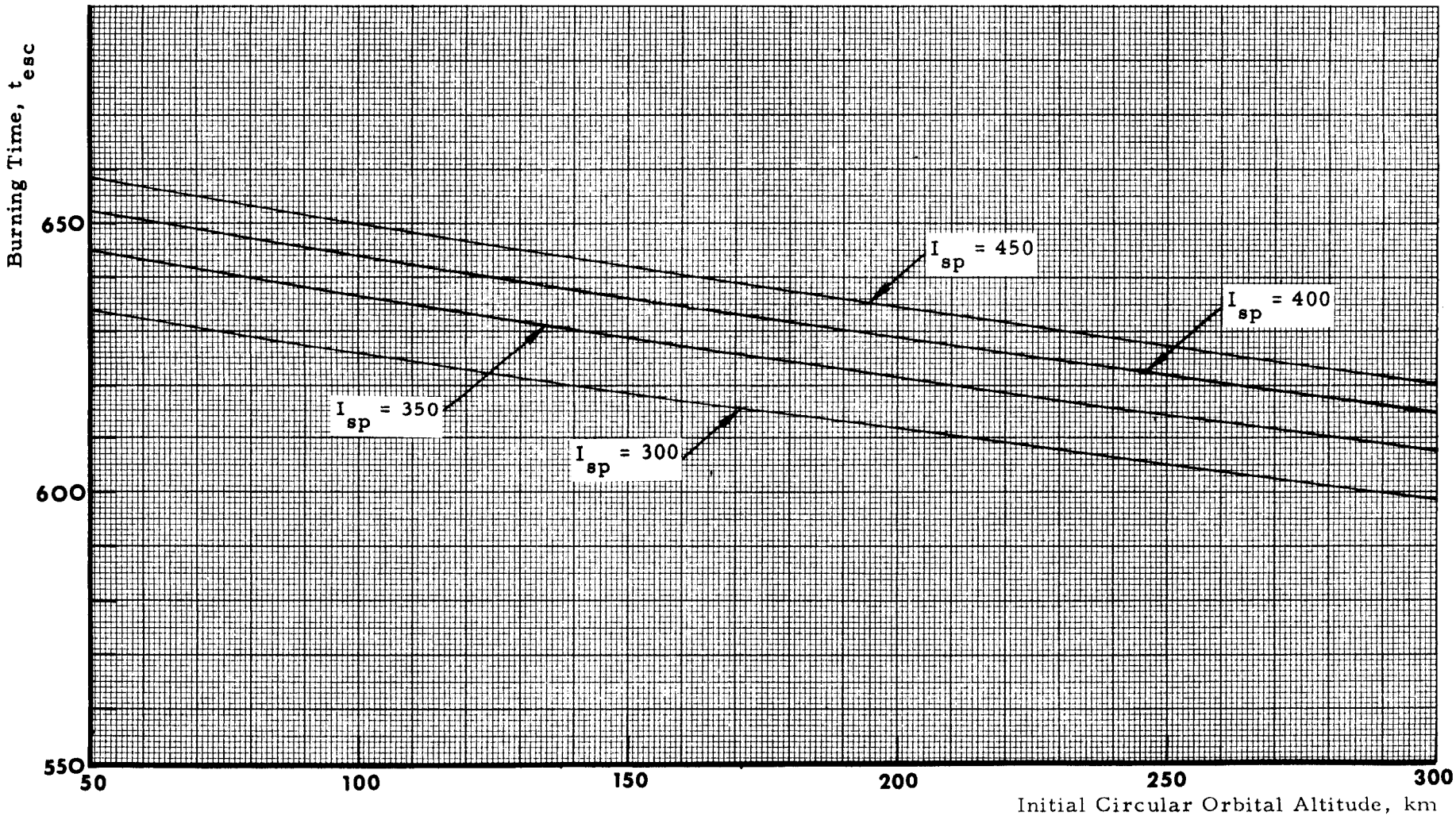

FIGURE 83. BURNING TIME TO ESCAPE VS INITIAL ORBITAL ALTITUDE FOR INITIAL LUNAR THRUST-TO-WEIGHT RATIO = 0.6.

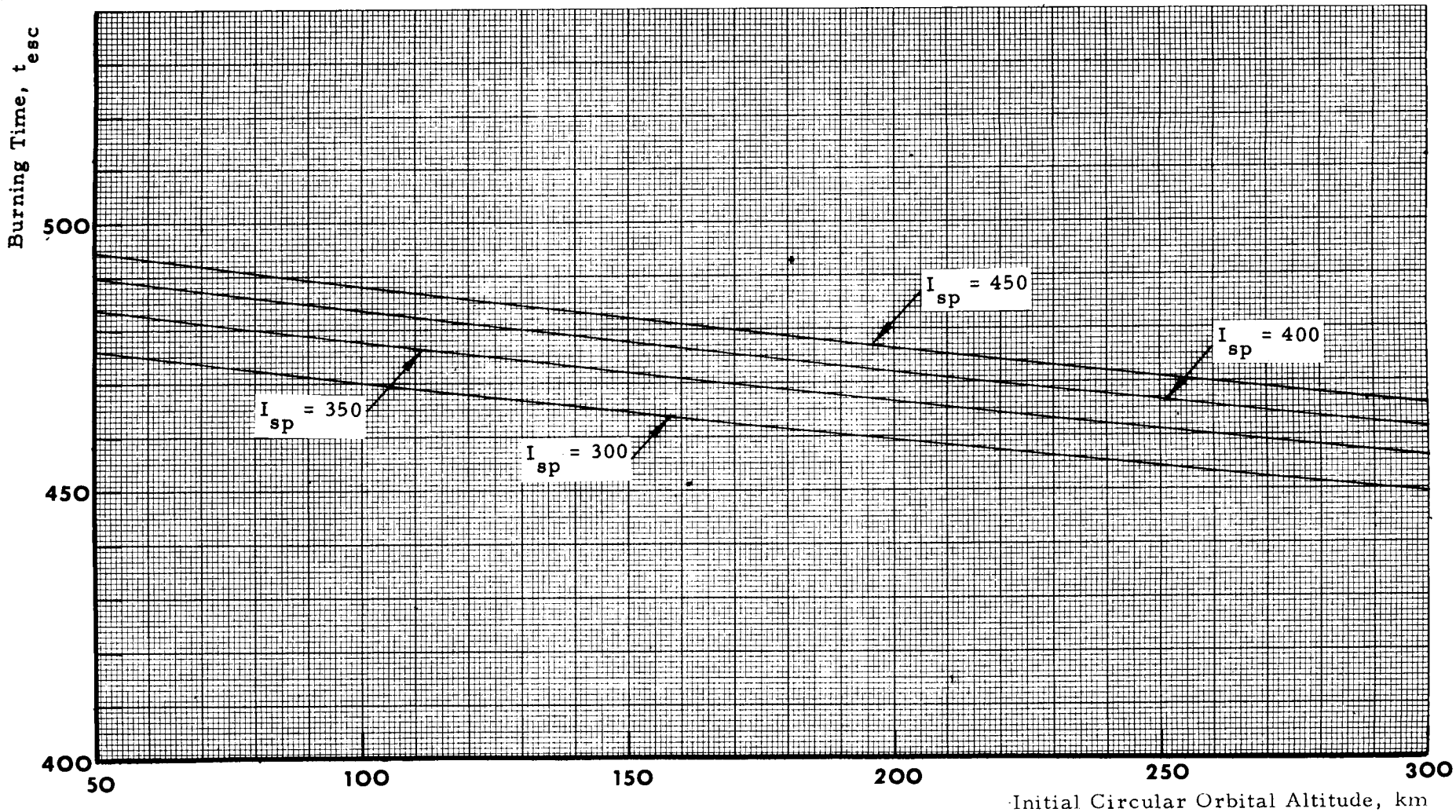

FIGURE 84. BURNING TIME TO ESCAPE VS INITIAL ORBITAL ALTITUDE FOR INITIAL LUNAR THRUST-TO-WEIGHT RATIO = 0.8.

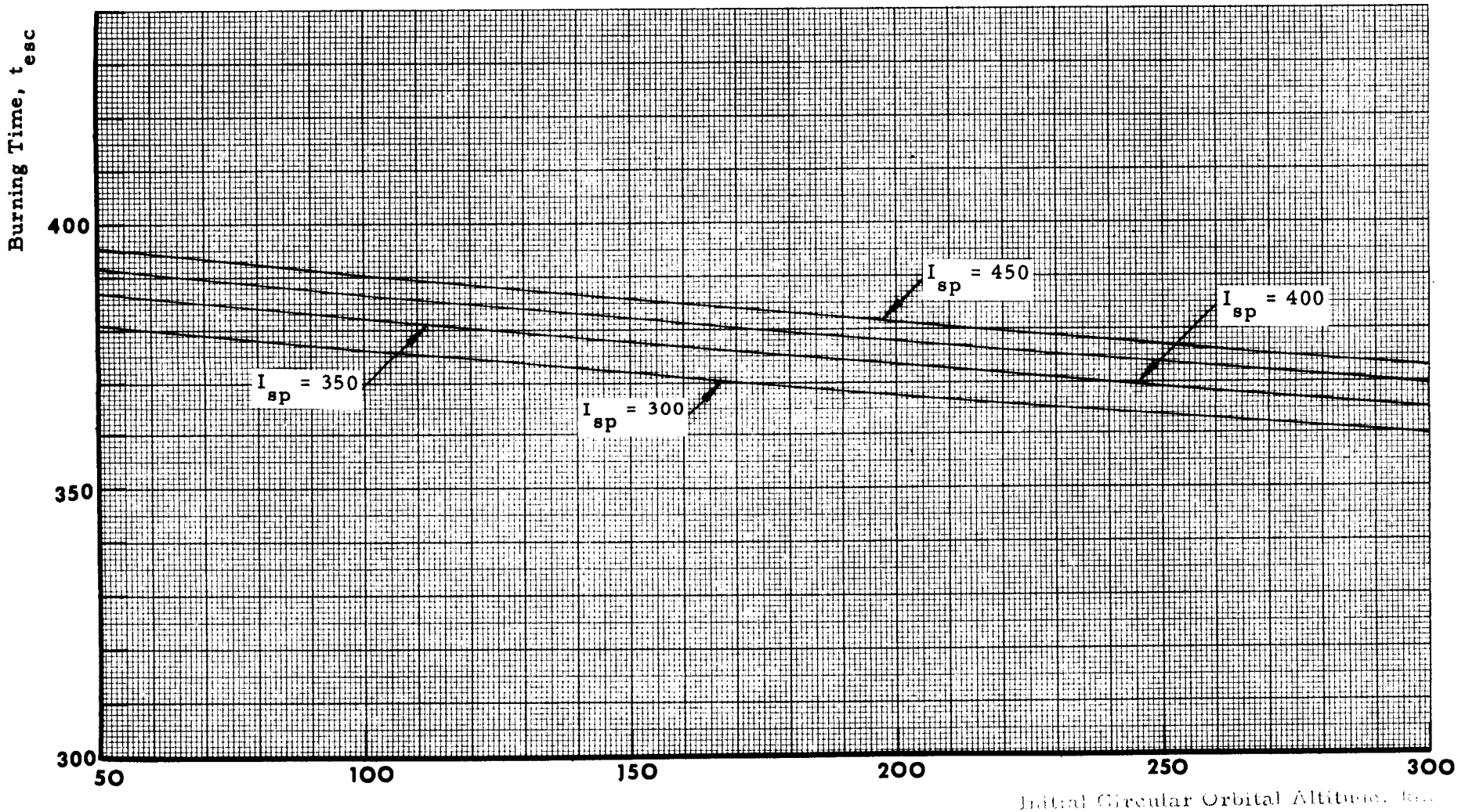

FIGURE 85. BURNING TIME TO ESCAPE VS INITIAL ORBITAL ALTITUDE FOR INITIAL LUNAR THRUST-TO-WEIGHT RATIO = 1.0.

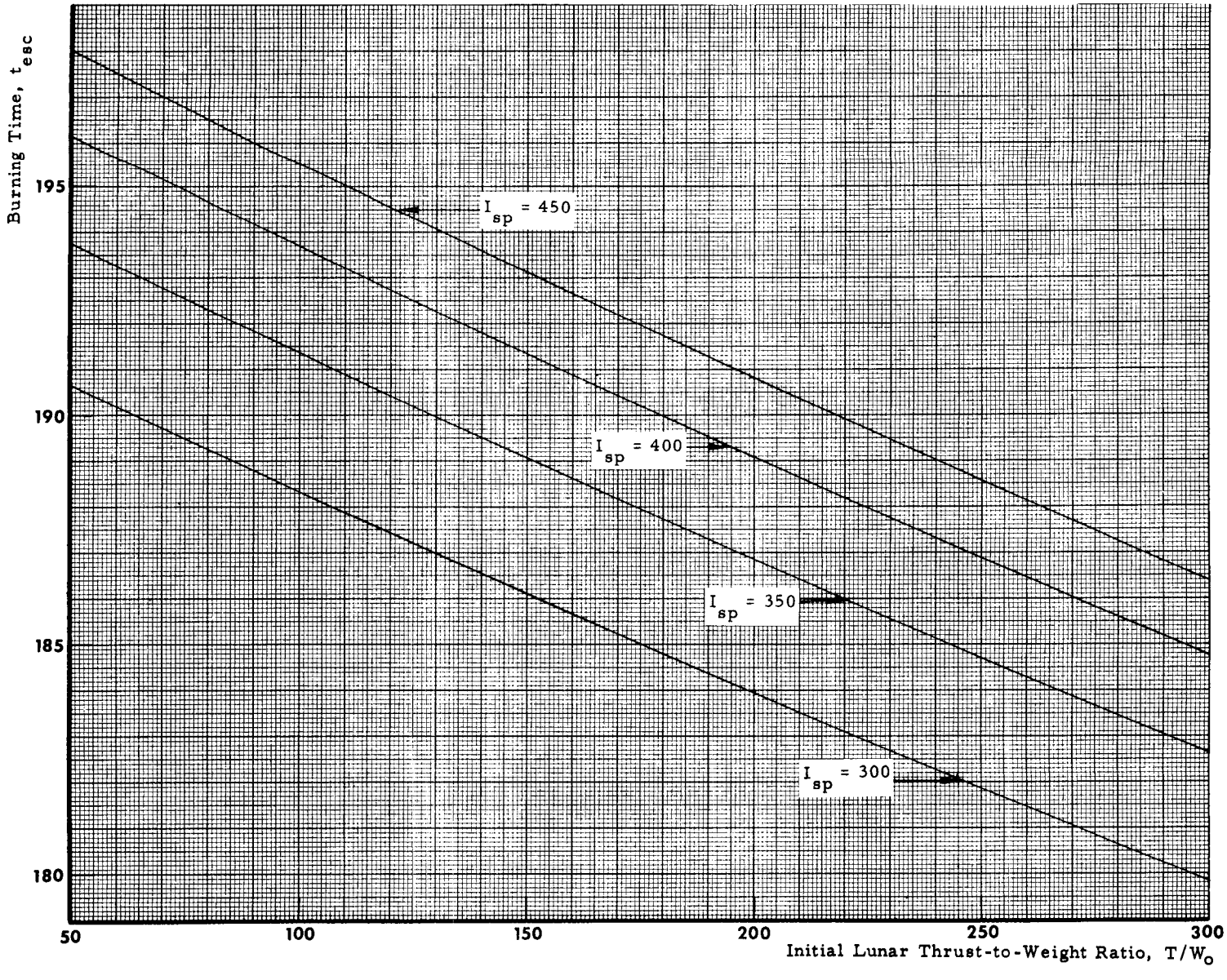

FIGURE 86. BURNING TIME TO ESCAPE VS INITIAL ORBITAL ALTITUDE FOR INITIAL LUNAR THRUST-TO-WEIGHT RATIO = 2.0.

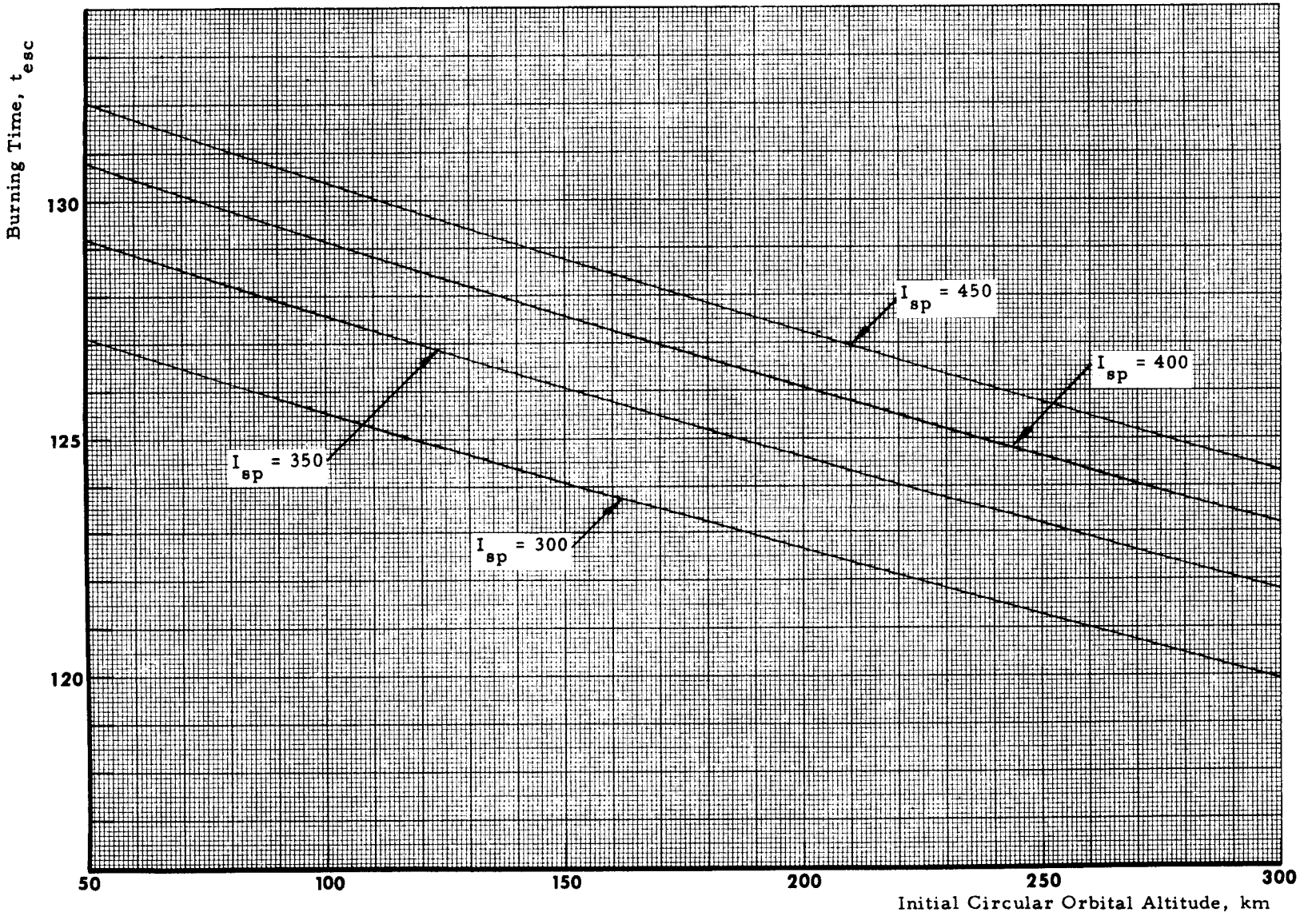

FIGURE 87. BURNING TIME TO ESCAPE VS INITIAL ORBITAL ALTITUDE FOR INITIAL LUNAR THRUST-TO-WEIGHT RATIO = 3.0.

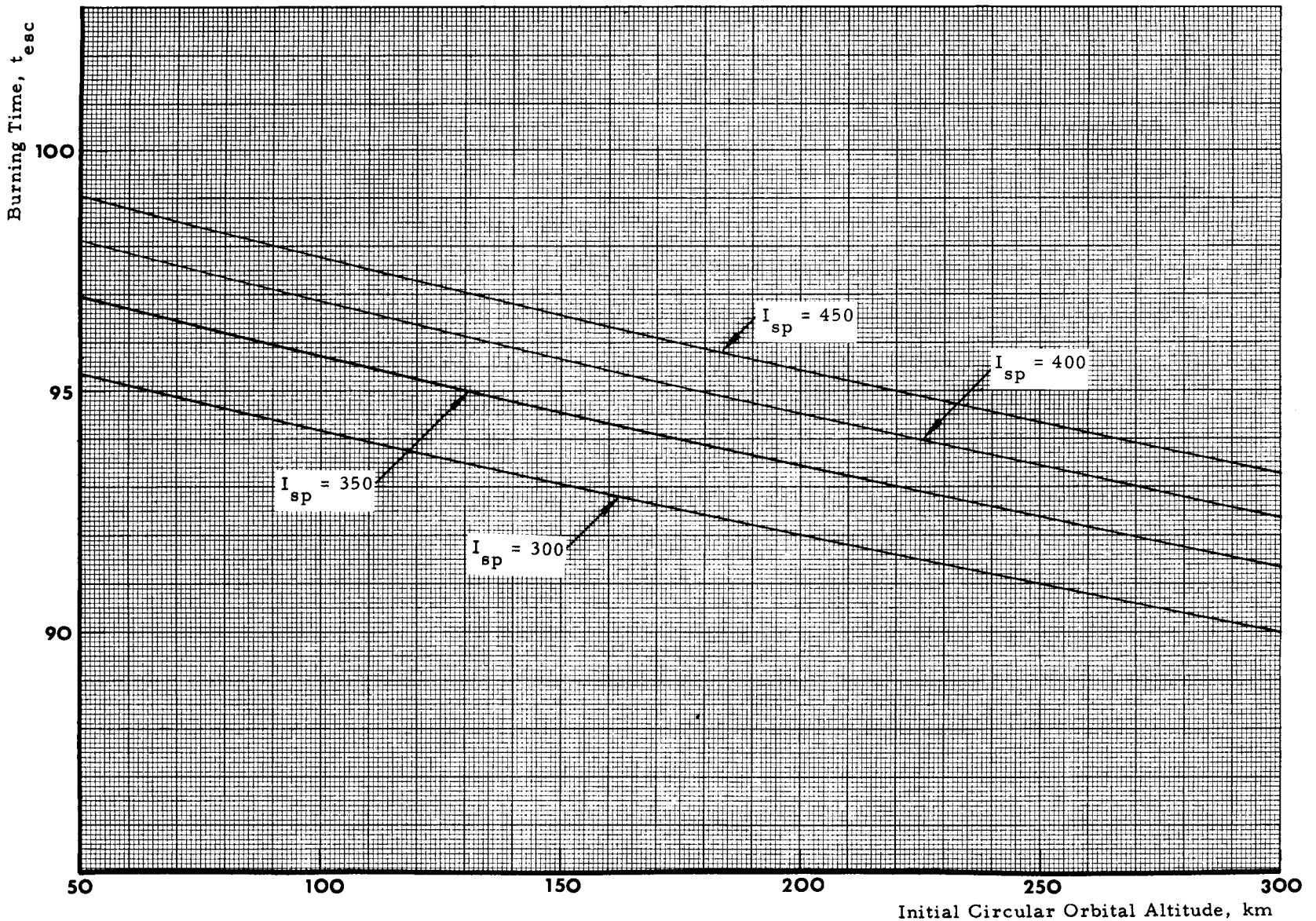

FIGURE 88. BURNING TIME TO ESCAPE VS INITIAL ORBITAL ALTITUDE FOR INITIAL LUNAR THRUST-TO-WEIGHT RATIO = 4.0.

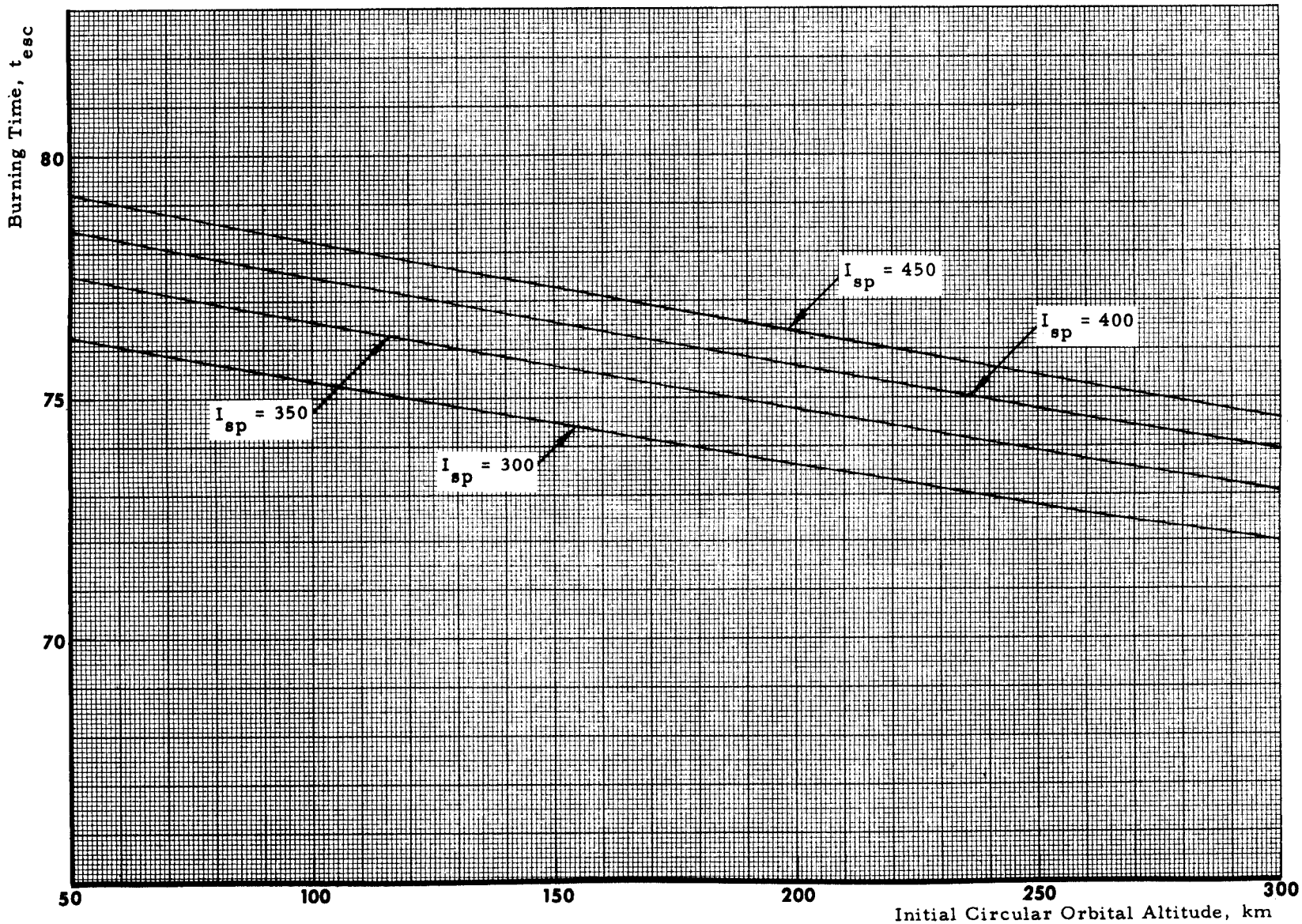

FIGURE 89. BURNING TIME TO ESCAPE VS INITIAL ORBITAL ALTITUDE FOR INITIAL LUNAR THRUST-TO-WEIGHT RATIO = 5.0.

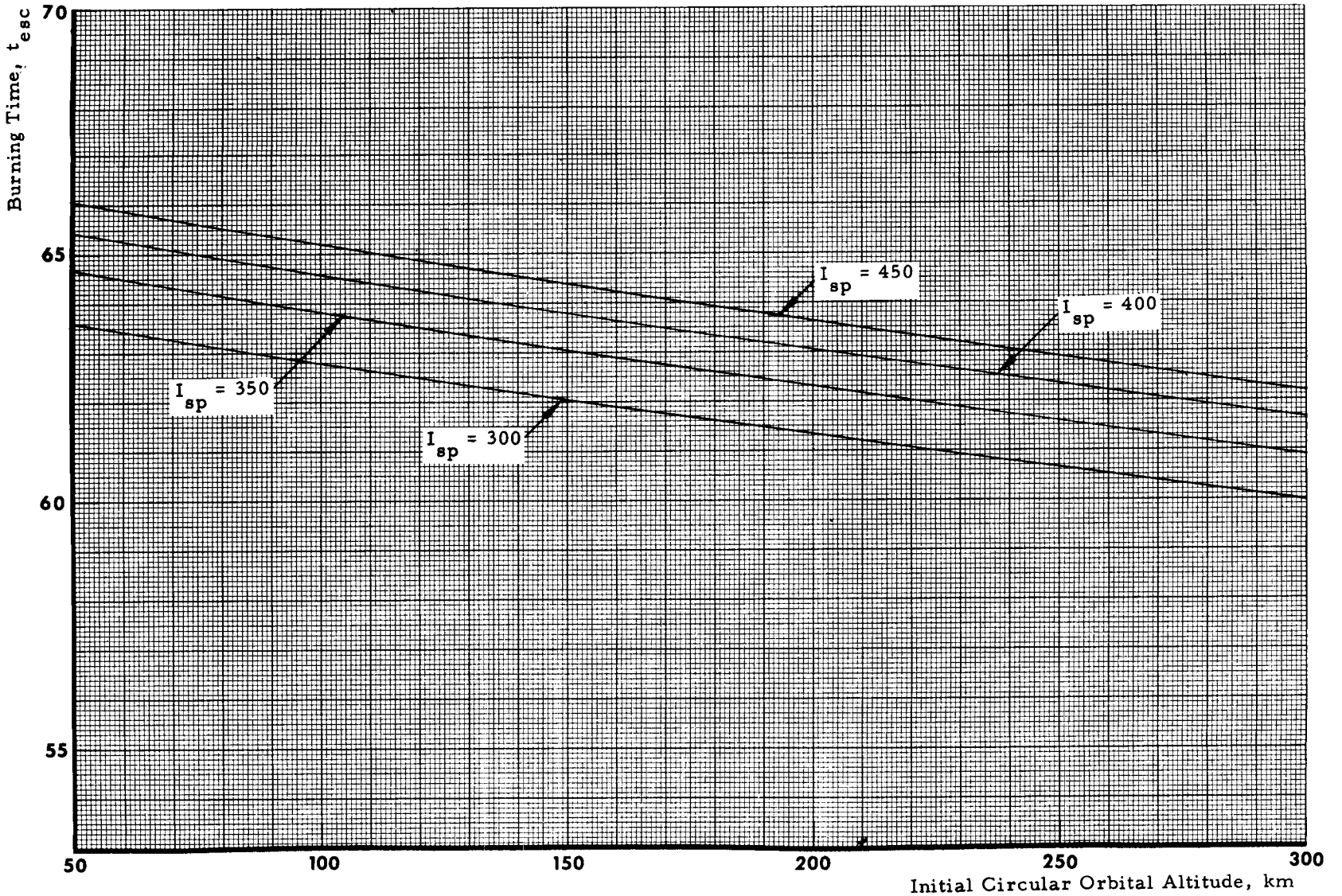

FIGURE 90. BURNING TIME TO ESCAPE VS INITIAL ORBITAL ALTITUDE FOR INITIAL LUNAR THRUST-TO-WEIGHT RATIO = 6.0.

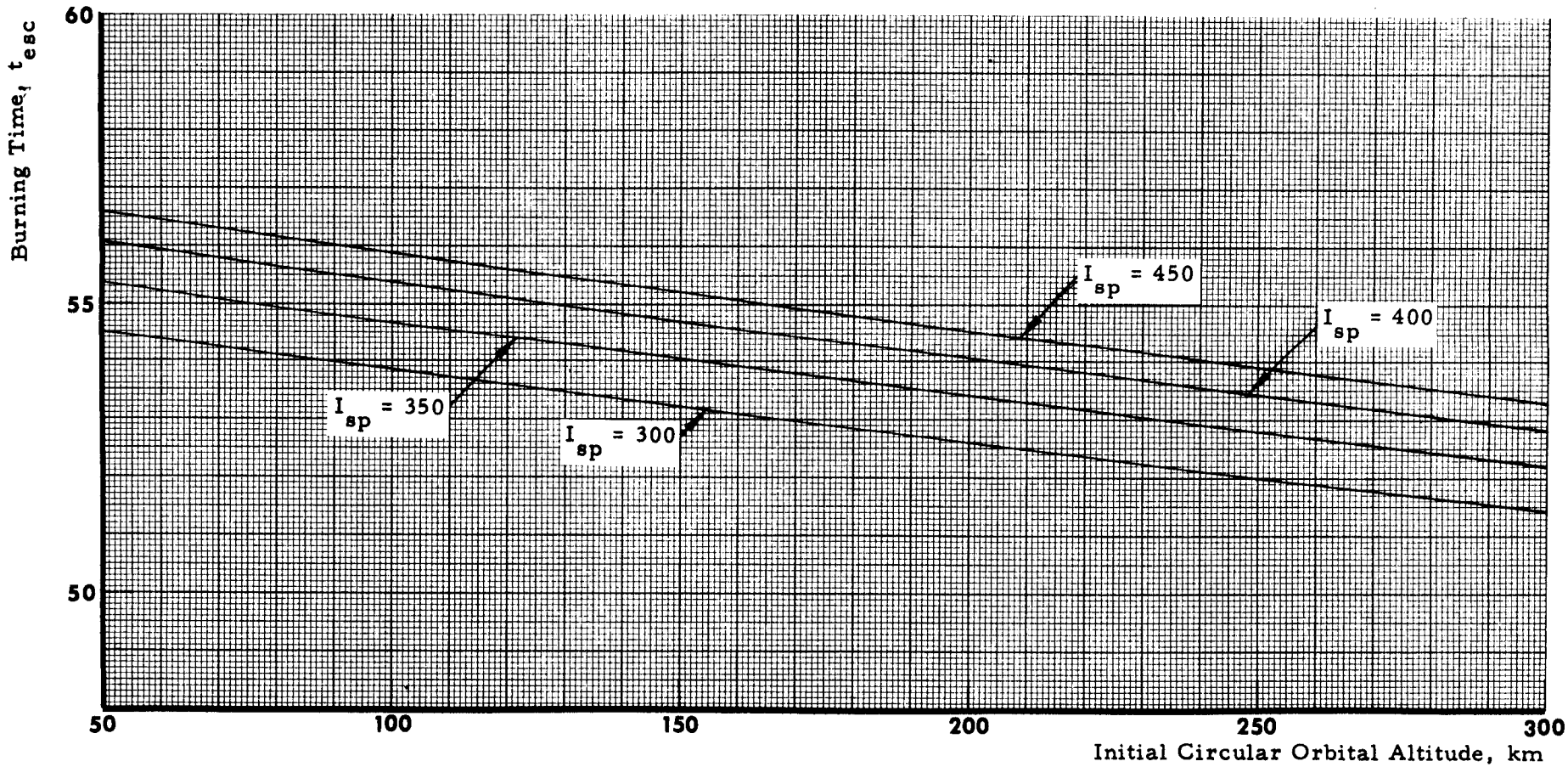

FIGURE 91. BURNING TIME TO ESCAPE VS INITIAL ORBITAL ALTITUDE FOR INITIAL LUNAR THRUST-TO-WEIGHT RATIO = 7.0.

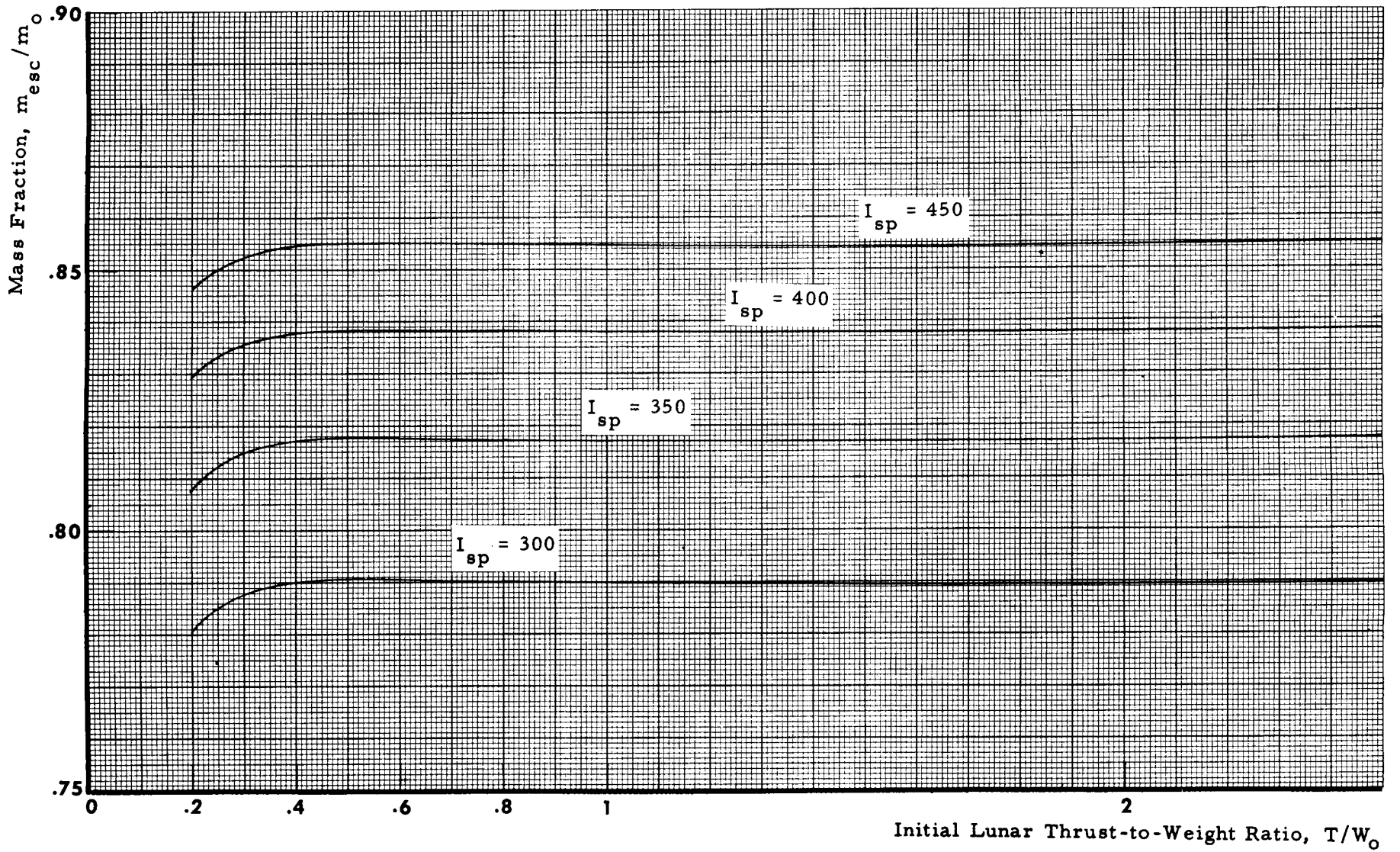

FIGURE 92. MASS FRACTION VS INITIAL LUNAR THRUST-TO-WEIGHT RATIO FOR INITIAL CIRCULAR ORBITAL ALTITUDE = 50 Km.

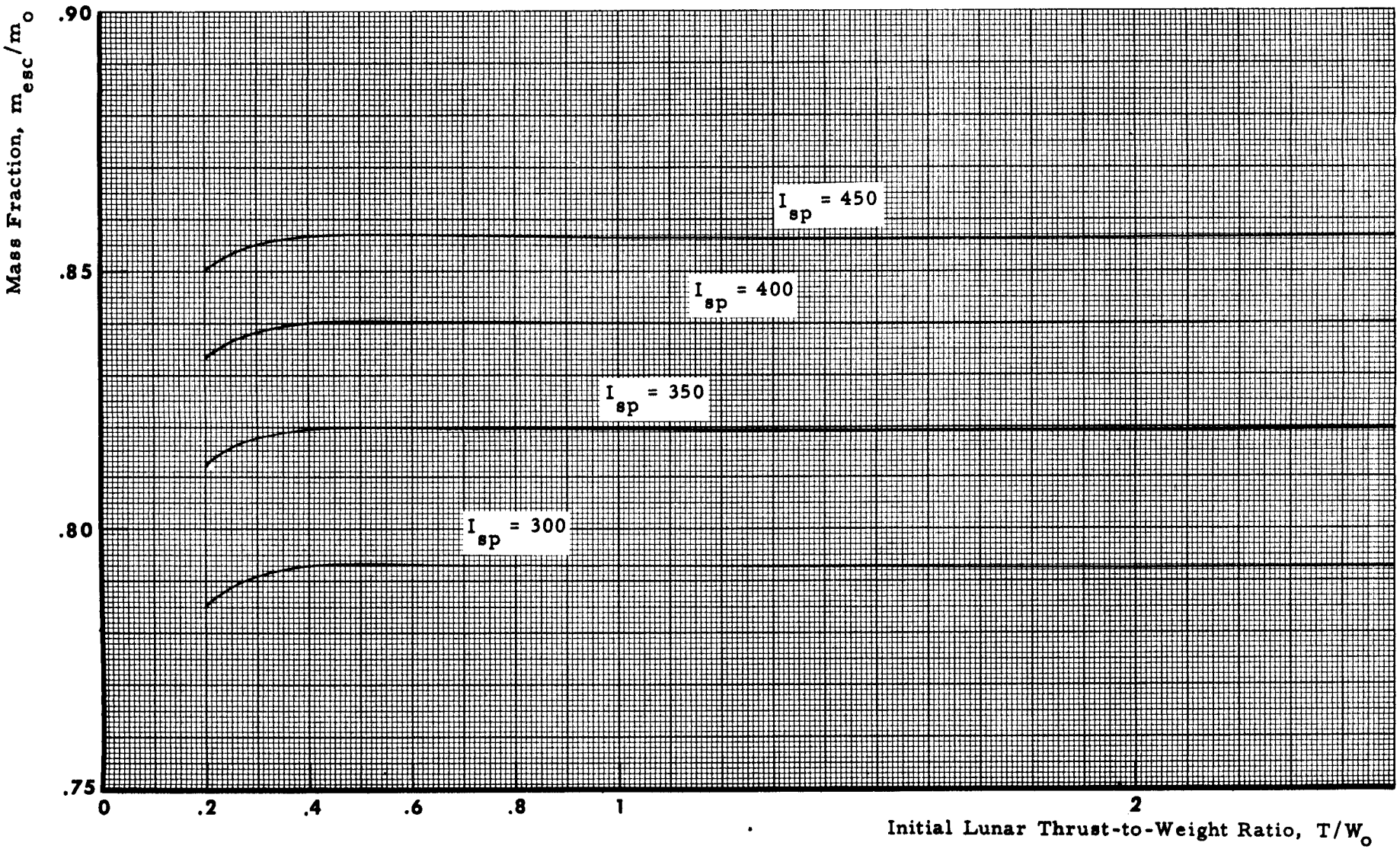

FIGURE 93. MASS FRACTION VS INITIAL LUNAR THRUST-TO-WEIGHT RATIO FOR INITIAL CIRCULAR ORBITAL ALTITUDE = 100 Km.

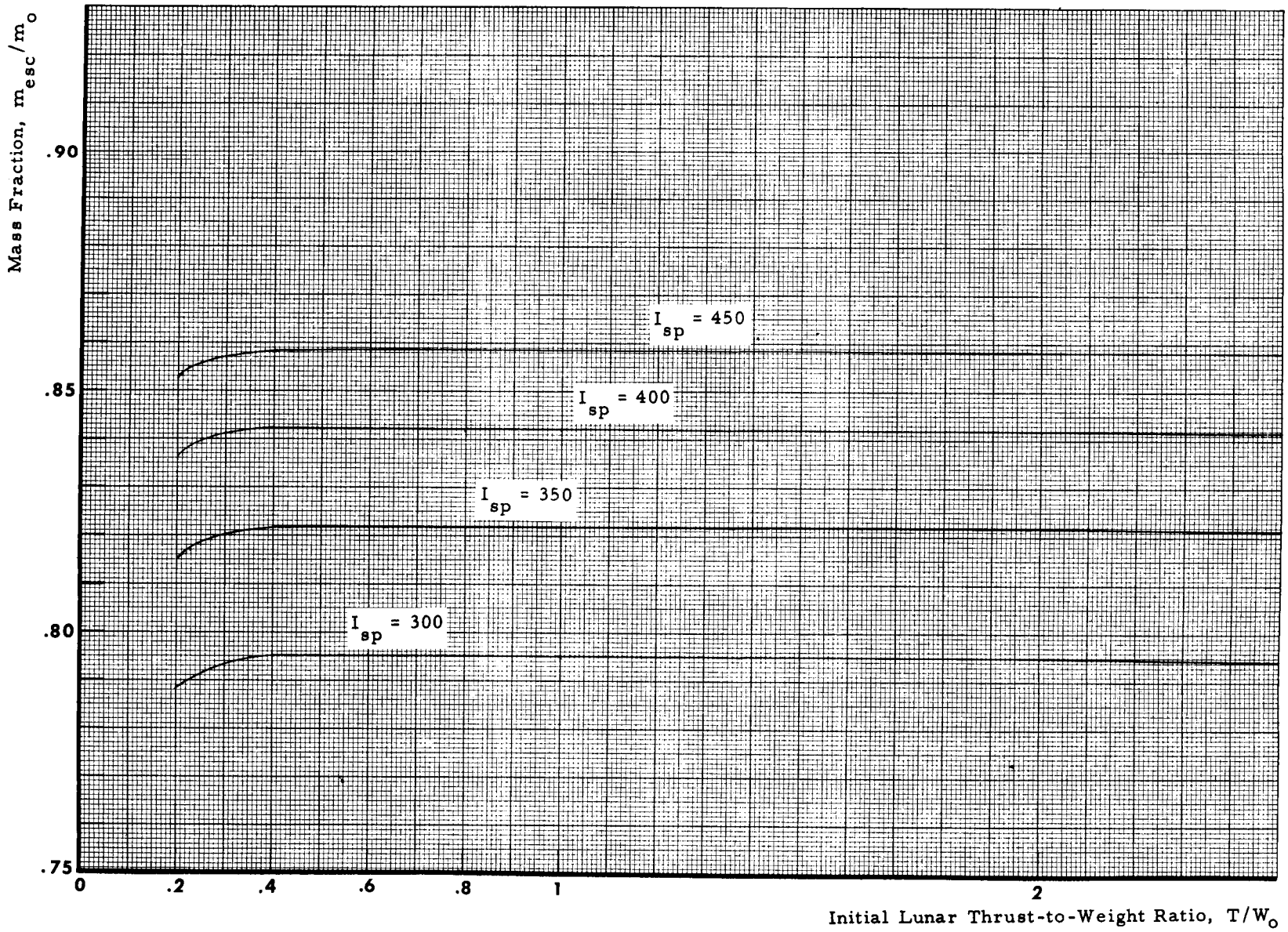

FIGURE 94. MASS FRACTION VS INITIAL LUNAR THRUST-TO-WEIGHT RATIO FOR INITIAL CIRCULAR ORBITAL ALTITUDE = 150 Km.

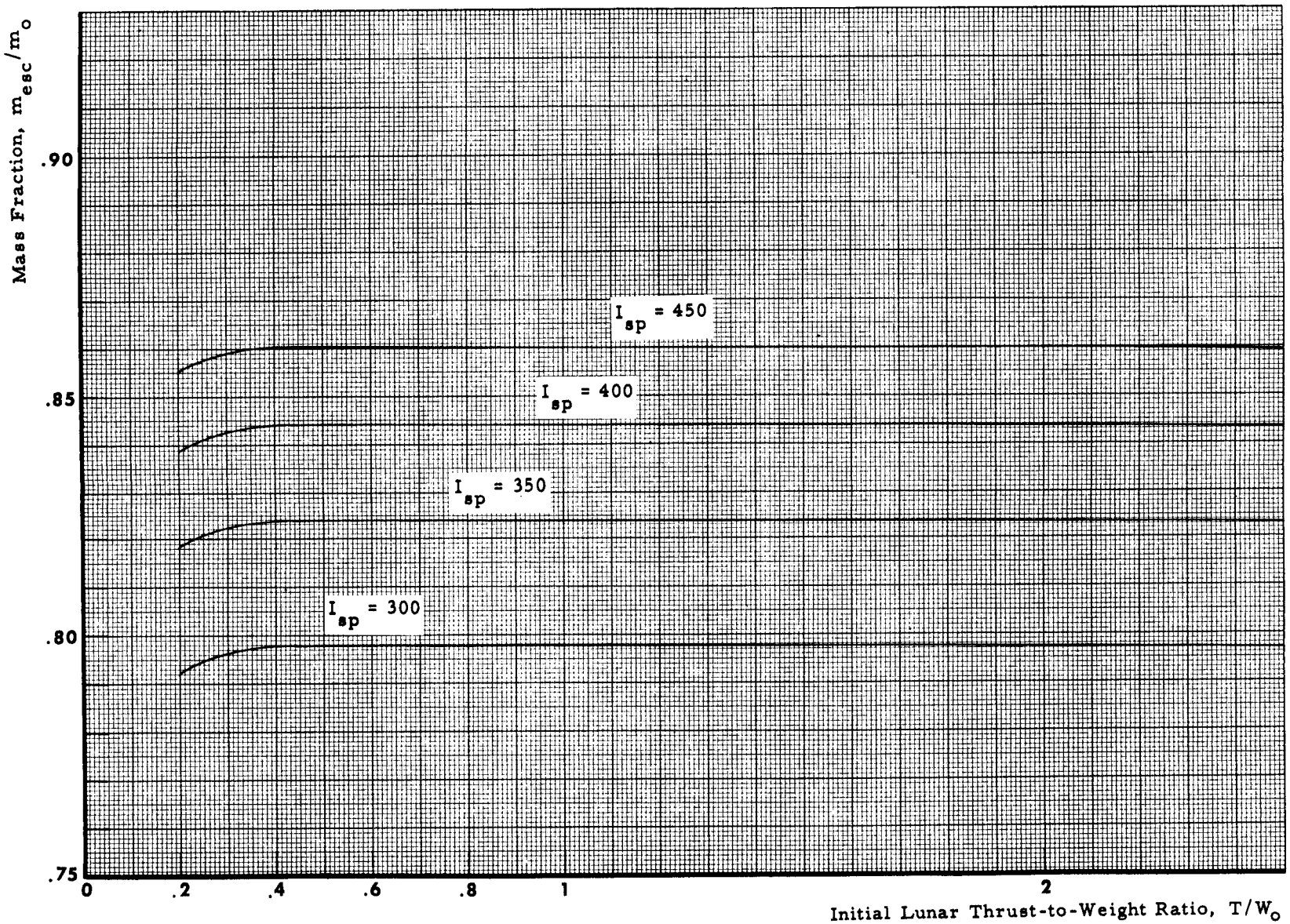

FIGURE 95. MASS FRACTION VS INITIAL LUNAR THRUST-TO-WEIGHT RATIO FOR INITIAL CIRCULAR ORBITAL ALTITUDE = 200 Km.

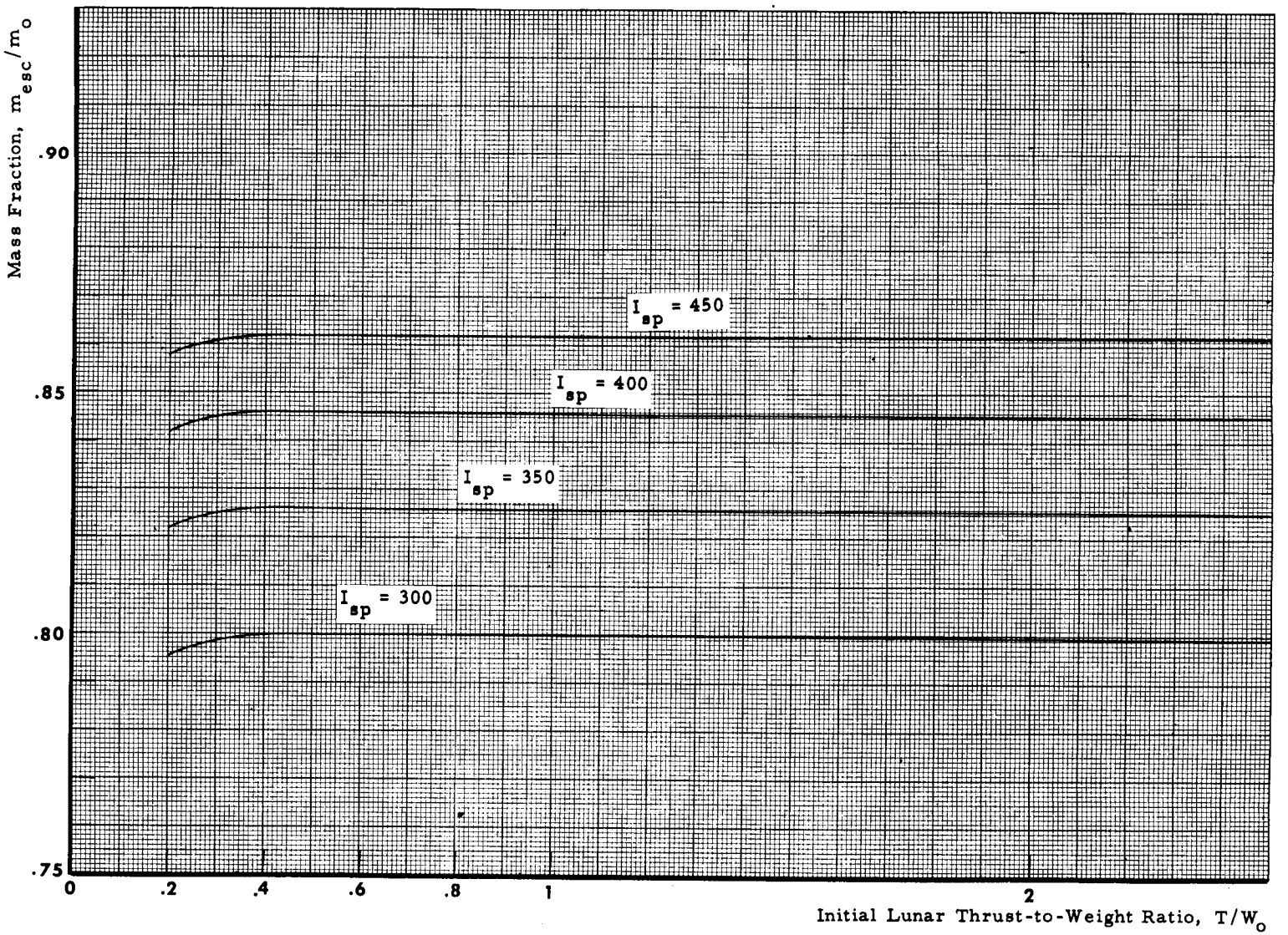

FIGURE 96. MASS FRACTION VS INITIAL LUNAR THRUST-TO-WEIGHT RATIO FOR INITIAL CIRCULAR ORBITAL ALTITUDE = 250 Km.

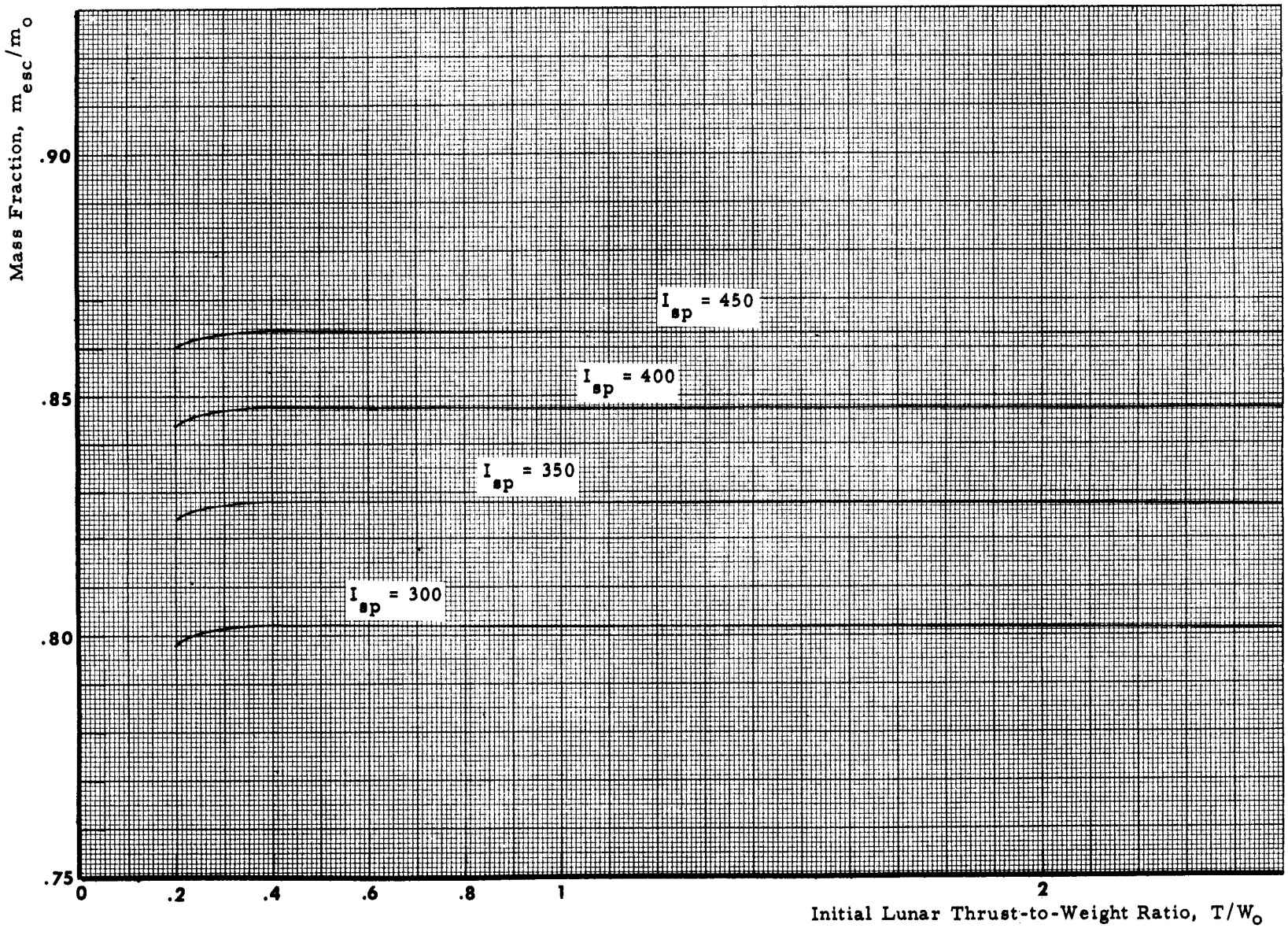

FIGURE 97. MASS FRACTION VS INITIAL LUNAR THRUST-TO-WEIGHT RATIO FOR INITIAL CIRCULAR ORBITAL ALTITUDE = 300 Km.

In the following four examples an attempt is made to illustrate a few of the possible uses of the above numerical data. These methods allow a first-pass determination of the various quantities that are usually of interest as well as provide estimates of the initial values of the Lagrangian multipliers necessary as input data to numerical calculations.

Example 1. Suppose that we desire to find the characteristic velocity, final value of gamma, burning time, and initial values of the multipliers λ_1, λ_4, and λ_5 required to perform a direct escape mission from the lunar surface to parabolic velocity. Assume that the vehicle has an initial lunar thrust-to-weight ratio of 2.7 and a specific impulse of 410 sec. Require that escape occurs at 15 kilometers altitude.

The solution begins with the use of FIG 3, 9, 10, 5, 7 and 8. If a vertical line is constructed on each of these graphs from $T/W_0 = 2.7$, the data presented in Table 98 are obtained.

Table 98
$(T/W_0) = 2.7$

I_{sp}	m_{esc}/m_0	γ_{esc}	t_{esc}	λ_1°	λ_4°	λ_5°
300	.4232	91.02	388	3.77	.0231	−8790.3
350	.4780	91.14	411	4.00	.0247	−8789.2
400	.5230	91.25	427	4.28	.0256	−8788.5
450	.5613	91.32	443	4.50	.0262	−8787.8

The next step is to isolate the given specific impulse, 410 sec. FIG 98 shows a plot of m_{esc}/m_0, γ_{esc}, and t_f vs I_{sp} for the necessary value of T/W_0 while FIG 99 shows a similar graph for λ_1, λ_4, and λ_5. For a value of $I_{sp} = 410$ on these graphs we read

Table 99

I_{sp}	m_{esc}/m_0	γ_{esc}	t_{esc}	λ_1°	λ_4°	λ_5°
410	.5310	91.27°	431	4.33	.0257	−8788.4

If we define u to be characteristic velocity we have

$$u = (g_0)_\oplus \; I_{sp} \ln\left(\frac{m_0}{m_{esc}}\right) = (g_0)_\oplus \; I_{sp} \ln \frac{1}{m_{esc}/m_0}$$

$$= (9.81)(410) \ln \frac{1}{.5310} = 4022.1 \ln (1.883) = 2545 \text{ m/sec}$$

Assume now that the vehicle had a lift-off weight of 35,000 earth pounds and the actual weight at escape is of interest. This may be obtained by multiplying the initial weight by the mass fraction at escape. Thus,

$$W_{esc} = W_0 \frac{m_{esc}}{m_0} = (35{,}000)(.5310) = 18{,}585 \text{ earth pounds}$$

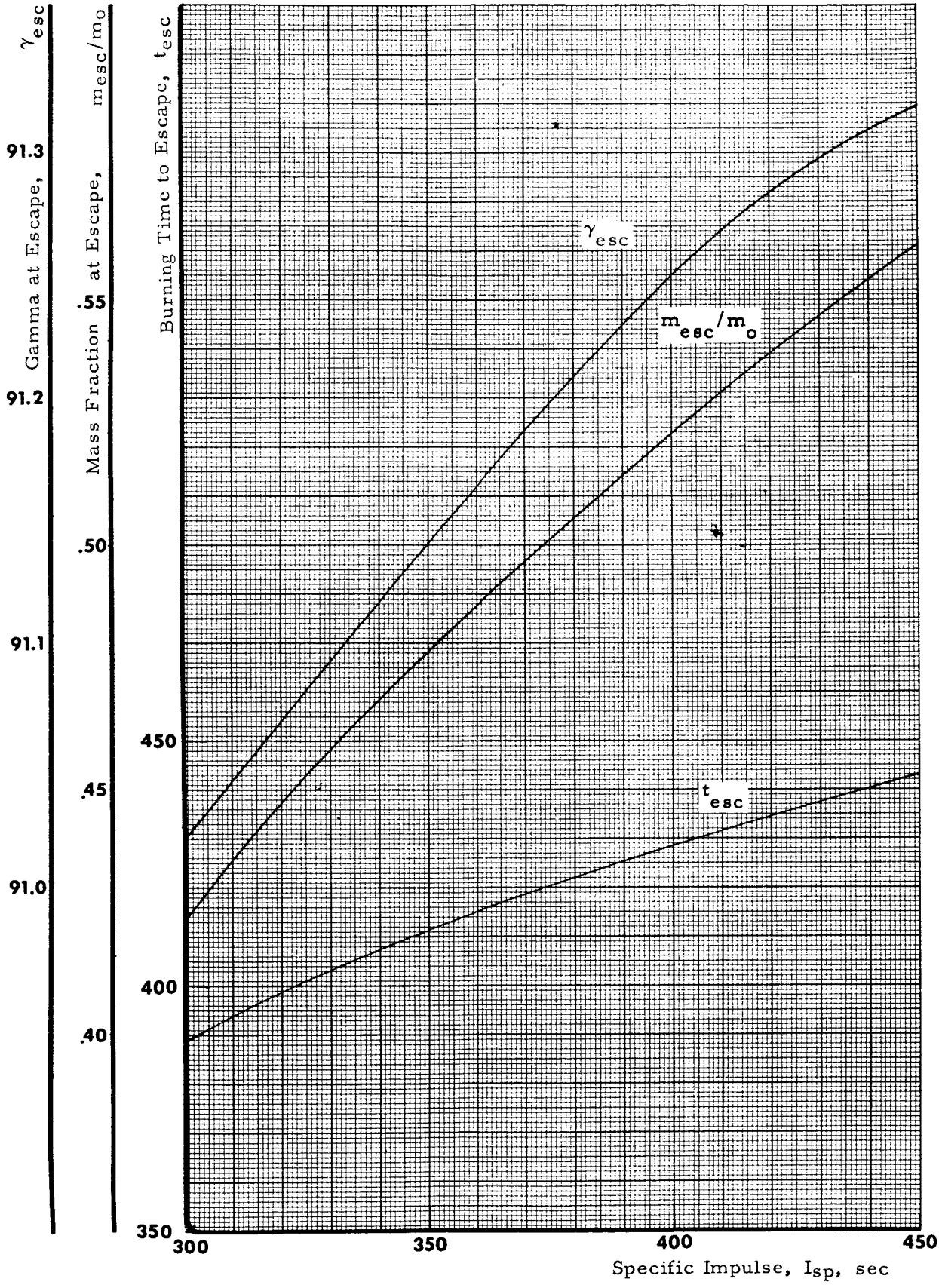

FIGURE 98. GAMMA, MASS FRACTION AT ESCAPE, AND TIME TO ESCAPE VS SPECIFIC IMPULSE FOR $T/W_o = 2.7$

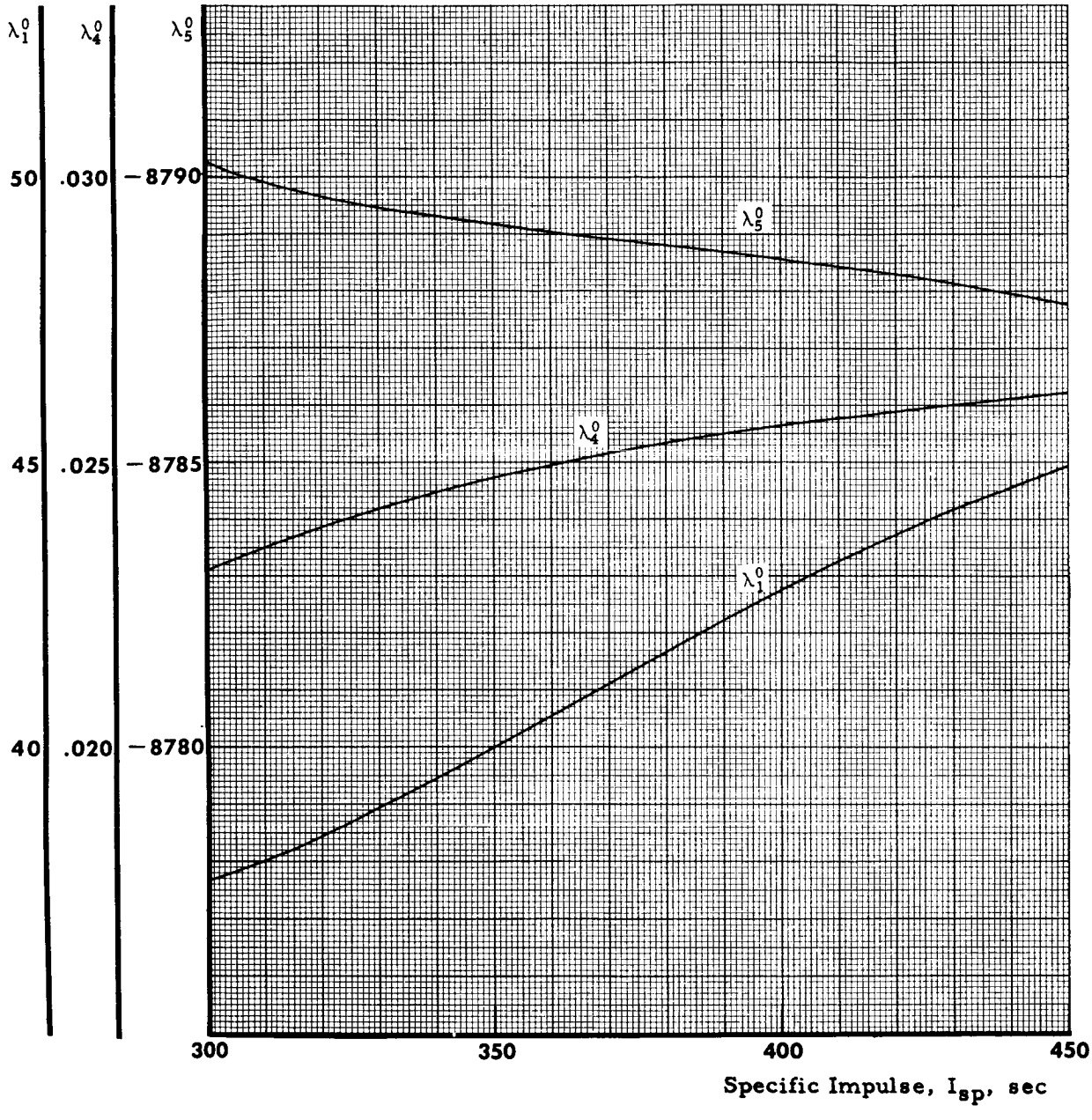

FIGURE 99. INITIAL VALUES OF λ_1, λ_4, AND λ_5 VS SPECIFIC IMPULSE FOR $T/W_o = 2.7$

The thrust acceleration at escape may also be derived from the given data. As shown in Reference 1, there exists a general relationship of the form

$$\frac{T}{m} = \frac{a\ (g_0)_{☾}\ (g_0)_{\oplus}\ I_{sp}}{(g_0)_{\oplus}\ I_{sp} - a\ (g_0)_{☾}\ t}$$

Since all quantities are known we can write, at escape,

$$\frac{T}{m_{esc}} = \frac{(2.7)(1.622169)(9.81)(410)}{(9.81)(410) - (2.7)(1.622169)(431)} = 8.25 \text{ m/sec}^2$$

converting this to the more familiar "g" we have

$$\frac{(T/m_{esc})}{(g_0)_{\oplus}} = \frac{8.25}{9.81} = .841\ g$$

This value can be used to calculate the total acceleration at cutoff by use of the equations of motion, if it is of interest.

As a final point of interest we can calculate the thrust level of the engine since we have previously specified the thrust-to-weight ratio and weight of the vehicle. We first convert the weight from earth pounds to lunar pounds by multiplying by the ratio of the gravitational accelerations; i.e.,

$$\frac{(g_0)_{☾}}{(g_0)_{\oplus}} = \frac{1.622169}{9.81}\ \frac{\text{m/sec}^2}{\text{m/sec}^2} = \frac{1}{6.047459}$$

because we know that

$$(W_0)_{\oplus} = (m_0)(g_0)_{\oplus}$$

and

$$(W_0)_{☾} = (m_0)(g_0)_{☾}$$

solving for m_0 (an invariant) in each of these equations we know that

$$\frac{(W_0)_{\oplus}}{(g_0)_{\oplus}} = \frac{(W_0)_{☾}}{(g_0)_{☾}}$$

since mass is an invariant. Thus,

$$(W_0)_{☾} = (W_0)_{\oplus}\ \frac{(g_0)_{☾}}{(g_0)_{\oplus}} = \frac{(35{,}000)}{6.047459} = 5787.55 \text{ lunar pounds}$$

From the original statement we now have

$$T = \left(\frac{T}{W_0}\right)_{☾} (W_0)_{☾} = (2.7)(5787.55) = 15{,}626 \text{ pounds}$$
$$= 69{,}508 \text{ newtons}$$

(The thrust, given in newtons, is an invariant.)

Example 2. To determine the mass fraction that may be propelled to direct escape from the lunar surface if escape occurs at 20 kilometers and the thrust and velocity vectors are to be aligned at escape. Assume a specific impulse of 375 sec.

This problem is of the class treated by Tables 11 through 20, and shown graphically in FIG 11 through 16. The altitudes, however, were matched with the corresponding thrust-to-weight ratios and specific impulses of those trajectories which ascend to a circular orbit and have a thrust and velocity vector alignment at orbit, but no alignment at escape. Graph 27 shows the altitude at escape as a function of initial thrust-to-weight ratio for either mode, and we begin the treatment of the problem here.

A horizontal line at an altitude of 20 kilometers on FIG 27 produces the data presented in Table 100.

Table 100
Final Altitude of 20 Km.

I_{sp}	T/W_0
300	3.20
350	3.37
400	3.51
450	3.61

FIG 100 shows T/W_0 plotted as a function of I_{sp}. For a specific impulse of 375 sec we may now read the initial thrust-to-weight ratio of 3.44. That is, this value of T/W_0 and an I_{sp} of 375 sec will produce an altitude of 20 kilometers for this mode.

From FIG 11 and 16 we can now read the data for $T/W_0 = 3.44$ given in table 101.

Table 101
$T/W_0 = 3.44$

I_{sp}	m_{esc}/m_0	t_{esc}
300	.4290	300
350	.4830	317
400	.5282	333
450	.5663	343

Adding these data to FIG 100 we obtain the results presented in Table 102.

Table 102

I_{sp}	m_{esc}/m_0	t_{esc}
375	.5061	326

Example 3. For a vehicle having a thrust of 20,000 pounds and a specific impulse of 330 sec, find (a) the maximum mass fraction that may be injected to escape, and (b) the maximum payload that may be injected to escape. Assume that the escape trajectory passes through a 15-kilometer circular orbit.

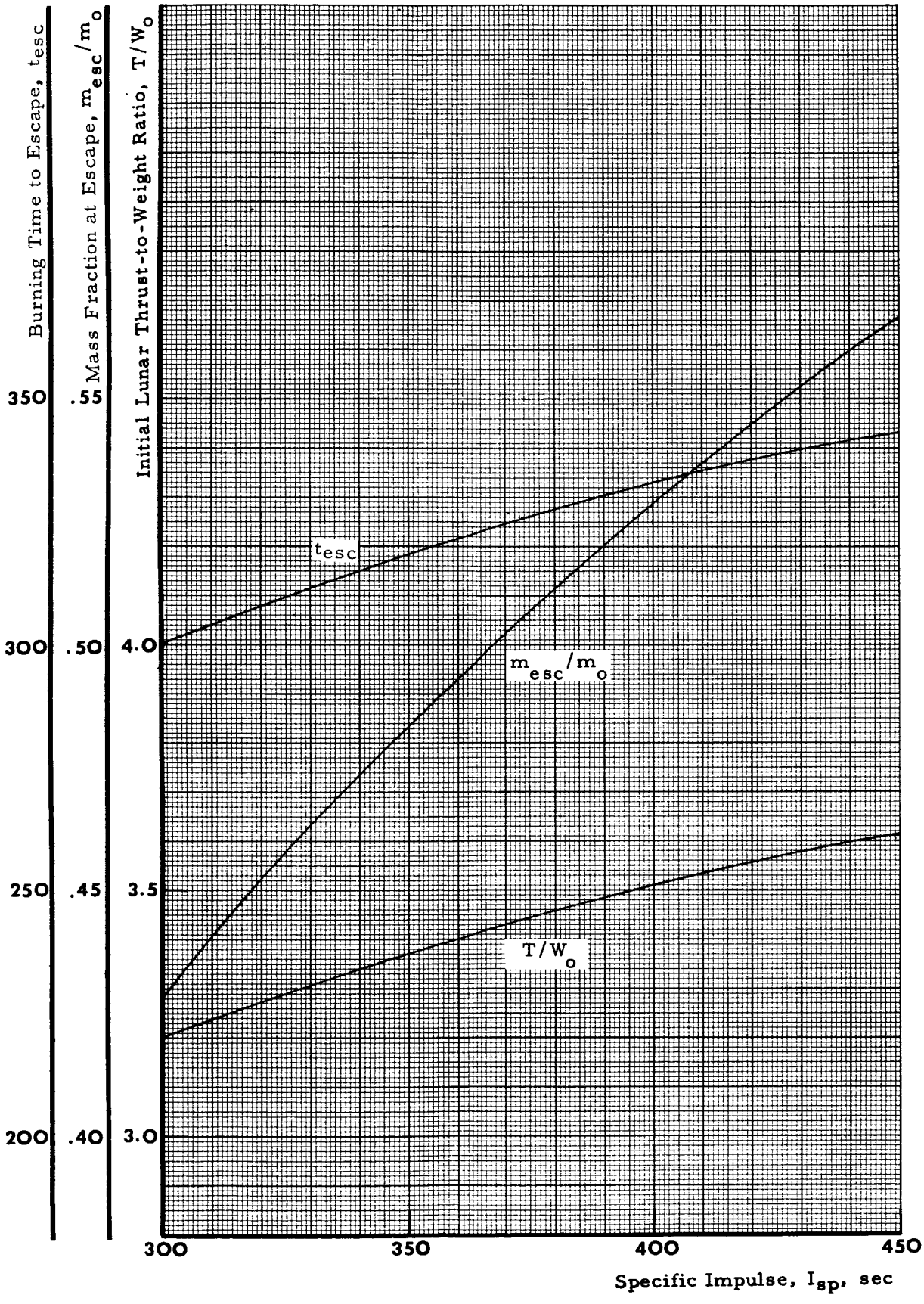

FIGURE 100. BURNING TIME TO ESCAPE, MASS FRACTION AT ESCAPE, AND INITIAL LUNAR THRUST-TO-WEIGHT RATIO VS SPECIFIC IMPULSE FOR $r_{esc} - r_o = 20$ km

As was noted in Reference 1, the two parts of this problem are not identical. We shall first investigate part (a).

Since no specification about thrust and velocity alignment at escape is given, we shall try all three possibilities (presented in this report) for trajectories which escape through a 15-kilometer orbit. We start with FIG 17 which maximizes mass fraction via a choice of T/W_0 and does not align thrust and velocity vectors at escape. From this graph we can directly read the following:

Table 103

I_{sp}	T/W_0	m_{esc}/m_0	$r_{esc} - r_0$
330	4.038	.4645	15.902

FIG 30 shows the similar data for escape through a 15-kilometer orbit with thrust and velocity aligned at escape by a discontinuity in the multiplier λ_4 at orbit. This graph produces

Table 104

I_{sp}	T/W_0	m_{esc}/m_0	$r_{esc} - r_0$
330	4.030	.4653	15.776

Similar results are achieved in FIG 45 for alignment via a λ_3 discontinuity. This graph shows

Table 105

I_{sp}	T/W_0	m_{esc}/m_0	$r_{esc} - r_0$
330	4.028	.4655	15.764

Since the last of these modes produces the greatest mass fraction at escape, we shall take this case to proceed with the investigation. Since the thrust was given as 20,000 pounds and since we have determined that

$$(T/W_0)_{\leftarrow} = 4.028$$

we find

$$(W_0)_{\leftarrow} = \frac{T}{4.028} = \frac{20{,}000}{4.028} = 4965 \text{ lunar pounds}$$

This may be converted to earth pounds as

$$(W_0)_{\oplus} = (4965)(6.047459) = 30{,}026 \text{ pounds (earth)}$$

The total weight which achieves escape is now given, in earth pounds, as

$$W_{esc} = \left(\frac{m_{esc}}{m_0}\right)(W_0)_{\oplus} = (.4655)(30{,}026) = 13{,}977 \text{ earth pounds}$$

The total propellant expenditure is, thus

$$W_{prop} = W_0 - W_{esc} = 16{,}049 \text{ earth pounds}$$

As was illustrated in Reference 1, the maximum *payload* to escape occurs at an initial lunar thrust-to-weight ratio of 1. This will now be used to solve part (b). From Table 66 we find

Table 106

I_{sp}	m_{esc}/m_0
300	.35280
350	.40212
400	.44421
450	.48048

By interpolation we find from FIG 101

I_{sp}	m_{esc}/m_0
330	.3855

Now, since

$$T/W_0 = 1$$

we have

$$W_0 = T = 15{,}000 \text{ pounds (lunar)}$$

or, in earth reference

$$W_0 = (15{,}000)(6.047459) = 90{,}712 \text{ pounds (earth)}$$

The payload, at escape, is now

$$W_{esc} = (.3855)(90{,}712) = 34{,}969 \text{ pounds (earth)}$$

The fuel expenditure for $(T/W_0)_1 = 1$ is, thus,

$$W_{prop} = 90{,}712 - 34{,}969 = 55{,}743$$

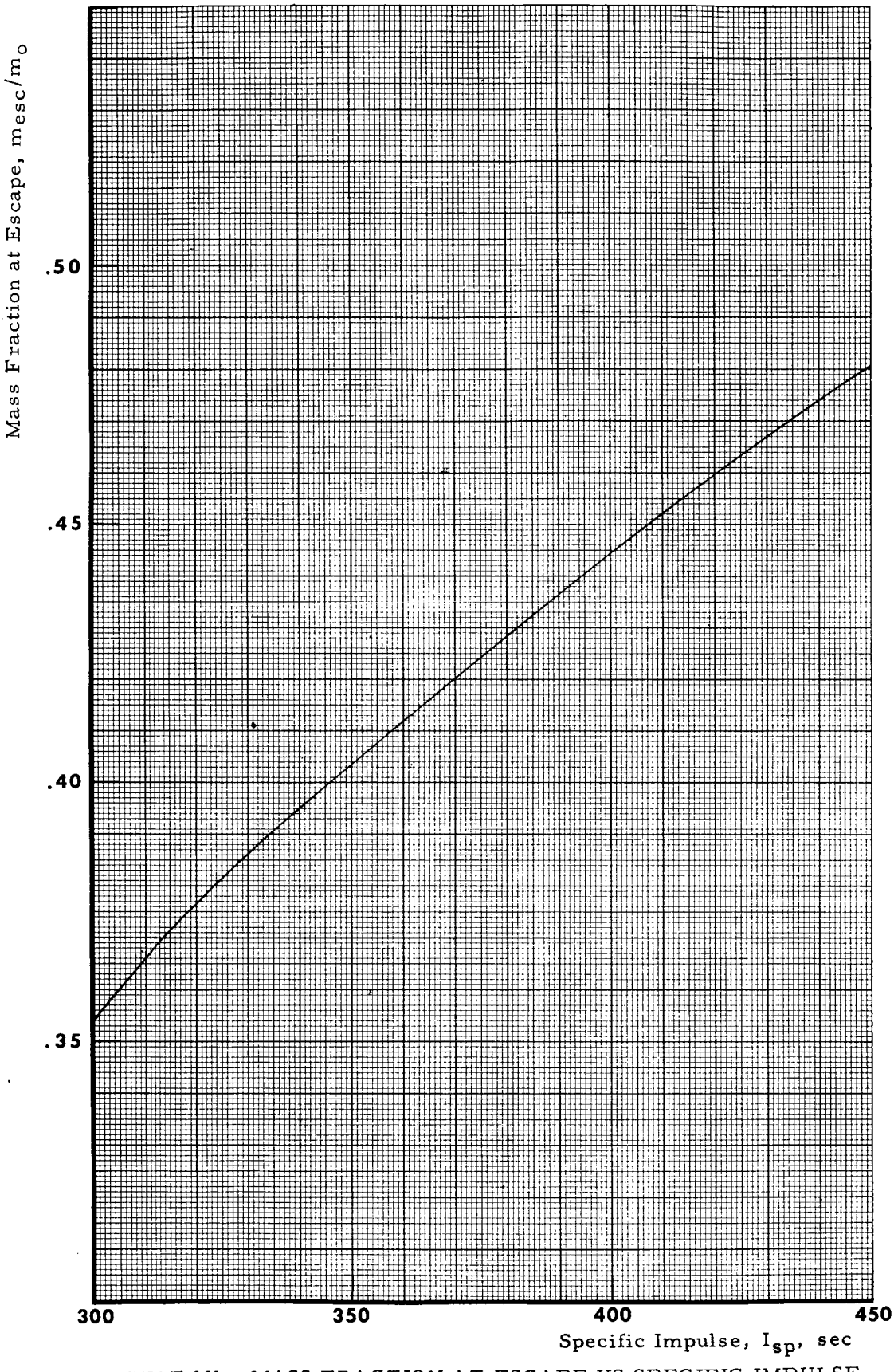

FIGURE 101. MASS FRACTION AT ESCAPE VS SPECIFIC IMPULSE FOR $T/W_o = 1$.

We thus obtain a larger payload at $(T/W_0)_{\text{☾}} = 1$ than at $(T/W_0)_{\text{☾}} = 4.028$, *but we have a far larger percentage of the lift-off weight expended as fuel during the ascent to escape.*

If we wish to retain the same payload (34,969 earth pounds) while minimizing the fuel expenditure, the problem above may be worked backwards to find the optimum thrust.

We have

$$W_{esc} = 34{,}969 \text{ pounds}$$

For an optimum T/W_0 (= 4.028) we have

$$\frac{m_{esc}}{m_0} = .4655$$

so that

$$W_0 = W_{esc}\left(\frac{m_0}{m_{esc}}\right) = \frac{34{,}969}{.4655} = 75{,}121 \text{ earth pounds}$$

Converting this to lunar pounds we find

$$(W_0)_{\text{☾}} = \frac{75{,}121}{6.047459} = 12{,}422 \text{ lunar pounds}$$

Now

$$(T/W_0)_{\text{☾}} = 4.028$$

$$T = (4.028)\,(W_0)_{\text{☾}} = (4.028)\,(12{,}422) = 50{,}036 \text{ pounds}$$

Thus, an engine of optimal thrust which produces a payload of 34,969 earth pounds has a thrust of 50,036 pounds.

The propellant expenditure for this engine is

$$W_0 - W_{esc} = 75{,}121 - 34{,}969 = 40{,}152 \text{ earth pounds}$$

The difference in propellant expenditure for the two engines is now

$$(W_{prop})_{15{,}000} - (W_{prop})_{50{,}036} = 15{,}591 \text{ earth pounds}$$

This may be regarded as almost pure weight saving simply by choice of the proper engine. This weight difference only accounts for the extra propellant expenditure required to attain escape velocity for the above payload; it does not account for the additional propellant required to land this on the lunar surface, the additional fuel necessary to escape the sum of these from earth, etc. Thus, even a small fuel saving can magnify when carried over several segments of a complicated mission.

Example 4. As a final example we shall consider the following: Determine the altitude at which escape occurs and the characteristic velocity required to attain escape for a vehicle which has an initial lunar thrust-to-weight ratio of 0.75 and a specific impulse of 425 if the escape trajectory originates in a 185-kilometer (≈ 100-nautical-mile) circular orbit about the Moon.

The procedure requires an additional step to those problems treated previously since we consider the circular orbital altitude as an additional parameter. The solution begins with the use of FIG 62, 63, 64, and 65 which show final altitude as a function of initial altitude for various parametric values of initial thrust-to-weight. The data are made available by constructing a vertical line from 185 kilometers on each of these graphs, and is available in Table 107.

Table 107
Initial Circular Orbital Altitude = 185 Km.

I_{sp}	T/W_0	$r_{esc} - r_0$	
300	.4	333	FIG 62
300	.6	256	
300	.8	226	
300	1	212	
300	2	192	
350	.4	339	FIG 63
350	.6	259	
350	.8	228	
350	1	212	
350	2	193	
400	.4	344	FIG 64
400	.6	261	
400	.8	229	
400	1	213	
400	2	193	
450	.4	346	FIG 65
450	.6	263	
450	.8	231	
450	1	215	
450	2	192	

FIG 102 shows a plot of final orbital altitude vs initial lunar thrust-to-weight ratio for an initial orbital altitude of 185 km. A vertical line from $T/W_0 = 0.75$ now produces the data given in Table 108.

Table 108
Initial Circular Orbital Altitude = 185 Km.
Initial Lunar Thrust-to-Weight Ratio = 0.75

I_{sp}	$r_{esc} - r_0$
300	231.5
350	233.5
400	235.0
450	236.5

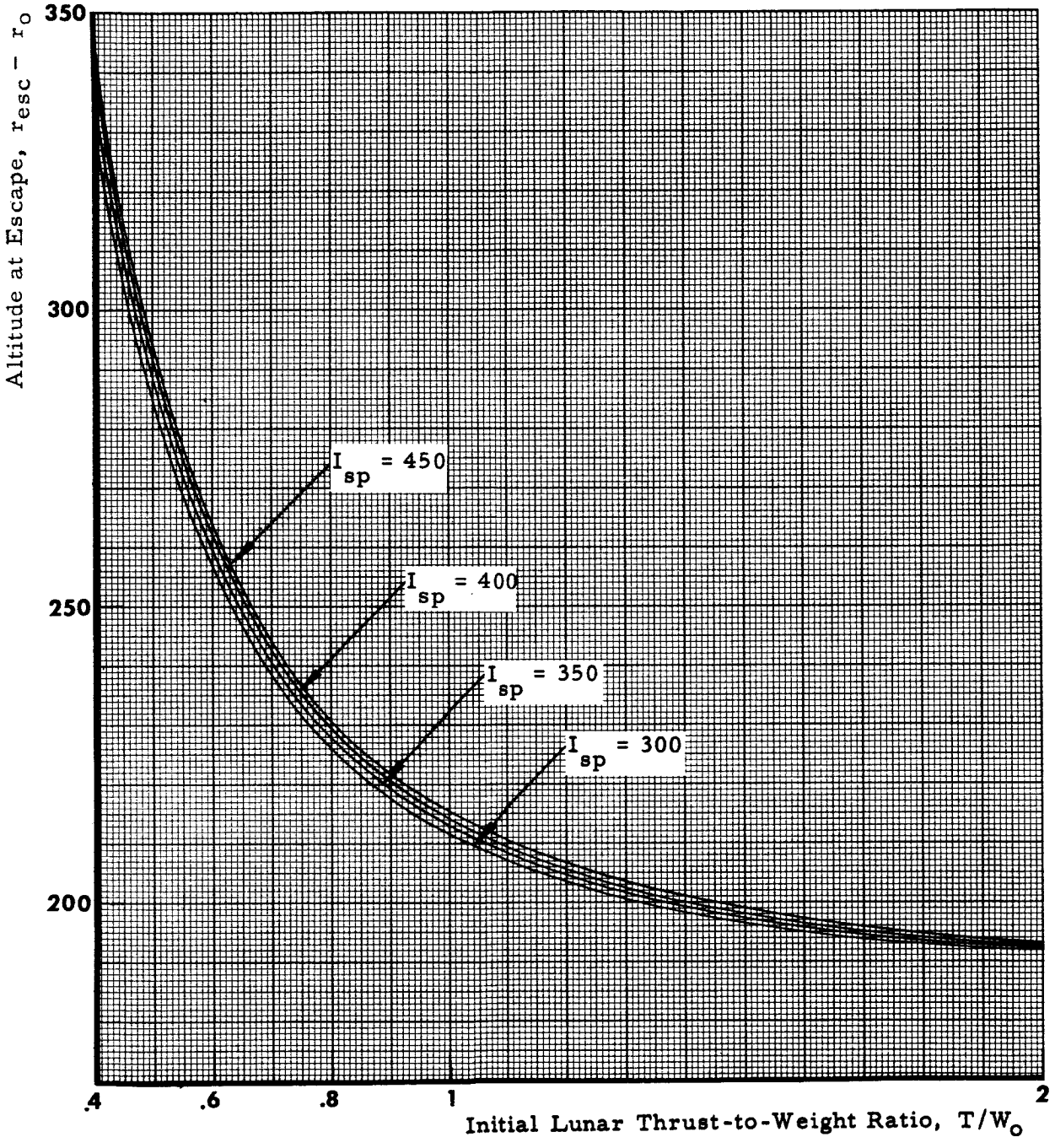

FIGURE 102. ALTITUDE AT ESCAPE VS INITIAL LUNAR THRUST-TO-WEIGHT RATIO FOR INITIAL CIRCULAR ORBITAL ALTITUDE OF 185 km.

(The reader will note that our significant figures mysteriously increase as we proceed; this example, however, is illustrating a technique rather than producing an answer.) FIG 103 now shows $r_{esc} - r_0$ vs I_{sp} for the above determined values of $r_{orb} - r_0$ and T/W_0. A vertical line from $I_{sp} = 425$ now yields

$$r_{esc} - r_0 = 235.7 \text{ km.}$$

as the altitude at which escape occurs.

To determine the characteristic velocity we first find m_{esc}/m_0. This may be done by the use of either FIG 66 through 76 or FIG 92 through 97. Choosing the former set, we first construct vertical lines from $r_{orb} - r_0 = 185$ kilometers on FIG 66 through 71 to obtain the data given in Table 109.

Table 109
Initial Circular Orbital Altitude = 185 Km.

$T/W_0 = .2$	I_{sp}	m_{esc}/m_0	
.2	300	.7910	FIG 66
.2	350	.8175	
.2	400	.8380	
.2	400	.8550	
.4	300	.7972	FIG 67
.4	350	.8233	
.4	400	.8438	
.4	450	.8600	
.6	300	.7970	FIG 68
.6	350	.8233	
.6	400	.8435	
.6	450	.8597	
.8	300	.7970	FIG 69
.8	350	.8230	
.8	400	.8435	
.8	450	.8594	
1.0	300	.7969	FIG 70
1.0	350	.8229	
1.0	400	.8432	
1.0	450	.8596	
2.0	300	.7966	FIG 71
2.0	350	.8230	
2.0	400	.8431	
2.0	450	.8591	

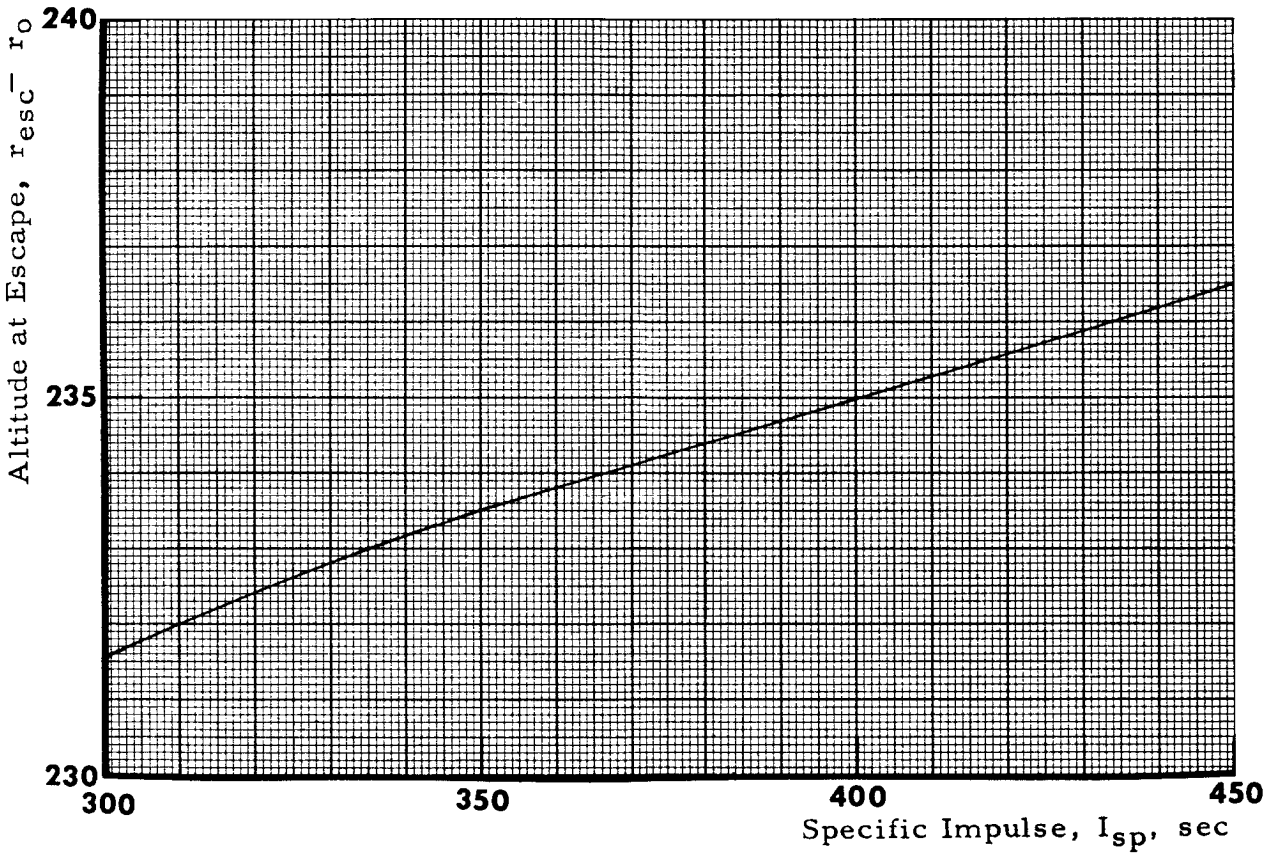

FIGURE 103. ALTITUDE AT ESCAPE VS SPECIFIC IMPULSE FOR INITIAL CIRCULAR ORBITAL ALTITUDE OF 185 km. AND INITIAL LUNAR THRUST-TO-WEIGHT RATIO OF 0.75

FIG 104 now shows mass fraction at escape vs initial lunar thrust-to-weight ratio for an initial orbital altitude of 185 kilometers. Construction of a vertical line from $T/W_0 = 0.75$ produces the data present in Table 110.

Table 110
Initial Circular Orbital Altitude = 185 Km.
Initial Lunar Thrust-to-Weight Ratio = 0.75

I_{sp}	m_{esc}/m_0
300	.7970
350	.8230
400	.8435
450	.8596

In FIG 105, m_{esc}/m_0 vs I_{sp} is plotted for the isolated values of Table 110. For $I_{sp} = 425$, we find

$$m_{esc}/m_0 = .8520$$

The required characteristic velocity for parabolic escape is now

$$u = g_0 I_{sp} \ln\left(\frac{m_0}{m_{esc}}\right) = (9.81)(425) \ln\left(\frac{1}{.8520}\right)$$

$$= 4169.25 \ln (1.1737) = (4169.25)(.16016) = 667.7 \text{ m./sec.}$$

The burning time to escape and necessary value of λ_4 at orbit are available by similiar techniques.

SECTION IX. CONCLUSIONS

The numerical data presented in this report have been chosen in an attempt to fulfill two purposes: firstly, to supply data for a nominal set of lunar escape missions, and secondly, to study the problems that arise in connection with the calculation of various escape modes to a sufficient degree that the given data may be readily extended to other cases of interest via numerical integration.

The most restrictive assumption is that of parabolic escape energy as a cutoff criterion. The initial values of the Lagrange multipliers are, however, relatively insensitive to small changes in the cutoff energy so that extensions to other cutoff criteria are not difficult. The numerical calculations involved in the extension of these results to other launch latitudes and other inclinations were discussed in Reference 1 and the results are valid for the present report. Finally, the choice of a 15-kilometer orbit for escape is arbitrary, but convenient. Similiar results can be obtained for any reasonable altitude (say, between 10 kilometers and 100 kilometers).

The insertion of a discontinuity into the steering program at circular orbit is simply a method of gaining an additional degree of freedom to match a desired end condition. This procedure may easily be justified on physical grounds but the mathematical significance of this encroachment is far more subtle and open to question. It may be noted that we may not necessarily expect that an arbitrary discontinuity in the steering program would lower performance since the variational technique predicts relative optima with respect to neighboring continuous steering functions.

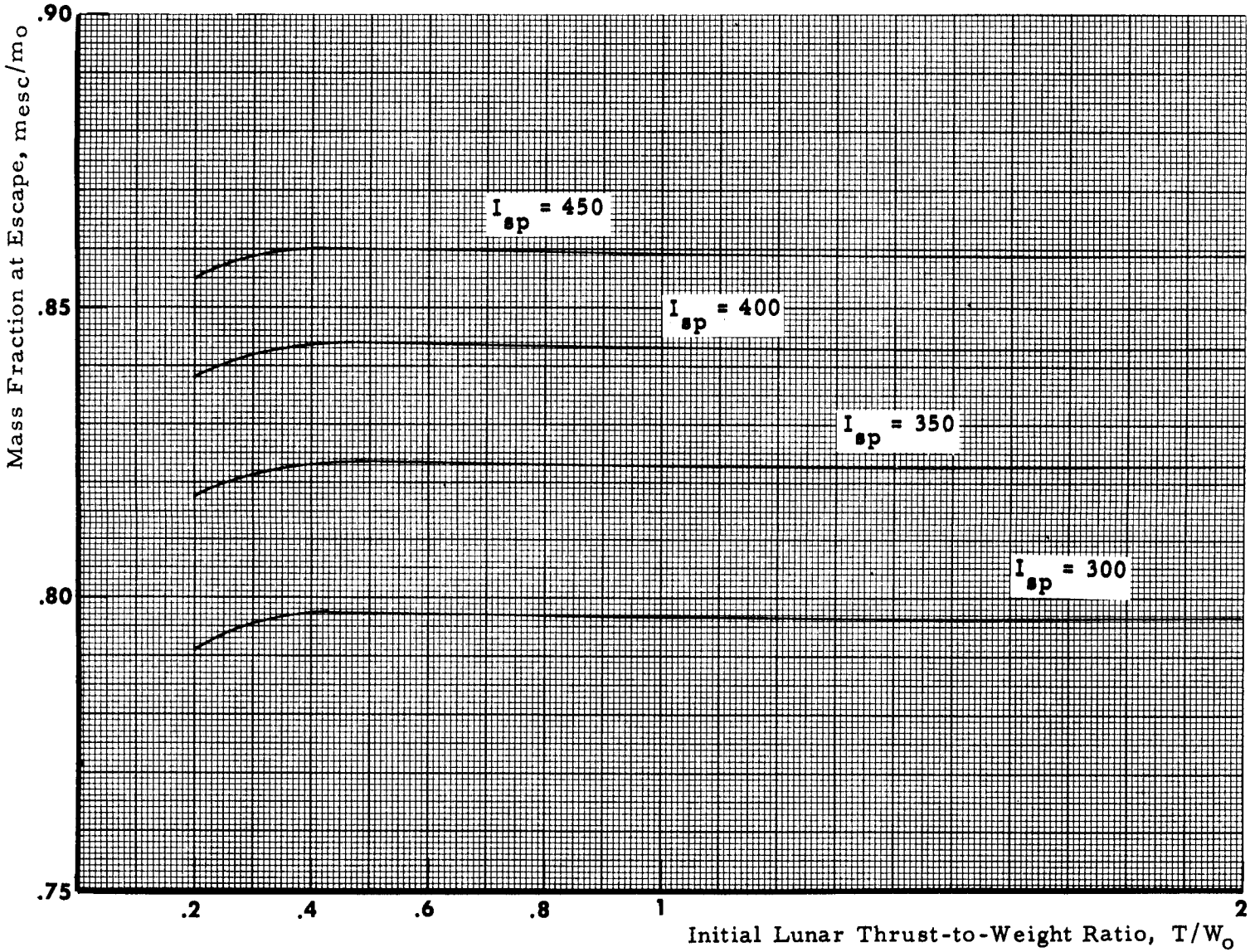

FIGURE 104. MASS FRACTION AT ESCAPE VS INITIAL LUNAR THRUST-TO-WEIGHT RATIO FOR INITIAL CIRCULAR ORBITAL ALTITUDE OF 185 km.

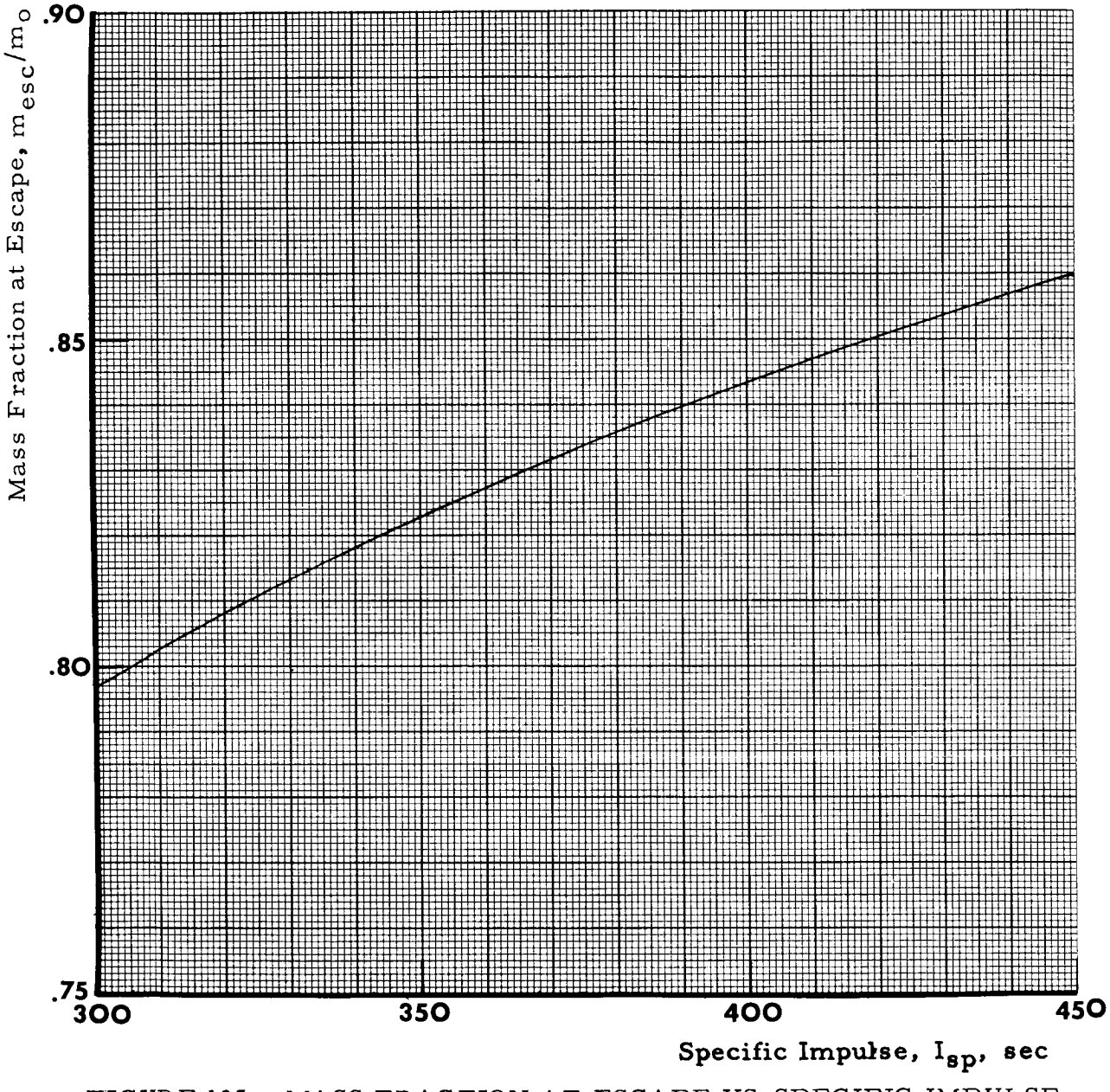

FIGURE 105. MASS FRACTION AT ESCAPE VS SPECIFIC IMPULSE FOR INITIAL CIRCULAR ORBITAL ALTITUDE OF 185 km. AND INITIAL LUNAR THRUST-TO-WEIGHT RATIO OF 0.75

APPENDIX
COMPUTER DIAGRAMS

GENERAL DATA FLOW

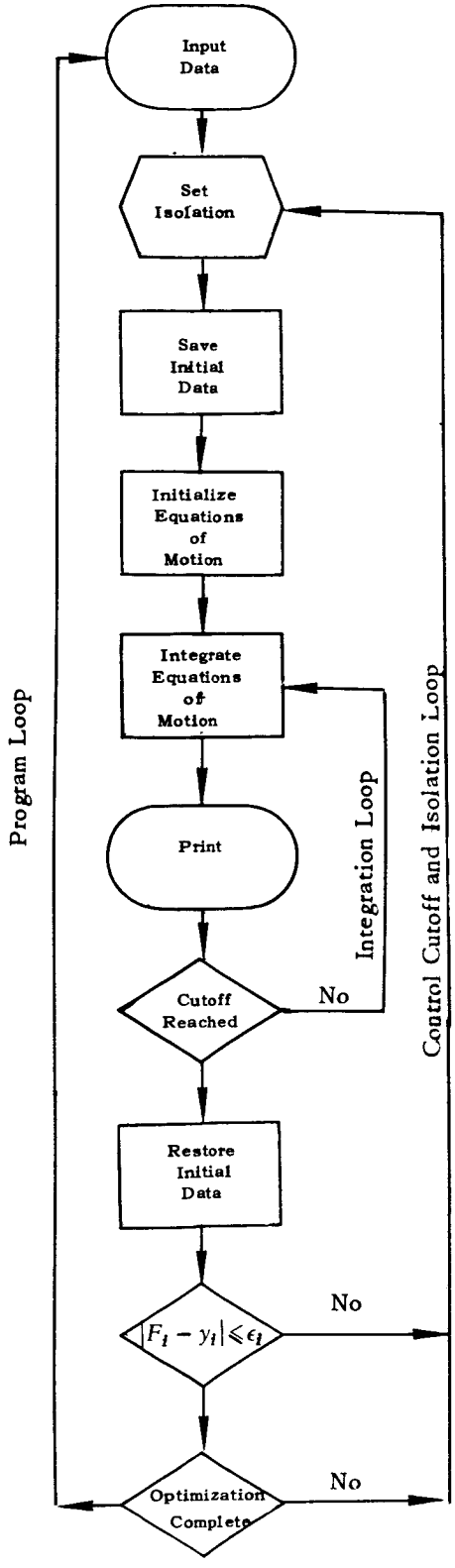

INPUT BLOCK

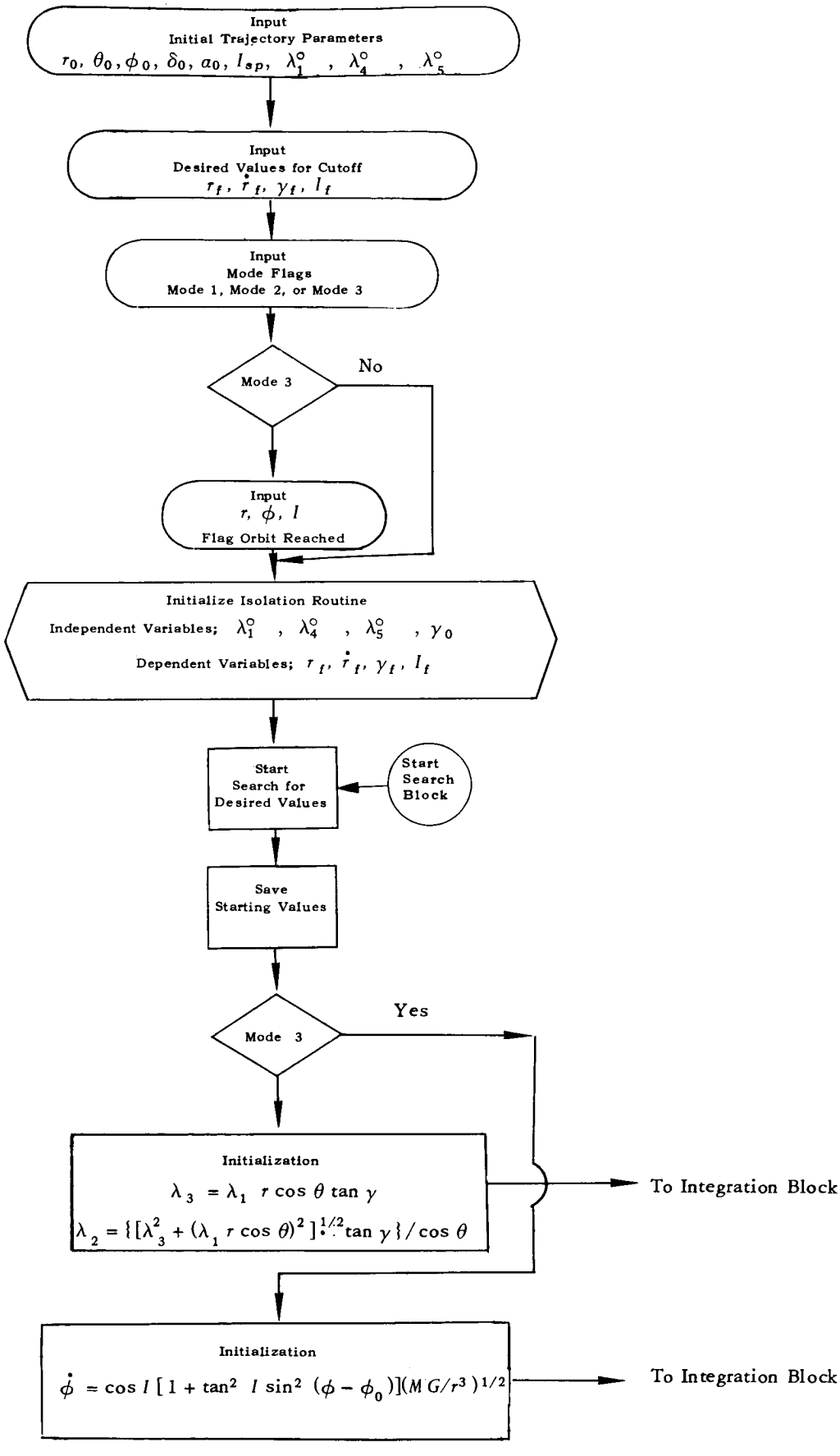
Input
Initial Trajectory Parameters
$r_0, \theta_0, \phi_0, \delta_0, a_0, I_{sp}, \lambda_1^\circ, \lambda_4^\circ, \lambda_5^\circ$
Input
Desired Values for Cutoff
$r_f, \dot{r}_f, \gamma_f, I_f$
Input
Mode Flags
Mode 1, Mode 2, or Mode 3
Mode 3
No
Input
r, ϕ, I
Flag Orbit Reached
Initialize Isolation Routine
Independent Variables; $\lambda_1^\circ, \lambda_4^\circ, \lambda_5^\circ, \gamma_0$
Dependent Variables; $r_f, \dot{r}_f, \gamma_f, I_f$
Start Search for Desired Values
Start Search Block
Save Starting Values
Mode 3
Yes
Initialization
$\lambda_3 = \lambda_1 \; r \cos\theta \tan\gamma$
$\lambda_2 = \{[\lambda_3^2 + (\lambda_1 \, r \cos\theta)^2]^{1/2} \tan\gamma\} / \cos\theta$
To Integration Block
Initialization
$\dot{\phi} = \cos I \, [1 + \tan^2 I \sin^2 (\phi - \phi_0)](MG/r^3)^{1/2}$
To Integration Block

INTEGRATION BLOCK

n = Typical Time Step and m = 1, 2, 3, 4, 5

Save

$r_n \to r_0;\ \theta_n \to \theta_0;\ \phi_n \to \phi_0;\ (\lambda_m)_n \to (\lambda_m)_0$

$\dot{r}_n \to \dot{r}_0;\ \dot{\theta}_n \to \dot{\theta}_0;\ \dot{\phi}_n \to \dot{\phi}_0;\ t_n \to t_0$

Compute

$r_1 = r_0 + \dot{r}_0\ \Delta t/2$

$\dot{r}_1 = \dot{r}_0 + \ddot{r}_0\ \Delta t/2$

$\theta_1 = \theta_0 + \dot{\theta}_0\ \Delta t/2$

$\dot{\theta}_1 = \dot{\theta}_0 + \ddot{\theta}_0\ \Delta t/2$

$\phi_1 = \phi_0 + \dot{\phi}_0\ \Delta t/2$

$\dot{\phi}_1 = \dot{\phi}_0 + \ddot{\phi}_0 \Delta t/2$

$(\lambda_m)_1 = (\lambda_m)_0 + (\dot{\lambda}_m)_0\ \Delta t/2$

$t_1 = t_0 + \Delta t/2$

Evaluate MR Block

$\ddot{r} = f(r_1, \dot{r}_1, t_1);\ \ddot{\theta} = f(\theta_1, \dot{\theta}_1, t_1);\ \ddot{\phi} = f(\phi_1, \dot{\phi}_1, t_1);\ \dot{\lambda}_m = f[(\lambda_m)_1, t_1]$

Compute

$r_2 = r_0 + \dot{r}_1\ \Delta t/2$

$\dot{r}_2 = \dot{r}_0 + \ddot{r}_1\ \Delta t/2$

$\theta_2 = \theta_0 + \dot{\theta}_1\ \Delta t/2$

$\dot{\theta}_2 = \dot{\theta}_0 + \ddot{\theta}_1\ \Delta t/2$

$\phi_2 = \phi_0 + \dot{\phi}_1\ \Delta t/2$

$\dot{\phi}_2 = \dot{\phi}_0 + \ddot{\phi}_1\ \Delta t/2$

$(\lambda_m)_2 = (\lambda_m)_0 + (\dot{\lambda}_m)_1\ \Delta t/2$

$t_2 = t_0 + \Delta t/2$

Evaluate MR Block

$\ddot{r} = f(r_2, \dot{r}_2, t_2);\ \ddot{\theta} = f(\theta_2, \dot{\theta}_2, t_2);\ \ddot{\phi} = f(\phi_2, \dot{\phi}_2, t_2);\ \dot{\lambda}_m = f[(\lambda_m)_2, t_2]$

Compute

$$r_3 = r_0 + \dot{r}_2 \, \Delta t$$
$$\dot{r}_3 = r_0 + \ddot{r}_2 \, \Delta t$$
$$\theta_3 = \theta_0 + \dot{\theta}_2 \, \Delta t$$
$$\dot{\theta}_3 = \dot{\theta}_0 + \ddot{\theta}_2 \, \Delta t$$
$$\phi_3 = \phi_0 + \dot{\phi}_2 \, \Delta t$$
$$\dot{\phi}_3 = \dot{\phi}_0 + \ddot{\phi}_2 \, \Delta t$$
$$(\lambda_m)_3 = (\lambda_m)_0 + (\dot{\lambda}_m)_2 \Delta t$$
$$t_3 = t_0 + \Delta t$$

Evaluate MR Block

$$\ddot{r} = f(r_3, \dot{r}_3, t_3); \; \ddot{\theta} = f(\theta_3, \dot{\theta}_3, t_3) \; ; \; \ddot{\phi} = f(\phi_3, \dot{\phi}_3, t_3) \; ; \; \dot{\lambda}_m = f[(\lambda_m)_3, t_3]$$

Compute

$$r_{n+1} = r_0 + (\dot{r}_0 \, \Delta t + 2 \dot{r}_1 \, \Delta t + 2 \dot{r}_2 \, \Delta t + \dot{r}_3 \, \Delta t)/6$$
$$\dot{r}_{n+1} = \dot{r}_0 + (\ddot{r}_0 \, \Delta t + 2 \ddot{r}_1 \, \Delta t + 2 \ddot{r}_2 \, \Delta t + \ddot{r}_3 \, \Delta t)/6$$
$$\theta_{n+1} = \theta_0 + (\dot{\theta}_0 \, \Delta t + 2 \dot{\theta}_1 \, \Delta t + 2 \dot{\theta}_2 \, \Delta t + \dot{\theta}_3 \, \Delta t)/6$$
$$\dot{\theta}_{n+1} = \dot{\theta}_0 + (\ddot{\theta}_0 \, \Delta t + 2 \ddot{\theta}_1 \, \Delta t + 2 \ddot{\theta}_2 \, \Delta t + \ddot{\theta}_3 \, \Delta t)/6$$
$$\phi_{n+1} = \phi_0 + (\dot{\phi}_0 \, \Delta t + 2 \dot{\phi}_1 \, \Delta t + 2 \dot{\phi}_2 \, \Delta t + \dot{\phi}_3 \, \Delta t)/6$$
$$\dot{\phi}_{n+1} = \dot{\phi}_0 + (\ddot{\phi}_0 \, \Delta t + 2 \ddot{\phi}_1 \, \Delta t + 2 \ddot{\phi}_2 \, \Delta t + \ddot{\phi}_3 \, \Delta t)/6$$
$$(\lambda_m)_{n+1} = (\lambda_m)_0 + [(\dot{\lambda}_m)_0 \, \Delta t + 2 (\dot{\lambda}_m)_1 \, \Delta t + 2 (\dot{\lambda}_m)_2 \, \Delta t + (\dot{\lambda}_m)_3 \, \Delta t]/6$$
$$t_{n+1} = t_0 + \Delta t$$

Evaluate MR Block

$$\ddot{r} = f(r_{n+1}, \dot{r}_{n+1}, t_{n+1}); \; \ddot{\theta} = f(\theta_{n+1}, \dot{\theta}_{n+1}, t_{n+1}) \; ; \; \ddot{\phi} = f(\phi_{n+1}, \dot{\phi}_{n+1}, t_{n+1}); \; \dot{\lambda}_m = f[(\lambda_m)_{n+1}, t_{n+1}]$$

To Control Block

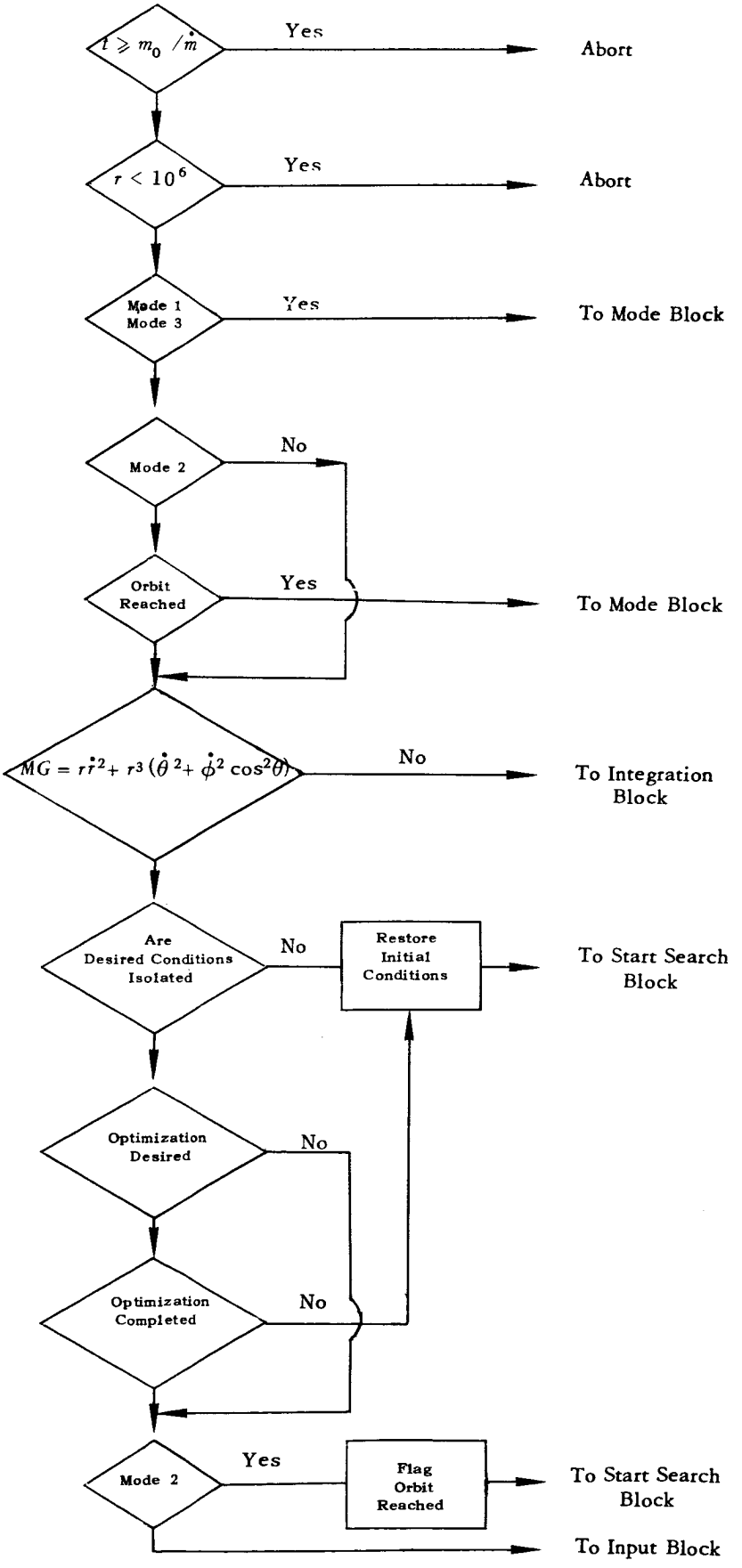

Mode 1 Direct to Escape
Mode 2 Via Orbit to Escape
Mode 3 From Orbit to Escape

CONTROL

MODE BLOCK

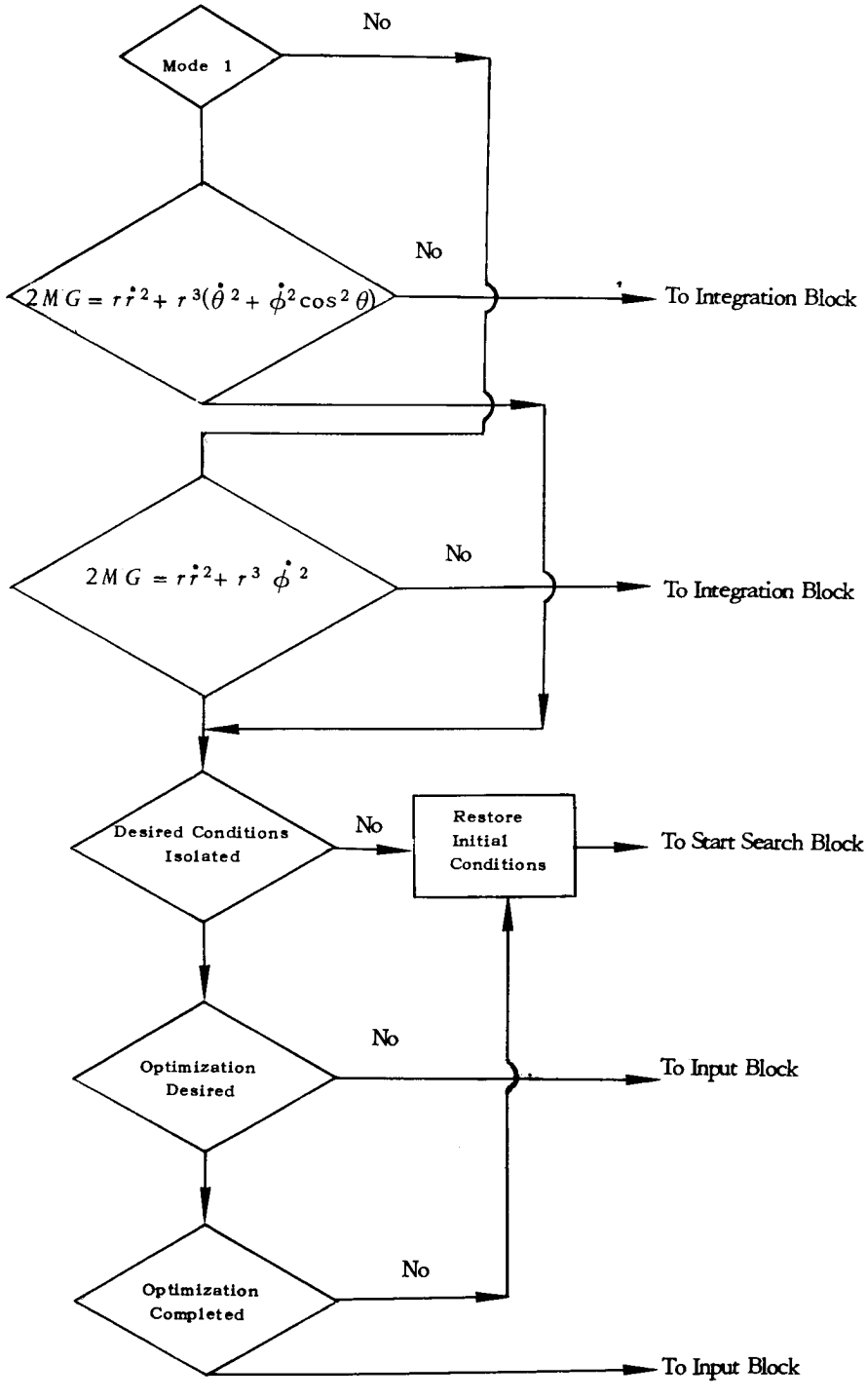

Orbit Reached

Compute

$$\ddot{r} = \left[\frac{a\,(g_0)_4\,(g_0)_\oplus\, I_{sp}}{(g_0)_\oplus\, I_{sp} - a\,(g_0)_4\, t}\right]\left[\frac{\lambda_1\, r\cos\theta}{\sqrt{(\lambda_1^2\, r^2 + \lambda_2^2)\cos^2\theta + \lambda_3^2}}\right] - \frac{MG}{r^2} + r(\dot{\theta}^2 + \dot{\phi}^2\cos^2\theta)$$

$$\ddot{\theta} = \left[\frac{a\,(g_0)_4\,(g_0)_\oplus\, I_{sp}}{(g_0)_\oplus\, I_{sp} - a\,(g_0)_4\, t}\right]\left[\frac{\lambda_2\cos\theta}{r\sqrt{(\lambda_1^2\, r^2 + \lambda_2^2)\cos^2\theta + \lambda_3^2}}\right] - \frac{2\dot{r}\dot{\theta}}{r} - \dot{\phi}^2\sin\theta\cos\theta$$

$$\ddot{\phi} = \left[\frac{a\,(g_0)_4\,(g_0)_\oplus\, I_{sp}}{(g_0)_\oplus\, I_{sp} - a\,(g_0)_4\, t}\right]\left[\frac{\lambda_3}{r\cos\theta\sqrt{(\lambda_1^2\, r^2 + \lambda_2^2)\cos^2\theta + \lambda_3^2}}\right] + 2\dot{\theta}\dot{\phi}\tan\theta - \frac{2\dot{r}\dot{\phi}}{r}$$

$$\dot{\lambda}_1 = \frac{2}{r}\,(\lambda_2\,\dot{\theta} + \lambda_3\,\dot{\phi}) - \lambda_4$$

$$\dot{\lambda}_2 = -2\left(\lambda_1\, r\,\dot{\theta} - \frac{\lambda_2\dot{r}}{r} + \lambda_3\,\dot{\phi}\tan\theta\right) - \lambda_5$$

$$\dot{\lambda}_3 = -2\left[(\lambda_1\, r\cos\theta - \lambda_2\sin\theta)\,\dot{\phi}\cos\theta + \lambda_3\left(\dot{\theta}\tan\theta - \frac{\dot{r}}{r}\right)\right] - C_1$$

$$\dot{\lambda}_4 = -\lambda_1\left[\frac{2MG}{r^3} + (\dot{\theta}^2 + \dot{\phi}^2\cos^2\theta)\right] - \frac{2\dot{r}}{r^2}\,(\lambda_2\,\dot{\theta} + \lambda_3\,\dot{\phi})$$

$$- \left[\frac{a(g_0)_4\,(g_0)_\oplus\, I_{sp}}{(g_0)_\oplus\, I_{sp} - a\,(g_0)_4\, t}\right]\left[\frac{(\lambda_2^2\cos^2\theta + \lambda_3^2)}{r^2\cos^2\theta\sqrt{(\lambda_1^2\, r^2 + \lambda_3^2)\cos^2\theta + \lambda_3^2}}\right]$$

$$\dot{\lambda}_5 = \dot{\phi}^2\,(\lambda_1\, r\sin 2\theta + \lambda_2\cos 2\theta) - 2\lambda_3\,\dot{\theta}\dot{\phi}\sec^2\theta$$

$$- \left[\frac{a(g_0)_4\,(g_0)_\oplus\, I_{sp}}{(g_0)_\oplus\, I_{sp} - a\,(g_0)_4\, t}\right]\left[\frac{\lambda_3^2\tan\theta\sec\theta}{r\sqrt{(\lambda_1^2\, r^2 + \lambda_2^2)\cos^2\theta + \lambda_3^2}}\right]$$

EXIT

Compute

$$\ddot{r} = \left[\frac{T}{m_0 - \dot{m}t}\right]\frac{\lambda_1\, r}{\sqrt{\lambda_1^2\, r^2 + \lambda_3^2\sec^2 I}} - \frac{MG}{r^2} + \frac{r\dot{\phi}^2\sec^2 I}{[1 + \sin^2(\phi - \phi_0)\tan^2 I]^2}$$

$$\ddot{\phi} = \left[\frac{T}{m_0 - \dot{m}t}\right]\frac{\lambda_3[1 + \sin^2(\phi - \phi_0)\tan^2 I]}{r\sqrt{\lambda_1^2\, r^2 + \lambda_3^2\sec^2 I}} + \frac{2\dot{\phi}^2\sin(\phi - \phi_0)\cos(\phi - \phi_0)\tan^2 I}{1 + \sin^2(\phi - \phi_0)\tan^2 I} - \frac{2\dot{r}\dot{\phi}}{r}$$

$$\dot{\lambda}_1 = \frac{2\lambda_3\,\dot{\phi}}{r}\left[\frac{\sec^2 I}{1 + \sin^2(\phi - \phi_0)\tan^2 I}\right] - \lambda_4$$

$$\dot{\lambda}_3 = -2\left[\frac{\lambda_1\, r\,\dot{\phi}}{1 + \tan^2 I\sin^2(\phi - \phi_0)}\right] - \frac{\lambda_3\,\dot{r}}{r}\Bigg] - C_1$$

$$\dot{\lambda}_4 = -\lambda_1\left[\frac{2MG}{r^3} + \frac{\dot{\phi}^2\sec^2 I}{[1 + \tan^2 I\sin^2(\phi - \phi_0)]^2}\right] - \frac{2\dot{r}\dot{\phi}\lambda_3\sec^2 I}{r^2[1 + \tan^2 I\sin^2(\phi - \phi_0)]}$$

$$+ \left[\frac{T}{m_0 - \dot{m}t}\right]\frac{\lambda_3^2\sec^2 I}{r^2\sqrt{\lambda_1^2\, r^2 + \lambda_3^2\sec^2 I}}$$

$$\theta = \tan^{-1}[\tan I\sin(\phi - \phi_0)]$$

$$\dot{\theta} = \frac{\tan I\cos(\phi - \phi_0)\,\dot{\phi}}{1 + \tan^2 I\sin^2(\phi - \phi_0)}$$

$$\lambda_2 = \lambda_3\tan I\cos(\phi - \phi_0)$$

$$\lambda_5 = \tan I\,[C_1\cos(\phi - \phi_0) - \lambda_3\,\dot{\phi}\sin(\phi - \phi_0)]$$

EXIT

REFERENCES

1. Burns, Rowland E. and Singleton, Larry G.: *Ascent from the Lunar Surface.** NASA TN D-1644, June 1963.

2. Silver, Sidney: Share; Book no. D-3, Installation JPL, Title, SRCH.

* The present report is an extension of Reference 1 to the problem of lunar escape. A portion of the numerical results of this reference disagree with the data of the present report due to a difference in the numerical integration step size. The results of the present report are to be preferred in all cases of discrepancy.

APPROVAL

LUNAR ESCAPE

By

Rowland E. Burns

and

Larry G. Singleton

The information in this report has been reviewed for security classification. Review of any information concerning Department of Defense or Atomic Energy Commission programs has been made by the MSFC Security Classification Officer. This report, in its entirety, has been determined to be unclassified.

Helmut G. L. Krause

H. G. L. KRAUSE
Scientific Advisor, Advanced Flight Systems Branch

Erich E. Goerner

ERICH E. GOERNER
Chief, Advanced Flight Systems Branch

W. A. Mrazek

W. A. MRAZEK
Director, Propulsion & Vehicle Engineering Division

DISTRIBUTION

M-DIR
  Dr. von Braun
M-DEP-R&D
  Dr. Rees
M-CP-DIR
  Mr. Maus
M-AERO-DIR
  Dr. Geissler
  Dr. Hoelker
M-AERO-TS
  Dr. Heybey
  Dr. Sperling
M-AERO-PS
  Mr. Braunlich
  Mr. Vaughn
  Mr. Schmidt
  Mr. Burrows
M-AERO-A
  Mr. Dahm
M-AERO-D
  Mr. Horn
  Mr. Baker
  Mr. Hart
  Mr. Callaway
  Mr. Redus
  Mr. Thomae
  Mr. Verderaime
M-AERO-F
  Dr. Speer
  Mr. Kurtz
M-AERO-G
  Mr. Dalton
M-AERO-P
  Mr. Miner
  Mr. Braud
  Mr. Dearman
  Mr. Hart
  Mr. Lisle
  Mr. Schmieder
  Mr. Schwaniger
  Mr. Silber
  Mr. Tucker
  Mr. Winch
M-AERO-S
  Mr. deFries
M-ASTR-DIR
  Dr. Haeussermann
M-ASTR-TSS
  Mr. Kroh
M-ASTR-A
  Mr. Digesu
M-ASTR-I
  Dr. Decher
M-ASTR-M
  Mr. Boehm
  Mr. Pfaff
M-ASTR-F
  Mr. Hosenthien
  Mr. Scofield
M-COMP-DIR
  Dr. Hoelzer
  Mr. Bradshaw
  Dr. Andrus
M-COMP-P
  Mr. Singleton (10)
M-COMP-TS
  Dr. Fehlberg
  Dr. Arenstorf
  Mr. Davidson
M-FPO
  Mr. Koelle
  Mr. Williams
  Dr. Ruppe
  Mr. Gradecak
M-MS-IP
M-MS-IPL (8)
M-PAT
M-P&VE-DIR
  Dr. Mrazek
  Mr. Weidner
  Mr. Hellebrand
M-P&VE-V
  Mr. Palaoro
M-P&VE-ADMP
M-P&VE-M
  Dr. Lucas
M-P&VE-F
  Mr. Goerner
  Mr. Barker
  Dr. Krause (5)
  Mr. Burns (50)
  Mr. Swanson
M-P&VE-FN
  Mr. Jordan
  Mr. Heyer
  Mr. Nixon
  Mr. Saxton
  Mr. Harris
  Mr. Kearns
  Mr. Manning
  Mr. Whiton
  Mr. Patton

DISTRIBUTION (Continued)

M-P&VE-FF
Mr. Voss
Mr. Galzerano
Mr. Fellenz
Mr. Russell
Mr. Akridge
Mr. Perry
Mr. Stafford
Mr. Thompson
Mr. Cohen
Mr. Kromis
Mr. Croft
Mr. Valentine
Mr. Wheeler
M-P&VE-FS
Mr. Neighbors
Mr. Laue
Mr. Wales
Mr. Schwartz
Mr. Orillion
Mr. Johns
M-P&VE-P
Mr. Paul
Mr. Gross
Mr. McKay
Mr. Swalley
Mr. Horner
M-P&VE-S
Mr. Kroll
Dr. Glaser
M-P&VE-E
Mr. Schulz
M-QUAL-DIR
Mr. Grau
M-RP-DIR
Dr. Stuhlinger
Mr. Heller
M-RP-N
Dr. Shelton
M-RP
Dr. Schocken
Mr. Naumann
Mr. Snoddy
Mr. Prescott
M-RP-T
Mr. Harrison
M-SAT-DIR
Dr. Lange
M-HME-P
Mr. Knox

M-TEST-DIR
Mr. Heimburg
M-MS-H
Mr. Akens

Headquarters
National Aeronautics and Space Administration
Washington 25, D.C.
Mr. Kurt Stehling,
Office of Plans & Program Evaluation

Office of Scientific and Technical Information
National Aeronautics and Space Administration
Washington 25, D.C.
Acquisitions and Dissemination Branch (AFSS-AD) (10)

Ames Research Center
National Aeronautics and Space Administration
Moffett Field, California
Library
Dr. Eggers

Goddard Space Flight Center
National Aeronautics and Space Administration
Greenbelt, Maryland
Library
Dr. J.W. Siry

Langley Research Center
National Aeronautics and Space Administration
Langley Field, Virginia
Library
Dr. J. C. Houbolt

Launch Operations Center
National Aeronautics and Space Administration
Cape Canaveral, Florida
Dr. Kurt Debus
Dr. A. Knothe

Lewis Research Center
National Aeronautics and Space Administration
2100 Brookpark Road
Cleveland 35, Ohio
Library
Dr. S. Himmel
Dr. W. E. Moeckel
Mr. Richard R. Burley
Mr. Richard J. Weber

Manned Spacecraft Center
National Aeronautics and Space Administration
Houston, Texas
Library
Mr. Fayet
Mr. Paul Thomas
Mr. Tom Price
Mr. Tom Kent
Mr. Don Jezewski

Jet Propulsion Laboratory
California Institute of Technology
4800 Oak Grove Drive
Pasadena, California
Library
Dr. Melbourne

Air Force Cambridge Research Center
L.G. Hanscom Field
Bedford, Massachusetts
Library

Defense Documentation Center
Cameron Station
Alexandria, Virginia 22314
Library

Ballistic Research Laboratories
Aberdeen Proving Ground, Maryland
Library
Dr. Boris Garfinkel

National Bureau of Standards
Washington, D.C.
Library

Smithsonian Astrophysical Observatory
Cambridge 38, Massachusetts
Library

U.S. Naval Observatory
Washington 25, D.C.
Library

U. S. Naval Postgraduate School
Monterey, California
Library
Dr. Frank D. Faulkner

Case Institute of Technology
University Circle
Cleveland 6, Ohio
Library
Dr. Sidney W. McCuskey
Dr. V. M. Blanco
Dr. Dettman
Dr. Robert S. Shankland

University of California
Los Angeles, California
Library

University of California
Berkeley 4, California
Library
Dr. George Leitmann

University of Oklahoma
Department of Mathematics and Astronomy
Norman, Oklahoma
Library
Dr. George Ewing

Aerospace Corporation
El Segundo, California
Library
Dr. E. Levin

Aerojet-General Corporation
Systems Analysis Department
Space Propulsion Division
Azusa, California
Library
Mr. L.C. Moore

Boeing Scientific Research Laboratories
Seattle 24, Washington
Library
Dr. Angelo Miele
Mr. David G. Hull

Chance Vought Corporation
Astronautics Division
Dallas 22, Texas
Library

DISTRIBUTION (Concluded)

Douglas Aircraft Corporation
Missile and Space Systems Division
3000 Ocean Park Boulevard
Santa Monica, California
Library
Mr. R. B. Canwrite

General Dynamics / Astronautics
San Diego, California
Library
Dr. Krafft A. Ehricke
Mr. F. Dore

General Electric Co.
Space Science Laboratory
3750 D Street
Philadelphia 24, Pa.
Library
Dr. V. G. Szebehely

Grumman Aircraft Engineering Corporation
Bethpaxe L.I., New York
Library
Dr. Henry Kelley

Lockheed Aircraft Corporation
Burbank, California
Library
Dr. R.M.L. Baker

Lockheed Aircraft Corporation
Missile and Space Division
Sunnyvale, California
Library
Dr. John V. Breakwell
Mr. Vane E. Jones
Dr. H. F. Michielson
Mr. Wilson B. Schramm

Martin Company
Space Systems Division, J-325
Baltimore 3, Maryland
Library

Martin Company, R.I.A.S.
7212 Bellona Ave.
Baltimore, Maryland
Library
Dr. R. E. Kalman

McDonnell Aircraft Corporation
St. Louis, Missouri
Library

North American Aviation
Space and Information Systems Division
Downey, California
Library
Dr. Laidlow
Mr. Stephen A. Jurovics
Mr. John E. McIntyre

Rand Corporation
Santa Monica, California
Library
Dr. Richard Bellman
Dr. Buchheim

Republic Aviation Corporation
Farmingdale L.I., New York
Library
Dr. Mary Payne

Space Technology Laboratories, Inc.
Redondo Beach, California
Library
Dr. P. Dergarabedian
Dr. Burton D. Fried
Dr. A. B. Michelwait

United Aircraft Corporation
Windsor Lockes, Connecticut
Library
Dr. Theodore N. Edelbaum
Mr. Robert P. Gregoire

Westinghouse Air Arm Division
M.S. 446, P.O. Box 746
Baltimore 3, Maryland
Library
Mr. Harold Shuster

Scientific and Technical Information Facility (2)
P. O. Box 5700
Bethesda, Maryland
NASA Representative (S-AK/RKT)